2007

An intelligent navigation system for an unmanned surface vehicle

Xu , Tao

THE UNIVERSITY OF PLYMOUTH

AN INTELLIGENT NAVIGATION SYSTEM FOR AN UNMANNED SURFACE VEHICLE

TAO XU

A THESIS SUBMITTED IN PARTIAL FULFILMENT FOR THE DEGREE
OF
DOCTOR OF PHILOSOPHY

IN THE
SCHOOL OF ENGINEERING

FACULTY OF TECHNOLOGY

IN COLLOBORATION WITH THE DEVONPORT MANAGEMENT LTD, J&S MARINE LTD
AND
SOUTH WEST WATER PLC

APRIL 2007

To my beloved family...

An Intelligent Navigation System for an Unmanned Surface Vehicle

Tao Xu

Abstract

A multi-disciplinary research project has been carried out at the University of Plymouth to design and develop an Unmanned Surface Vehicle (USV) named *Springer*. The work presented herein relates to formulation of a robust, reliable, accurate and adaptable navigation system to enable *Springer* to undertake various environmental monitoring tasks. Synergistically, sensor mathematical modelling, fuzzy logic, Multi-Sensor Data Fusion (MSDF), Multi-Model Adaptive Estimation (MMAE), fault adaptive data acquisition and an user interface system are combined to enhance the robustness and fault tolerance of the onboard navigation system.

This thesis not only provides a holistic framework but also a concourse of computational techniques in the design of a fault tolerant navigation system. One of the principle novelties of this research is the use of various fuzzy logic based MSDF algorithms to provide an adaptive heading angle under various fault situations for *Springer*. This algorithm adapts the process noise covariance matrix (Q) and measurement noise covariance matrix (R) in order to address one of the disadvantages of Kalman filtering. This algorithm has been implemented in *Springer* in real time and results demonstrate excellent robustness qualities. In addition to the fuzzy logic based MSDF, a unique MMAE algorithm has been proposed in order to provide an alternative approach to enhance the fault tolerance of the heading angles for *Springer*.

To the author's knowledge, the work presented in this thesis suggests a novel way forward in the development of autonomous navigation system design and, therefore, it is considered that the work constitutes a contribution to knowledge in this area of study. Also, there are a number of ways in which the work presented in this thesis can be extended to many other challenging domains.

Acknowledgements

I would like thank the many individuals that have contributed to make this project a success, and my educational experience at the University of Plymouth so enjoyable.

The biggest thanks goes to my Director of studies Professor Robert Sutton. His immense intelligence astounds me. More importantly, his work ethic greatly overshadows his god-given ability. I'll never know exactly how much time he spend reviewing my work. I sometimes wonder if his work ethic drove him to put more effort into my education than I did. I am deeply indebted to him for his help along this education journey, and I am inspired by the effort he puts in at MIDAS everyday.

Also gratitude goes to my pervious Director of studies Dr. John Chudley who had given so many suggestions and considerations before he left the University of Plymouth. I am also extremely thankful to my co-supervisors Dr. Ming Dai, Dr. Sanjay Sharma and Mr. Andy Stamp, for their suggestions and kind support.

I also need to express my gratitude to the *Springer* team members: Dr Wasif Naeam for his cooperation and help during the project, Mike Sloman for his technical help and keeping us safe on the boat, also William Stephenson, Gregory Nash and Craig Holmes. Without their work this project would not have been possible. Special thanks also go to the other members in MIDAS: Dr Dedy Loebis, Dr Seon Tan for their intellectual discussions. Thanks are also due to EPSRC for the overall funding of this project.

Finally I wish to thank the most important people in my life, my parents and my sister, Deru Xu, Hui-min Wang and Xin Xu. They laid the foundation for everything I have achieved and become today. This thesis would not have been possible without their encouragement on the telephone every night.

Declaration

I hereby declare that the thesis submitted in partial fulfilment for the requirements for the degree of Doctor of Philosophy that

- the thesis comprises only of my original work,
- due acknowledgment has been made in the text to all other material used,
- during the candidature, I have not been registered for any other award at any other institution,
- this study was financed with the aid of a studentship from the Engineering and Physical Sciences Research Council, UK,
- relevant scientific seminars and conferences were regularly attended at which work was often presented; external institutions were visited for consultation purpose and several papers prepared for publication,
- the thesis is below 31 000 words in length, exclusive of tables, bibliographies and appendices.

Tao Xu
April 2007

Table of Contents

List of Figures

List of Tables

Nomenclature

α_i	Uncertain parameter in elemental Kalman filter
β_i	Information feedback factor
ΔR_k	Adjustment of R matrix
Δs	The scale-factor error
δ	Dirac delta function
$\hat{C}_{Inn_k}$	Actual covariance value of innovation
$\hat{x}_k$	States estimate of the state space model
$\hat{z}_k$	Estimated measurement
ν_k	Measurement white noise of the state space model
ω_k	Process white noise of the state space model
ϕ_k	Transition matrix
ψ	The angle between north axis in the navigation-frame coordinate and u axis in the body-frame coordinate
d_k	System external disturbance
$DoMI_k$	Degree of Mismatch
e	System disturbance
F	System matrix of the state space model
f_k	Output of fuzzy logic observer
G	Matrix that relates the control input to the state vector
$H(.)$	Measurement matrix of the state space model

Inn_k	Innovation
j_0	The first sample inside the moving window
k	Discrete time index
M	Size of the moving estimation window
n	The number of elementary Kalman filters
p	Hypothesis conditional probability
P_k	State error covariance
q^{-1}	System delay operator
Q_k	Process noise covariance
r	Kalman filter residuals
R_k	Measurement error covariance
S_k	Theoretical covariance value of innovation/Residual covariance
T_n^b	The transformation matrix that converts a vector from the body-frame coordinate to the navigation-frame coordinate
u	System input
x_k	States of the state space model
y	System output
z_k	Measurement vector of the state space model
Z_k^*	A growing length measurement history vector consisting of all measurement vectors from z_0 to z_{k-1}
(u,v)	The velocity components in the body-frame coordinate
AAV	Autonomous Aerial Vehicle
AGV	Autonomous Ground Vehicle
AI	Artificial Intelligence
AMR	Anisotropic Magneto-Resistive

ANN	Artificial Neural Network
AOSN	Autonomous Ocean Sampling Networks
ARMAX	Auto-Regressive Moving Average with eXogenous variable
ARX	Auto-Regressive with eXogenous variable
ASIMOV	Advanced System Integration for Managing the Coordinated Operation of Robotic Ocean Vehicles
ASW	Anti-Submarine Warfare
AUV	Autonomous Underwater Vehicle
CAS	Collision Avoidance System
CKF	Centralised Kalman Filter
CSB	Combat Support Boat
DAQ	Data Acquisition
DGPS	Differential Global Positioning System
DKF	Decentralised Kalman Filter
DoD	Department of Defense
DOF	Degree Of Freedom
DR	Dead Reckoning
DSOR	Dynamical Systems and Ocean Robotics
DVL	Doppler Velocity Log
EKF	Extended Kalman Filter
EMS	Energy Management System
EPSRC	Engineering and Physical Sciences Research Council
FIS	Fuzzy Inference System
FKF	Federated Kalman Filter
FLA-CKF	Fuzzy Logic Adaptive Centralised Kalman Filter

FLA-DKF	Fuzzy Logic Adaptive Decentralised Kalman Filter
FLA-FKF	Fuzzy Logic Adaptive Federated Kalman Filter
FLA-KF	Fuzzy Logic Adaptive Kalman Filter
FLO	Fuzzy Logic Observer
FM	Frequency Modulated
GA	Genetic Algorithm
GLONASS	Global Orbiting Navigation Satellite System
GPS	Global Positioning System
HF	High Frequency
HMR	Honeywell Magneto-Resistive
INS	Inertial Navigation System
ISR	Institute for Systems and Robotics
IST	Instituto Superior Técnico
KF	Kalman Filter
LADC	Local Area Differential Correction
LAN	Local Area Network
LoS	Line of Sight
LQG	Linear Quadratic Gaussian
LQR	Linear Quadratic Gaussian with loop transfer Recovery
MAROV	Marine habitats of the Azores using Robotic Ocean Vehicle
MCM	Mine Counter Measures
MIT	Massachusetts Institute of Technology
MMAE	Multiple Model Adaptive Estimation
MMS	Mission Management System
MPC	Model Predictive Control

MPRS	Man Portable Robotics System
MSDF	Multiple Sensor Data Fusion
MWATH	Medium WAterplane Twin Hull
NAVSTAR	NAVigation System with Time And Ranging
NGC	Navigation Guidance Control
NI	National Instrument
NM	Nautical Mile
NMEA	National Marine Electronics Association
PD	Proportional Derivative
PDF	Probability Density Function
PID	Proportional Integral Derivative
RF	Radio Frequency
RHIB	Rigid Hull Inflatable Boats
RMS	Remote Minehunting System
RMSE	Root Mean Square Error
ROV	Remotely Operated Vehicle
SESAMO	SEa Surface Autonomous MOdular unit
SI	System Identification
SISO	Single Input Single Output
SWATH	Small WAterplane Twin Hull
SWIMS	Shallow Water Influence Mine Sweeping
USBL	Ultra Short Baseline Unit
USCG	United State Coast Guard
USV	Unmanned Surface Vehicle
VHF/UHF	Very/Ultra High Frequency
WADC	Wide Area Differential Correction

Chapter 1

INTRODUCTION

1.1 Motivation

Over the past century the global growth of heavy industry and manufacturing has come with a dramatic increase in pollution. The adverse consequence of this increase is climate change. In particular, research carried out in the last decade emphasized the role played by ocean/water pollution in the prediction of global climate condition (Heal and Kriström 2002). Therefore, pollutant tracking and environmental surveying have become very important issues. However, only 5% of the oceans have been characterized. One obvious reason is that the ocean environment is complex which could contain unknown biological, chemical, and mineral (National Research Council,USA 2003). Hence, the exploration tasks are extremely difficult, expensive and dangerous for human beings.

In order to explore the unknown ocean environment, in recent years, there has been significant progress in the development of Autonomous Underwater Vehicles (AUVs) and Remotely Operated Vehicles (ROVs), and a number of AUVs and ROVs have been successfully implemented in offshore industrial, military and commercial areas (Butler and Hertog 1993, Griffiths *et al.* 1999, Yoerger *et al.* 2000, Loebis *et al.* 2006). However, in

shallow or inland waters, AUVs and ROVs have limited capabilities for undertaking tracking and surveying tasks. Currently, worldwide interest is gathering a pace into the design and development of cost effective Unmanned Surface Vehicles (USVs) to undertake surveys in shallow waters, such as pollutant tracking and hydrographic tasks can be carried out in a more economical manner than is currently possible.

To date, the USV market in the USA and Europe has grown significantly with several USVs on the horizon. The US Navy spent $55 million to develop their *Spartan* USV system (Tiron 2002), in Portugal, *Delfim* and *Caravela* 2000 USVs have been designed in order to undertake oceanographic research (Dynamical Systems and Ocean Robotics (DSOR) Laboratory 2000). Whilst in German, the *Measuring Dolphin* USV has been employed for shallow water survey missions (Majohr *et al.* 2000). More details of on-going USV projects are presented in Chapter 2. In the UK research interest in this key area appears mainly confined to that being undertaken by Corfield (Corfield 2002) who has developed variants of the *Mimir* USVs for naval and surveying missions. More details of on-going USVs are introduced in Chapter 2. From the relevant literature, it is clear that there is a widening technology gulf between the UK and other countries in this technologically interesting and extremely important area of study. Thus developing an USV in the UK cannot only close the gap in this field but also provide a low cost solution for environment monitoring and relevant pollutant investigations.

1.1.1 *Springer* project objectives

The *Springer* USV project commenced in early 2004 at the University of Plymouth. The *Springer* USV is intended to be a mobile, rapidly sampling, remotely operated sensor platform which can undertake various hydrological surveys, including real time mapping of pollutant spills, tracking of pollutant spills to their sources, quantification of sharp pollutant and other scientifically important gradient phenomena.

The *Springer* vehicle is easily deployable and can accommodate various requirement without varying the existing payload. Hence, the *Springer* can also be used as a test bed platform for other academic and scientific institutions involved in environmental data gathering, sensor and instrumentation technology, control systems engineering and power systems based on alternative energy sources. More details of the *Springer* are introduce in Chapter 3.

1.1.2 Navigation, Guidance and Control (NGC)

Onboard NGC system play a vital role in autonomous vehicle operation. The navigation system provides information related to the target. The guidance system manipulates the outputs from the navigation system and by utilizing proper guidance laws generates suitable trajectories to be followed by the vehicle. The control system is responsible for keeping the vehicle on course as specified by the guidance processor(Lin 1992). In remotely operated systems, guidance commands are sent from a ground station by a trained human operator whilst autonomous vehicles have an onboard guidance processor. A generic block diagram of a integrated NGC system of a vehicle is depicted in Figure 1.1.

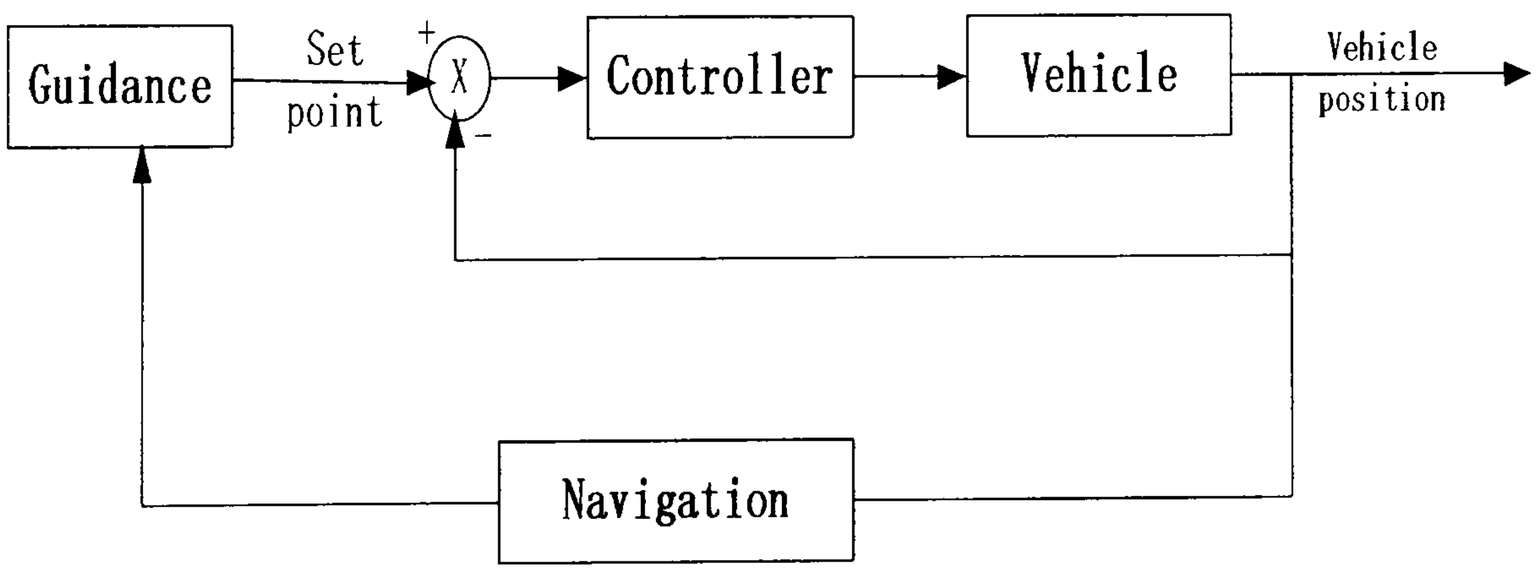

Figure 1.1: Navigation, Guidance and Control process

The navigation system is responsible for accurate positioning of the USV, it should be able to cope with any kind of sensor noise/faults that may occur during an operation. For this purpose. Multi-Sensor Data Fusion (MSDF) algorithms which combines data from various

onboard sensors and provides the best estimate for the vehicle are always used to achieve intrinsic redundancy. More techniques involved in navigation systems will be presented throughout the thesis.

The guidance and control system plays a vital role in bringing autonomy to the system and keeping the vehicle on the proper trajectory. A good account of several guidance laws employed by AUVs have been documented by Naeem et al. (2004). For *Springer*, an intelligent fuzzy logic based model predictive controller, a fuzzy logic Linear Quadratic Gaussian (LQG) controller and LQG with Loop Transfer Recovery (LQR) algorithms have been implemented (Naeem *et al.* 2007).

1.2 Aim and objectives of the research

Intelligent multi-sensor navigation system design has recently received a great deal of interest, in particular hybrid MSDF algorithms with Artificial Intelligence (AI) techniques. However, until now, such an approach has not been employed on modern autonomous vehicles. An intelligent navigation approach must have the ability to learn a process, adapt its behaviour in light of process change, store and recall relevant information and autonomously improve its performance when required to do so. It is therefore important that such a system can adapt to register new information.

The overall aim of the thesis is to develop an intelligent navigation system for the *Springer* vehicle. This also entails the implementation and cooperation with a guidance and control system in real time. The main objectives of this research include the onboard navigation sensor modelling, user interface development , fault tolerant MSDF navigation strategy design and full scale real time trial and evaluations.

Broken down as submodules, the objectives of this research are provided as follows:

- Critically review current autonomous navigation techniques.

- Survey current USV projects and analysis the features of different applications.

- Develop a friendly user interface which can allow the user access an onboard NGC system remotely. Also design a practicable communication manner between the NGC system for real time trials.

- Design a novel fault tolerant fuzzy logic based MSDF system for *Springer* as an onboard navigation system.

- Design a Multi-Model Adaptive Estimation (MMAE) algorithm as an alternative navigation solution.

- Evaluate the proposed navigation strategy performances in simulations for various scenarios.

- Employ a simulated navigation strategy in the full scale trials, and evaluate the experimental performance results.

All of the objectives mentioned here will be revisited at the end of the thesis.

1.3 Thesis overview

Accordingly, the thesis is constructed as follows,

Chapter 2 elaborates upon the related research, technologies and projects relating to the USVs. This review is sub-divided into two distinct parts, the autonomous navigation techniques and the details of on-going USV projects. The first part surveys the autonomous navigation strategies and navigation sensors. Whilst, the second part provides a broad review on the current military, research and commercial USVs all over the world.

Since there was no previous hardware details of *Springer* in the literature, it was deemed necessary to disseminate this information in Chapter 3. The contents includes the hardware setup, navigation sensor suite, controller and other equipment. The user interface design is also emphasized. The fault tolerant Data AcQuisition (DAQ) system, data processing and the data transmitting structure of the NGC system is also included.

Chapter 4 delves into sensor modelling. Clearly, in order to design a proper Kalman filter, an accurate sensor model must be available. Consequently, a first principle algorithm is used to derive the model of a Global Positioning System (GPS) , whilst a System Identification (SI) method is implemented in deriving the models for the onboard compasses.

With the knowledge gained through the aforementioned survey, it was decided that this research would focus on the development of an intelligent MSDF navigation algorithm. Its intriguing properties coupled with its strong potential for practical implementation rendered it a worthy topic of research. Hence, Chapter 5 presents the development of various cascaded Kalman filters combined with fuzzy logic. Also, a fuzzy logic observer is designed to offer an observation window for the user in order to tune the fuzzy rules and membership functions. The fault tolerant capabilities of each algorithm are examined under different types of sensor fault. As a result, a fuzzy logic based federated Kalman filter with adaptive information feedback was selected as an onboard navigation system.

Following the success of the MSDF simulations conducted in Chapter 5, an alternative fault tolerant multiple sensor navigation approach based on a MMAE algorithm is developed in Chapter 6. Three elemental filters are utilised for each sensor in order to derive an estimate for the actual state. Then the individual estimates are combined together by using a fuzzy logic centralised Kalman filter. In the process of the development of this MMAE approach, the measurement noise covariance matrix (R) and the process covariance matrix (Q) are varying for each elemental filter. The residual and probability simulation results are shown.

Chapter 7 presents the experimental results from several *Springer* trials. The experimental setup is elucidated. A Model Predictive Control (MPC) algorithm is implemented as the control strategy, and a Federated Kalman Filter (FKF) with and without fuzzy logic algorithms are implemented. The results demonstrate that the proposed MSDF strategies perform remarkably well in a real time environment despite the existence of wind/wave disturbances.

Concluding remarks, a summary of the thesis achievements and recommendations for future research are presented in Chapter 8.

In addition, Appendix A provides the author's published work. The features of different types of USVs are compared in Appendix B. The details of the onboard sensor strings are presented in Appendix C, and Appendix D briefly introduces model predictive control and Genetic Algorithm (GA) based MPC for completeness.

1.4 Contributions of the thesis

The major research contributions of the thesis are seen as:

- Providing an up-to-date comprehensive review of the current autonomous navigation techniques with special attention to on-going USV projects.
- A user interface which enables the user access and to monitor the vehicle is developed using LabView.
- Onboard navigation sensor models are developed using first principle and system identification techniques.
- A novel fuzzy logic MSDF algorithm with fault tolerance is proposed. To author's knowledge, this is the first study of an USV implementation of this particular tech-

nique. Q and R matrices are adapted on-line in order to improve the robustness of the navigation system.

- A modified MMAE algorithm is offered as an alternative solution for the navigation system for the *Springer*.

From the above it is deemed that a contribution to knowledge has been made in the area of **fuzzy logic based federated Kalman filter with adaptive information feedback, fault tolerant capability analysis of fuzzy logic based cascaded Kalman filter, fuzzy logic based MMAE algorithm, adaptive Q and R matrices and their performance analysis, navigation sensor modelling** and **a fault tolerant user interface**.

Chapter 2

RELATED RESEARCH AND LITERATURE SURVEY

A comprehensive literature review of autonomous navigation systems which have been widely adopted by autonomous air and marine vehicles is provided in this chapter. Also the details of navigation strategies, navigation sensors and multi-sensor navigation algorithms are given. In addition, an in-depth survey of on-going USV projects is carried out in this chapter. The features and specifications of different USVs are also summarized and compared.

2.1 Autonomous navigation

Navigation is the process of accurately determine the position and velocity of a body relative to a known reference and to plan and execute the manoeuvres necessary to move between desired locations (Farrell and Barth 1999). Autonomous navigation means a vehicle can move to a desired destination or along a desired path purposefully without human

intervention. The following capabilities for a vehicle are thus required:

- The ability to execute elementary goal achieving actions or reaching a given location;
- The ability to react in real time to unexpected events;
- The ability to form plans that pursue specific goals or avoid undesired situations;
- The ability to adapt to changes in the environment.

A navigation system constantly evaluates the vehicle's position, anticipates dangerous situations well before they arise, and always keeps "ahead of the vehicle"(Farrell and Barth 1999). Methods of navigation have changed throughout history. each new method has enhanced the vehicle's ability to complete a voyage safely and expeditiously.

There are four main methods widely used in autonomous navigation, including satellite navigation, dead reckoning navigation, inertial navigation and multiple sensor navigation system.

2.1.1 Satellite navigation

Satellite navigation techniques have the advantage that their signals have Line of Sight (LoS) propagation to almost an entire hemisphere of the Earth. Currently, there are three satellite navigation systems all over the world:

- NAVigation System with Time And Ranging Global Positioning System (NAVSTAR GPS), developed and operated by the USA Department of Defense(DoD);
- Global Orbiting Navigation Satellite System (GLONASS) operated by the Russian Space Forces;

- GALILEO developed by the European Union and the European Space Agency.

Among the satellite navigation systems which have been used in real applications, GPS has matured rapidly since being fully operated in 1995 (Grewal *et al.* 2000). The GPS combines a network of 24 or more satellites which continuously transmit radio signals, containing a variety of data including time and distance data that can be picked up by any GPS receiver, thereby allowing the user to pinpoint their position anywhere on Earth (Farrell and Barth 1999). For most of GPS, the clock is inaccuracy which result the GPS accuracy degrades over time. Also signals are often reflected off tall buildings before reaching the receiver. The signal is delayed therefore information provided is inaccurate. The satellite signal could slow down when it passes through inclement weather. As GPS has such disadvantages, for accurate and fault tolerant navigation system, it still cannot be employed independently. More details of GPS technique will be introduced in Section 2.1.6.

2.1.2 Dead Reckoning (DR) navigation

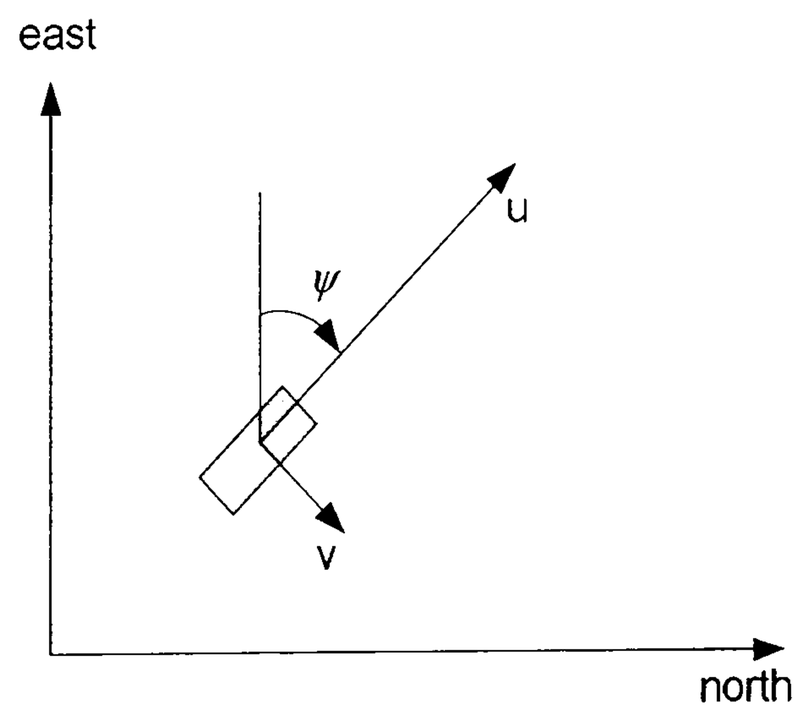

Figure 2.1: Ideal two dimensional DR (Farrell and Barth 1999)

DR navigation was used by Columbus in 1492 on his voyage of discovery to the New World (Bowditch 1995). It is the process of estimating the vessel's position when starting from a

known position and moving at a known course and speed (Farrell and Barth 1999). Speed and heading information are two basic measurements for this navigation technique.

In a modern DR navigation system, electronic sensors are used to measure the body-frame velocity and heading, the navigation-frame velocity and heading are determined at a high rate. Figure 2.1 describes the ideal two dimensional DR navigation system, and the differential Equations 2.1 gives the details of this approach,

$$\begin{bmatrix} \dot{n}(t) \\ \dot{e}(t) \end{bmatrix} = \begin{bmatrix} \cos(\psi(t)) & -\sin(\psi(t)) \\ \sin(\psi(t) & \cos(\psi(t))) \end{bmatrix} \begin{bmatrix} u(t) \\ v(t) \end{bmatrix} \tag{2.1}$$

Where (n, e) is the north and east position component in a navigation-frame coordinate, (u, v) is velocity components in the body-frame coordinate, ψ is the angle between the north axis in navigation-frame and u axis in the body-frame. Matrix T_n^b shown in Equation 2.2 is a transformation matrix that converts a vector from the body-frame coordinate to the navigation-frame coordinate.

$$T_n^b = \begin{bmatrix} \cos(\psi(t)) & -\sin(\psi(t)) \\ \sin(\psi(t) & \cos(\psi(t))) \end{bmatrix} \tag{2.2}$$

It should be noted that the DR approach described in Equation 2.1 is in an ideal situation. Whilst in real applications, the sensors and various environmental effects will generate disturbances which act upon a DR navigation system. As a result the actual DR navigation system is described in Figure 2.2, and the equation should be changed to include various system errors as shown in Equation 2.3:

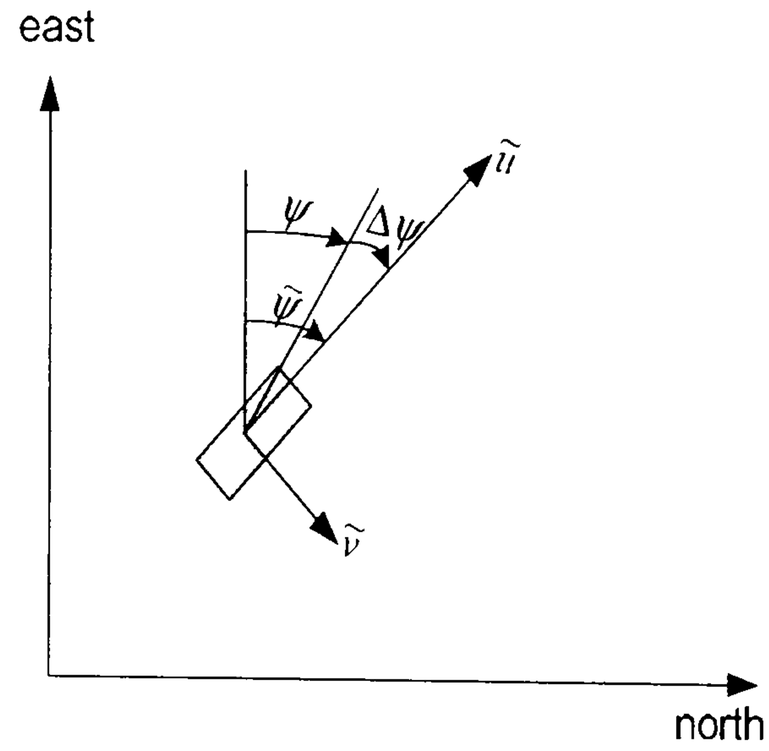

Figure 2.2: Actual two dimensional DR (Farrell and Barth 1999)

$$\begin{bmatrix} \dot{\hat{n}}(t) \\ \dot{\hat{e}}(t) \end{bmatrix} = \begin{bmatrix} \cos(\tilde{\psi}(t)) & -\sin(\tilde{\psi}(t)) \\ \sin(\tilde{\psi}(t) & \cos(\tilde{\psi}(t))) \end{bmatrix} \begin{bmatrix} \tilde{u}(t) \\ \tilde{v}(t) \end{bmatrix} \tag{2.3}$$

Where $\tilde{\psi} = \psi + \Delta\psi$;

$\tilde{v} = v + \Delta v$;

$\tilde{u} = (1 + \Delta s)u + \Delta u$;

Where $\Delta\psi, \Delta v, \Delta u$ are the bias terms which assume generated by wind, wave and sensor measurement errors. And Δs is the scale-factor error.

Assuming $\tilde{v} = 0$, and $\Delta v = -v$, Equation 2.3 is simplified to Equation 2.4,

$$\begin{bmatrix} \dot{\hat{n}}(t) \\ \dot{\hat{e}}(t) \end{bmatrix} = \begin{bmatrix} \cos(\psi(t) + \Delta\psi(t)) & -\sin(\psi(t) + \Delta\psi(t)) \\ \sin(\psi(t) + \Delta\psi(t)) & \cos(\psi(t) + \Delta\psi(t)) \end{bmatrix} \begin{bmatrix} (1 + \Delta s)u(t) + \Delta u(t) \\ v(t) + \Delta v(t) \end{bmatrix} \quad (2.4)$$

Applying Taylor's Theorem and dropping all errors greater than first order, linear error differential equations are obtained in Equation 2.5,

$$\begin{bmatrix} \dot{\hat{n}}(t) \\ \dot{\hat{e}}(t) \end{bmatrix} = \begin{bmatrix} \cos(\psi(t)) & -\sin(\psi(t)) \\ \sin(\psi(t)) & \cos(\psi(t)) \end{bmatrix} \begin{bmatrix} u(t) \\ v(t) \end{bmatrix} +$$

$$\begin{bmatrix} -u(t)\sin(\psi(t)) & u(t)\cos(\psi(t)) & \cos(\psi(t)) & -\sin(\psi(t)) \\ u(t)\cos(\psi(t)) & u(t)\sin(\psi(t)) & \sin(\psi(t)) & \cos(\psi(t)) \end{bmatrix} \begin{bmatrix} \Delta\psi(t) \\ \Delta s(t) \\ \Delta u(t) \\ \Delta v(t) \end{bmatrix} \quad (2.5)$$

As $\Delta\dot{n} = \dot{n} - \dot{\hat{n}}$ and $\Delta\dot{e} = \dot{e} - \dot{\hat{e}}$, taking the difference of Equation 2.1 and Equation 2.5, the linear error differential equation is yielded in Equation 2.6:

$$\begin{bmatrix} \Delta\dot{n} \\ \Delta\dot{e} \end{bmatrix} = \begin{bmatrix} 0 & 0 \\ 0 & 0 \end{bmatrix} \begin{bmatrix} \Delta n \\ \Delta e \end{bmatrix} -$$

$$\begin{bmatrix} -u(t)\sin(\psi(t)) & u(t)\cos(\psi(t)) & \cos(\psi(t)) & -\sin(\psi(t)) \\ u(t)\cos(\psi(t)) & u(t)\sin(\psi(t)) & \sin(\psi(t)) & \cos(\psi(t)) \end{bmatrix} \begin{bmatrix} \Delta\psi(t) \\ \Delta s(t) \\ \Delta u(t) \\ \Delta v(t) \end{bmatrix} \quad (2.6)$$

In Equation 2.6, $\begin{bmatrix} \Delta\psi(t) \\ \Delta s(t) \\ \Delta u(t) \\ \Delta v(t) \end{bmatrix}$ is considered as various sensing errors which result in growth in position errors. The initial position errors $\begin{bmatrix} \Delta n \\ \Delta e \end{bmatrix}$ result in constant position off sets for all future time. It is worth noting that the errors in position cannot be detected or corrected without additional sensor.

2.1.3 Inertial navigation

Since 1960s, an advanced navigation technique known as an inertial navigation system (INS), which consists of a sensor package has been in use in aircraft, ships and submarines. This type of navigation which is based on Newton's laws of motion relies on knowing the initial position, velocity and attitude and thereafter measuring the attitude rates and accelerations from the sensors without needing any reference from land or other vehicles (Grewal *et al.* 2000).

The basic sensors for INS are accelerometers and gyroscopes. The accelerometers provide measurements of the vehicle's accelerations along the body-fixed translation axes, and the vehicle's position can be calculated easily by using a second order integration with respect to time. The gyroscopes measure the rates and angular information of rotation. The accuracy of these systems is determined by the sensitivity of their internal components and the degree of error introduced over time (Lawrence 1998). The general working process of INS is depicted in Figure 2.3.

The GPS has superior long-term error performance but poor short-term accuracy. It is not sufficient for providing position for vehicle navigation system, whilst general INS sensors

are self-contained and provide high frequency and continuous information. However, the accelerometers and gyroscopes drift can result in significant misalignments between the instrument and the Earth referenced frame degrading INS accuracy over time. Owing to their complementary characteristics, INS is often integrated with GPS. With decreasing prices in both GPS and INS sensors and processor technologies, this sort of integrated approach has been used for many autonomous navigation systems in robotics, AUVs and autonomous airborne vehicles (AAVs) (Kim *et al.* 2002, McGhee *et al.* 1995, Moore *et al.* 2003).

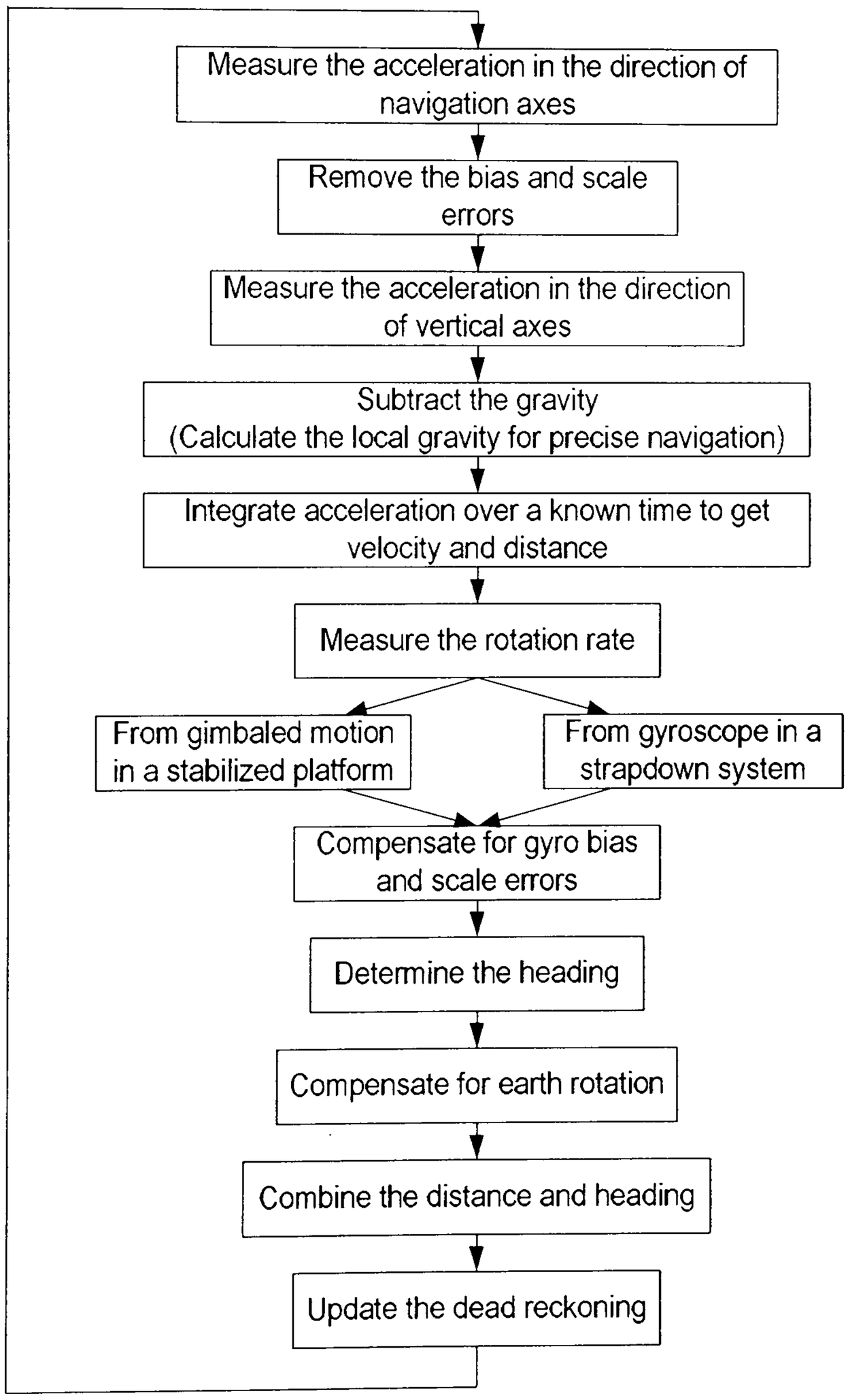

Figure 2.3: INS working process

2.1.4 Multi-sensor navigation system

Advanced technology brings the navigation system into a new era. the modern navigation system gathers information from every available source which is measured by different sensors in order to produce more accurate information (Brown and Hwang 1997). For instance, a compass can determine the direction relative to the local magnetic north, and the speed log produces accurate information about the speed of the vehicle. Various sensors provide their own distinguished outputs to provide a navigation solution. Therefore, more than one sensor is involved so as to not only determine the navigation states at a certain time but also to supply a continuous navigation trajectory. The term, 'multi-sensor navigation system', is therefore often used. Such systems are typically operated with multi-sensors referenced to a common platform and synchronized to a common time base (Brooks and Iyengar 1998). Each sensor contributes its own stream of data and all the data is optimally processed. From the evaluation of this data, the navigation system determines a fix, and compares that fix with its pre-determined position. The core technique of a multi-sensor navigation strategy is Multi-Sensor Data Fusion (MSDF).

MSDF is an evolving technology that is concerned with the problem of how to fuse data from multiple sensors. It has several significant advantages over single source data (Varshney 1997):

- MSDF systems produce accurate information by combing readings from several redundant sensors or different sensors in order to achieve better data interpretation or improved decision making;
- MSDF systems will be more clearly insensitive to sensor failures than a system using a single sensor;
- MSDF is low cost algorithm which uses several inexpensive sensors in a synergistic manner to provide data that are same or even better than data from much more

expensive single sensor devices.

As results of all these advantages, MSDF has been used widely and successfully in many fields, such as: onboard navigation, object detection, recognition, identification and classification, tracking monitoring, and change detection (Shahbazian *et al.* 2000, Shahbazian *et al.* 1997, Loebis *et al.* 2003). In particular, it has been successfully applied in autonomous navigation techniques (Luo *et al.* 2002).

The sensing process of MSDF generally proceeds in the following patterns: detection, pre-processing, fusion and data interpretation (Brooks and Iyengar 1998). The schematic diagram is shown in Figure 2.4.

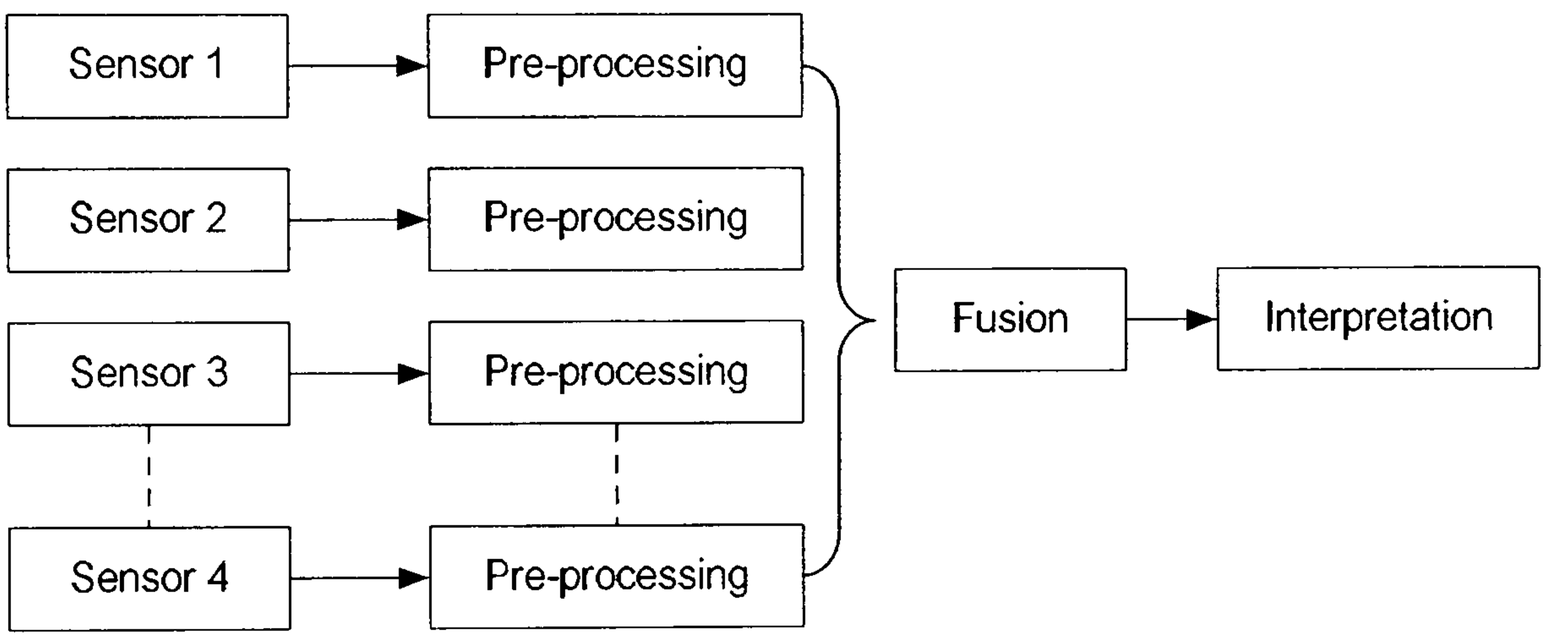

Figure 2.4: The schematic diagram of MSDF process

Every sensor must detect some aspect of the state of its environment. The interaction may, for example, involve detecting electromagnetic radiation originating from the environment, recording reflection of radiation emitted by the sensor, or direct physical contact with obstacles in the environment.

After detection, pre-processing is necessary. Tasks that are generally part of pre-processing include noise reduction, sensor recalibration, de-skewing individual readings and activities peculiar to one specific type of sensor.

When the sensor reading has been pre-processed, it is appropriate to put the data in a

specified form. Therefore the readings from several sensors can be fused into a single reading. This fused reading will be in the same form as the pre-processed data.

After the data from various sensors have been fused, it will be interpreted. The process of interpretation is task-specific and consists of finding the best fit possible for the data within the information requirement of the system.

Among the various estimation algorithms available for MSDF, the Kalman Filter (KF) based approach has been applied successfully to many practical problems, particularly in navigation (Welch and Bishop 2004). The KF uses the statistical characteristics of a measurement model to determine estimates recursively for the fused data that are optimal in a statistical sense. If the system can be described by a linear model and both the system and sensor errors can be modelled as white Gaussian noise, the KF will provide unique statistically optimal estimates for the fused data. In addition to eliminate the need for storing the entire past observed data, the KF is computationally more efficient than non-recursive methods (Kalman 1960). The KF is very powerful in several aspects: it supports estimations of past, present, and even future states, and it can do so even when the precise nature of the modeled system is unknown.

KF has been has been used extensively for data fusion. Simone et al. (2000) proposes a multi-scale Kalman filter for the fusion of radar images, acquired by different radars operating with different resolutions. Boucher et al. (2001) use KF tracks the features through data sequences and estimates 3D position. Amditis et al. (2005) utilise a KF based information fusion system in automotive forward collision warning systems.

More details of KF computation process is introduced in Chapter 5.

2.1.5 Hybrid MSDF

Hybrid MSDF refers to the actual combination of Kalman filtering with other techniques such as fuzzy logic, Artificial Neural Networks (ANNs) and Genetic Algorithms (GAs) (Loebis *et al.* 2004, Chen and Huang 2001, Liu *et al.* 2003). All the MSDF approaches need exact knowledge about the sensed environment and sensors, however, in real applications only certain information is known about the sensed environment and sensors are rarely perfect. With the rapid growth in MSDF techniques, there is scope for the development of Kalman filter based MSDF architectures capable of adaptation to changes in the sensed environment and to deal with sensor faults.

In order to deal with complex problems, fuzzy logic based MSDF techniques have become the most popular approach. By using fuzzy logic, the uncertainty in sensor readings can be directly represented in the fusion process by allowing each proposition to be assigned a real number to indicate its degree of truth (Yan *et al.* 1995). Furthermore, a fuzzy logic based adaptive MSDF has the ability to combine information from different classes of variable by means of Fuzzy Inference Systems (FISs), so it can solve complex problems using imprecise inputs from several different sensors and thereby provide approximate solutions.

Three fuzzy logic related adaptive MSDF methods are now briefly presented. Loebis et al. (2004) used a fuzzy logic based adaptation scheme to cope with a divergence problem which was caused by insufficient knowledge of *a priori* filter statistics. Also GA techniques are used to choose the fuzzy membership functions for the adaptation scheme. This algorithm was proposed as a navigation application for an AUV.

Prajitno and Mort (2001) produced a fuzzy model based MSDF algorithm which was applied in target tracking applications. First the algorithm was used to predict the future sensor states to validate the measurement data. Then the valid sensor data was used to generate the decision output, and finally a corrector or filter unit provided the final decision

on the value of the current state based on the current measurement (fused output) and the predicted state.

Whilst Doyle and Harris (1996) introduced a neuro-fuzzy KF based MSDF method which was used for real time tracking of obstacles occurring during the flight of a helicopter. Several different sensors were used to estimate the location of obstacles around the helicopter, a B-spline trained ANN was implemented to construct the dynamic and observation models of the helicopter. A KF was then deployed to perform state estimation.

2.1.6 Navigation sensors

In various modern navigation techniques, onboard sensors including GPS, magnetic compass, inclinometer, INS instruments and depth/speed sensors etc. are very important for different applications. Among these sensors, the essential sensors are the magnetic compass and GPS.

Compass

The magnetic compass was developed in China more than seventeen hundred years ago works on the basis of Earth magnetic field available everywhere, requiring no environmental modification as compared with other positioning senors (Bells 2000). Currently, the most commonly used electronic magnetic compass are based on the flux-gate effect, magneto-inductive effect or Anisotropic Magneto-Resistive(AMR) effect (Brooke 2005).

The flux-gate effect employs two or more small coils of wire around a core of highly permeable magnetic material. The idea of a flux gate effect is that when the core is saturated it essentially disappears and when it's out of saturation it bends the Earth's magnetic field lines which cross the coil. The magnetic change of the core generate a voltage accord-

ing to Faraday's law (Brooke 2005). This voltage value will decide the compass's heading output. Some flux-gate compass systems, for instance, the KVH C100 flux-gate compass offers modules incorporating both rate gyros that compensate for errors from acceleration, as well as inclinometers that provide accurate readings of heading, pitch, and roll (KVH Industries, Inc. 2004).

The magneto-inductive effect sensor simply uses a single winding coil for each axis on a ferromagnetic core that changes permeability within the Earth's field. The sensor's coil serves as the inductance element in a L/R relaxation oscillator. The oscillator's frequency is proportional to the field being measured, and a microprocessor outputs the magnetic field value which calculates the orientation in the Earth's field. The PNI's TCM series electronic compass are based on the magneto-inductive effect. The TCM2 compass combines a two axis inclinometer to measure the tilt and roll. It has simpler design with low operating power than flux-gate effect sensor(PNI, Co. 2004).

The magneto-resistive effect is based on the resistance of element changes due to magnetic field strength. It is highly sensitive and well adapted for low fields. The Honeywell Magneto-Resistive (HMR) compass uses three perpendicular sensors and a fluidic tilt sensor to provide a tilt-compensated heading (Honeywell International, Inc. 2004).

The table below shows the comparison of these three electronic compass techniques,

Table 2.1: comparison of electronic compass techniques

	Flux-gate effect	Magneto-inductive effect	AMR effect
Sensibility	Low	High	High
Power consumption	High	Low	Medium
Design	Complex	Simple	Complex
Disturbance tolerance capability	Low	Low	High

GPS/DGPS

Every point on the surface of the Earth is identified by two sets of numbers called coordinates. These coordinates represent the exact point where a line parallel to the equator, known as latitude, crosses a line parallel to the polar axis, known as longitude. The GPS technique employs trilateration which is the algorithm of determining position by measuring distances to points at a known coordinate (Kennedy 2002).

The GPS includes three major segments:

- the space segment
- the control segment
- the user segment

The space segment consists of the GPS satellites. The GPS operational constellation includes 24 or more satellites approximately positioned in six orbits with 60 degree separation. The orbits are nearly circular with 55 degree inclination relative with the equator. The radius of the orbits is about 26,600 km. This constellation ensues the user located anywhere on the surface of the Earth can use more than 4 satellites under a clear view of the sky. The satellites broadcast signal contains data which identifies the satellite and provides the positioning, timing, ranging data, satellite status and corrected orbit parameters of the satellite.

The control segment has responsibility for monitoring and maintaining the space segment. This includes monitoring the health and status of the satellites and maintaining the satellites in their proper position and function. The control segment includes one master control station, six remote control stations spread around the globe in longitude and four large ground antennas. The remote monitor stations keep tracking and gathering code from the

satellites and transmit this data to the master control station where any adjustments or updates needed to upload to the satellites via ground antennas are corrected.

The user segment typically referred to as a GPS receiver can decode the satellite transmissions to provide the position, velocity and time information to the users.

Differential GPS, or DGPS, uses position corrections to attain greater accuracy by utilizing two GPS receivers. One receiver is located in a reference station whose position is a known point. Another receiver is operated as a mobile receiver. Since the precise location of the reference station is known, it can compare that position with the signals from the GPS satellites and thus correct satellite pseudo-range to the true range. Therefore this correction information can be calculated and transmitted to the mobile receiver in order to remove most of the satellite signal error and improve accuracy.

Methods of differential correction fall into two broad categories: Local Area Differential Correction (LADC) and wide area differential correction (WADC).The LADC can be accomplished by:

- using Frequency Modulated (FM) radio stations;
- using United States Coast Guard (USCG) beacon signals;
- using a user purchased base station.

WADC corrects the signal by using the same algorithm as with LADC. Also WADC covers a much larger area than LADC by implementing stationary satellites (geo-referenced). These satellites are very similar to television satellites and are not part of the GPS. These geo-referenced satellites track all the GPS satellites and broadcast the differential corrections to the users (Shearer *et al.* 2005).

2.2 Current USV projects

The discussion that now follows focuses on a variety of USVs which have been successfully designed and developed during the past few years. According to the different purpose of the vehicles, diverse shapes of the vehicle have been designed. different propulsion systems implemented and various sensors combined to supply the data for the NGC system.

For most of the USVs reviewed in this section, the simplicity of the launch and recovery operation is a common characteristic in USV design. Therefore small or medium size hulls are deployed in the current USVs. Today, USVs have been designed with a number of different hull types including (Corfield and Young 2006):

- jetski
- Rigid Hull Inflatable Boats (RHIB)
- catamaran
- custom tri-hulls
- patrol craft mono-hulls

The choice of the type of the hull depends on the desired USV operation requirements and its numbers, types and masses of the onboard payload equipment and sensors. The flexibility and safety of the manoeuvres are key considerations. Also, cost constraints are very important.

In this section, USVs are reviewed in three main categories: military applications, academic research applications and commercial applications.

2.2.1 Military applications

The first military USV application can be traced back to 1588 when eight unmanned fire ships were arranged by Howard and Drake to disrupt the Spanish Armada fleet (Roberts and Sutton 2006). During the World War II, the Canadian Navy tried to develop a torpedo USV *COMOX* to lay smoke during the Normandy invasion. Unfortunately, the *COMOX* was not deployed even though successful tests were completed (Veers and Bertram 2006). After the coordinated terrorist suicide attacks by Islamic extremists on the United States at the 11 September 2001, the USA military launched a global anti-terrorism programme on December 2001. It is aim to expand the line of defence for preventing terrorism attack, as well as strengthening the USA forces anti-terrorism capabilities. Following the spread of this programme, more investment has been made in designing and purchasing modern vehicles and weapons (Moiré Inc. 2003).

The military market has grown significantly faster than predicted. Several modern navies, such as, UK, Canada and Germany have started to put a stronger focus on the design of USVs. Hence the functions of the USVs are broadly defined as:

- navy coastal warfare;
- Anti-Submarine Warfare (ASW) surveillance;
- battle space preparation and awareness;
- battle damage assessment;
- port and coastal reconnaissance;
- force protection;
- targeting;
- amphibious open area reconnaissance:

- Mine Counter Measures (MCM);
- mine sweeping and clearing;
- riverine operation and other special force operations;
- hydrography and oceanography survey etc.

Owl MK II

The *Owl MK II* USV shown in Figure 2.5 is a high-speed, military surveillance vehicle with a low-profile hull for increased stealth and payload, and operated in a remotely controlled mode. It is designed to undertake multi-missions, including hydrographic survey, optical surveillance, data collection and mine detection by utilizing a sonar.

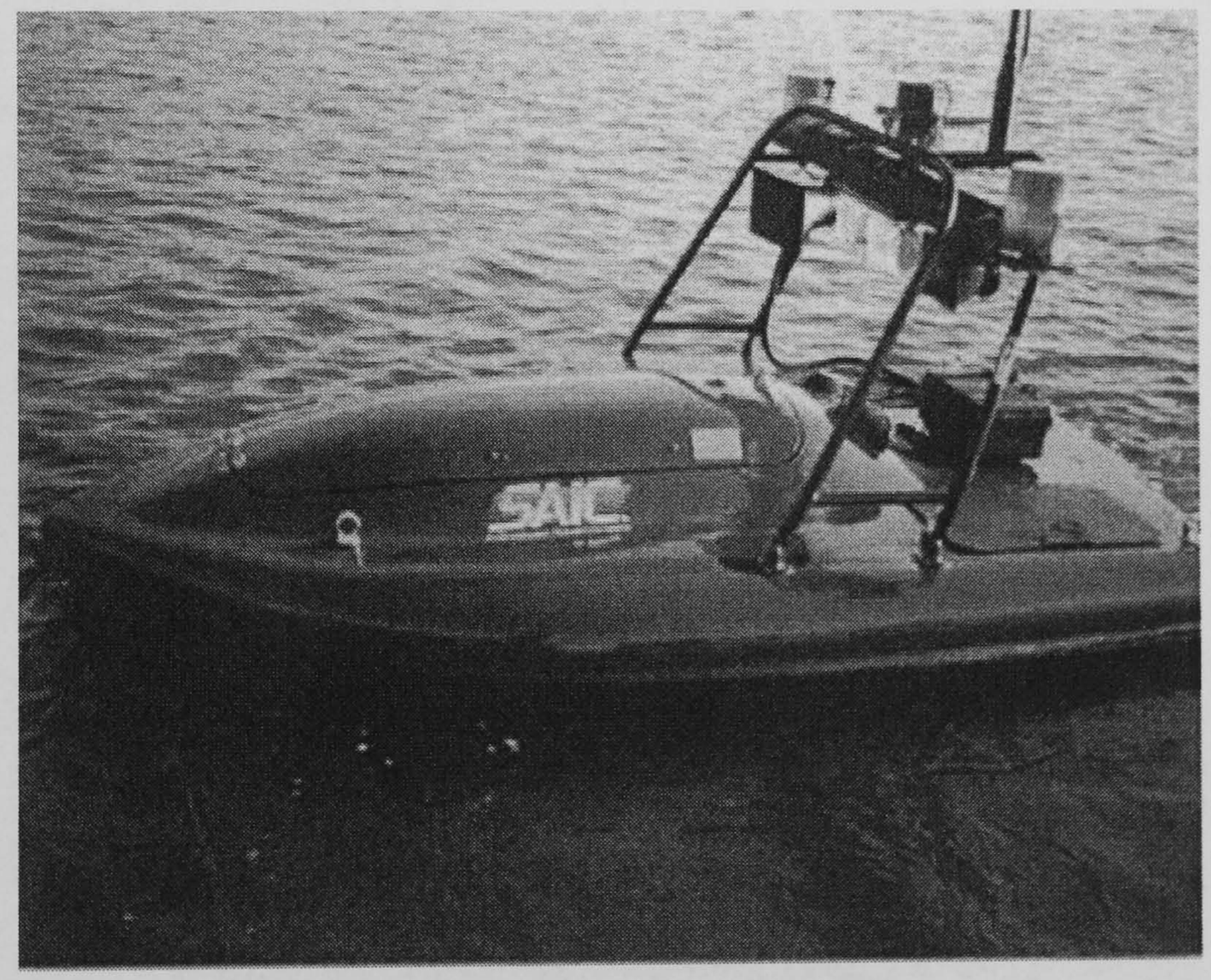

Figure 2.5: *OWL Mark II* vehicle (Hornsby 2005)

The *Owl MK II* is powered by a modified jetski propulsion system which is capable of speeds up to 45 knots. As a military vehicle, the *Owl MK II* is accommodated with several surface and subsurface detection sensors, such as, a side scan sonar, visual sensors, a magnetometer and a bathymetry sensor (Hornsby 2005).

The *Owl MK II* has several outstanding capabilities. It can conduct side scan surveys in 20 m water depths to 12 NMs: the operator can control the USV and receive excellent video information within 10 NMs. The USV is capable of undertaking either day time or night time waterside security missions.

The *Owl MK II* USV has been considered for a role in harbour security and has provided potential solutions for a number of technical issues in an USV area including long range command and control and in theatre launch and recovery.

Spartan

Since 2002, the U.S. Navy has spent $55 million over 6 years to develop a high speed unmanned surface vehicle named *Spartan* which can be operated remotely and autonomously. The *Spartan* shown in Figure 2.6 is a 11 m RHIB integrating with a defence and weapon system onboard. It can conduct a wide array of missions including littoral ASW, mine warfare, torpedo defence and intelligence, surveillance and reconnaissance with an endurance of up to 8 hours (Tiron 2002).

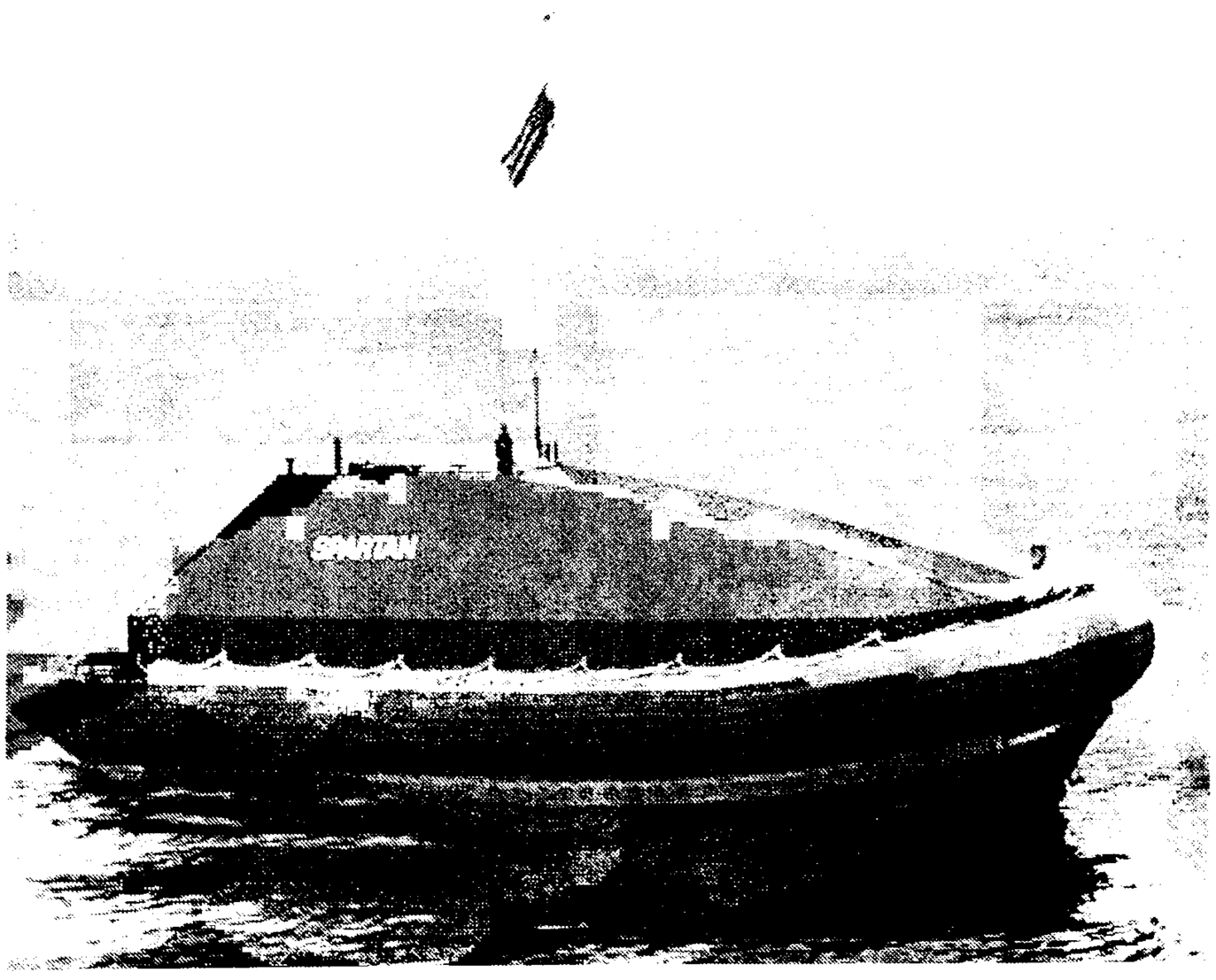

Figure 2.6: *Spartan* USV (Tiron 2002)

The navigation system includes a surface search radar which can be used to detect incoming threats. An onboard side scan sonar conducts bottom-mapping and search for undersea mine threats. The communications system is designed to allow the *Spartan* to act as a node for over-the-horizon communications.

The significant achievement in *Spartan* is the development of modular mission payload which can be simply and rapidly integrated onto the main *Spartan* platform to meet the requirements for the various roles that are contemplated.

The *Spartan* operated successfully during the Iraq war.

Protector

The *Protector* is a 9 m RHIB developed by BAE Systems North America and Rafael Armament Development Authority Ltd., Israel. The *Protector* as shown in Figure 2.7 features a single Diesel engine which drives water jets that propel the boat to speeds of 40 knots. The onboard navigation system includes a radar, a GPS, a INS with gyro and a mounted video camera. This camera allows for day and night operation and has a forward-looking infrared laser range finder capability to detect and track targets in the near vicinity . The *Protector* is armed with a Raphael stabilized mini-Typhoon weapon system and a variety of stabilized cameras. (BAE Systems, North America 2003).

The *Protector* is described as new generation USV which is highly autonomous and linked with a highly effective command and control system from land-based or mother ship stations. The communications unit maintains a constant link between *Protector* and the control station. Jam resistant communication technology is implemented on the *Protector* to allow it to send secured digital video and telemetry to the command centre (point-to-point) through a downlink channel. Command data can be transmitted in an uplink channel, which is maintained even in the most hostile electromagnetic environments.

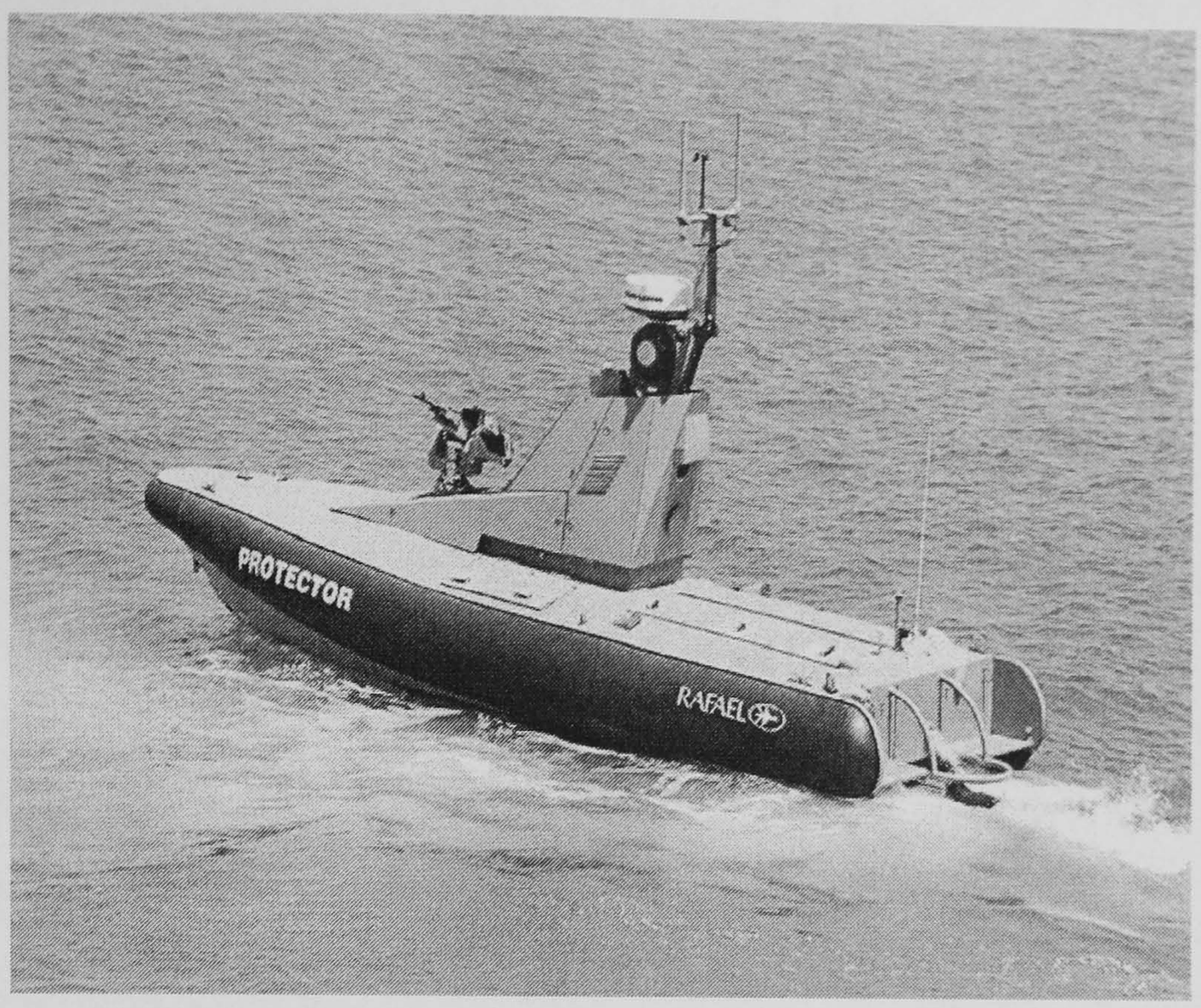

Figure 2.7: *Protector* USV (BAE Systems, North America 2003)

Shallow Water Influence Mine Sweeping (*SWIMS*)

SWIMS system was designed to support MCM operations during the Iraq War in 2003. It is a self-contained system designed to perform high-speed mine sweeping missions using multiple USVs in a shallow water environment. Existing Combat Support Boats (CSBs) operated by the British Army were selected as the vehicle which could be converted into USVs. These USVs are used to tow mine sweeping equipment. Currently, 12 USVs are involved in the *SWIMS* system.

The *SWIMS* control system was accomplished by National Instrument (NI) equipments with a LabView user interface and a custom control console. Ultra High Frequency (UHF) data link is utilised to transmit the onboard sensor information, such as, GPS and compass etc to the main control station.

The *SWIMS* system operates ahead of a main mine hunting system within a 9 km range. It provided protection for the main hunting vehicle and undertook simultaneous sweeping and searching operations. It is highly maneuverable in shallow waters and is capable of

running at speeds of up to 40 knots (Corfield and Young 2006).

Other military USVs

Besides the USVs discussed above, several other military USVs has been developed to meet the requirement of the fast growing USV market.

Seastar and *SSC San Diego* USV

In Figure 2.8, two similar USV design *Seastar* (left) and *SSC San Diego* (right) are presented.

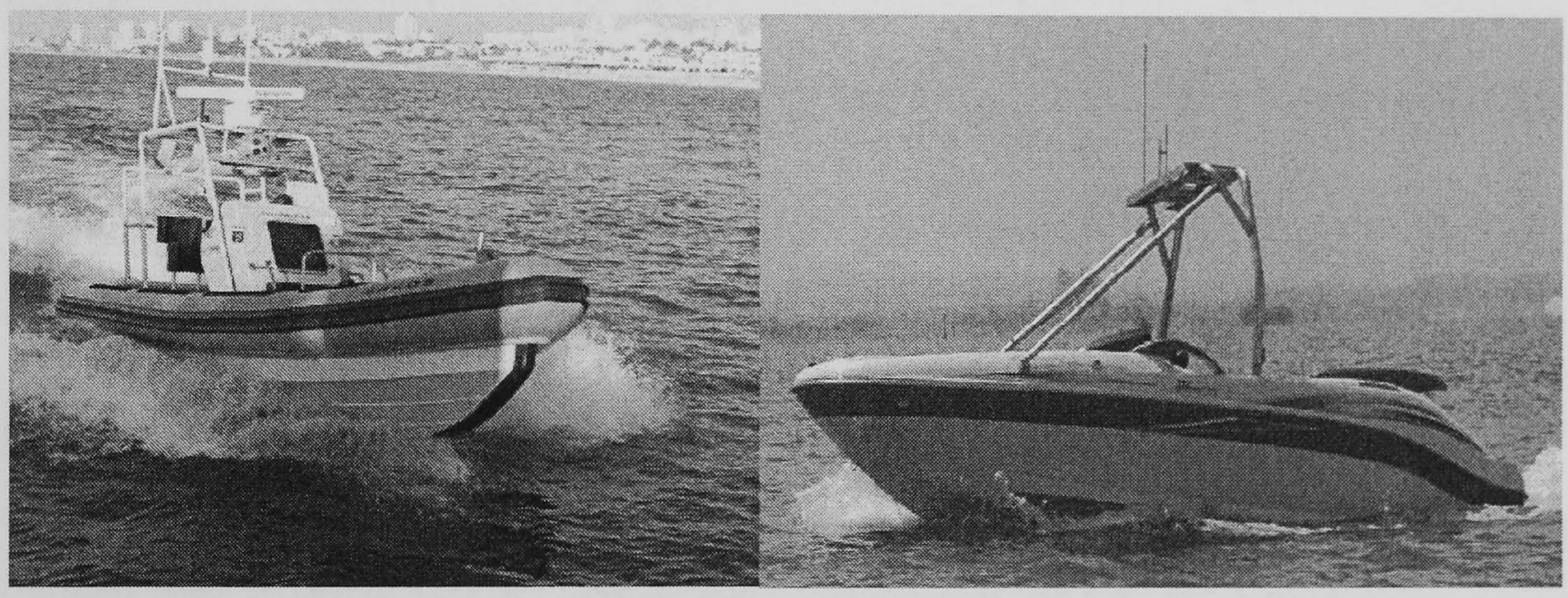

Figure 2.8: *Seastar* (left) (Aeronautics Defense systems Ltd. 2003) and *SSC San Diego* (right) (SPAWAR Systems Center San Diego 2002) USVs

The USA Aeronautics Inc. developed the *Seastar* USV that is a versatile platform for various missions even in hazardous sea conditions. The command and control station can be located on any marine, aerial and ground vehicles.

Whilst the Robotics Group at the US Space and Naval Warfare Systems Center in San Diego have developed an USV called *SSC San Diego*. It is designed as a test-bed for rapid prototyping and testing of new concepts.

The *SSC San Diego* has a Man Portable Robotics System (MPRS), Kalman filter and

waypoint navigation system. The USV can download the waypoint information before a mission, and an operator can stop, pause or resume the mission at any time. In order to provide full autonomy, Collision Avoidance System (CAS) using radar and machine vision technologies are being developed (Ebken *et al.* 2005).

Sea Fox and *Roboski*

The *Sea Fox* is a 16 foot aluminum RHIB manufactured by Northwind Marine Inc., USA. Whereas RoboTek Engineering produced a small size USV called *Roboski* which has a similar style to *Sea Fox*. They are both depicted in Figure 2.9.

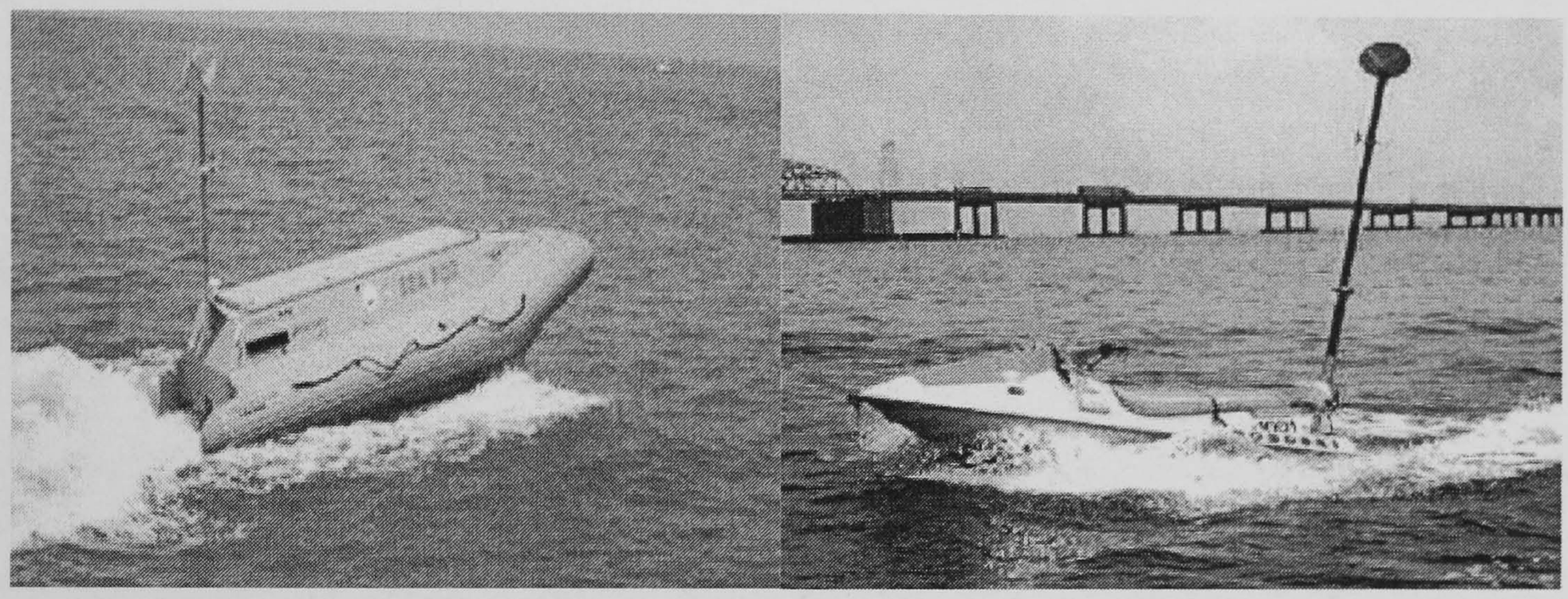

Figure 2.9: *Sea Fox* (left) (Autonomous Flight Systems Laboratory, University of Washington 2005) and *Roboski* (right) (RoboTek Engineering Inc. 2004) USVs

They are designed as ship deployable, high speed low cost expendable small size USVs that contained a mast mounted at the rear of the vehicle. Stabilized cameras and a laptop remote control program are implemented in these USVs.

Stingray and *Basil*

In Figure 2.10, the *Basil* (left) and *Stingray* (right) USVs are shown. They have both adopted a small size mono-hull with a mast carrying a communication aerial.

The *Basil* is a low speed USV that can operate on a long operating time scale. While

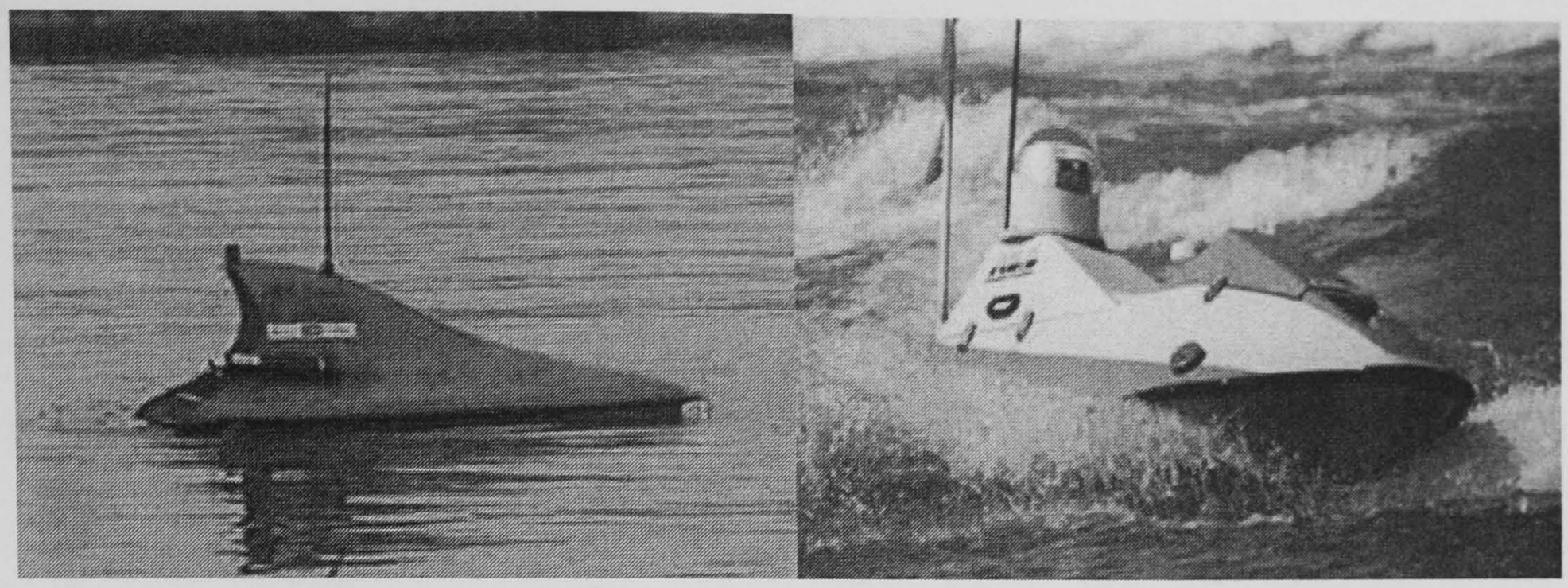

Figure 2.10: *Basil* (left) (Veers and Bertram 2006) and *Stingray* (right) (Elbit Systems 2005) USVs

the *Stingray* is capable of undertaking day or night missions in remote control or with pre-programmed waypoint navigation.

Features

According to the review of current military USVs, the following features can be summarized:

- high speed (up to 45 knots);
- small/medium size of the vehicle, usually in RHIB;
- safe, reliable, simple launch and recovery;
- usually remote operate from the control console;
- precise navigation system including video cameras;
- strong communication capability to extend the range that the USV can operate;
- usually have night mission and stealth capability;
- onboard weapon and sensor systems depending upon the applications.

2.2.2 Academic research applications

Worldwide, academic research groups in engineering and oceanography are becoming more interested in the USV area. As a result, several USVs have been designed and applied in scientific missions.

Measuring Dolphin

Since 1998, USV *Measuring Dolphin* was developed within the German cooperation project *MESSIN*. *Measuring Dolphin* is an unmanned and independently operated catamaran having been designed as a carrier for multiple measuring devices. It can be applied in the field of oceanography, water ecology and hydrology in shallow waters combined with a high precision positioning and navigation system (Majohr *et al.* 2000).

Measuring Dolphin is a Small WAterplane Twin Hull (SWATH) catamaran using a hybrid power supply. An Energy Management System (EMS) was designed to check the power condition. When insufficient power is found, the EMS will switch off the unimportant equipment or reduce the driving speed to guarantee a secure return. A hierarchical structure was designed in order to achieve a fault tolerant performance. A mission can be carried out in either a remote control mode or a fully autonomous mode.

In order to develop a navigation system with high precision, high reliability and high availability, the *Measuring Dolphin* integrates several sensors to collect the navigational data, such as, heading, speed and depth. The most important one is the DGPS. A DGPS receiver incorporates the correctional data via a Very High Frequency (VHF) radio system from its reference station and receives the correctional data from the DGPS reference station via a High Frequency (HF) beacon receiver. A smooth course behaviour is obtained by an electronic compass which supported by a yaw rate gyro, vehicle speed is measured by an

echo sounder speed log. For a simple check of the vehicle's speed condition, an impeller-log and a newly developed electromagnetic log are used. Any anti-collision manoeuvre is based on hydro-acoustic depth sensors which are used to determine exactly the depth of the water and to recognize obstacles ahead regarding their distance and bearing (Majohr and Buch 2006).

Delfim and *Caravela 2000*

Over the past few years, Dynamical Systems and Ocean Robotics (DSOR) Laboratory at Institute for Systems and Robotics (ISR) of the Instituto Superior Técnico (IST) has focused on designing the unmanned marine vehicles and their NGC systems. Development work has led to the construction of the *Delfim* and *Caravela 2000* shown in Figure 2.11 and Figure 2.12 respectively.

Delfim is a small catamaran (3.5 m long and 2.0 m wide) equipped with onboard resident systems for NGC, as well as for mission control. *Delfim* is an electric propelled vehicle

Figure 2.11: *Delfim* vehicle (Dynamical Systems and Ocean Robotics (DSOR) Laboratory 2000)

which can manoeuvre autonomously and perform precise path following while carrying out automatic marine data acquisition and transmission to a remote control centre on a support vessel or on shore (Pascoal *et al.* 2006).

An attitude reference unit, a Doppler Velocity Log (DVL). and a high precision DGPS have been integrated into its navigation system to provide accurate navigational information. The position of the vehicle can be observed from the DGPS with a mobile segment onboard. heading and tilt angles are provided by the attitude reference unit, velocity is obtained by the DVL. The vehicle has a similar wing shaped central structure as *Measuring Dolphin* that carries all acoustic transducers and is lowered during operations at sea.

A new navigation strategy has been reported by Pascoal and Oliveira (2003) which uses simple kinematics relationships. The vehicle's velocity and position can be estimated by implementing multi-rate time-varying complementary filters based on motion sensor data.

Figure 2.12 shows the *Caravela 2000* USV which was designed as a low cost autonomous vehicle which is able to perform a large number of oceanographic missions without any support. It has a 10 m long yacht shaped hull, under the keel a 'torpedo' shaped structure is employed to house the sensors and other equipment. It is a long range autonomous research vessel currently being planned with a range of operation at least 2000 NMs with an average speed of 5 knots and with a duration period of two to three weeks. (Dynamical Systems and Ocean Robotics (DSOR) Laboratory 2000).

Caravela 2000 will operate in either autonomous or remotely controlled mode. To realize the precise navigation, the system includes GPS/DGPS, DVL, gyrocompass, heave, pitch and roll sensors. The sensor data can be sent to land or any sea platform via a remote Radio Frequency (RF)/satellite communication link. This link can also transmit commands to the vehicle in order to re-direct the mission. In case of complete communication link failure. the vessel will adopt a pre-programmed plan to return to a point near its base (Pascoal *et*

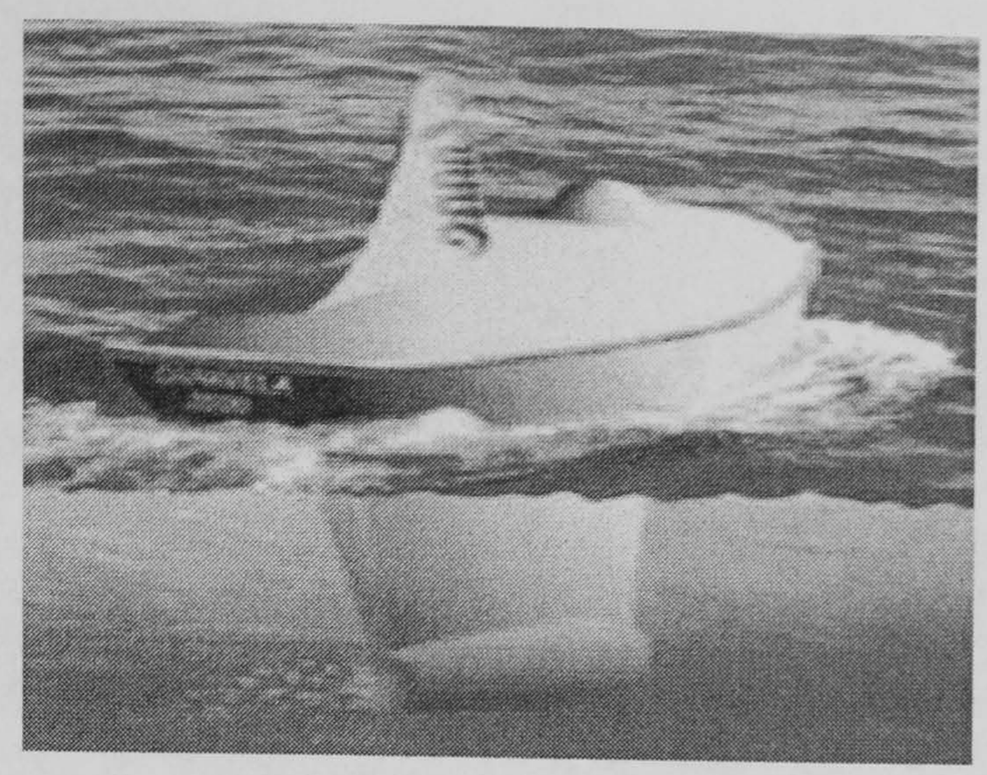

Figure 2.12: *Caravela 2000* vehicle (Dynamical Systems and Ocean Robotics (DSOR) Laboratory 2000)

al. 2006).

SEa Surface Autonomous MOdular unit (*SESAMO*)

SESAMO depicted in Figure 2.13 was developed by Robotlab of Italy and it is an electric propelled autonomous catamaran for data acquisition and sampling for biological, chemical and physical investigations on the air-sea interface. Two propellers are powered by two electrical thrusters and the steering of the vehicle is based on the differential propeller revolution rate (Caccia *et al.* 2005).

The navigation system of the vessel is combined with a GPS, an azimuth gyrotrac which is used to compute the true north given the measured magnetic north and GPS supplied geographic coordinates. A video camera is fitted in the vehicle to supply the real time image of the operating environment and a weather station sensor is utilised to provide wind speed, direction and the air temperature just above the sea surface. Auto-heading and LoS guidance algorithms with a Proportional Derivative (PD) controller have been successfully employed in *SESAMO* (Caccia *et al.* 2005).

SESAMO can operate in fully autonomous, tele-operated and Internet based tele-operated modes. This allows the operator to control and observe the vessel not only from a support

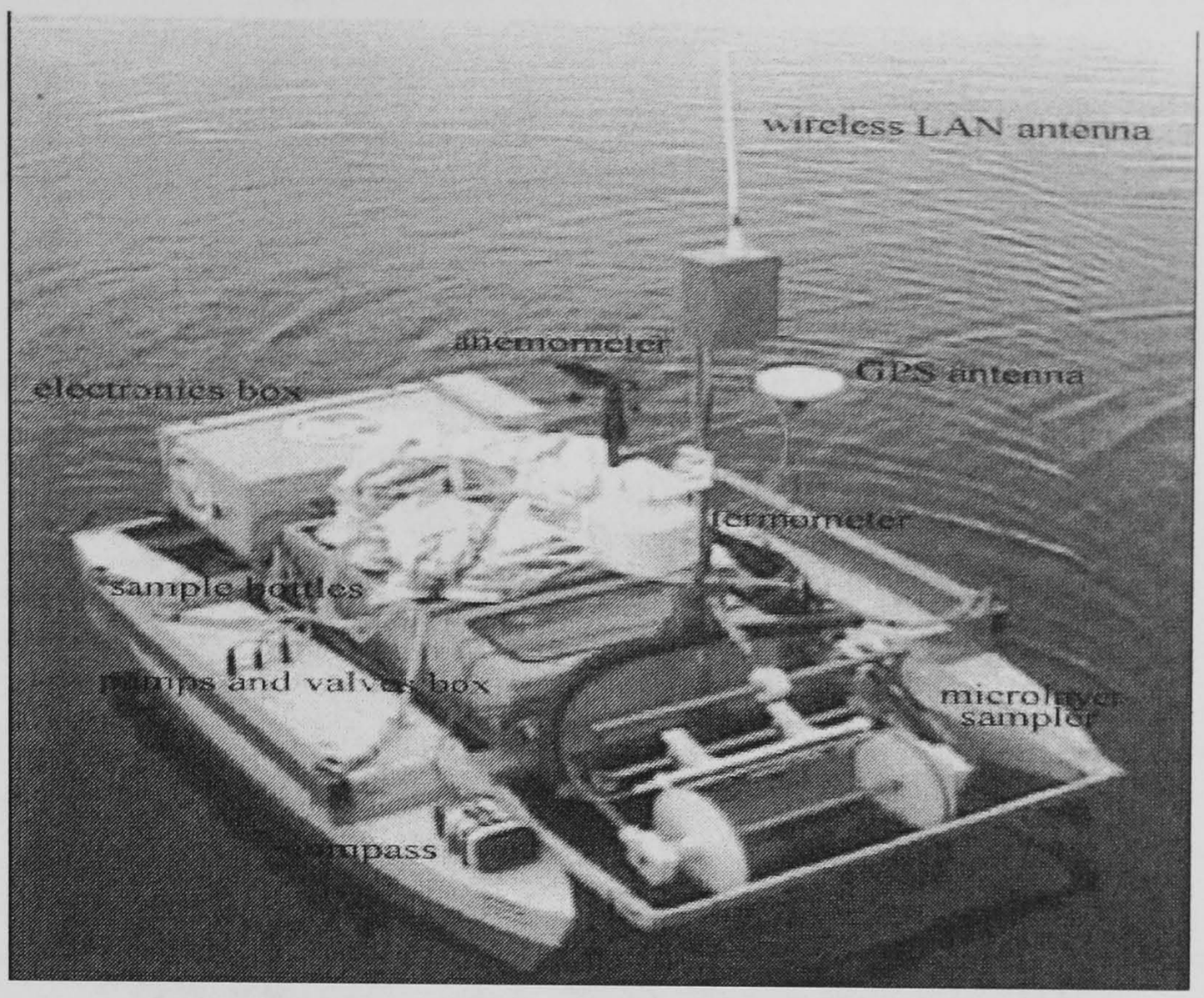

Figure 2.13: SESAMO platform (Caccia *et al.* 2005)

vessel through a radio wireless Local Area Network (LAN) within 550 m range, but also from their laboratories via the Internet.

From *Artemis* to *AutoCat*

Since 1993 the Massachusetts Institute of Technology (MIT) Autonomous Vehicles Laboratory began to develop USVs, *Artemis* being the first craft to be designed. The vehicle is primarily designed to generate bathymetric maps (MIT AUV Lab 2000).

A digital fluxgate compass, a depth sounder and a DGPS are used to provide navigation information. A simple dead reckoning algorithm uses the vehicle's heading and speed to estimate the vehicle's position between GPS update, and each new GPS position fix re-initialize the dead reckoning algorithm. A Kalman filter was implemented to propagate vehicle's speed based on GPS position updates (Vaneck 1997).

Since 1998 a series of mechanical, power and propulsion improvements have been made to the vehicle, the USV being renamed *AutoCat* (shown in Figure 2.14). The changes

enhanced the vehicle's reliability and manoeuvrability (Manlay *et al.* 2000). Now *AutoCat* is fitted with precise navigation systems and a novel instrument named high-frequency sub-bottom profiler. The vehicle cannot only undertake sub-bottom profiler surveys but also operate as a link between AUVs and ships or shore laboratories.

Figure 2.14: *AutoCat* vehicle (MIT AUV Lab 2000)

Features

In academic research applications, USVs are often used as a testbed for intelligent NGC systems, the features of these vehicles include:

- normally in catamaran hulls (high stability and reasonable payload capability);
- medium/low speed, normally around 5 knots;
- low cost;
- operate either in remote or fully autonomous mode;
- onboard intergrated NGC system.

2.2.3 Commercial applications

Following the USV developments in military and academic research, industrial organizations realized the significant growing market in this area and then they began to develop user friendly USVs.

MIMIR

QinetiQ Ltd. in the UK has a wide experience of designing and operating unmanned vehicles. In 2001, QinetiQ began to develop the *MIMIR* system, which uses multiple low cost USVs to accomplish networked mobile control through the land based command centre via wireless communication. The *MIMIR EV1* is one of the USVs in the *MIMIR* system, it was designed to investigate the USV's search and survey capabilities in shallow waters (Corfield and Young 2006).

MIMIR EV1 has a tri-hull design with a dedicated sensor pod that can be lowered through the water column during an operation. It is powered by a 9hp single cylinder Diesel engine and can endure more than 8 hours continuous performance at speeds of 3 to 4 knots. The navigation subsystem uses a DGPS and a fluxgate compass as the primary sensors. A sonar and a video camera are also used to provide real time information. Sonar image data and camera video data can be passed to the operator console in the mobile command centre via commercial telecommunications technology. The *MIMIR* mobile command centre is based on a commercial four wheel drive vehicle which is fitted with the PC-based command segment of the Mission Management System (MMS), data post-processing capabilities, a wireless communications system and commercial data telecommunications systems. System operators monitor and control the vehicle from the command centre (Corfield 2002).

When the *MIMIR EV1* is driven to an operation area over an agreed transit path, then a

pre-programmed automatic survey pattern is implemented to accomplish the survey mission. The vehicle can also halt within a small area to undertake water sampling or other measurements. Upon completion of missions, *MIMIR EV1* can either be reprogrammed with another mission or proceed to a designated nominal recovery point.

Kan-Chan

In order to gather sufficient quality data about global warming and weather pattern changes, *Kan-Chan* shown in Figure 2.15 was designed by the Yamaha Motor Co. to perform a mobile data gathering mission in the Pacific Ocean. It is the world's first unmanned ocean atmosphere observation boat which can collect data in great extensions of the ocean over long periods (700 hours). In order to realize the long duration of operation, *Kan-Chan* is fitted with AC and DC generators powered by a Diesel engine plus a wind turbine generator. The atmospheric observation instruments and water testing instruments are located at the bow and midships respectively (YAMAHA Motor Co., Ltd 2003).

The vehicle navigation system consists of a GPS positioning system, a speed log, a compass, a wind direction and speed gauges. The system receives waypoint information from the control unit, and controls the rudder by comparing the waypoint information with the current position as read by the GPS. The waypoint is always defined as a circle with a radius of 50 m, once the vehicle is within the circular area of the waypoint, the motor will stop running and the vehicle starts to drift. As soon as the vehicle's position outside the waypoint circle, the motor will start automatically and run towards the next waypoint (Enderle *et al.* 2004).

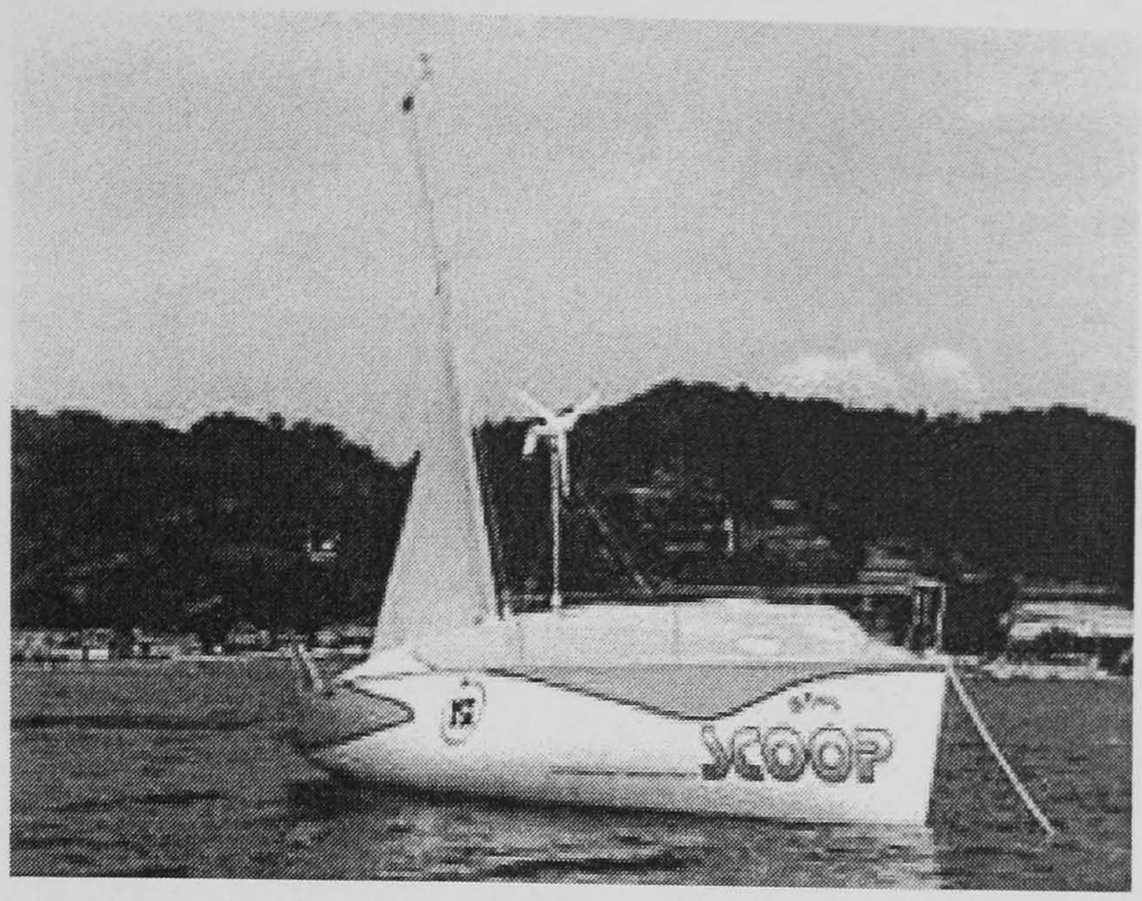

Figure 2.15: *Kan-Chan* USV (YAMAHA Motor Co., Ltd 2003)

Search and Rescue Portable, Air-Launchable (*SARPAL*)

A long established need has existed for searching and rescuing victims in the water in all weather and sea states. ISE has addressed this lack by employing an autonomous rescue vehicle *SARPAL* that will lessen human casualties.

Figure 2.16: *SARPAL* USV (ISE group of companies 2000)

SARPAL was initially developed by the Department of National Defense Canada for the purpose of search and rescue. It is a remotely-operated, air-droppable, Diesel-powered marine vehicle. The *SARPAL* is a RHIB configuring with 2 cylinder Yanmar Diesel which can continuously operate 24 hours. Uniquely the *SARPAL* is launched by a CC-130 aircraft over the crisis site and operated from the aircraft using command, control and live video.

The onboard mission package includes GPS navigation. VHF communication. video and self-propulsion, all of which are remotely operated from the aircraft. Realtime video are transferred to the control console over a single channel from four onboard cameras. The fore cameras are used for searching for victims. and as video feedback for manually steering the vehicle from the aircraft. The aft camera monitors the aft periphery of the vehicle and victims as they embark the vehicle using the recovery ramp. while the interior camera allows for monitoring the condition of the recovered survivors. Also waypoint navigation algorithm is used for defining search patterns or rendezvous points for recovery (ISE group of companies 2000).

Features

In summary commercial USVs have the following common characteristics:

- flexible control modules for the user required missions;
- easy to be reconfigured to meet a user's unique requirements;
- friendly user interface;
- easy maintained;
- usually in remote control.

2.3 USV, AUV and AAV coordinate network applications

Great achievements have been made in the various AUV, USV and AAV projects separately. while recently researchers set the goal of fulfilling coordinated operation of AUV, USV and

AAV in order to establish a fast direct communication link between these autonomous vehicles and undertake a variety of missions in multiple dimensions. Effective employment of these autonomous vehicles can meet a critical need in today's military, academic and commercial applications.

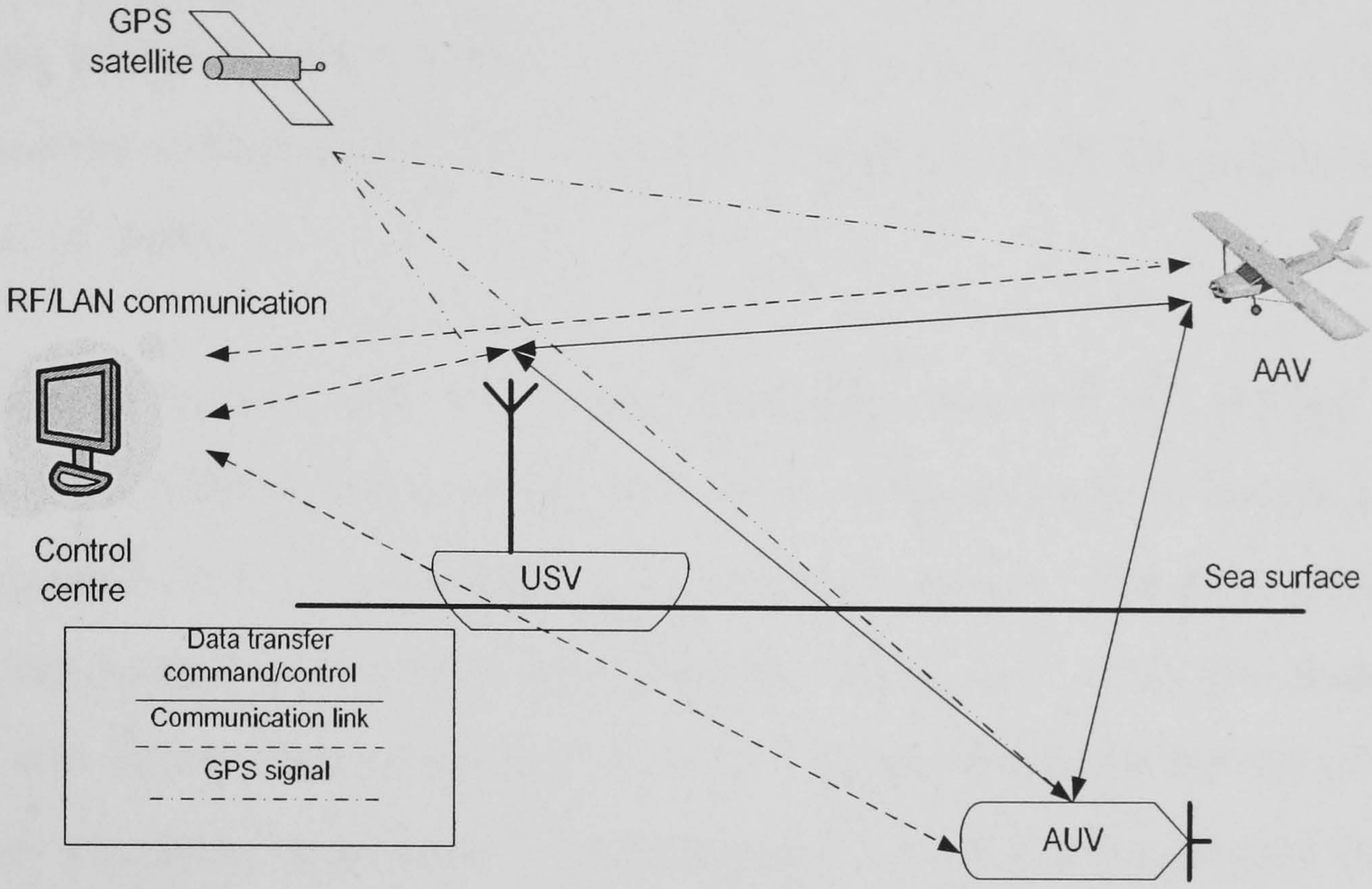

Figure 2.17: Pictorial view of a coordinate operation of AUV, AAV and USV

An obvious limitation to the use of USVs by themselves in the marine environment is the limited field of view of the theatre of operations. For instance, LoS are often obstructed by other vehicles in the water. These shortcomings are readily overcome if the USVs are supported by an AAV that can act as communication relay as well as providing clear view in the sky over the interest area. In a similar manner, an USV can also serve as communication relay for an AUV, in addition the USV can survey in the shallow water where the AUV cannot access. The USVs can reduce the cost of expensive navigation sensors for AUV by acquiring position update information from an USV through a RF uplink system. The remote control console can transmit/receive command or data to the vehicles via a RF/LAN link. The general structure of this coordinated system can be seen from Figure 2.17. The cooperating system of AUV, USV and AAV must be relatively inexpensive, fault tolerant as well as simple to operate.

Autonomous Advanced System Integration for Managing the coordinated operation of robotic Ocean Vehicles (*ASIMOV*)

In DSOR, AUV *Infante*and USV *Delfim* (discussed in Section 2.2.2) demonstrated sound autonomous capabilities. In order to expand the operating coordination. the *ASIMOV* project was proposed with the aim to move individual operation to more autonomous group operation, whilst ensuring a fast reliable communication link between the two vehicles (Pascoal *et al.* 2000).

As discussed in Section 2.2.2, the *Delfim* is equipped with a DGPS receiver, an Ultra Short BaseLine (USBL) unit , a radio link, and a high data rate communications link with the *Infante* AUV that is optimized for a vertical channel. The *Infante*'s navigation system is integrated by an attitude reference unit, a DVL and a set of free floating buoys equipped with DGPS. These buoys receive acoustic emissions from the *Infante* and compute the *Infante*'s position underwater. The computed *Infante* position is then transmitted to the *Delfim*. Thus, by properly manoeuvring the *Delfim* to remain in the vicinity of a vertical line along the *Infante*, a fast communications channel can be established to transmit navigational data from the USV to the AUV, and scientific data from the AUV to the USV. A space stabilized sonar with associate transducer elements is installed to realize collision avoidance and bubble detection (Dynamical Systems and Ocean Robotics (DSOR) Laboratory 2000).

Mapping of Marine Habitats of the Azores using Robotic Ocean Vehicle (*MAROV*)

The University of the Azores developed a similar project as *ASIMOV*, called *MAROV*. The key scientific contribution of this project is to generate a set of detailed maps in the Azores with the objective of deriving guidelines for EU habitats directive management in the future (The University of Azores 2001).

Autonomous Ocean Sampling Network (*AOSN*)

AOSN was designed by the MIT AUV laboratory, and one of the important results was the development of acoustic modems for sub-sea communication with AUVs. Utilizing GPS navigation and RF/satellite communications the surface vehicles in such a network will act as a link to the underwater vehicles and allow the entire system to be monitored or controlled from ship or shore stations (MIT AUV Lab 2000).

FENRIR

The *FENRIR* project developed by the QinetiQ Ltd. utilised a set of small USVs which focused on contributing to the network enabled operation in a broad range of roles and scenarios, particularly in warfare (Corfield and Young 2006).

AAV

A number of AAVs, such as Eagle Eye from USCG have achieved significant performances in completing various missions over the sky. While, at present they have not been successfully applied in cooperation with AUVs and USVs. It believed to be a essential and crucial feature for undertaking multi-demission missions in the future.

2.4 Concluding remarks

In this chapter, autonomous navigation systems and main types of autonomous navigation methods have been reviewed. Also a survey has been conducted for a number of on-going USV projects. The features of these USVs are compared in Appendix B Table B.1.

For safe operation, a hierarchical structure as shown in Figure 2.18 is often adopted by most of the on-going USVs . It is normally be divided into two levels: the lower level includes steering, engine control and payload operation; and the higher level includes NGC

system. reactive planning and tactical planning.

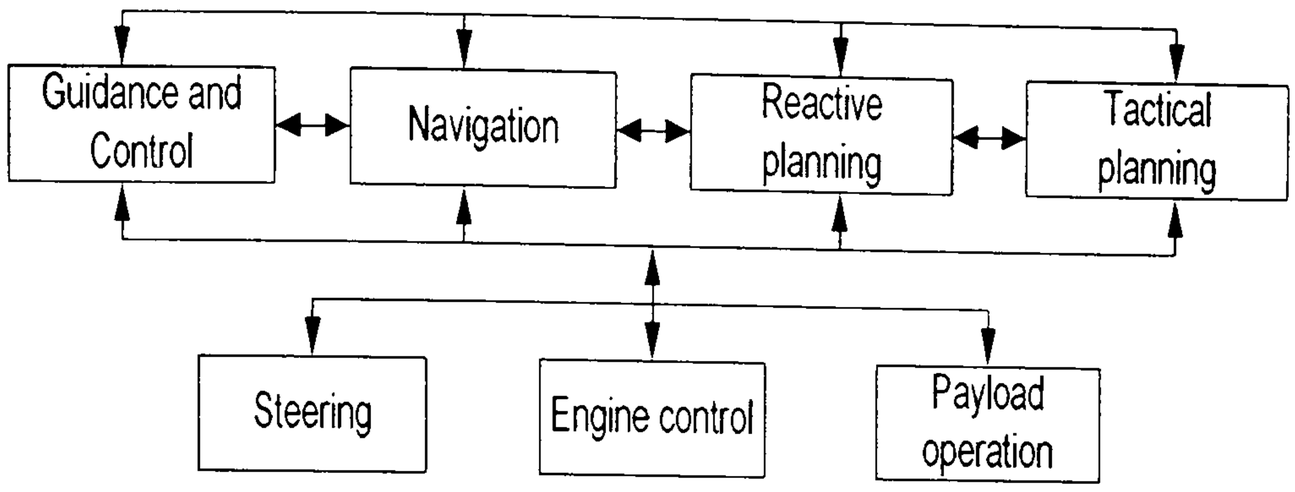

Figure 2.18: USV operation hierarchical structure

The lower level is designed to support and supply data for the higher level, whilst the higher level focuses on manoeuvring the vehicle towards the target and making reactive decision when the vehicle experiencing onboard faults or environmental change. Once the higher level failed in operation, the vehicle can guarantee a safe return to the base via remote control.

USVs will play increasing roles in the future, so the improvements in the autonomous capabilities are crucial to their future development. Of particular importance is the ability of these systems to adapt intelligently in sensor fault situations. As the motion sensors play a vital role in the vehicle, it is inevitable that the sensors will experience faults, and their onboard sensing systems should indicate such changes. The onboard systems must be capable of recognizing the changes and adapting the navigation strategy accordingly without the human interventions.

From the review, it has been shown that multi-sensor navigation systems are successfully employed by most current USVs. USV guidance systems usually use heading and waypoint based guidance algorithms which has been successfully applied on AUVs (Naeem *et al.* 2004). According to the different purpose of the vehicles, different navigation sensors are combined to realize robust and accurate navigation. For a high precision positioning and navigation system, GPS/DGPS is normally employed supplemented by compass, motion and speed sensors. For a long range data transformation vessel, effective RF/wireless LAN

or satellite communication link are utilised. For high speed military USVs, side scan sonar and visual sensors are necessary. High resolution video cameras are usually used to allow remote control to take place.

USVs normally operate in open water with little environment knowledge, therefore the risk of collision with other vessels or obstructions could be high and the consequences is serious. Most of the current USVs employ onboard video cameras to monitor the traffic on the water, the operate control console will send the USV appropriate steering command while collision is detected.

Research has focused on the design of autonomous CAS during the last two decades (Tan *et al.* 2004). High resolution visual, infrared, sonar or radar sensors are implemented to detect the collision in advance. Consequently, the CAS will replan the mission in order to avoid obstructions. At present, CASs have been successfully applied in AUVs, nevertheless, as the expensive sensors are needed currently there are only a few USVs that utilise CASs.

Whilst Section 2.3 briefly introduces the unmanned vehicle network operations, It is considered there is an increasing need for onboard autonomy that can facilitate the employment of multiple cooperative unmanned vehicles. In the near and medium term, it is likely that enhanced performances and benefits will arise from coordinated operation unmanned vehicles.

A comprehensive survey has been conducted in this chapter. The next chapter elaborates on the hardware and software development of the *Springer* including the design of a user interface.

Chapter 3

THE *SPRINGER* UNMANNED SURFACE VEHICLE

Springer is being developed as an autonomous catamaran in order to conduct environmental and geographical surveys in shallow waters. An equally important secondary role envisaged for *Springer* is as a platform for research and student to test their own onboard systems. Therefore user-friendly interfaces, effective Data AcQuisition (DAQ) systems as well as easy maintained hardware are highlighted in this chapter. Also details regarding the onboard electrical components, navigation sensors, controller as well as an environmental sensor are given.

3.1 *Springer* hardware and sensor suite

3.1.1 Hardware setup

The *Springer* USV was designed as a Medium WAterplane Twin Hull (MWATH) vessel which is versatile in terms of mission profile and payload. The catamaran type of the hull ensures high stability and a reasonable payload capability. It is approximately 4 m long and 2.3 m wide with a displacement of 0.6 tonnes. Each hull is divided into three watertight compartments. The NGC system is carried in two watertight Peli cases and secured in a bay area between the crossbeams. This facilitates the quick substitution of systems on shore or at sea. The batteries which are used to provide the power for the propulsion system and onboard electronics are carried within the hulls and are accessed by a watertight hatch. In order to prevent any catastrophe resulting from an ingress of water, leak sensors are utilised within the motor housings. If a breach is detected the onboard computer immediately issues a warning to the user and/or stops the motors in order to minimize damage to the onboard electronics (Naeem *et al.* 2006).

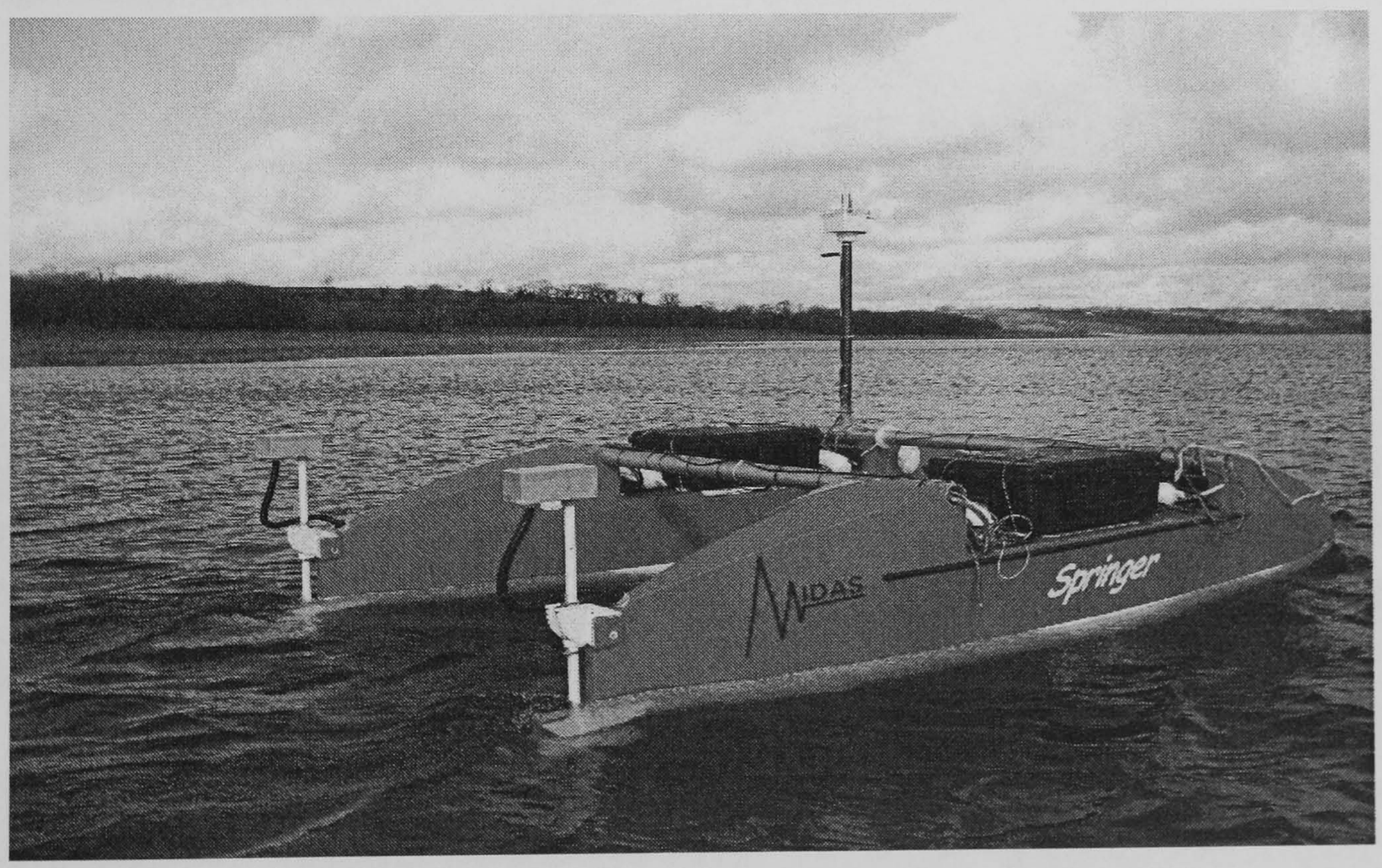

Figure 3.1: The *Springer*

A mast is installed to carry the GPS and wireless antennas. The wireless antenna is used as a means of communication between the vessel and its user and is intended to be utilized for remote monitoring purpose, intervention in the case of erratic behaviour and to alter the mission parameters. The *Springer* is shown in Figure 3.1 and the arrangement inside hulls is depicted in Figure 3.2. Whilst, the Peli case layouts are presented in Figure 3.3.

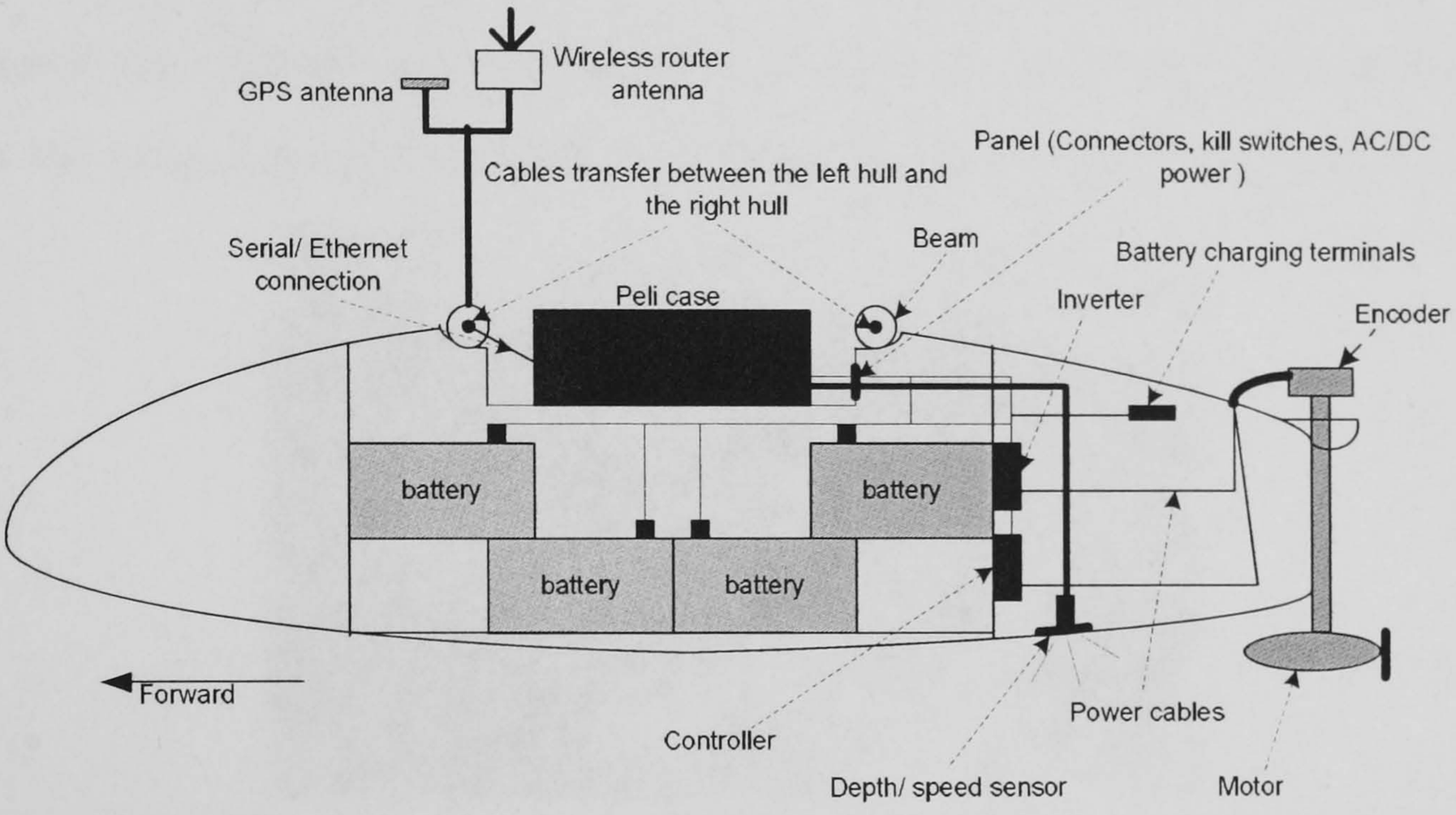

Figure 3.2: Side view of the *Springer*

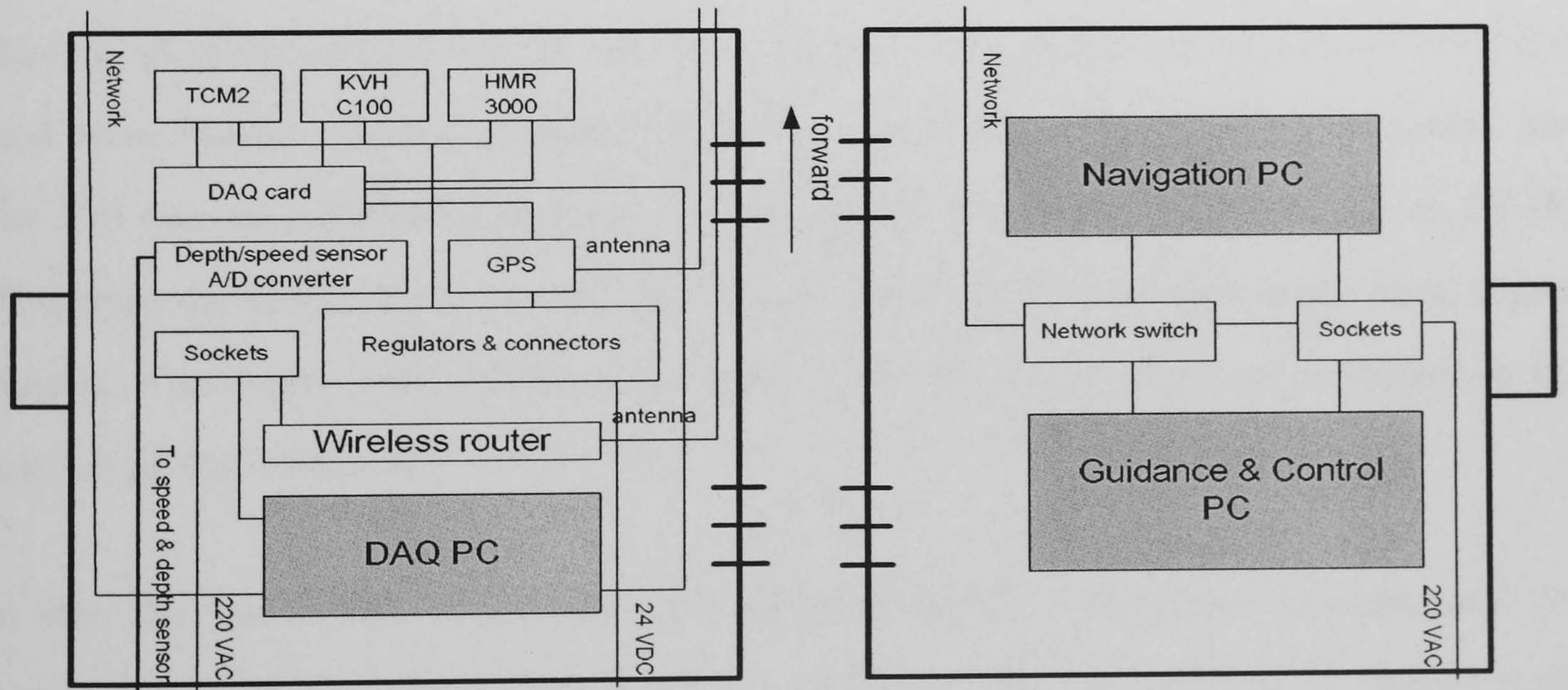

Figure 3.3: Peli case layouts

The *Springer* propulsion system consists of two propellers powered by a set of $24V$ $74lbs$ Minn Kota Riptide transom mounted saltwater trolling motors. Steering of the vessel is

based on differential propeller revolution rates.

In order to maintain the temperature inside the Peli cases, an effective but economical cooling system based on heat sinks were installed as depicted in Figure 3.4. This is vital for the onboard sensors otherwise the heat generated by the onboard computers gradually builds up to a level which could go well outside the operating temperature of the sensors. An experiment was carried out with and without the heat sinks in the Peli cases and it was found that the heat sinks facilitated the regulation of temperature within the cases.

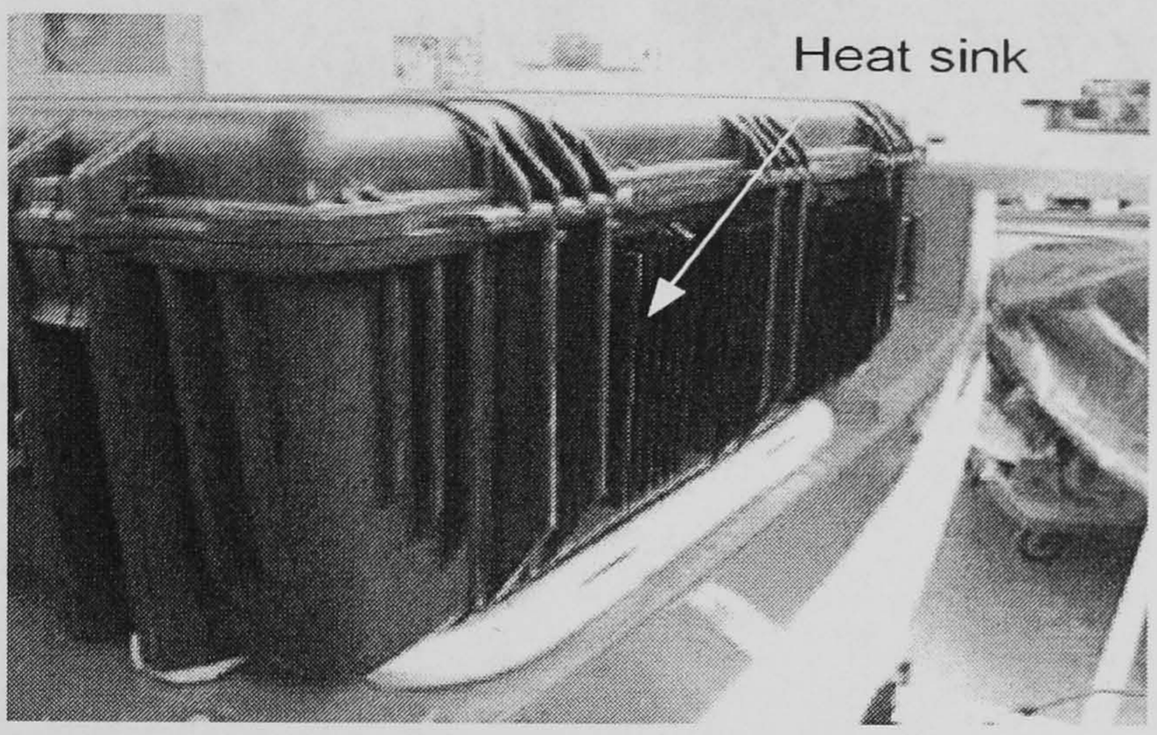

Figure 3.4: Cooling system based on heat sinks is installed to regulate the temperature within the Peli cases

Almost all of the sensors are placed within the Peli cases with the exception of the depth and speed sensors which are located at the bottom of the hulls. They are connected into the Peli case via a E85001 interface box (Raymarine, Ltd. 2001*a*, Raymarine, Ltd. 2001*b*). Therefore speed and depth sensors' SEATALK output can be translated into serial digital output. The depth sensor is shown in Figure 3.5 whilst the speed sensor is located at the bottom of the other hull.

Within the rear section of the hulls, the motor controller, radio control systems and AC power source for the onboard computers are located. These are mounted on custom made plates which are simple to install and replace as depicted in Figure 3.6.

The link from the onboard electronics to the Peli cases is created through front panels, shown in Figure 3.7 which are especially designed to accommodate various connectors, cable

Figure 3.5: Depth sensor at the bottom of the hull

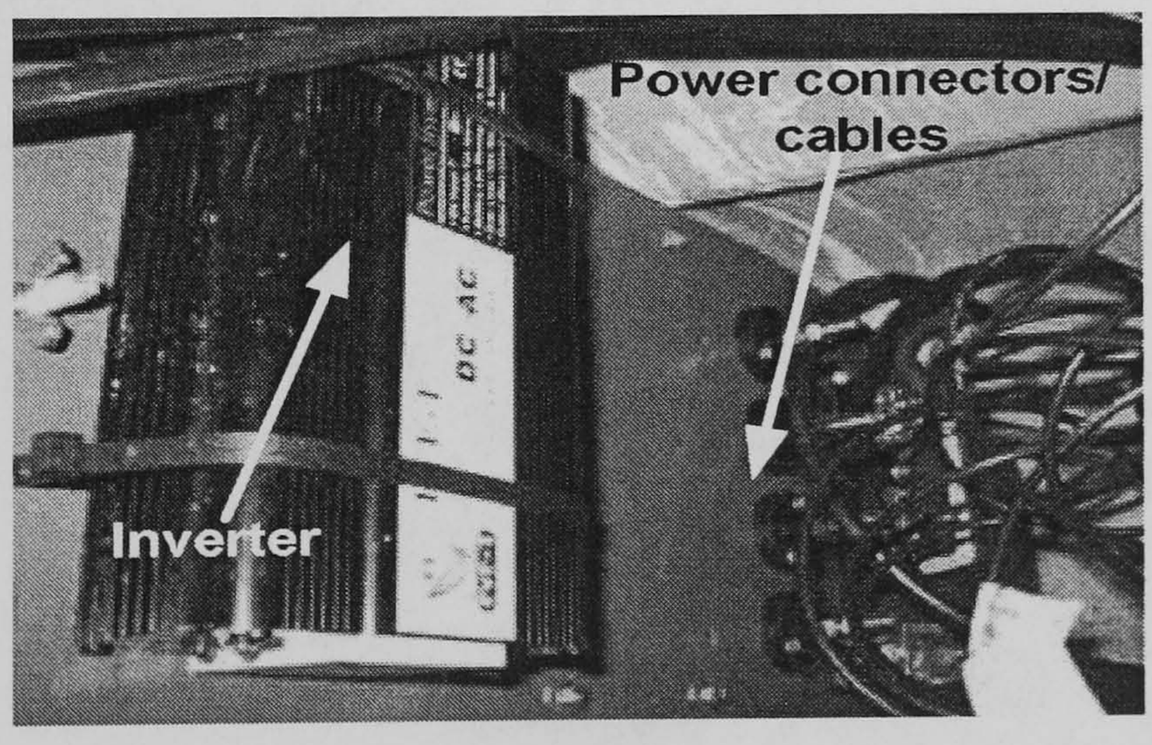

Figure 3.6: AC power source and other components are installed on a custom-made plate placed within the rear section of each hull

glands, isolators and emergency kill switches. The purpose of the isolators is to separate the batteries terminals from the electronics circuitry whilst being recharged. Whereas the emergency kill switches are installed on both panels and are manually operated.

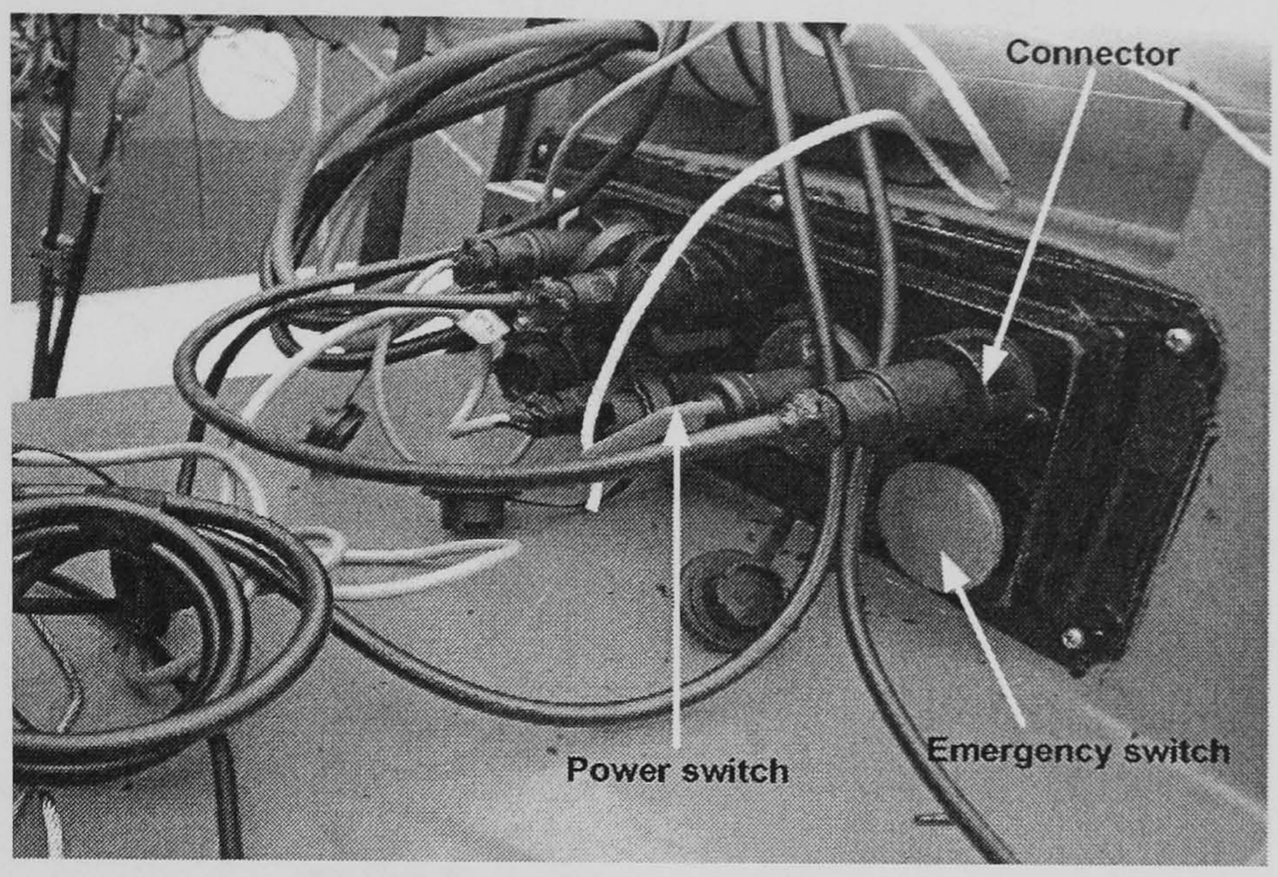

Figure 3.7: One of the front panels showing the connectors, power switch and an emergency switch

3.1.2 Navigation sensor suite

In *Springer*, the integrated sensor suite combines a GPS, three different types of compass, a speed log and a depth sensor. All of these sensors are interfaced to a PC via a NI-PCI 8430/8 (RS232) serial connector. Each of the sensors can output NMEA's 0183 standard sentences. The navigation sensor suite is shown in a block diagram form in Figure 3.8. The specifications of three compasses are summarized in Table 3.1.

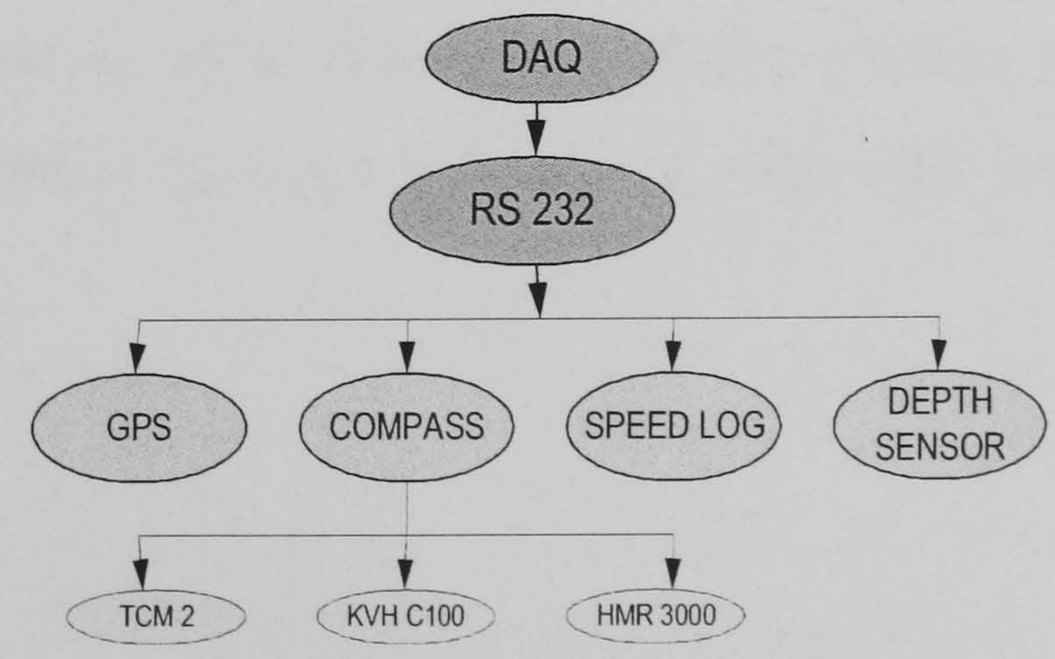

Figure 3.8: *Springer* sensor suite

Table 3.1: Specifications of each compass

	TCM2	HMR 3000	KVH C100
Dimension (mm)	73.5x50.8x32.75	114.0x46.0x28.0	74.9x30.5x25.0
Weight (oz)	1.6	0.75	2.25
Baudrate	300-38400	300-9600	1200-38400
Supply Voltage (VDc)	+5	+12	+5
Current (mA)	15-20	< 40	35
Frequency (Hz)	≈ 10	≈ 10	≈ 10
Temperature (C^o)	-20 - 70	-40 - 65	-20 - 70
Tilt range (degree)	± 50	± 80	± 40
Output	Digital NMEA 0183 /Analogue	Digital NMEA 0183 /Analogue	Digital NMEA0183 /Analogue

Three different compasses, TCM2, KVH C100 and HMR 3000, are employed in the navigation system of the *Springer*. TCM2 compass are based on the magneto-inductive effect. It combines a two axis inclinometer to measure the tilt and roll. (PNI, Co. 2004).

KVH C100 is a flux-gate compass which offers modules incorporating both rate gyros that compensate for errors from acceleration, as well as inclinometers that provide accurate readings of heading, pitch, and roll (KVH Industries, Inc. 2004).

HMR 3000 use AMR effect, it includes three perpendicular sensors and a fluidic tilt sensor to provide a tilt-compensated heading (Honeywell International, Inc. 2004).

The TCM2 compass has simple design with low operating power, however it is very sensitive to the electrical and environmental disturbances. The flux-gate compass KVH C100 can output accurate heading while it has more power consumption. Among these three compasses, the HMR 3000 is the most accurate compass with disturbance resistant capability.

Sensor strings

All the sensors data strings output in a specified form. The strings normally include the

string head, main body of the string as well as check sum at the end. The details of the main parameters of the strings are introduce in Appendix C.

3.1.3 Controller

To control the speed of the propulsion motors and hence the speed of the vessel, a two channel RoboteQ's AX2850 is installed in the vehicle. The AX2850 is a highly configurable, microcomputer-based, dual channel digital speed or position controller with built-in high power drivers. The controller is designed to interface directly to high power DC motors in computer controlled or remote controlled mobile robotics and automated vehicle operations. The AX2850 controller can accept speed or position commands in a variety of ways such as pulse-width based control from a standard radio control receiver, analogue voltage commands, or RS-232 commands from a microcontroller or wireless modem. For *Springer*, the commands to the controller are sent using the serial port communication from the onboard guidance and control PC (Naeem *et al.* 2006).

The controller's two channels can be operated independently or can be combined to set the forward/reverse direction and steering of the vehicle by coordinating the motion on each side of the vehicle. In the speed control mode, the AX2850 can operate in open loop or closed loop. In closed loop operation, actual speed measurements from tachometers or optical encoders are used to verify that the motor is rotating at the desired speed and direction and to adjust the power to the motors accordingly (Roboteq 2005).

3.1.4 Environmental monitoring sensor

The primary purpose of *Springer* is to undertake pollutant tracking and to carry out environmental and hydrographic surveys. Hence the need for an environmental monitoring

unit is of paramount importance. A YSI 6600 environmental monitoring system was thus procured which can be installed in a foil suspended between the hulls. The YSI 6600 is a multi-parameter, water quality measurement and data collection system. It is mainly intended for use in research, assessment and regulatory compliance applications. It consists of a sonde which is a torpedo-shaped water quality monitoring device that is placed in the water to gather water quality data. The YSI 6600 sonde has multiple probes where each probe has one or more sensors that read water quality data. The specifications of the YSI 6600 sonde is provided in Table 3.2 below. This device can operate in fresh, sea or polluted water up to a depth of 200 m. A 384 kilobytes onboard memory can store approximately 150,000 individual parameter readings. A computer interface using RS-232 can also be established which allows importing data directly into a digital computer (YSI 2005).

Table 3.2: The YSI 6600 environmental monitoring unit specifications

	YSI 6600 Sonde
Available Sensors	Temperature, conductivity, dissolved oxygen, pH, ORP, Ammonium nitrate, chloride, depth (shallow, medium, deep, shallow vented), turbidity, chlorophyll and rhodamine WT.
Weight (kg)	3.18
Operating Temperature (C^o)	-5-45
Operating Depth (m)	0 - 200
Interface	RS-232, SDI-12
Power	8 C-size alkaline batteries or external 12VDC
Battery Life	Approximately 90 days at 20 C^o at 15 minute logging intervals

Whilst this sensor suite is yet to be integrated into the *Springer* USV, it has included for information and completion.

3.1.5 Other hardware

Besides all the measurement sensors, the *Springer* is equipped with three onboard PCs running Windows XP. They are contained in the two Peli cases with an serial/ethernet link

connecting them together. These machines can be termed as DAQ PC, navigation PC and the control PC. The DAQ PC runs LabView whilst the navigation and control PCs use Matlab software.

The DAQ PC acquires all the data of the sensors and transmits them over the serial/ethernet cable to the navigation and control PCs by concatenating the desired data in one string. The transmit rate from the DAQ PC is $5Hz$, the actual sampling rate can be specified by the user to tune the navigation and controller parameters. The navigation PC provides estimates of the states of the vehicle by combining data using a MSDF technique. The controller PC issues commands directly to the speed controller which produces a differential thrust (if needed) in order to steer the vehicle on the desired course.

3.2 *Springer* user interface

A user interface is created in DAQ PC to monitor sensor readings and to alter the mission parameters if required. This user interface is accessible on a remote laptop through the wireless connection. A schematic diagram is shown in Figure 3.9.

There are three main blocks in the user interface. The first block is the DAQ system with data logging capability, this block is an essential requirement for the user interface. The second block is for pre-processing, whilst the third block is for data transmitting/receiving to/from NGC PC.

3.2.1 DAQ system

In a multiple sensor system, the DAQ program becomes the crucial issue. The *Springer* gathers data in parallel from several sensors via a NI DAQ card which contains 8 serial

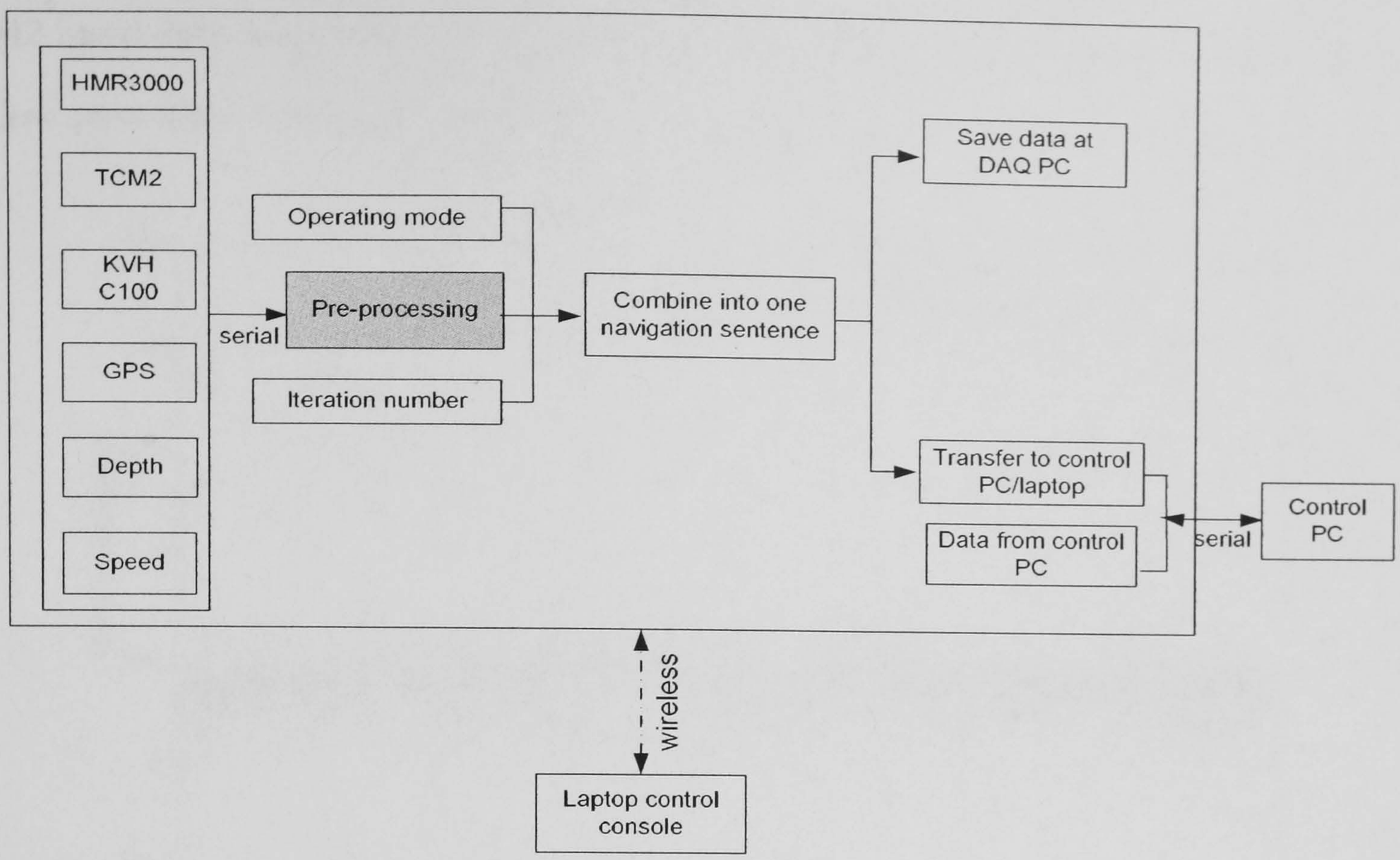

Figure 3.9: *Springer* user interface structure diagram

ports. The sensor data is then logged separately as text files on the DAQ PC. The Labview program receives the data from the compasses at $5Hz$, whilst the GPS and depth/speed sensors are running at $1Hz$. Therefore the DAQ program will repeat the previous GPS and depth/speed data until a new measurement is available. Besides the normal data acquisition, the DAQ system will continuously check the sentence head and specified characters in the sensor strings. If the sensor gives a wrong output the previously sentence will be used to replace the wrong sentence.

3.2.2 Sensor raw data pre-processing

As discussed in Section 2.1.6, the TCM2 compass use the magneto-inductive effect technique, this type of compass is very sensitive to electrical disturbances. Therefore, the TCM2 output is a noisy measurement when operating inside the Peli case where several electrical connectors/equipment are running. A simple low pass filter was designed to minimize these disturbances. In order to test the performance of this low pass filter, raw TCM2 data and

TCM2 fused data were collected while the vehicle was still. In Figure 3.10, the result shows the low pass filter effectively reduced the disturbances.

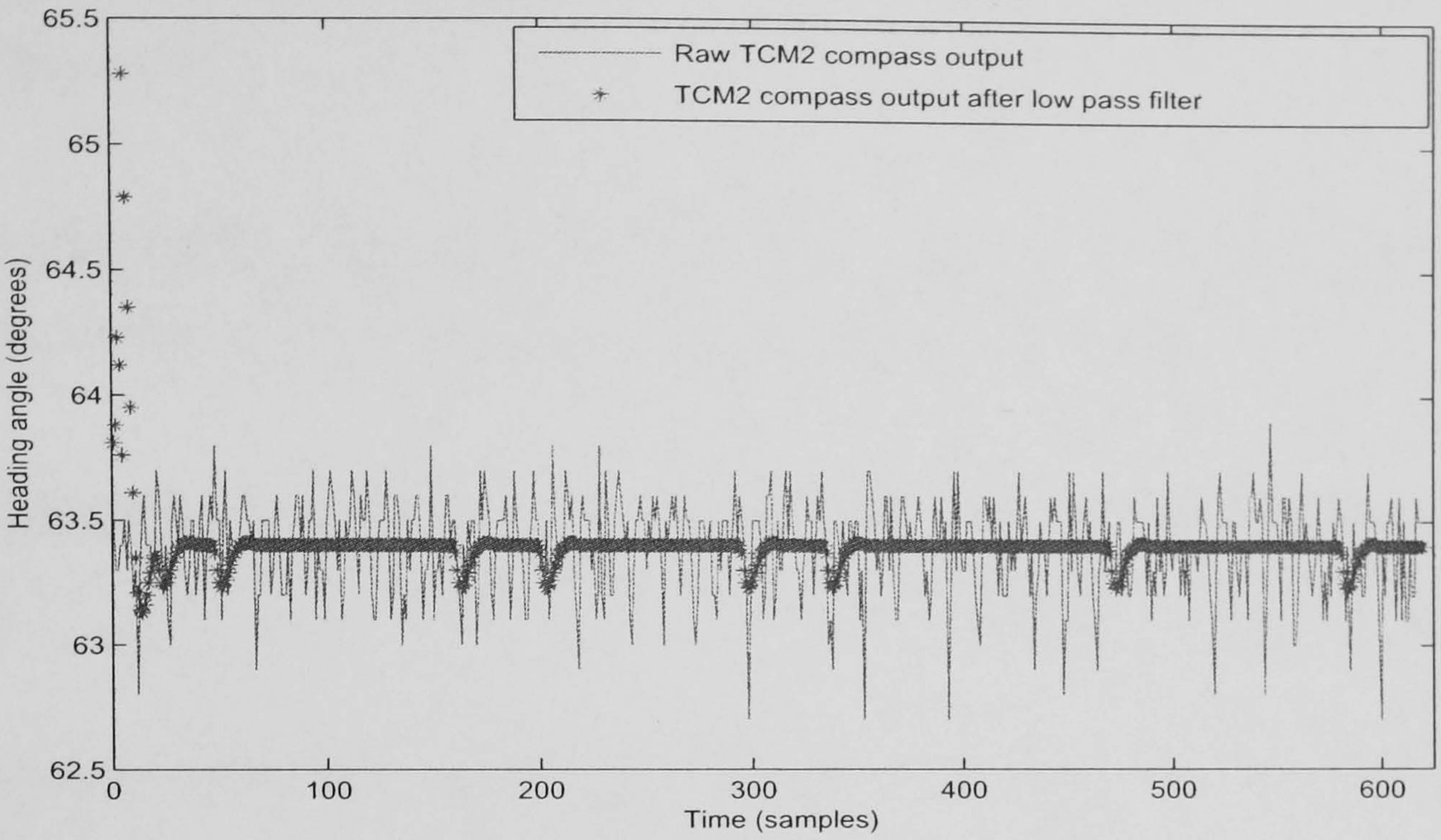

Figure 3.10: TCM2 output with low pass filter

In order to reduce the transmitting sentence length, the sentence head and check sum are reduced to a simple character. For instance, the 'GPRMC' is replaced by 'G'.

3.2.3 Data transmitting/receiving

When the sensor data has been pre-processed, the information from the sensor will be combined into one transmitting sentence. This sentence will be sent to the NGC PC immediately in the following form.

rX & HMR3000 data& TCM2 data & KVH C100 data & GPS data & depth/speed data & desired heading angle & navigation parameter & MPC parameter & LQG parameter & file name indicator & counter &)

rX is operating mode prefix which will be used to call the different program in NGC PC.

For instance, 'r0' is used when the vehicle runs out of space or the data collected is assumed to be sufficient enough for further analysis. 'r1' is used when the control system wishes change the heading. Currently, 15 run types have been designed. the details of which are given in Chapter 7.

desired heading angle, navigation parameter, MPC parameter and LQG parameter are used to tune the navigation and control program parameters by the user,

file name indicator is used to save the data in different files, otherwise the data will be rewritten,

counter is use to record the iteration number of the program,

) is the checksum of this sentence,

& is used to separate different data.

The user interface program can also receive the data from NGC PC which allow the user to observe the control program. Therefore the user can stop the vehicle if an error is received from the NGC PC.

3.3 Concluding remarks

This chapter has detailed the hardware, sensors and user interface required to automate the *Springer* USV. The hardware has been designed in order to allow for easy access to the various systems on shore or in the water. In addition the electrical propulsion system eradicates any Diesel pollution.

The user interface is aimed to provide a convenient interaction tool for users to observe

and modify the NGC program.

Having given a detailed description of *Springer*, the next chapter will start to discuss the sensor modelling process.

Chapter 4

SENSOR MODELLING

System modelling is one of the most important issues for a multiple sensor navigation system. A good model should be simple enough to be implementable, whilst, at the same time, still represent the physical situation with a reasonable degree of accuracy.

There are mainly two categories of modelling methods: first principle and System Identification (SI) (Aris 1995). First principle methods implement a solution to the physical governing equations that expresses the relevant dynamics of the plant (Gershenfeld 1998). Whereas with SI data is collected through experimentation and which then correlated with a suitable mathematical expression that representing the plant dynamics (Ljung 1999). The first principle approach offers a significant advantage in that it enables early testing of a system and a thorough exploration of design options. The SI approach, however, offers confidence in the accuracy of the model, and possibly provides a more efficient model building process.

This Chapter describes the mathematical models employed in the computer simulation studies herein in order to acquire deeper insights and to evaluate the suitability of the proposed algorithms in MSDF.

4.1 GPS modelling

Assume a GPS receiver is mounted at a moving vehicle. therefore the state equation for the position and velocity of the vehicle are approximately:

$$x(t+\Delta t) = x(t) + \dot{x}(t)\Delta t + \frac{1}{2}a(t)(\Delta t)^2$$
$$\dot{x}(t+\Delta t) = \dot{x}(t) + a(t)\Delta t \tag{4.1}$$

As the acceleration is an unknown parameter, it can be treated as a random disturbance.

$$a(t) \sim N(0, \sigma_a^2) \tag{4.2}$$

The measurement of the GPS observer can be expressed as Equation 4.3

$$z(t+\Delta t) = x(t+\Delta t) + \nu(t+\Delta t) \tag{4.3}$$

where

$$\nu(t) \sim N(0, \sigma_\nu^2) \tag{4.4}$$

Consequently, the above equations can be rewritten as Equation 4.5:

$$x_{k+1} = \begin{bmatrix} 1 & \Delta t \\ 0 & 1 \end{bmatrix} x_k + \omega_k$$
$$Q_k = \begin{bmatrix} \frac{1}{4}(\Delta t)^4 & \frac{1}{2}(\Delta t)^3 \\ \frac{1}{2}(\Delta t)^3 & (\Delta t)^2 \end{bmatrix} \sigma_a^2 \tag{4.5}$$

$$R_k = \sigma_\nu^2 \tag{4.6}$$

The measurement frequency is $1Hz$, and assume the measurement error is less than $100m$. therefore,

$\Delta t = 1$, $\sigma_a^2 \cong 21$ and $\sigma_\nu^2 \cong 2500$

4.2 Magnetic compass modelling

Magnetic compasses play a vital role in the navigation system for *Springer*, consequently, to obtain accurate compass models is of utmost importance for the whole MSDF process. On the other hand, a magnetic compass is a very sensitive and complex sensor, therefore SI is chosen to derive a model which can replicate the sensor behaviour as closely as possible.

SI offers an alternate route to model a sensor. This approach is quite useful for providing reliable and accurate models in a short time using input/output experimental data. It consists of the following steps:

- data collection;
- characterization;
- identification/estimation;
- validation.

The first and most important step is to collect the input/output data of the system to be

identified. The choice of input signal is crucial in SI. Psuedo-Random Binary Sequence (PRBS) input, multiple level input and step input are always chosen as the input signals. Whereas for the magnetic compasses, as the compasses cannot achieve instant corresponding output to the PRBS signal, PRBS is not suitable for deriving the compass models. Therefore a multiple input signal is used here to identify the system models.

The second step is characterization which aims to define the structure of the system to be identified. This includes selection of a suitable model structure, e.g. Auto-Regressive with eXogenous variable (ARX), Auto-Regressive Moving-Average with eXogenous variable (ARMAX), and error type selection. If there is significant amount of noise in the data then it could be modelled separately by specifying an appropriate model type. A generic input-output linear model for a single output system can be written as (Ljung 1999):

$$A(q^{-1})y(k) = \sum_{i=1}^{nu} B_i(q^{-1})u_i(k - nn_i) + C(q^{-1})e(k) \tag{4.7}$$

where u and y are the input and output respectively, and u_i represents the ith input. A,B_i and C are polynomial in the delay operator q^{-1}, nn_i denotes the time delay in the system and e is the disturbance. All the above mentioned models can be obtained from the generic model structure by substituting the appropriate values of the polynomials.

The third step is identification/estimation, which involves determining the numerical values of the structure parameters, which minimize the error between the system to be identified and its model. Common estimate methods are least squares, instrumental variable, maximum likelihood and prediction error models. A common criterion used in most optimization

methods is the quadratic error function given by (Ljung 1999):

$$\min_{\Gamma} J = \frac{1}{N}\sum_{i=1}^{N}(\hat{y}(k) - y)^2 \tag{4.8}$$

where $\hat{y}$ is the predicted output from the model, y denotes the actual output, N represents the number of data points and Γ contains the coefficient to be estimated in a given model structure.

The final step is model validation which consists of relating the system to the identified model in time or frequency domain to instil confidence in the obtained model. Residual analysis and cross validation tests are always employed for model validation. Residuals ϵ are defined as the difference between the model output and the measured output. For a perfect model, the residuals should reduce to an uncorrelated sequence e with zero mean and finite variance. Correction based tests are employed to verify if

$$e(t) = \varepsilon(t) \tag{4.9}$$

This is achieved by verifying if the correction functions are within the confidence intervals, i.e.

$$\phi_{\varepsilon\varepsilon}(n) = E[\varepsilon(k-n)\varepsilon(n)] = \delta(n) \tag{4.10}$$

$$\phi_{u\varepsilon}(n) = E[u(k-n)\varepsilon(n)] = 0 \tag{4.11}$$

where $\phi_{\varepsilon\varepsilon}$ and $\phi_{u\varepsilon}$ represents the autocorrelation of residuals and cross correlation of residuals and input respectively. u is the excitation signal to the system and δ is the dirac delta

function defined as:

$$\delta(k) = \begin{cases} 0 & \text{if } k \neq 0: \\ 1 & \text{if } k = 0; \end{cases} \tag{4.12}$$

if the cross correlation test in Equation 4.11 is not verified. this means that there is something in the residuals which is originating from the input and has not been properly taken care of by the model and thus the model needs further tuning.

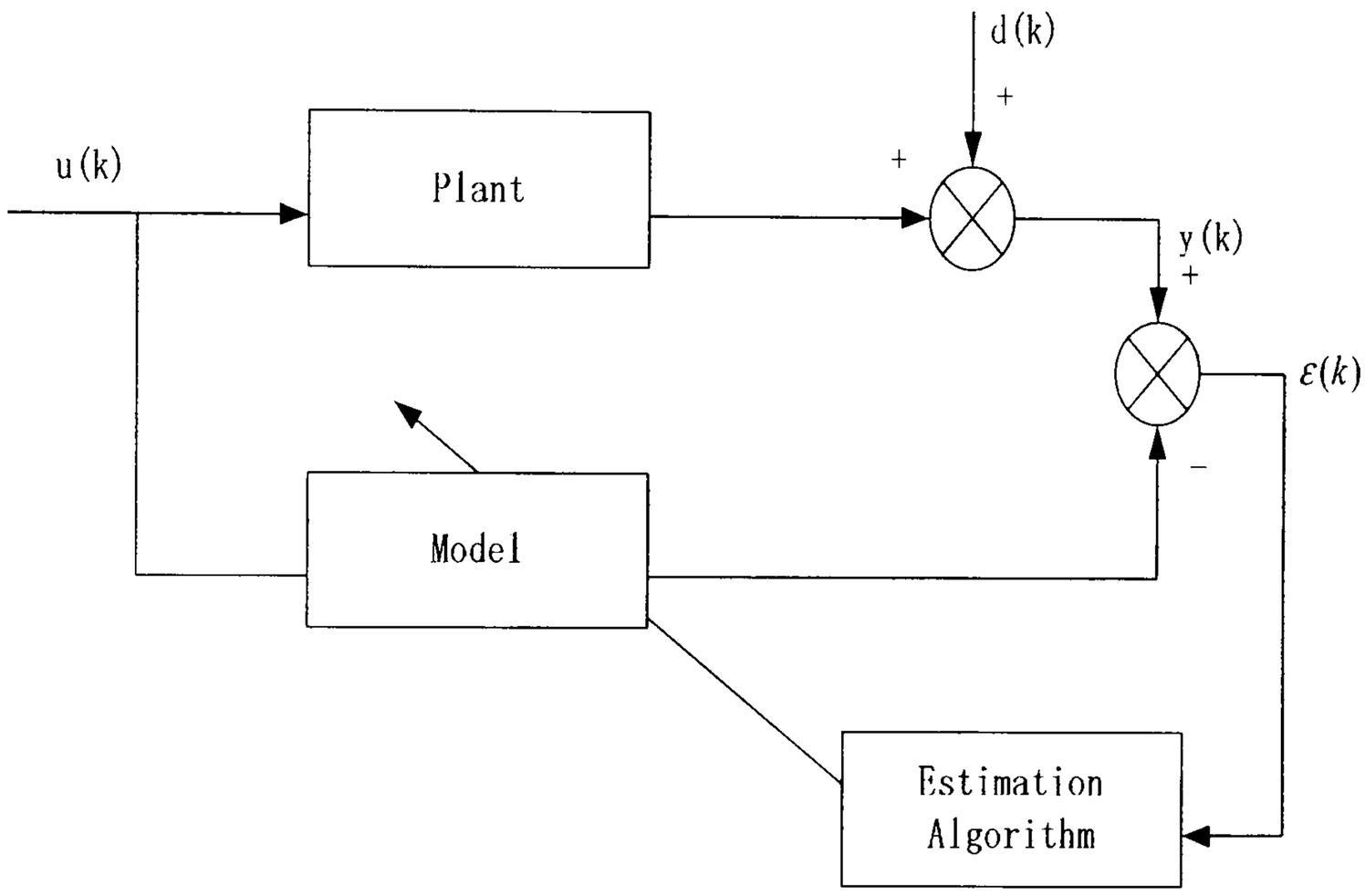

Figure 4.1: The overall SI structure

The above mentioned features of SI are symbolically indicated in Figure 4.1 where $d(t)$ is the external noise or disturbance to the plant. SI theory is well established and the reader is referred to Ljung (1999) for a comprehensive treatment.

4.2.1 SI for the compasses

The compass SI experiments were carried out many times, one of the experimental results are presented here to show the whole process.

The magnetic compasses were installed inside a Peli case, a multiple level input signal was given as the excitation signal. The outputs of the three compasses were recorded and are shown in Figure 4.2.

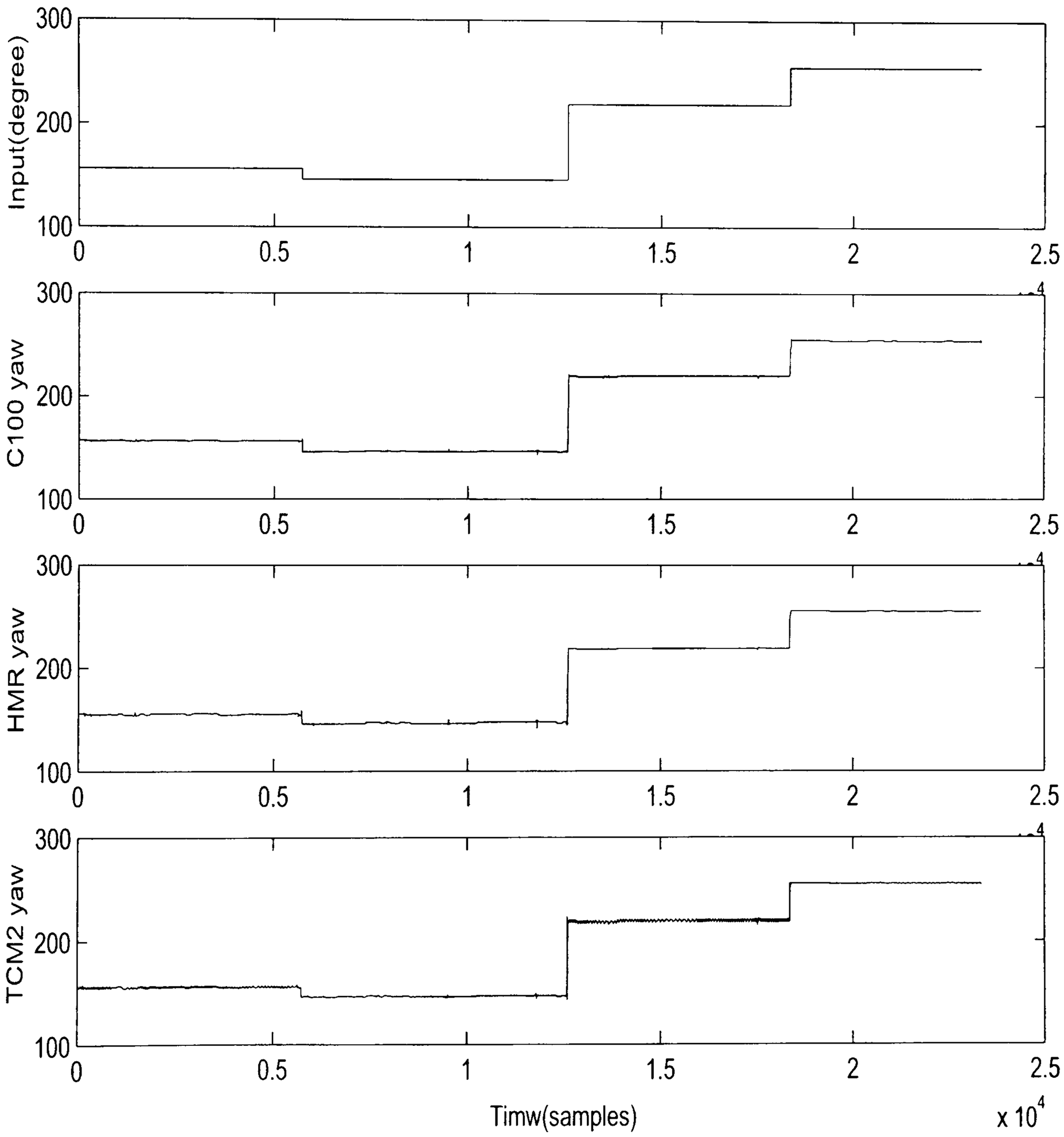

Figure 4.2: Data collection for SI

ARMAX model was selected for the sensor models because it has more flexibility in the

handling of disturbance modeling than other models.

The General structure of an ARMAX model is expressed in Equation 4.13:

$$A(q^{-1})x(k+n) = B(q^{-1})u(k) + C(q^{-1})e(k) \tag{4.13}$$

The prediction error model method is being used to estimate the system model. As a result, the compass models are shown as follow:

TCM2

$$A(q) = 1 - 0.2796q^{-1} - 0.6971q^{-2}$$
$$B(q) = 0.4364q^{-1} - 0.407q^{-2}$$
$$C(q) = 1 + 0.1334q^{-1}$$

HMR

$$A(q) = 1 - 0.978q^{-1} - 0.0204q^{-2}$$
$$B(q) = 0.03386q^{-1} + 0.03549q^{-2}$$
$$C(q) = 1 + 0.1392q^{-1}$$

KVH C100

$$A(q) = 1 - 0.4783q^{-1} - 0.5124q^{-2}$$
$$B(q) = 0.5504q^{-1} - 0.5411q^{-2}$$
$$C(q) = 1 + 0.1068q^{-1}$$

The ARMAX models identified above can be simplified as state space models:

TCM2 state space model:

$$x_{k+1} = \begin{bmatrix} 0.2796 & 0.6971 \\ 1 & 0 \end{bmatrix} x_k + \begin{bmatrix} 0.4364 & 0 \end{bmatrix} u_k + \omega \tag{4.14}$$

$$z_k = \begin{bmatrix} 1 & 0 \end{bmatrix} x_k + \nu \tag{4.15}$$

HMR state space model:

$$x_{k+1} = \begin{bmatrix} 0.978 & 0.0204 \\ 1 & 0 \end{bmatrix} x_k + \begin{bmatrix} 0.03886 & 0 \end{bmatrix} u_k + \omega \tag{4.16}$$

$$z_k = \begin{bmatrix} 1 & 0 \end{bmatrix} x_k + \nu \tag{4.17}$$

KVH C100 state space model:

$$x_{k+1} = \begin{bmatrix} 0.4783 & 0.5124 \\ 1 & 0 \end{bmatrix} x_k + \begin{bmatrix} 0.5504 & 0 \end{bmatrix} u_k + \omega \tag{4.18}$$

$$z_k = \begin{bmatrix} 1 & 0 \end{bmatrix} x_k + \nu \tag{4.19}$$

where ω and ν are random variables.

$$\omega_k \sim N(0, Q_k)$$
$$\nu_k \sim N(0, R_k) \tag{4.20}$$

4.3 Model validation

The SI approach is a black box modelling technique meaning that no physical quantities are directly involved in this process in contrast to first principle modelling. All that is of interest is the cause and effect phenomena and then identifying the black box in between, that can produce the measured system output as closely as possible for the same input. Some insight can be gained into systems behaviour by analysising the estimated model.

Various techniques were employed to measure the model quality and its capability to predict accurately the measured response. Correlation tests are performed here to validate if all the sensor dynamics have been captured. The result of the correlation tests of the three compasses are presented in Figure 4.3 to Figure 4.5. A cross validation test is carried out on the TCM2 compass, the result is shown in Figure 4.6.

The autocorrelation and cross correction of the residuals for each compass are within the confidence bands indicating that the extracted models fit well with the measured data and thus are deemed adequate for further analysis. The cross validation result for the TCM2 compass denotes that the measured and simulated outputs are in harmony, i.e. the model output is closely following the measure response.

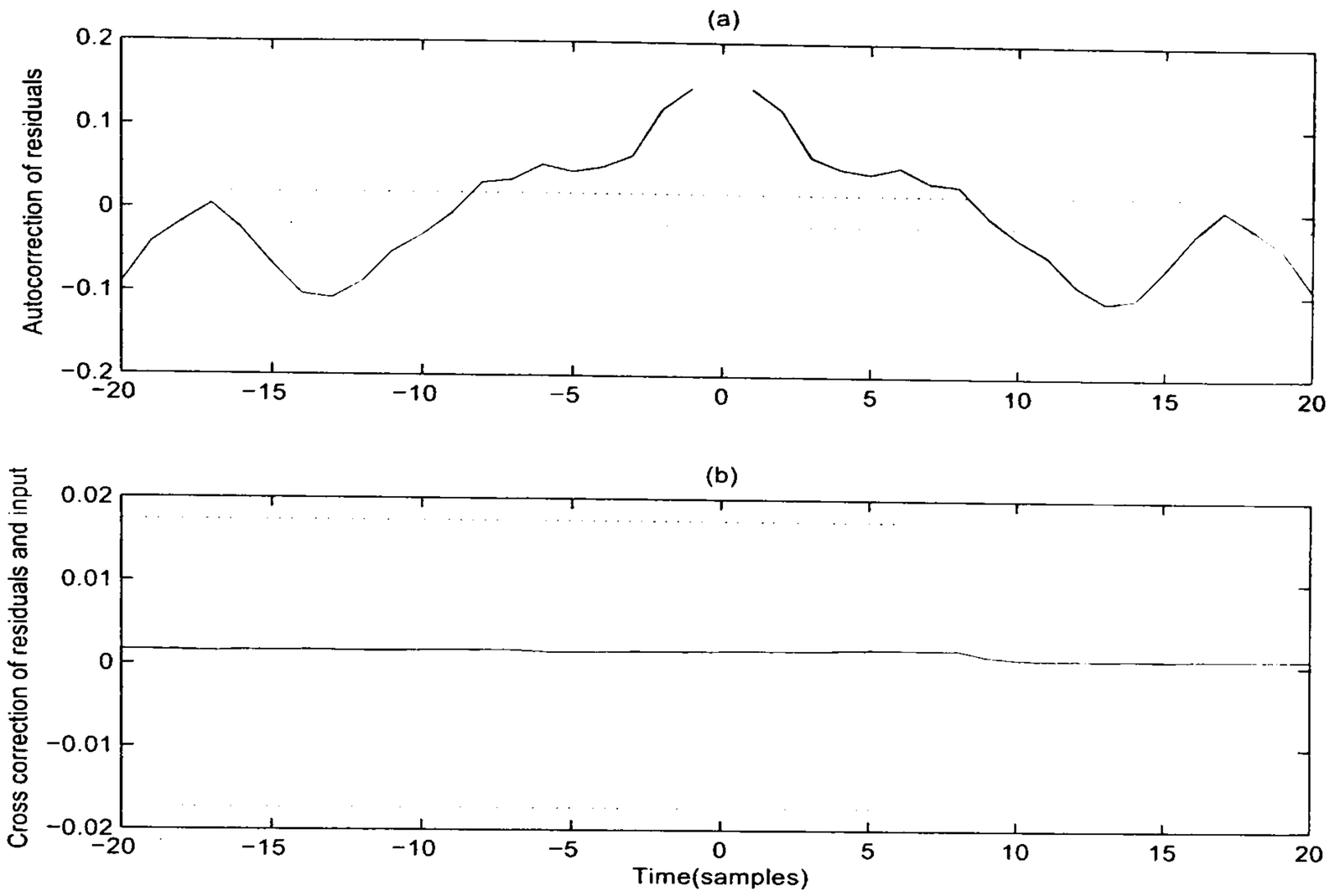

Figure 4.3: Correlation test for TCM2 compass model (a)Autocorrelation of residuals and (b)Cross correction of residuals and the input

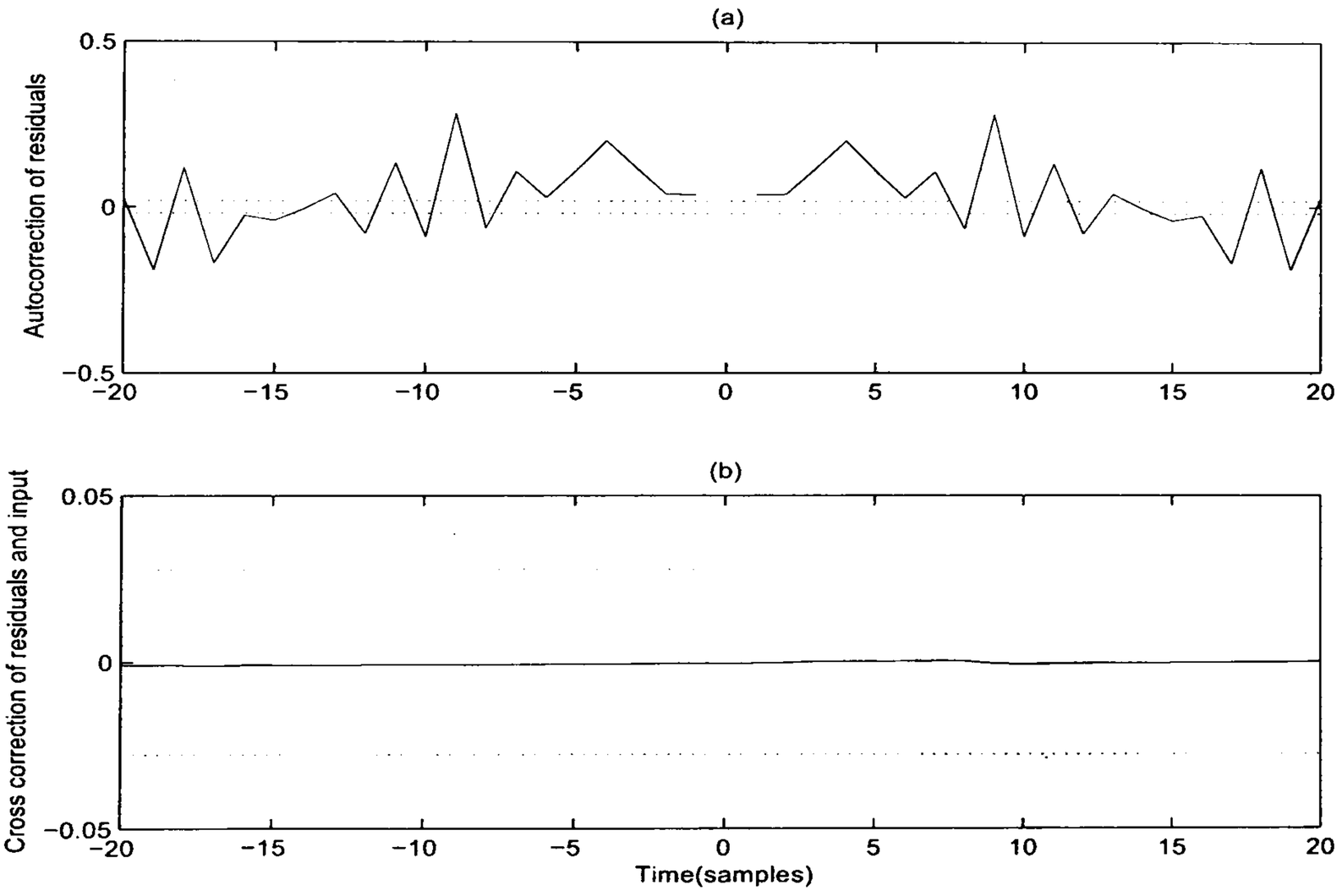

Figure 4.4: Correlation test for HMR 3000 compass model (a)Autocorrelation of residuals and (b)Cross correction of residuals and the input

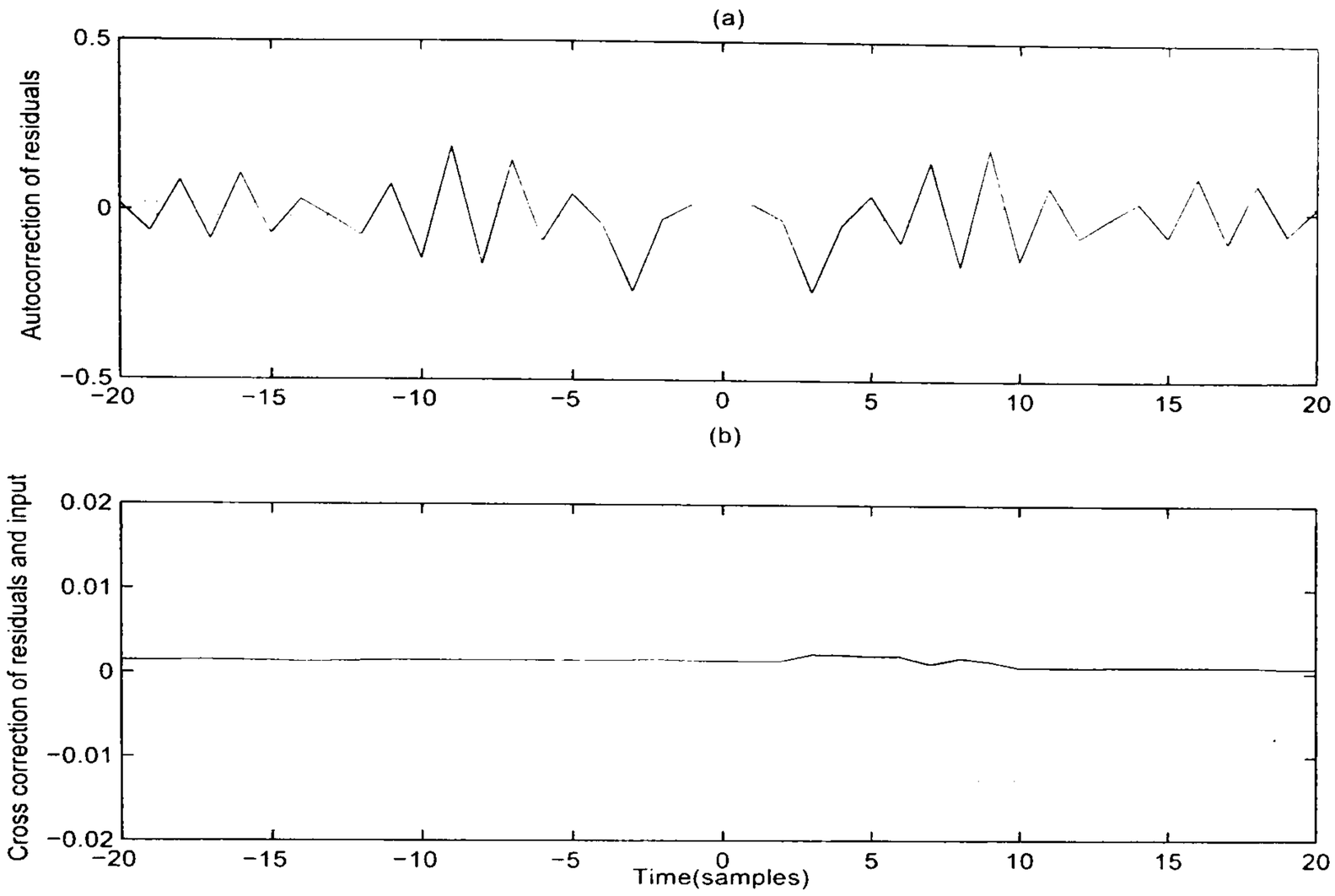

Figure 4.5: Correlation test for KVH C100 compass model (a)Autocorrelation of residuals and (b)Cross correction of residuals and the input

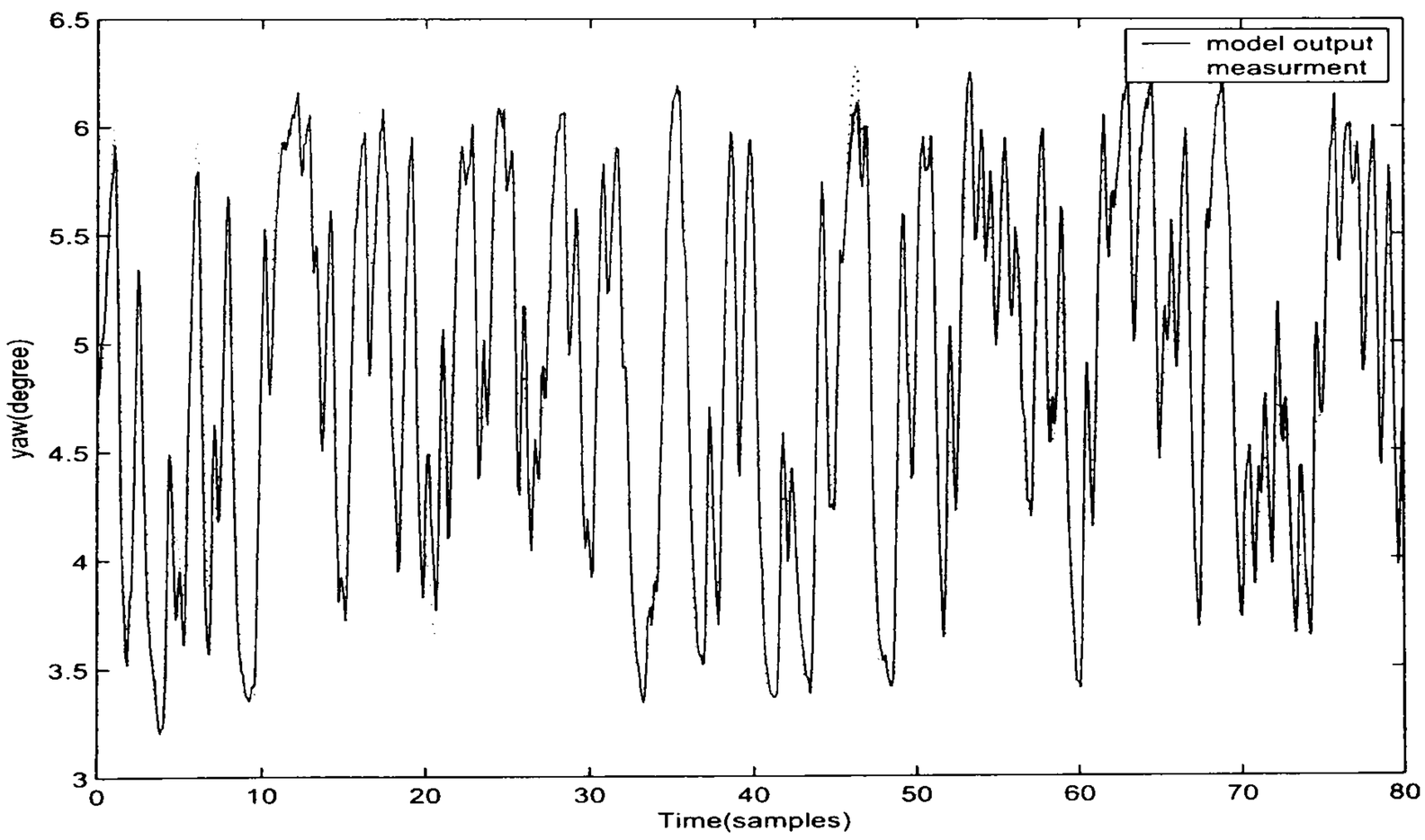

Figure 4.6: Cross validation test for the TCM2 compass

4.4 Concluding remarks

Mathematical modelling is very important in design of a MSDF system. Details with regards to modelling of a GPS and three magnetic compasses have been presented in this Chapter. Two different practical ways are elaborated. The GPS model was derived based on the first principle method and knowledge gained from the experiment. An alternative method using SI was implemented to produce three compass models based on input/output data. The results were analysised and validated. Moreover, all the compasses have a build in stabilized filter in order to reduce cross-coupling effects generated from the pitch and roll axes. The cross-coupling effects therefore assumed to be small and, as a result, are ignored here for simplicity.

This chapter completes the sensor modelling, whilst in the forthcoming Chapter, a novel fuzzy logic based MSDF technique will be described and simulation results will be presented.

Chapter 5

MULTI-SENSOR DATA FUSION

Multiple Sensor Data Fusion (MSDF) refers to the acquisition, processing and synergistic combination of data from several redundant sensors or different sensors in order to achieve better data interpretation or improved decision making (Varshney 1997). In this chapter, a fuzzy logic adaptive technique is used to adjust the measurement noise covariance matrix (R) in Kalman filter to fit the actual statistics of the noise profile present in the incoming sensor measured data using a covariance matching method. Whilst, the process noise covariance (Q) matrix in a Federated Kalman Filter (FKF) is tuned by an adaptive information sharing strategy. This strategy enables the more accurate sensors to make larger contribution to the global estimation.

Simulations are carried out using various fuzzy logic cascaded Kalman filter algorithms under different sensor fault situations.

5.1 Kalman filter

In 1960, R.E. Kalman introduced a recursive solution to the discrete-data linear filtering problem which is now known as the Kalman filter. The Kalman filter is a set of mathematical equations that provides an efficient computational (recursive) means to estimate the state of a process, in a way that minimizes the mean of the squared error (Welch and Bishop 2004).

The computation process of the Kalman filter can be divided into a time update process and a measurement update process. The time update process projects the current state estimate ahead in time. Whilst the measurement update adjusts the projected estimate by an actual measurement at that time.

Considering the following system described in Equation 5.1:

$$z_k = H_k x_k + \nu_k \tag{5.1}$$

where $x \in \Re^m$ is a state vector, $H \in \Re^{n \times m}$ is a matrix of the state space model, and $\nu \in \Re^n$ is the measurement white noise of the state space model.

The state vector satisfies a linear discrete time state transition, it is defined in Equation 5.2:

$$x_{k+1} = \Phi_k x_k + G_k u_k + \omega_k \tag{5.2}$$

where $\Phi \in \Re^{n \times m}$ is the system state space model, $G \in \Re^{m \times q}$ is the control model. $u \in \Re^q$ is a known control input, and $\omega \in \Re^m$ is the input noise.

In Equation 5.3 to 5.5, matrix Q and matrix R are defined as the process noise covariance and the measurement noise covariance respectively, where

$$E[\omega_k \omega_j^T] = \begin{cases} Q_k & \text{if } j = k; \\ 0 & \text{if } j \neq k; \end{cases} \tag{5.3}$$

$$E[\nu_k \nu_j^T] = \begin{cases} R_k & \text{if } j = k; \\ 0 & \text{if } j \neq k; \end{cases} \tag{5.4}$$

$$E[\omega_k \nu_j^T] = 0, \text{for all k and i.} \tag{5.5}$$

It is assumed the system of Equation 5.2 starts from an initial state x_0, which is a Gaussian random vector with mean and covariance by Equation 5.6:

$$E[x_0] = \hat{x}_0$$

$$E\{[x_0 - \hat{x}_0][x_0 - \hat{x}_0]^T\} = P_0 \tag{5.6}$$

The time update process is presented in Equations 5.7 and 5.8:

$$\hat{x}_{k+1}^- = \Phi_k \hat{x_k} + G_k u_k \tag{5.7}$$

$$P_{k+1}^- = \Phi_k P_k \Phi_k^T + Q_k \tag{5.8}$$

The measurement update process is shown in Equations 5.9 to 5.11:

$$K_k = P_k^- H_k^T [H_k P_k^- H_k^T + R_k]^{-1} \tag{5.9}$$

$$\hat{x}_k = \hat{x}_k^{-1} + K_k[z_k - H_k \hat{x}_k] \tag{5.10}$$

$$P_k = [I - K_k H_k] P_k^{-1} [I - K_k H_k]^T + K_k R_k K_k^T \tag{5.11}$$

The measurement update equations incorporate a new observation into the *priori* estimate from the time update equations to obtain an improved *posteriori* estimate. In the time and measurement update equations, $\hat{x}_k$ is an estimate of the system state vector x_k, K_k is the Kalman gain and P_k is the covariance matrix of the state estimation error. The 'super minus' in the equation reminds the reader that it is *a priori* estimate before the measurement. The 'super plus' denotes the estimate after the measurement update.

5.2 Cascaded Kalman filter

In the literature, three main Kalman filter based MSDF architectures are suggested (Gao and Abousalem 1993): Centralized Kalman Filter (CKF), Decentralized Kalman Filter (DKF) and Federated Kalman Filter (FKF). All the systems have their own advantages and disadvantages.

5.2.1 Centralised Kalman filter

A CKF based MSDF system is shown in Figure 5.1. It communicates and processes all measured sensor data in a central site using simple KF computation techniques. The advantage of this method is that it involves minimal information loss, however, it can result in a high computational load. In addition the CKF is not robust enough when there is spurious data in any of the sensors.

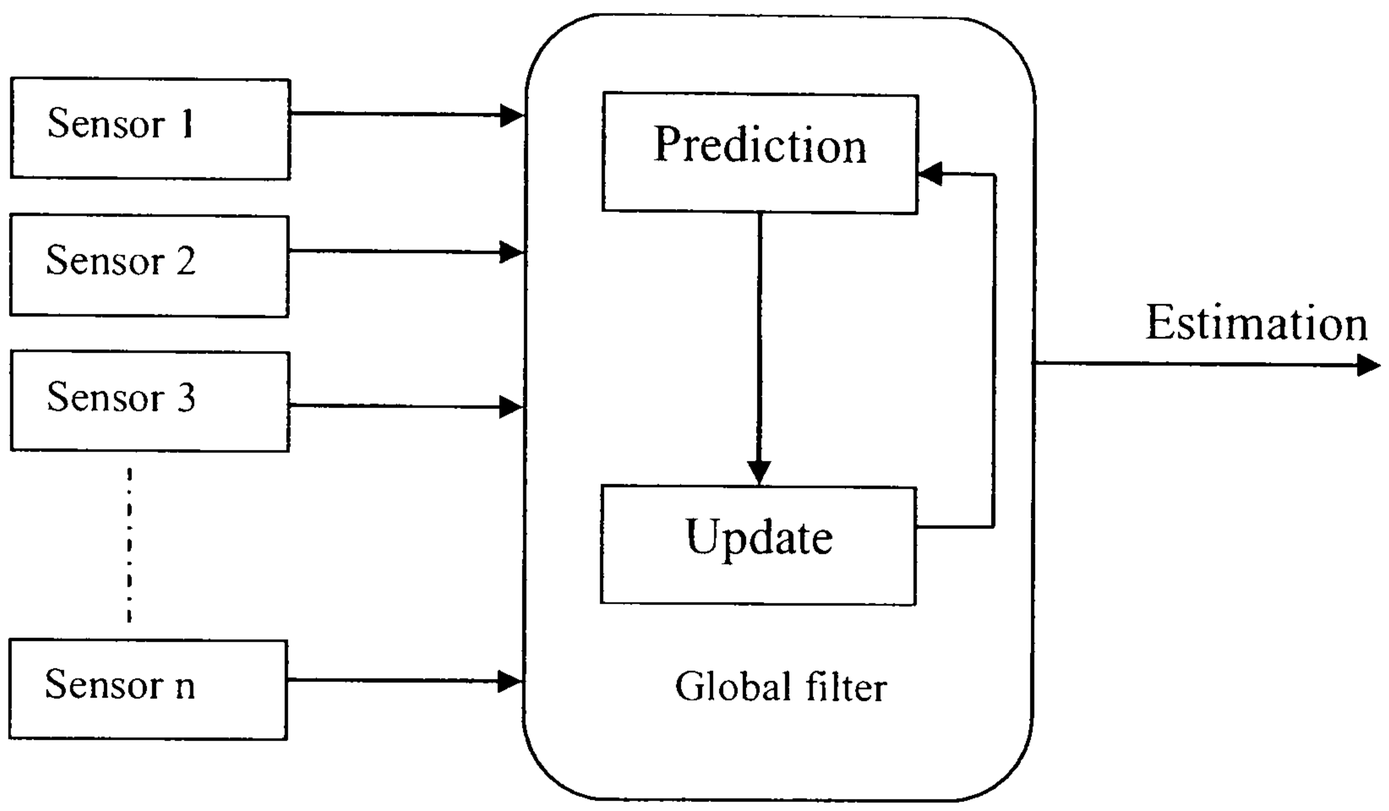

Figure 5.1: Centralized Kalman Filtering (CKF)
(Gao and Abousalem 1993)

5.2.2 Decentralised Kalman filter

In Figure 5.2, a DKF based MSDF system is shown, it is a two stage data processing technique which divides the standard Kalman filter into local filters and a master filter. Firstly, the local filters process their own data in parallel to yield the best possible local estimates, then the master filter fuses the local estimates to generate the best global solution, so that the data computation is efficient. Since the individual and global estimates for the state vector can be compared, decentralization leads to easy fault detection and isolation.

In a standard Kalman filter, all the measurements are always input directly to a single

filter. Whilst in DKF, N sensor measurements are processed by N local Kalman filters in parallel to yield the best possible local estimations. and then, a master filter accepts the N local filters' output to generate the global estimation.

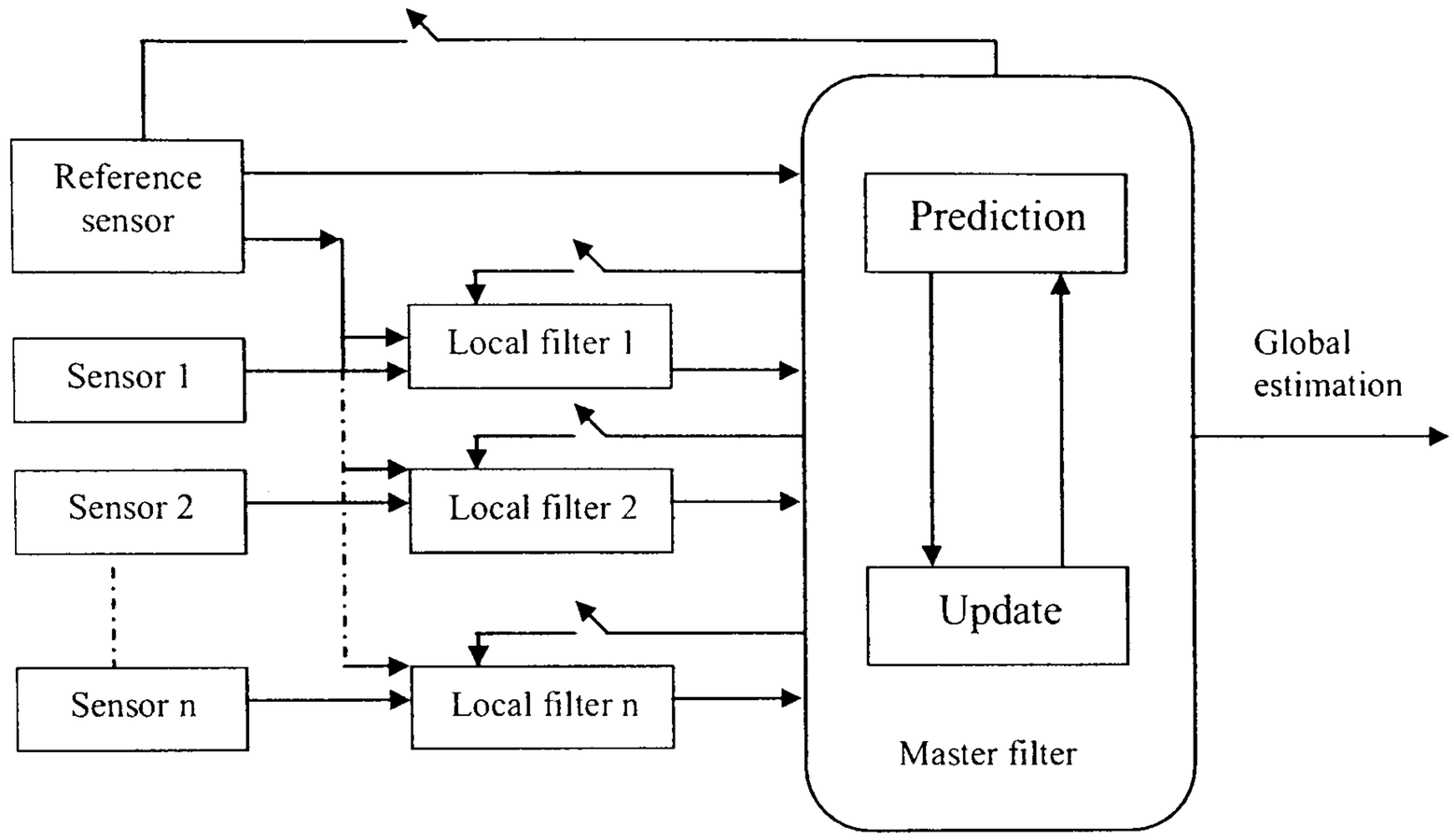

Figure 5.2: Decentralized Kalman Filtering (DKF) (Gao and Abousalem 1993)

The computation sequence of a DKF is described as follows.

In the local Kalman filters:

$$\hat{x}^-_{i(k+1)} = \Phi_{i(k)}\hat{x}^+_{i(k)} + G_{i(k)}u_{i(k)} \tag{5.12}$$

$$P^-_{i(k+1)} = \Phi_{i(k)}P^+_{i(k)}\Phi^T_{i(k)} + Q_{i(k)} \tag{5.13}$$

invert to get ${P^-_{i(k+1)}}^{-1}$

$$K_{i(k)} = P^-_{i(k)}H^T_{i(k)} + [H_{i(k)}P^-_{i(k)}H^T_{i(k)} + R_{i(k)}]^- \tag{5.14}$$

$$\hat{x}^+_{i(k)} = \hat{x}^-_{i(k)} + K_{i(k)}[z_{i(k)} - H_{i(k)}\hat{x}^-_{i(k)}] \tag{5.15}$$

$$P^{+}_{i(k)} = [I - K_{i(k)}H_{i(k)}]P^{-1}_{i(k)}[I - K_{i(k)}H_{i(k)}]^T + K_{i(k)}R_{i(k)}K^T_{i(k)} \tag{5.16}$$

invert to get ${P^{+}_{i(k)}}^{-1}$ where $i = 1, \ldots, N$

In the master filter:

$$\hat{x}^{-}_{(k+1)} = \Phi_{(k)}\hat{x}^{+}_{(k)} + G_{(k)}u_{(k)} \tag{5.17}$$

$$P^{-}_{(k+1)} = \Phi_{(k)}P^{+}_{(k)}\Phi^T_{(k)} + Q_{(k)} \tag{5.18}$$

invert to get ${P^{-}_{(k+1)}}^{-1}$

$${P^{+}_{(k)}}^{-1} = {P^{-}_{(k)}}^{-1} + \sum_{i=1}^{N} {P^{+}_{i(k)}}^{-1} - \sum_{i=1}^{N} {P^{-}_{i(k)}}^{-1} \tag{5.19}$$

and then invert to get $P^{+}_{(k)}$

$$\hat{x}^{+}_{(k)} = P^{+}_{(k)}[{P^{-}_{(k)}}^{-1} + \sum_{i=1}^{N} {P^{+}_{i(k)}}^{-1}\hat{x}^{+}_{i(k)} - \sum_{i=1}^{N} {P^{-}_{i(k)}}^{-1}\hat{x}^{-}_{i(k)}] \tag{5.20}$$

5.2.3 Federated Kalman filter

A FKF based MSDF system is shown in Figure 5.3 which differs from the DKF by employing information feedback. It combines local estimates in the master filter in order to yield the global optimal estimate and then includes feedback information from the master filter to the

local filters in given proportions. The challenge in the design of a FKF is to determine the feedback factor values in order to achieve higher fault tolerance and efficient computation.

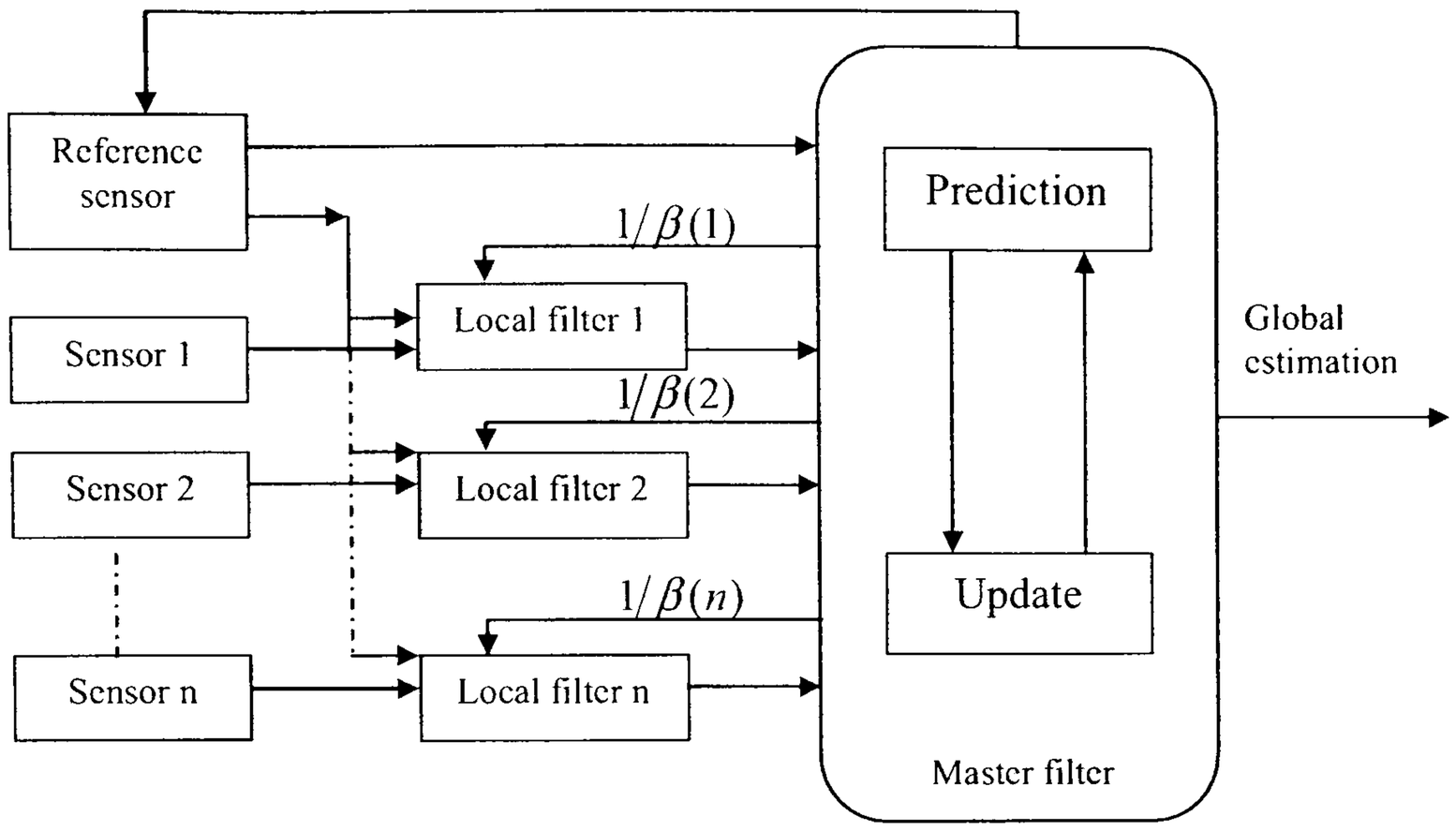

Figure 5.3: Federated Kalman Filtering (FKF)
(Gao and Abousalem 1993)

First of all, the global information is divided as:

$$Q_{i(k)} = (1/\beta_i)Q_{(k)} \tag{5.21}$$

$$P^+_{i(k)} = (1/\beta_i)P^+_{f(k)} \tag{5.22}$$

$$\hat{x}^+_{i(k)} = (1/\beta_i)x^+_{f(k)} \tag{5.23}$$

In the local Kalman filters:

$$\hat{x}^+_{i(k)} = \hat{x}^+_{f(k)} \tag{5.24}$$

where $i = 1, \ldots, N$, subject to

$$\sum_{i=1}^{N} \beta_i = 1 \tag{5.25}$$

$$\hat{x}^-_{i(k+1)} = \Phi_{i(k)}\hat{x}^+_{i(k)} + G_{i(k)}u_{i(k)} \tag{5.26}$$

$$P^-_{i(k+1)} = \Phi_{i(k)}P^+_{i(k)}\Phi^T_{i(k)} + Q_{i(k)} \tag{5.27}$$

$$K_{i(k)} = P^-_{i(k)}H^T_{i(k)} + [H_{i(k)}P^-_{i(k)}H^T_{i(k)} + R_{i(k)}]^- \tag{5.28}$$

$$\hat{x}^+_{i(k)} = \hat{x}^-_{i(k)} + K_{i(k)}[z_{i(k)} - H_{i(k)}\hat{x}^-_{i(k)}] \tag{5.29}$$

$$P^+_{i(k)} = [I - K_{i(k)}H_{i(k)}]P^{-1}_{i(k)}[I - K_{i(k)}H_{i(k)}]^T + K_{i(k)}R_{i(k)}K^T_{i(k)} \tag{5.30}$$

where $i = 1, \ldots, N$

invert to get ${P^+_{i(k)}}^{-1}$

For the master filter:

$$\hat{x}^-_{M(k+1)} = \Phi_{M(k)}\hat{x}^+_{M(k)} + G_{M(k)}u_{M(k)} \tag{5.31}$$

$$P^-_{M(k+1)} = \Phi_{M(k)}P^+_{M(k)}\Phi^T_{M(k)} + Q_{M(k)} \tag{5.32}$$

invert to get ${P^-_{M(k+1)}}^{-1}$

$${P^+_{f(k)}}^{-1} = \sum_{i=1}^{N} {P^+_{i(k)}}^{-1} - {P^-_{M(k)}}^{-1} \tag{5.33}$$

invert to get $P^+_{f(k)}$

$$\hat{x}^+_{f(k)} = P^+_{f(k)}[{P^-_{M(k)}}^{-1}\hat{x}^-_{i(k)} + \sum_{i=1}^{N} {P^+_{i(k)}}^{-1}\hat{x}^+_{i(k)}] \tag{5.34}$$

5.3 Fuzzy logic adaptive Kalman filter

As discussed in Section 2.1.5, since it has the capability to deal with complex problems, Fuzzy Logic Adaptive Kalman Filter (FLA-KF) techniques have become a popular approach.

5.3.1 Fuzzy logic based adaptive Kalman filter

A significant difficulty in designing a Kalman filter can often be traced to incomplete *a priori* knowledge of the matrix Q and matrix R. These matrices are often initially estimated from experience or are even unknown. However, it has been shown that insufficient *priori* knowledge can reduce the precision of estimation, or even can lead to divergence (Welch and Bishop 2004).

The adaptation here is in the sense of adaptively tuning the measurement noise covariance matrix to fit the actual statistic of the noise profiles present in the incoming measured data. The adaptation is based on a technique known as covariance matching (Mebra 1970).

At a sample time k, the innovation Inn_k is the difference between the real measurement z_k and estimated value $\hat{z}_k$ from the filter.

The actual covariance is defined as an appropriation of the Inn_k sample through averaging inside a moving estimation window of size M (Mohamed and Schwarz 1999). and it has the following form:

$$\hat{C}_{Inn_k} = \frac{1}{M}\sum_{j=j_0}^{k} Inn_k Inn_k{}^{\mathrm{T}} \tag{5.35}$$

where $j_0 = k - M + 1$ is the first sample inside the window, M is chosen empirically to give some statistical smoothing (Escamilla-Ambrosio and Mort 2003). Experiments by the author have shown that a good size for the moving window is 15.

The theoretical covariance of the innovation sequence is defined in Equation 5.36:

$$S_k = H_k P_k^- H_k{}^{\mathrm{T}} + R_k \tag{5.36}$$

If a discrepancy is found between the actual covariance and theoretical covariance, then a FIS produces adjustments for the diagonal elements of R_k based on the size of this discrepancy. The discrepancy is defined in Equation 5.37 by a variable called the degree of mismatch (DoM_k):

$$DoM_k = S_k - \hat{C}_{Inn_k} \tag{5.37}$$

If the actual covariance is greater than its theoretical value, the value of R_k should be decreased. If the actual covariance is less than its theoretical value, the value of R_k should be increased. So that, three fuzzy rules can be generated as shown Table 5.1:

Table 5.1: Fuzzy rules for FLA-KF

If DoM_k	Then R_k
> 0	DECREASE
< 0	INCREASE
$\cong 0$	MAINTAIN

Therefore, the adjustment can be applied to R_k:

$$R_k = R_{k-1} + \Delta R_k \tag{5.38}$$

Hence, a Single Input Single Output (SISO) FIS is produced to adjust the element in R_k. FIS can be implemented considering three fuzzy sets for DoM_k: N=Negative, Z=Zero and P=Positive. For ΔR_k, also three fuzzy sets are specified: I=Increase, M=Maintain and D=Decrease. The membership functions are shown in Figure 5.4. The shape of the membership function should be representative of the variable. In order to determine the shape of the fuzzy logic membership, several simulations were carried out to observe the DoM_k values and adjust the corresponding R_k. Therefore the shape of the membership functions having been derived heuristically.

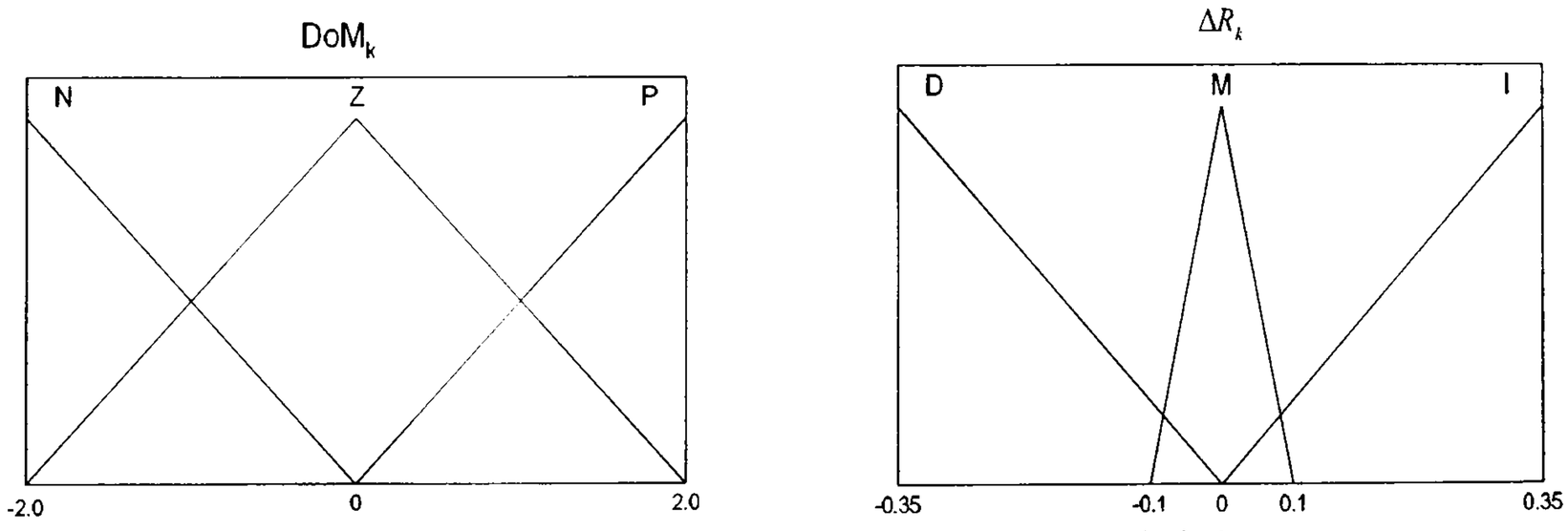

(a) DoM_k (b) ΔR_k

Figure 5.4: Membership functions for DoM_k and ΔR_k

5.3.2 An adaptive determination method for the information feedback factors

The information feedback factors (β_i) in the FKF represent the unitary portion of estimation information from the local KF in the total fusion estimation. The higher the value of β_i, the larger the contribution made from the local filter to the master filter at the next sampling time $(k+1)$. In order to make the FKF adaptive with the estimation accuracies, an adaptive method is presented here to change the feedback factors on-line according to the corresponding eigenvalues of a matrix P. The eigenvalues of the matrix P in the KF equation represent the covariance of their corresponding state vectors (Xu *et al.* 2006*a*).

In the FKF, the covariance matrix of the ith local filter P_i can be decomposed as:

$$P_i = L\Lambda_i L^{\mathrm{T}} \tag{5.39}$$

where $\Lambda_i = diag(\lambda_{i1}, \lambda_{i2}, \ldots, \lambda_{iN})$, $\lambda_{i1} \sim \lambda_{iN}$ are the eigenvalues of P_i, and L is the corresponding eigenvectors matrix.

Herein, $P_i^{\mathrm{T}} P_i$ is used to replace P_i to perform the eigenvalue decomposition.

$$P_i^{\mathrm{T}} P_i = L'\Lambda_i'(L')^{\mathrm{T}} \tag{5.40}$$

where $\Lambda_i' = diag(\lambda_{i1}', \lambda_{i2}', \cdots, \lambda_{im}')$, $\lambda_{ij}' = \lambda_{ij}^2, j = 1, 2, \cdots, N$

As a result its information feedback factor values are given by:

$$\beta_i = \frac{tr\Lambda_i'}{tr\Lambda_1' + tr\Lambda_2' + \cdots + tr\Lambda_n' + tr\Lambda_m'} \tag{5.41}$$

5.4 Fuzzy logic observer

In order to monitor the process of the FLA-KF, a Fuzzy Logic Observer (FLO) is implemented on-line. It uses linguistic rules to identify the quality of the fuzzy logic process. It was employed here as it allows the user to adjust the fuzzy logic membership functions if needed. This FLO assigns a weight of confidence to the FLA-KF with a number on the interval of $[0, 1]$ (Xu *et al.* 2006*b*). $|DoM_k|$ and ΔR_k are employed as two inputs for the FLO with labels: small, medium and large. The output of FLO, $f_k \in [0, 1]$, is the weight of confidence for each FLA-KF. Three fuzzy singletons are defined for the output and labelled as: good, normal and poor.

From the FLA-KF performances, the heuristic fuzzy rules for the FLO is summarized as:

- IF $|DoM_k|$ is Small OR R_k is Small THEN $f_k \cong 1$ FLA-KF is in a Good situation;
- IF $|DoM_k|$ is Large OR R_k is large THEN $f_k \cong 0$ FLA-KF is in a Poor situation;
- Otherwise, FLA-KF is in a Normal situation.

The FLO membership functions are shown in Figure 5.5 and fuzzy rules are given in Table 5.2. The shape and result of the membership functions were derived heuristically.

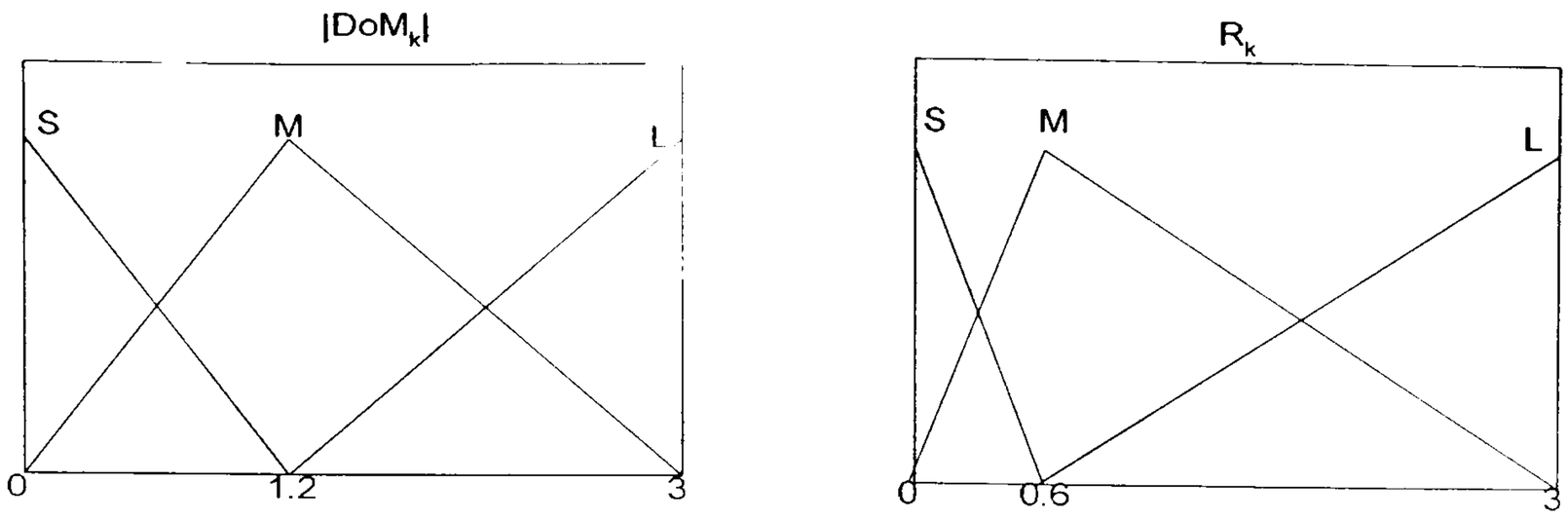

(a) $|DoM_k|$ (b)ΔR_k

Figure 5.5: FLO Membership functions for $|DoM_k|$ and ΔR_k

Table 5.2: Fuzzy rules for FLO

$\|DoM_k\|$	ΔR_k		
	Small	Medium	Large
Small	Good	Good	Normal
Medium	Good	Normal	Poor
Large	Normal	Poor	Poor

5.5 Fault tolerant design

It has been proven that multiple motion sensors play a vital role in autonomous navigation (Luo *et al.* 2002). In real situations there is always the possibility of sensor failure, therefore, to realise reliable and robust navigation for *Springer*, fault detection and isolation are major concerns.

At any time, a sensor may stop sending information under three kinds of sensor fault: transient, persistent or permanent (Escamilla-Ambrosio and Mort 2004). In this paper these three types of fault are defined as:

- Transient fault: the fault lasts on the sensor for 1 sampling time and then recovers to the normal operating condition.

- Persistent fault: the fault lasts on the sensor for a few sampling periods and then recovers to the normal operating condition.

- Permanent fault: the fault remains on the sensor until the sensor is isolated physically.

In any of the above cases, the navigation system must immediately identify the failed sensor and act in such a way that data from the failed sensor will not corrupt the global estimates. This action can be to isolate the sensor from the list of active sensors.

Based on the above discussion, a modified Fuzzy Logic Adaptive Federated Kalman Filter (FLA-FKF) based MSDF architecture is proposed in Figure 5.6 to realise fault tolerant multi-sensor navigation for *Springer*.

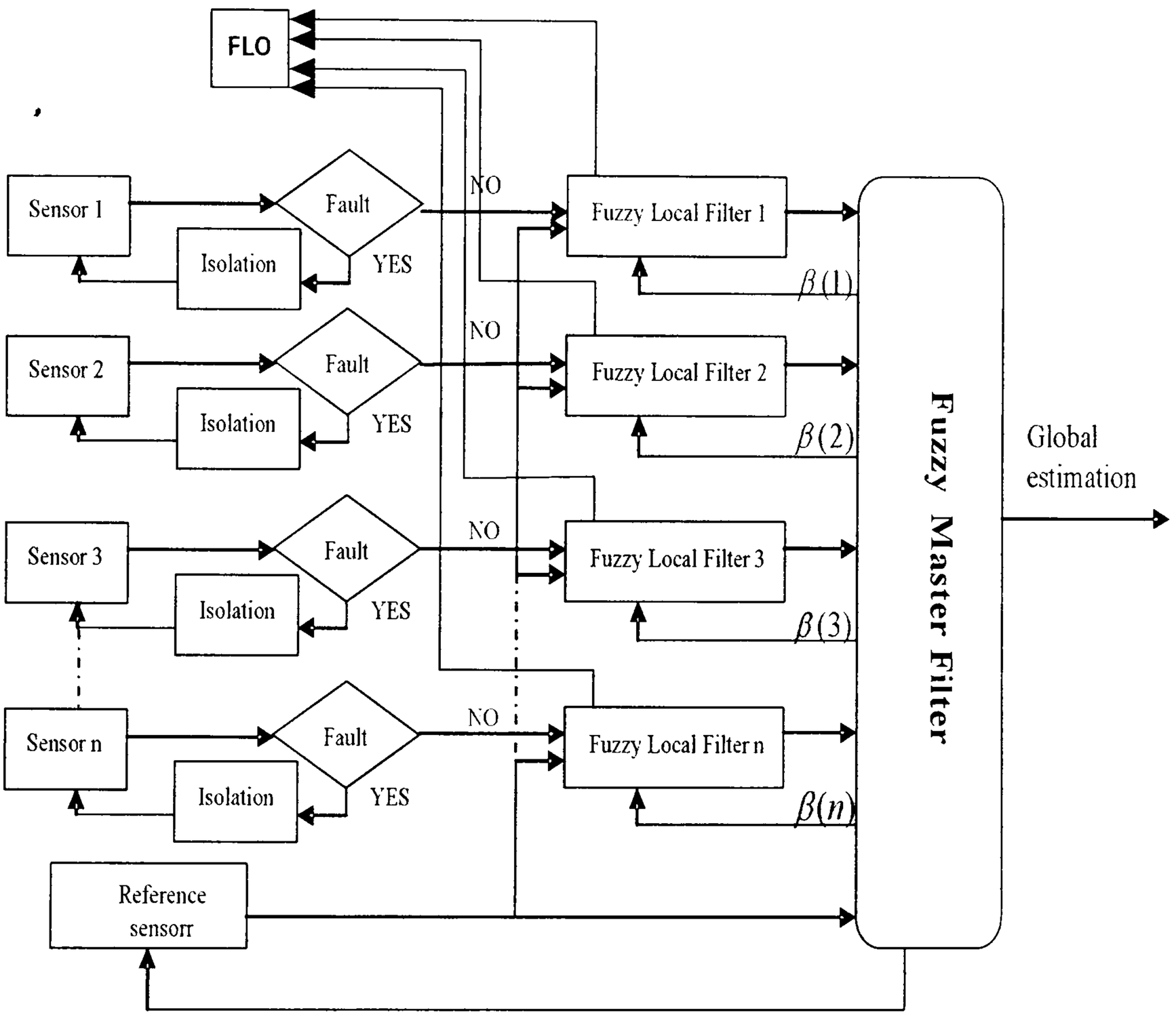

Figure 5.6: MSDF strategy with fault tolerant feature

A simple checking process is added before the FLA-FKF to ensure that the sensor data is functioning continuously. The system will check the NMEA sentence's header, checksum and specific characters. If the sensor's output does not have a complete sentence, the system

will recognize this output as a fault. If the sensor gives a fault output less than 8 sampling times, which is approximately 1 second, the system will use the previous measurements instead of the current one. If the sensor continues giving the fault output (use previous values) for more than 10 seconds, the program will not request output from this sensor immediately. This mechanism can improve the computation efficiency when the system is working under a large and complex sensor network.

At the same time, a GPS output is requested by the system at $10Hz$. The GPS information cannot only provide location of the vehicle but also guarantee successful operation even if all of the compasses have faults.

After checking, the successful sensors' datum will be processed by the FLA-FKF MSDF algorithm. The local Kalman filters progress each sensor's data in parallel to yield the best estimations, according to the difference between the actual value and theoretical value of covariance. Fuzzy logic is then implemented to adjust the R matrix in order to decrease the fault sensor influence. Finally, a master Kalman filter fuses the local outputs to generate the global estimation. During this fusion process the feedback factors are determined depending on the accuracy of the local Kalman filter estimation.

5.6 Simulation results

In order to produce a more accurate heading angle for *Springer*, FLA-CKF, FLA-DKF and FLA-FKF algorithms were investigated. Three magnetic compasses, TCM2, KVH C100 and HMR 3000, were used in the simulation. Details of these compasses can be seen from Section 3.1.2. Transient, persistent and permanent faults were simulated on the TCM2 and HMR 3000 compasses to test the algorithms' fault tolerant capability. Similar results were achieved when the faults occurred on the KVH C100 compass. Owing to the similarity of the results, in the interest of brevity, herein only the unstable compass TCM2 and most

accurate compass HMR 3000 are presented. The results are compared based on the Root Mean Square Error (RMSE) of the heading angle. MATLAB code was developed and used to simulate and test the proposed algorithms.

The experiments were carried out in the laboratory. Three compasses and a GPS, an Inertial Measurement Unit (IMU) were mounted on a trolley. The real position data were collected from an IMU and a GPS, the mean value of the measurements are used for real position.

Recalling the compass models from Section 4.2.1, the initial values for Q and R matrix are given below, other initial parameters are chosen as 0.

$$Q_{TCM2} = Q_{HMR} = Q_{C100} = \begin{bmatrix} 0.1 & 0 \\ 0 & 0.1 \end{bmatrix} \tag{5.42}$$

$$R_{TCM2} = \begin{bmatrix} 2^2 & 0 \\ 0 & 2^2 \end{bmatrix} \tag{5.43}$$

$$R_{HMR} = \begin{bmatrix} 0.7^2 & 0 \\ 0 & 0.7^2 \end{bmatrix} \tag{5.44}$$

$$R_{C100} = \begin{bmatrix} 1.5^2 & 0 \\ 0 & 1.5^2 \end{bmatrix} \tag{5.45}$$

5.6.1 Fuzzy logic based MSDF algorithm with transient faults on the TCM2 compass

In this section , FLA-CKF, FLA-DKF and FLA-FKF are employed for the three compasses of *Springer*. In order to compare the robustness of each algorithm, transient faults were introduced to the TCM2 compass at 100, 200, 300 and 400 samples.

FLA-CKF

Using the fuzzy logic algorithm discussed in Section 5.3.1, a FLA-CKF fuses the three compass measurements and a global estimation was consequently achieved. The performance is shown in Figure 5.7, the sensor faults have not been effectively reduced in the overall fusion result, apparently, this algorithm is not robust when sensor transient fault situations prevail.

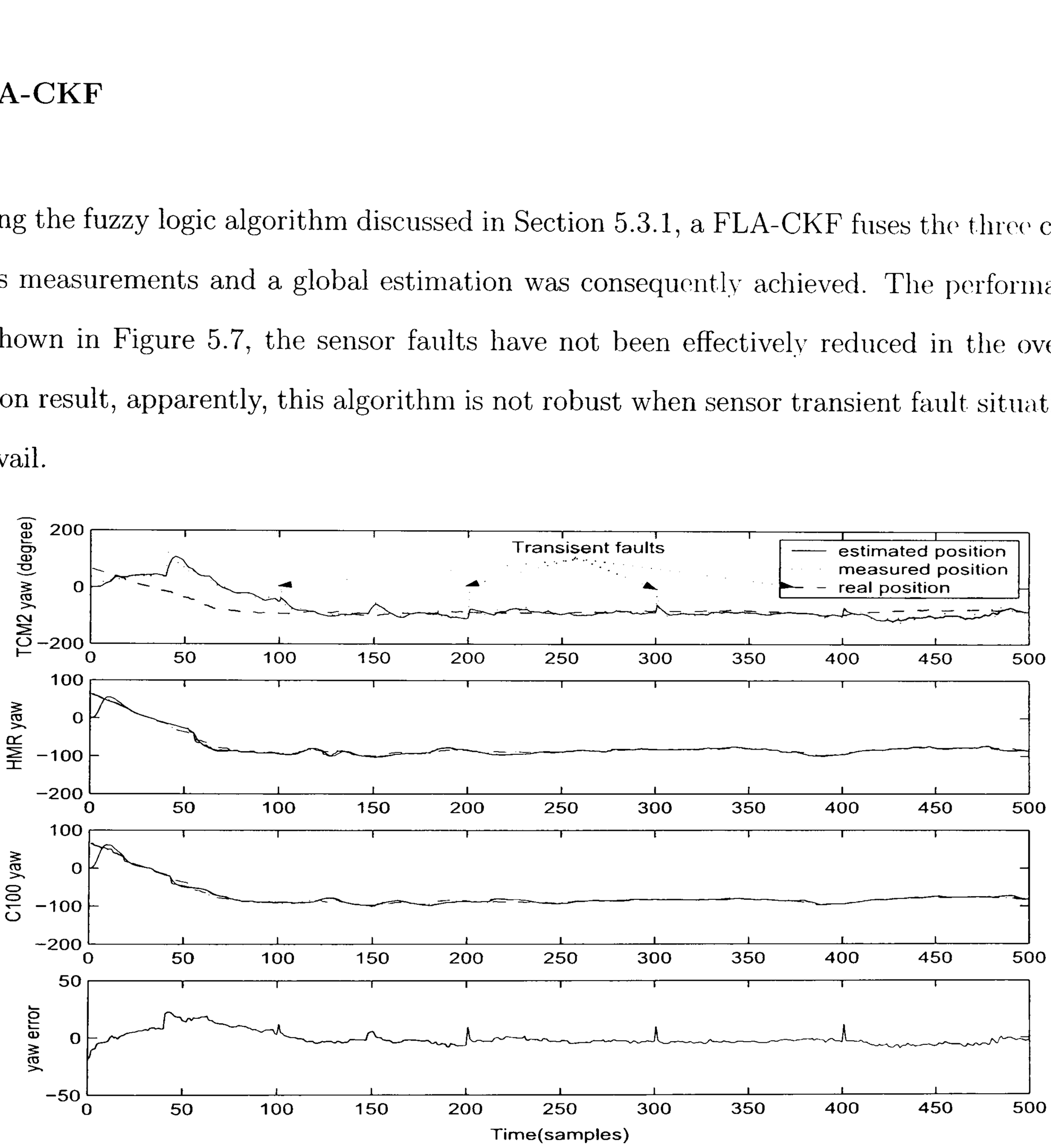

Figure 5.7: FLA-CKF performance with transient faults on the TCM2

FLA-DKF

Figure 5.8 presents the results for the FLA-DKF. the three compass measurements are fused locally before the master fusion procedure. The result demonstrates that FLA-DKF can reduce the sensor transient faults and output fault tolerant fusion result.

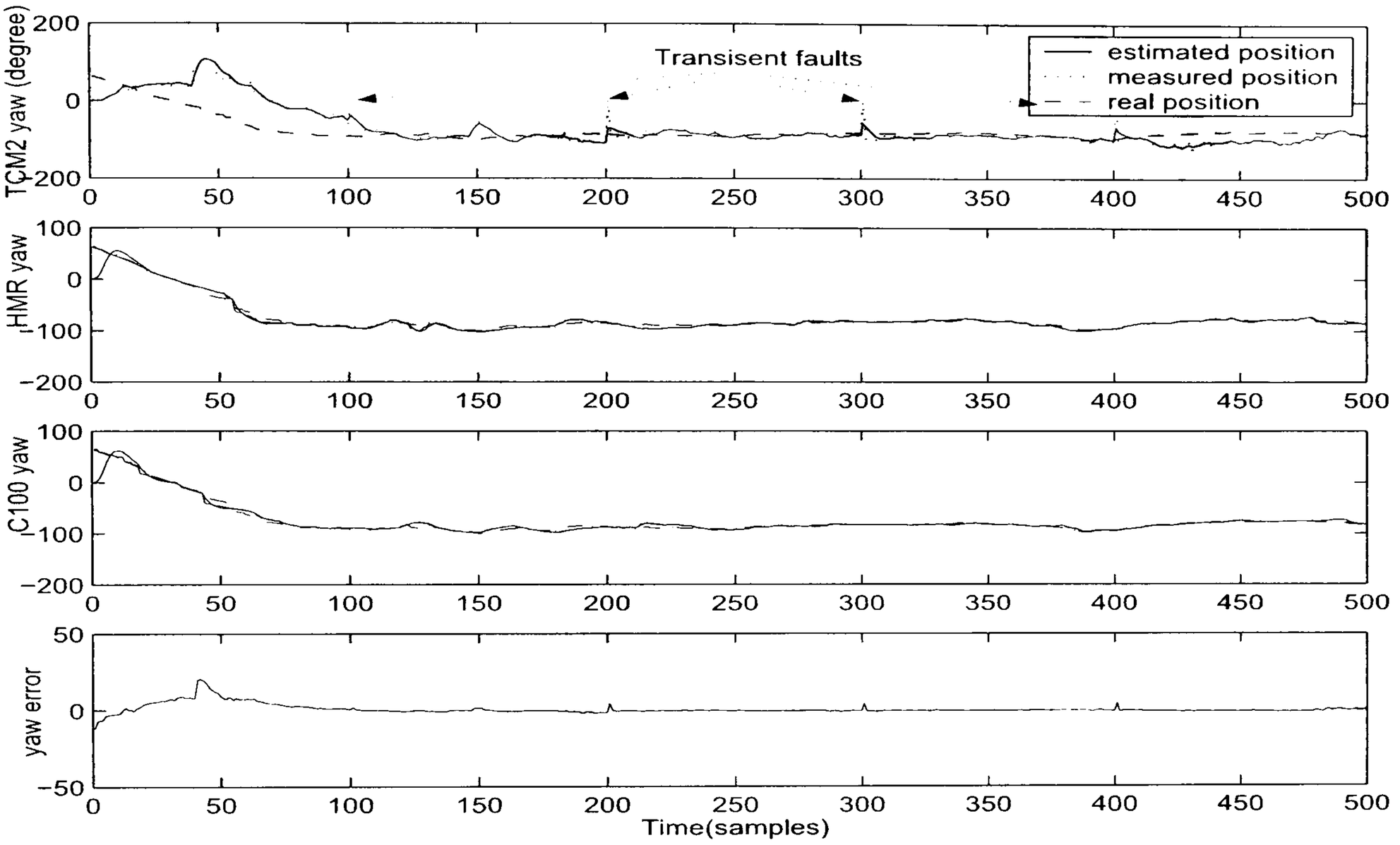

Figure 5.8: FLA-DKF performance with transient faults on the TCM2

FLA-FKF with fixed feedback factors

The performance of a FLA-FKF is presented in Figure 5.9, in which the sensor's accuracy decides the feedback factors in the FKF. After experiments, the most accurate compass was found to be the HMR 3000 and was given a 0.5 feedback factor. Whilst for KVH C100 and TCM2 the feedback factors were 0.35 and 0.15 respectively. The global estimation accuracy of this algorithm is higher than the FLA-DKF algorithm.

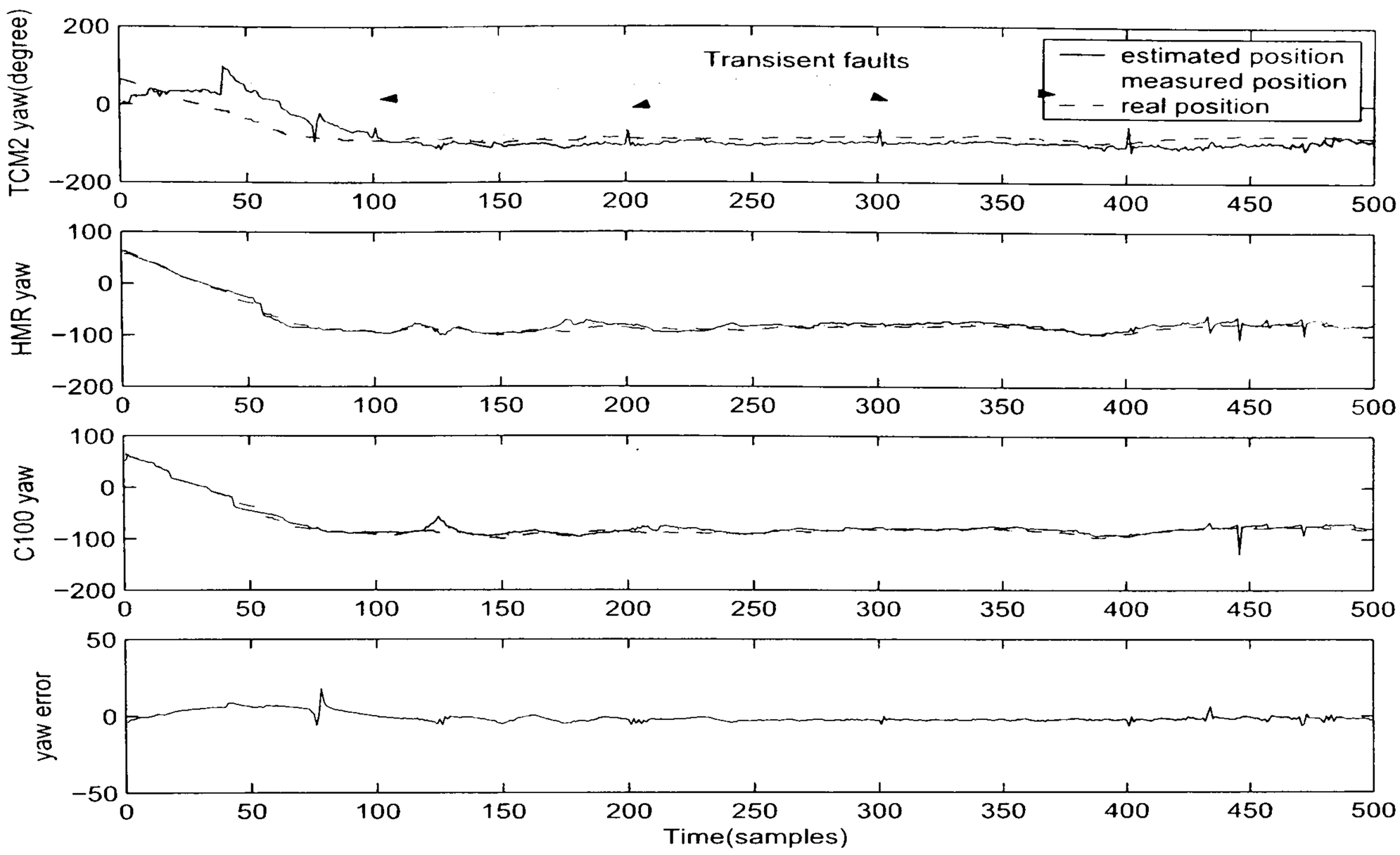

Figure 5.9: FLA-FKF with fixed feedback factors under transient faults on the TCM2

FLA-FKF with adaptive feedback factors

In Figure 5.10 the results for the FLA-FKF, which include the adaptive feedback factors, are presented. The feedback factor values are shown in Figure 5.11. Compared with previous simulation results, this algorithm outputs the best fusion result under transient sensor faults. The information feedback factors were tuned continuously according to the accuracies of each local Kalman filters.

In this section, with transient faults on the TCM2 compass, FLA-CKF, FLA-DKF and FLA-FKF are employed to fuse the sensor measurements. In Figure 5.7, the FLA-CKF algorithm was implemented with transient faults in the TCM2 compass. When the transient faults occurred in the TCM2, the KVH C100 and HMR 3000 compasses operated under normal conditions. The result shows that the FLA-CKF cannot minimize the transient fault disturbances effectively. Therefore the FLA-CKF is not suitable for a fault tolerant multi-sensor navigation system. FLA-DKF and FLA-FKF with fixed feedback algorithm can reduce the sensor faults, however the FLA-FKF algorithm with adaptive feedback can

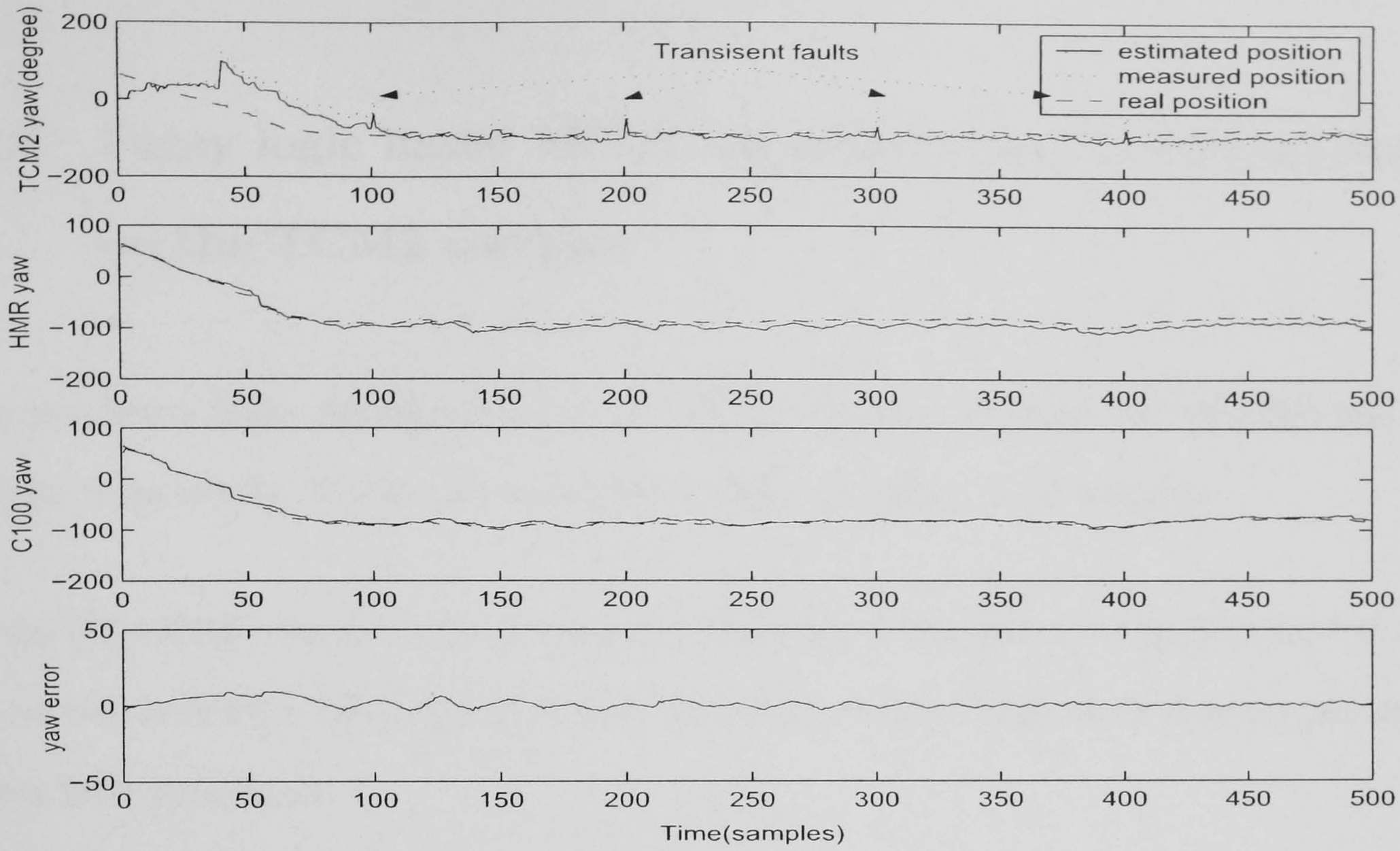

Figure 5.10: FLA-FKF with adaptive feedback factors under transient faults on the TCM2

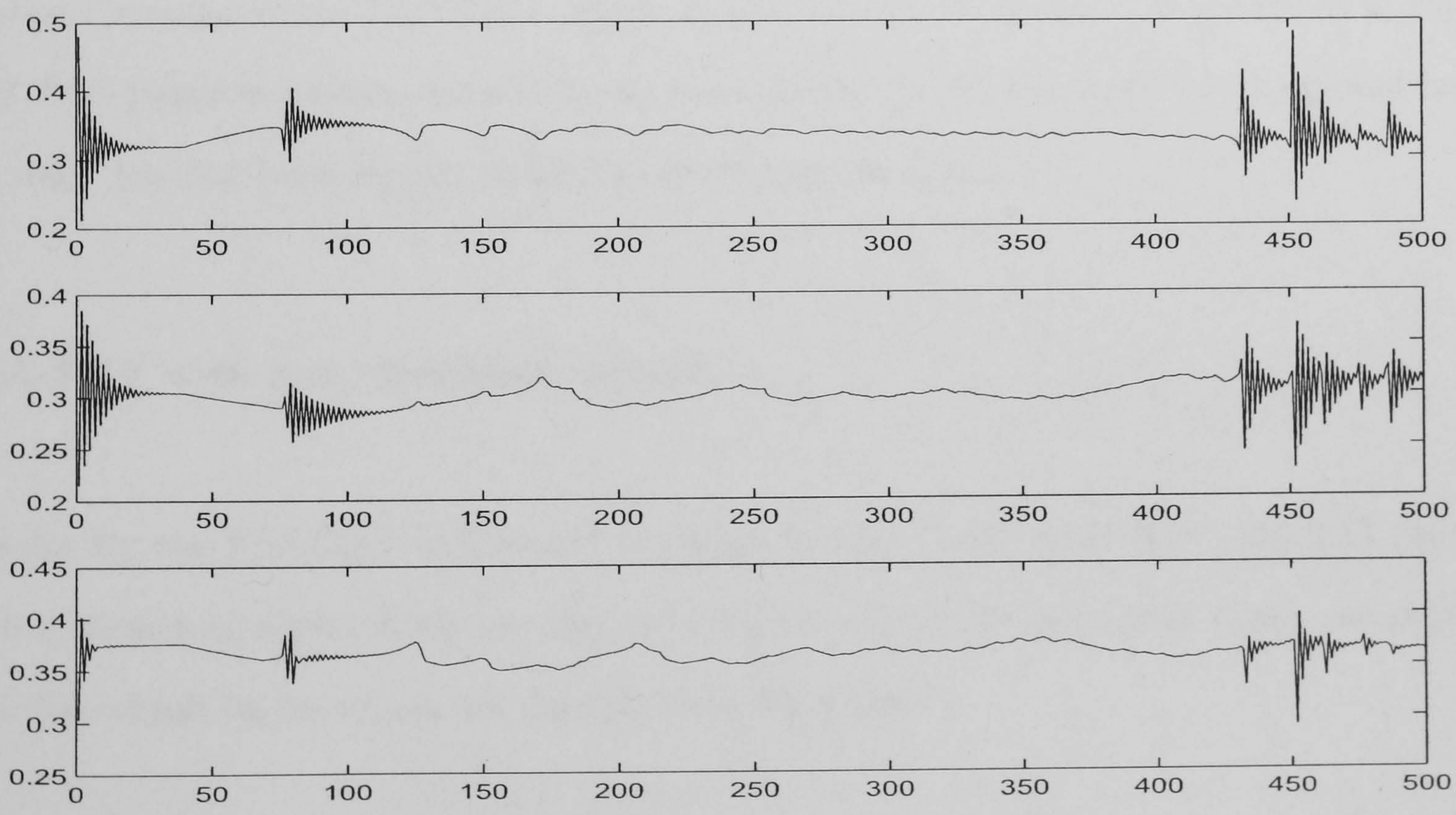

Figure 5.11: Information feedback factors (β_i)under transient faults on the TCM2

effectively improve the fusion accuracy.

5.6.2 Fuzzy logic based MSDF algorithms with persistent faults on the TCM2 compass

Four persistent faults are simulated on the TCM2 compass at times 100, 200, 300 and 400 samples respectively. Fixed values are given with a duration of 10 samples.

As the FLA-CKF was not robust enough to tolerate transient faults in Section 5.6.1, in this section only FLA-DKF and FLA-FKF algorithms will be implemented under persistent sensor fault conditions.

FLA-DKF

The performance of the FLA-DKF under a persistent fault condition is presented in Figure 5.12. The persistent faults are effectively reduced in local filters, therefore the global fusion accuracy has not been largely disturbed by the sensor faults.

FLA-FKF with fixed feedback factors

Results for the FLA-FKF with fixed feedback factors (same as in Section 5.6.1) running with a persistent sensor fault are shown in Figure 5.13. The persistent faults are reduced and the overall fusion errors are smaller than FLA-DKF.

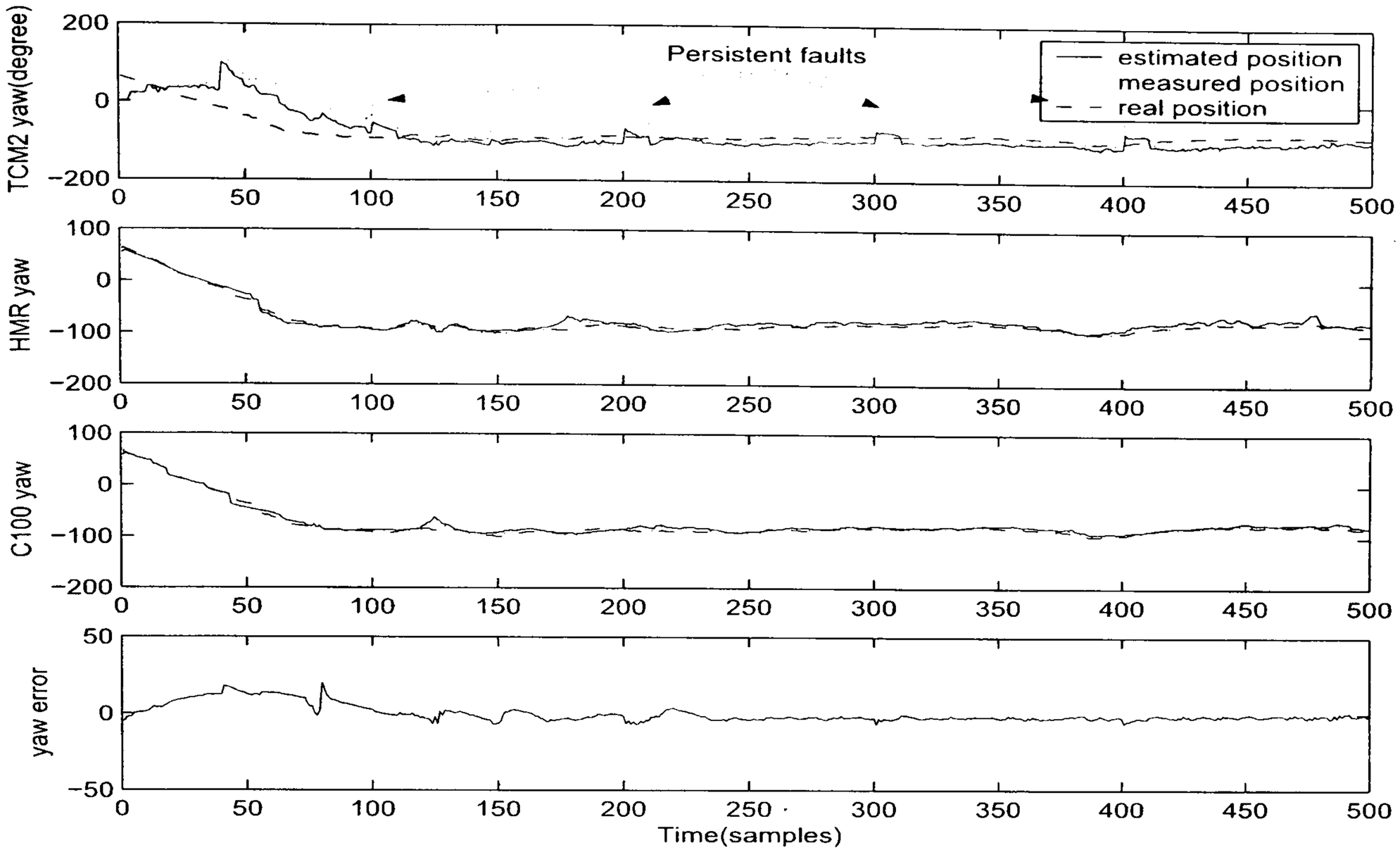

Figure 5.12: FLA-DKF under persistent faults on the TCM2

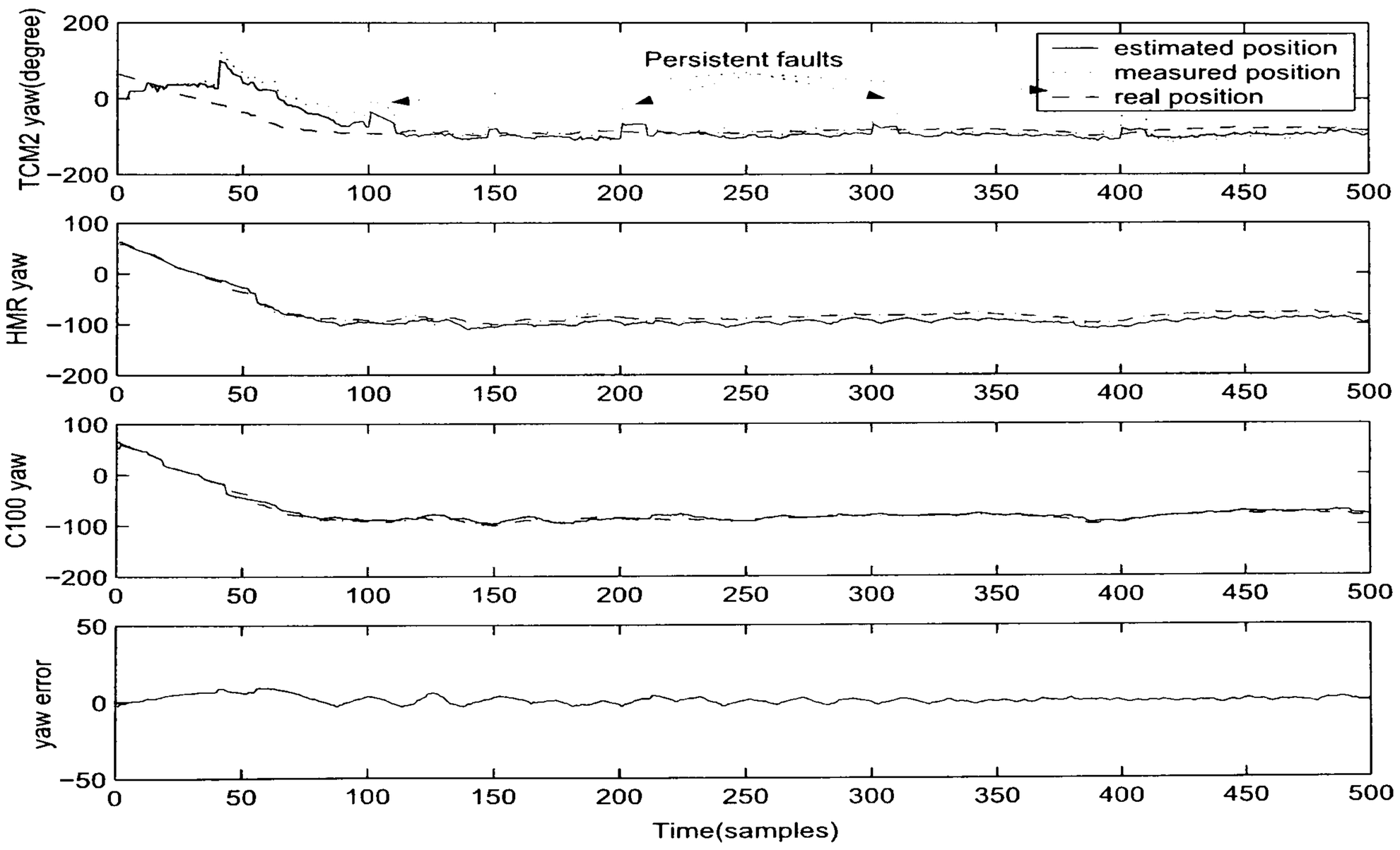

Figure 5.13: FLA-FKF with fixed feedback factors under persistent faults on the TCM2

FLA-FKF with adaptive feedback factors

The performance of the FLA-FKF with adaptive feedback is shown in Figure 5.14, where the feedback factors for the FLA-FKF are shown in Figure 5.15. Similar with the transient fault situations, FLA-FKF with adaptive feedback approach gives the best fusion accuracy, and the information feedback factors are adaptive according to the local filters' output.

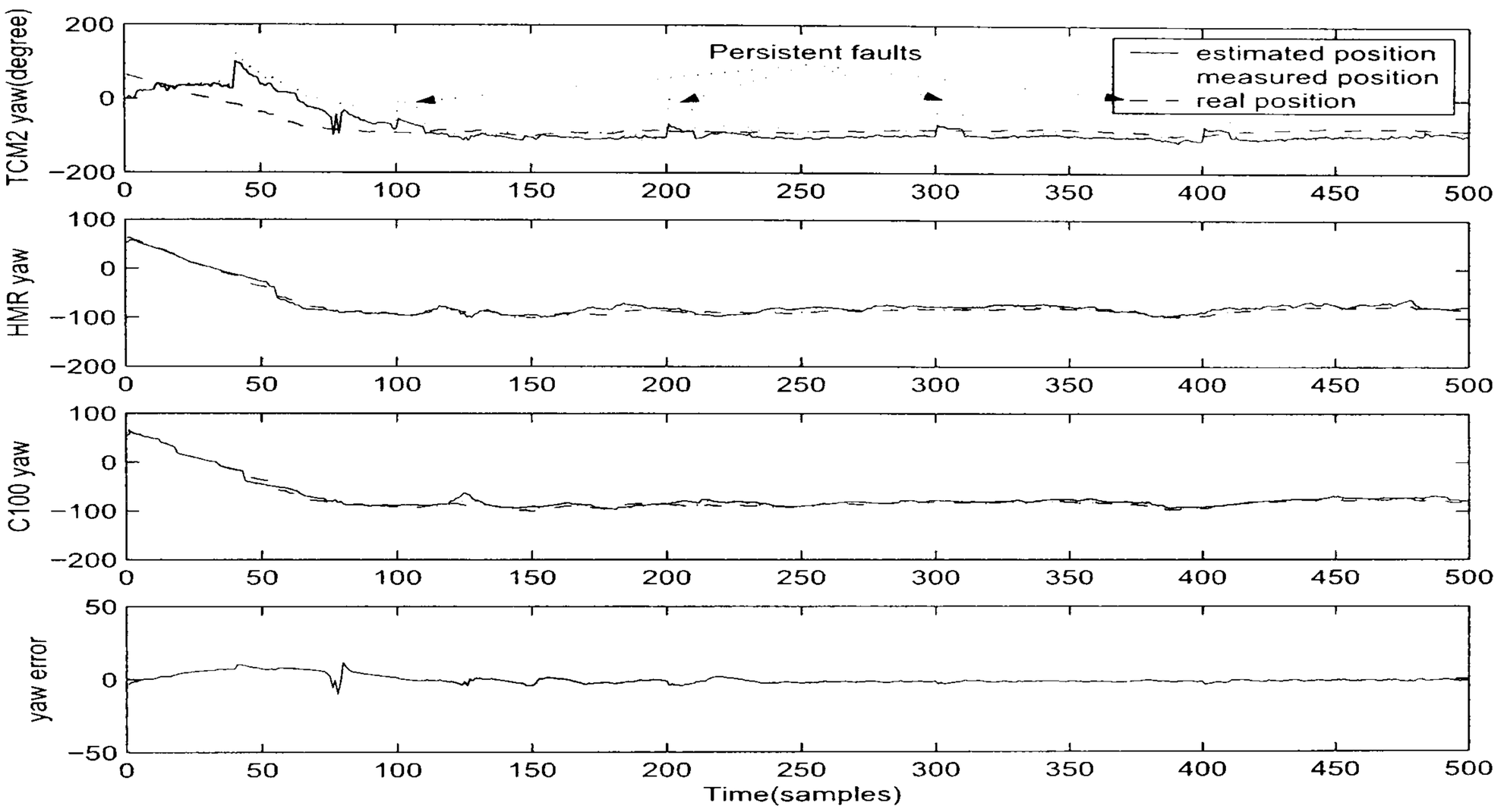

Figure 5.14: FLA-FKF with adaptive feedback factors under persistent faults on the TCM2

Figure 5.8 and Figure 5.12 present the performance of the FLA-DKF with the transient and persistent faults in the TCM2 respectively. The results demonstrate that the FLA-DKF can output a stable global estimation. In comparing fusion accuracy, the FLA-DKF reduced the heading RMSE (from 201 to 500 samples) to 0.8520 degree, which is nearly $\frac{2}{3}$ that of the FLA-CKF. For the FLA-DKF with persistent faults in the TCM2, the heading RMSE(from 201 to 500 samples) increases to 0.9230 degree. The reason for the increase in error is that the persistent faults were simulated on the TCM2 for 10 samples, while the transient faults last on the TCM2 only for 1 sample each time.

Figure 5.9 and Figure 5.13 show the performances of the fixed feedback FLA-FKF algorithm, where the feedback factors were distributed according to the sensors' stability. This

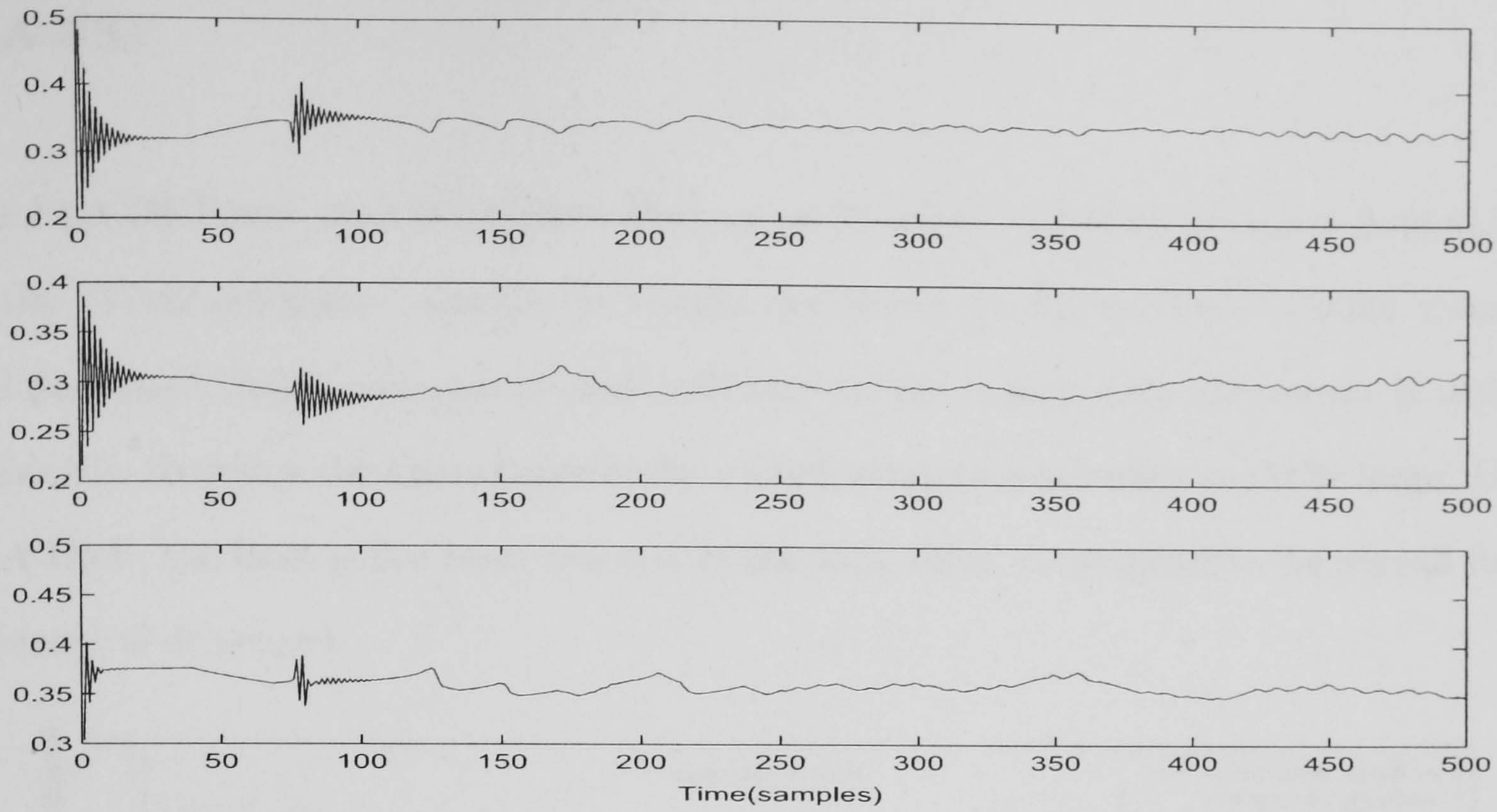

Figure 5.15: Information feedback factors (β_i)under persistent faults on the TCM2

approach gives a higher fusion accuracy compared with the FLA-DKF.

Whereas, in Figure 5.10 and Figure 5.14, the FLA-FKF with an adaptive feedback algorithm produced the most accurate and robust performance under transient and persistent fault situations. The information feedback factors shown in Figure 5.11 and Figure 5.15 were tuned continually according to the accuracies of each local Kalman filter. The feedback factors play a vital role in improving the MSDF robustness and accuracy.

5.6.3 Fuzzy logic based MSDF algorithms with a permanent fault on the TCM2 compass

In this section, a permanent fault is simulated on the TCM2 compass from 300 samples with an output of zero.

FLA-DKF

The FLA-DKF was used to estimate the yaw angle when a permanent sensor fault existed in the TCM2 compass. Simulation results are shown in Figure 5.16. Unlike transient and persistent faults, permanent fault will last on the sensor until the sensor is isolated physically, therefore the disturbance to the global estimation accuracy could be large. Using FLA-DKF, the fault is not been reduced in the local filter. consequently, the overall fusion accuracy is decreased.

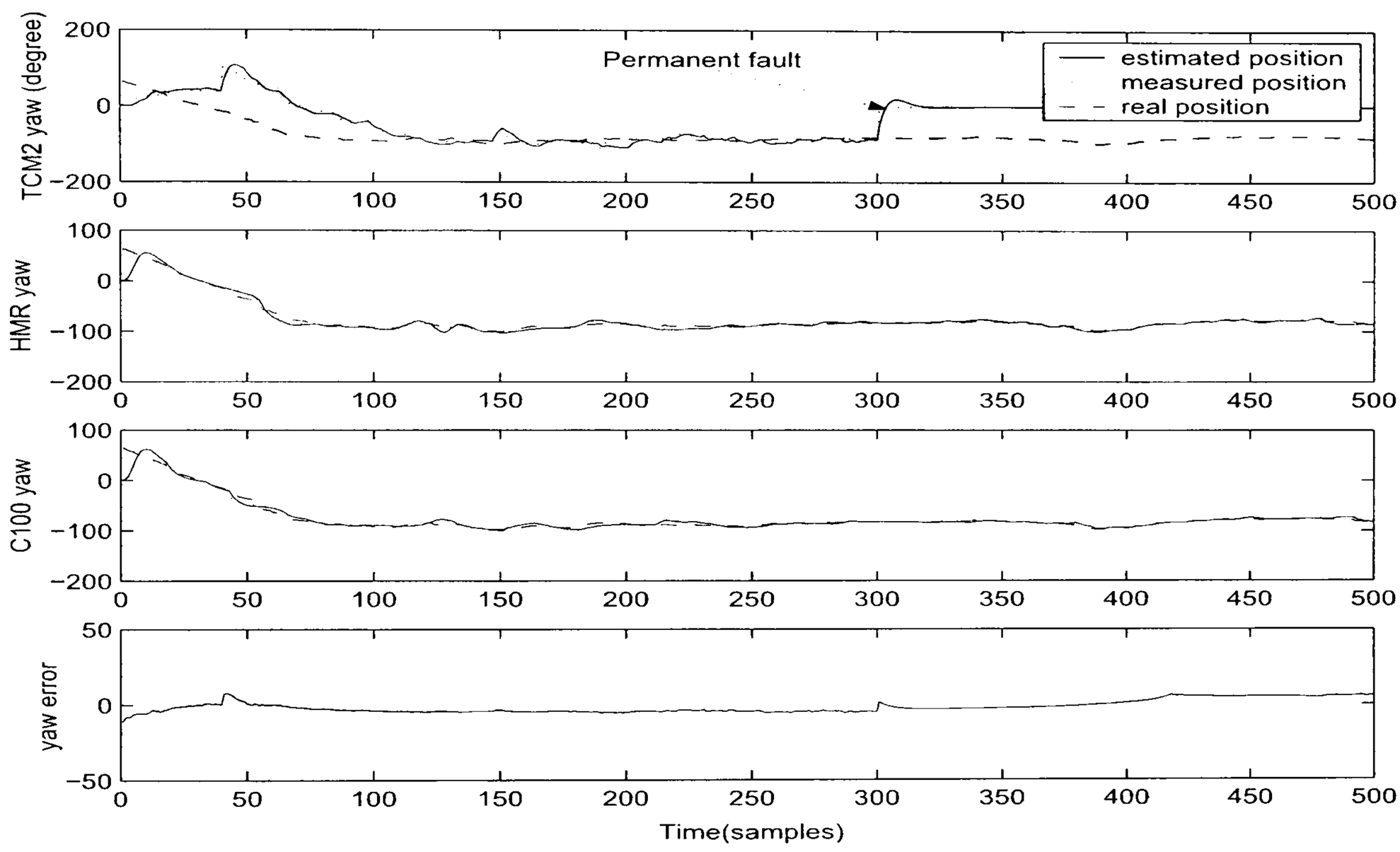

Figure 5.16: FLA-DKF under a permanent fault on the TCM2

FLA-FKF with fixed feedback factors

Also for the permanent fault situation, the FLA-FKF algorithm performance with fixed feedback factors (same as in Section 5.6.1) is presented in Figure 5.17. The permanent fault is reduced in local KF, therefore the overall fusion accuracy is better than FLA-DKF.

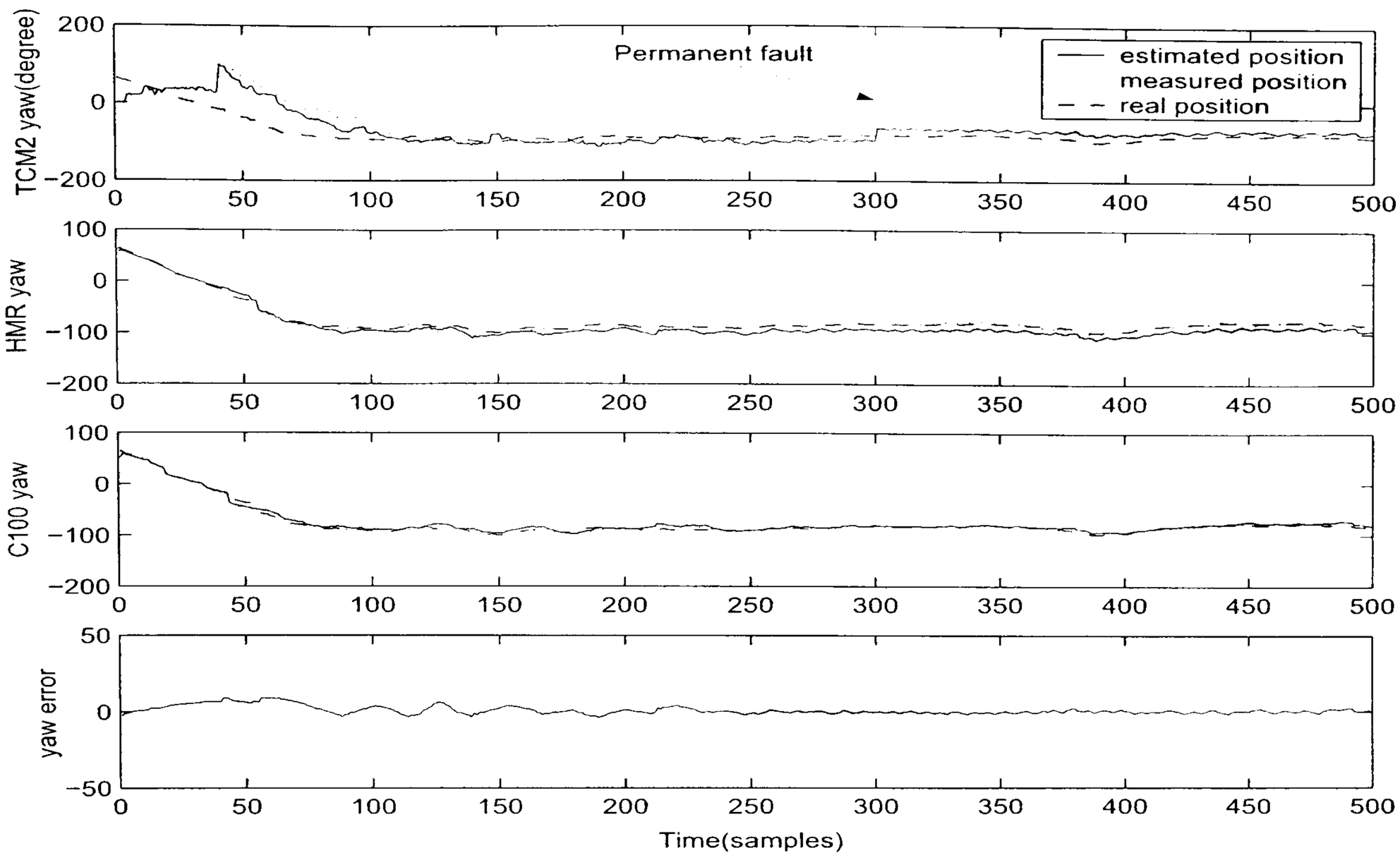

Figure 5.17: FLA-FKF with fixed feedback factors under a permanent fault on the TCM2

FLA-FKF with adaptive feedback factors

The FLA-FKF algorithm with adaptive feedback was applied to the compasses, whilst operating under a permanent sensor fault condition in the TCM2 compass. The simulation results are presented in Figure 5.18 and the adaptive feedback factors are shown in Figure 5.19. Using this approach, the permanent fault is effectively reduced and global estimation error is decreased.

A permanent fault rarely occurs under normal operating condition, however it brings serious problems to a navigation system if such an event takes place. In Section 5.6.3, a permanent fault is simulated on the TCM2 to verify the fault tolerance capabilities of the algorithms.

From Figure 5.16 to Figure 5.19, the FLA-DKF and FLA-FKF algorithms were employed under a permanent fault condition in the TCM2. Comparing with the FLA-DKF, the fixed feedback FLA-FKF gave more accurate global estimations. In the FLA-DKF, three local fuzzy logic Kalman filters were treated evenly in the master filter, also there is no infor-

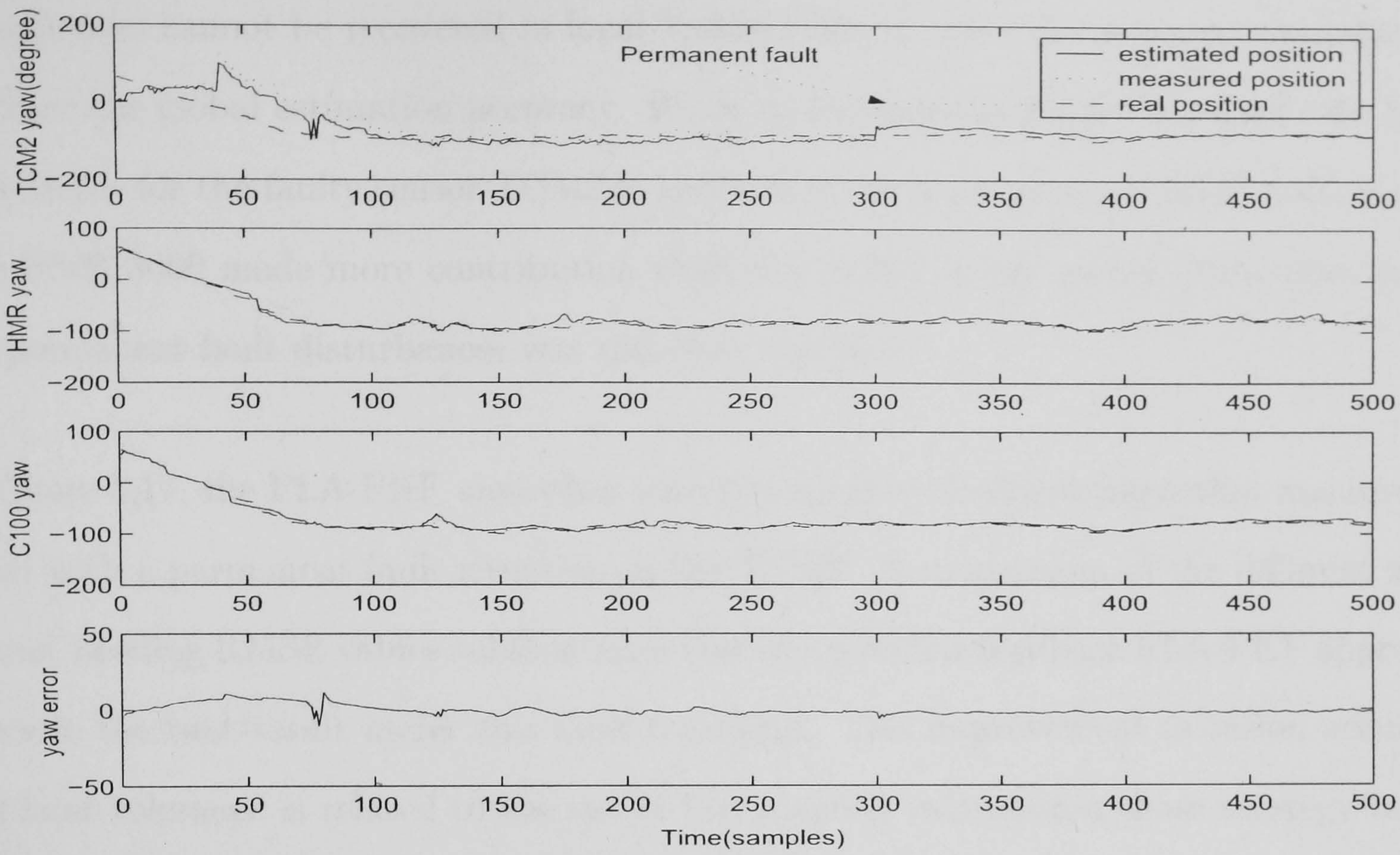

Figure 5.18: FLA-FKF with adaptive feedback factors under a permanent fault on the TCM2

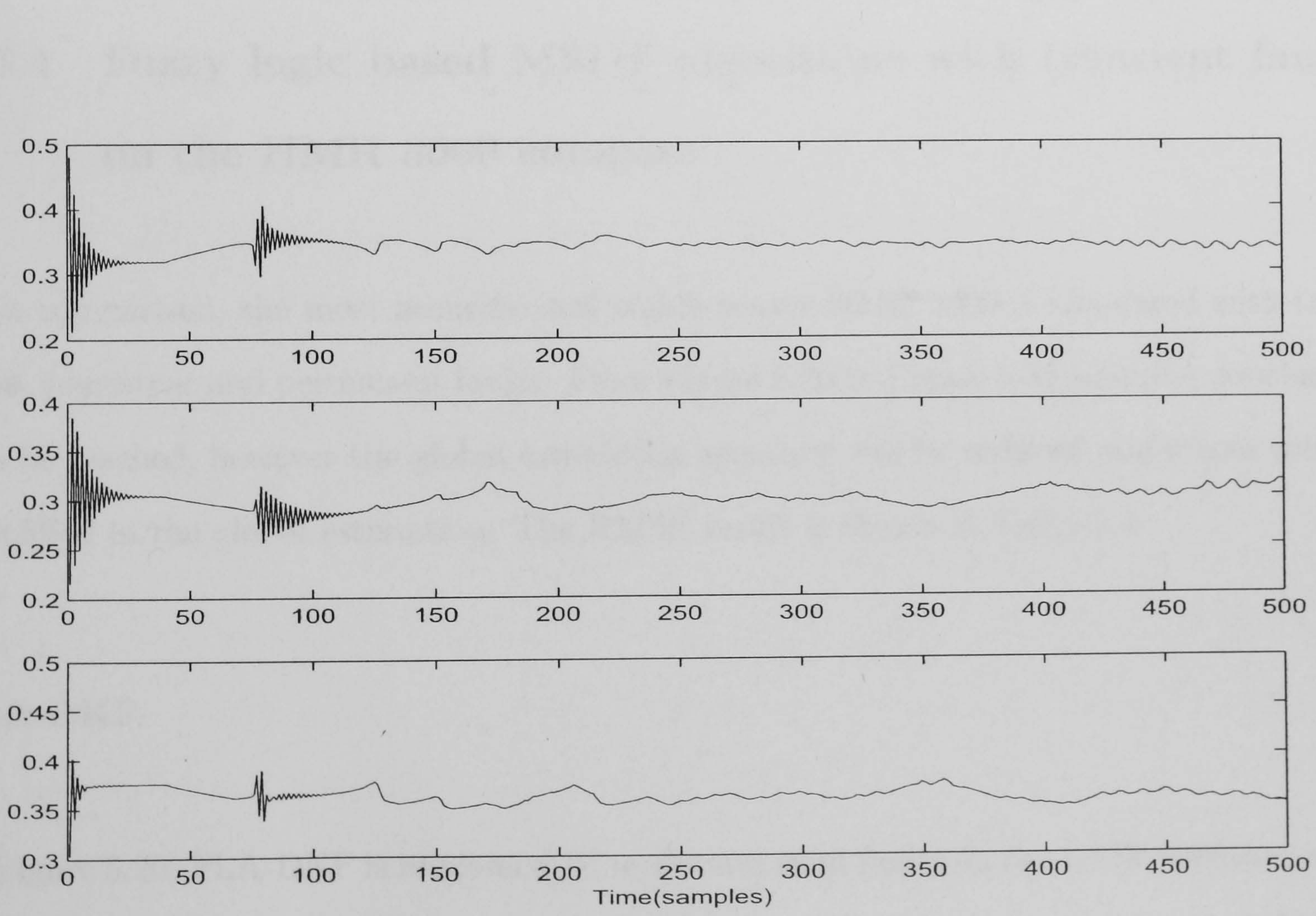

Figure 5.19: Information feedback factors (β_i)under a permanent fault on the TCM2

mation feedback from the master filter to the local filters, so when the permanent fault disturbances cannot be recovered in local Kalman filters, these disturbances consequently decrease the global estimation accuracy. While in the fixed feedback FLA-FKF, the feedback factor for the faulty sensor TCM2 is lower than the most accurate HMR 3000 sensor. The HMR 3000 made more contribution than the TCM2 to the global estimation, hence the permanent fault disturbances was therefore reduced.

In Figure 5.17, the FLA-FKF algorithm with the adaptive feedback algorithm was investigated with a permanent fault situation in the TCM2. A comparison of the different algorithms' heading RMSE values substantiates that the adaptive feedback FLA-FKF approach provides the best result under this fault condition. This improvement in fusion accuracy and fault tolerance is related to the use of the adaptive information share strategy in the FLA-FKF.

5.6.4 Fuzzy logic based MSDF algorithms with transient faults on the HMR 3000 compass

As a comparison, the most accurate and stable sensor HMR 3000 is simulated with transient, persistent and permanent faults. From Figure 5.20 to Figure 5.31 a similar conclusion can be reached, however the global estimation accuracy will be reduced and errors will be amplified in the global estimation. The RMSE result is shown in Table 5.4.

FLA-DKF

In Figure 5.20, FLA-DKF is implemented under transient faults on the HMR 3000 compass. The transient faults are reduced in local filter and global estimation error is reduced.

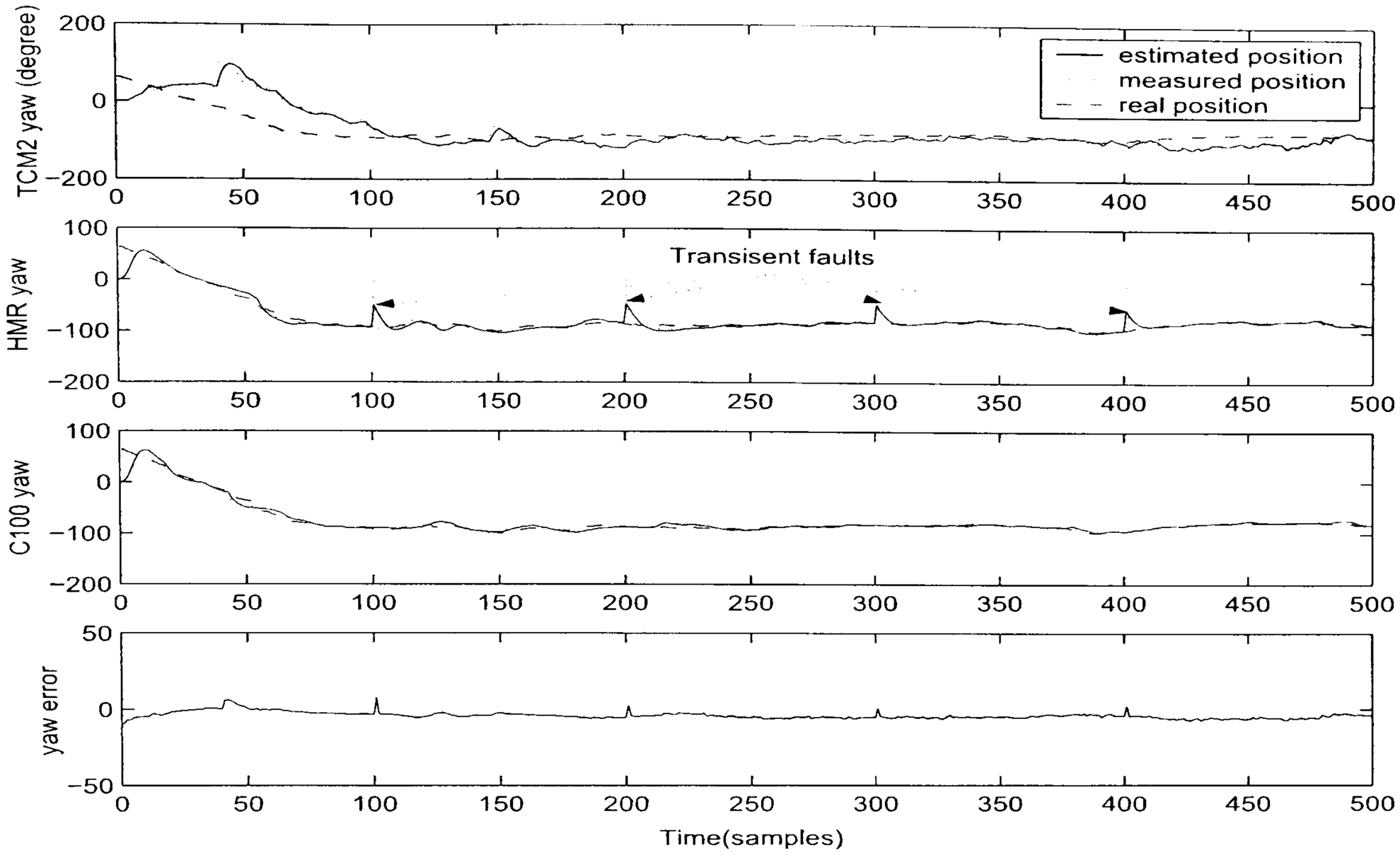

Figure 5.20: FLA-DKF performance with transient faults on the HMR 3000 compass

FLA-FKF with fixed feedback factors

Figure 5.21 presents the simulation result of FLA-FKF with a fixed feedback factor algorithm under transient faults on the HMR 3000 compass. Comparing with Figure 5.20, the FLA-FKF with fixed feedback algorithm output more accurate fusion results than FLA-DKF.

FLA-FKF with adaptive feedback factors

FLA-FKF with an adaptive feedback factor algorithm is employed, the simulation result and feedback factors are shown in Figure 5.22 and Figure 5.23 respectively. This approach presents the best fusion results and it can effectively reduce the fault disturbances by employing adaptive information feedback factors.

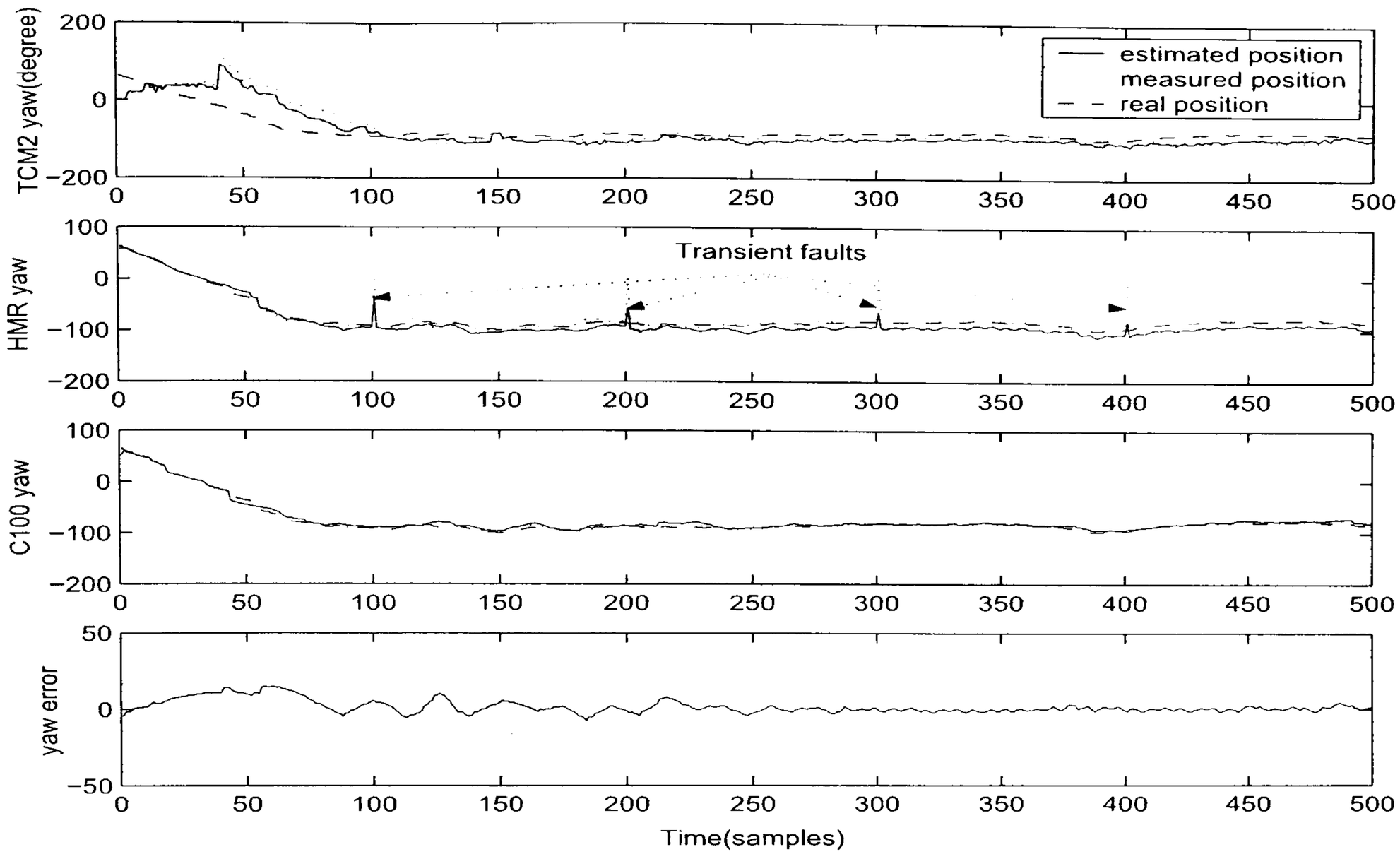

Figure 5.21: FLA-FKF performance with fixed feedback factors under transient faults on the HMR 3000 compass

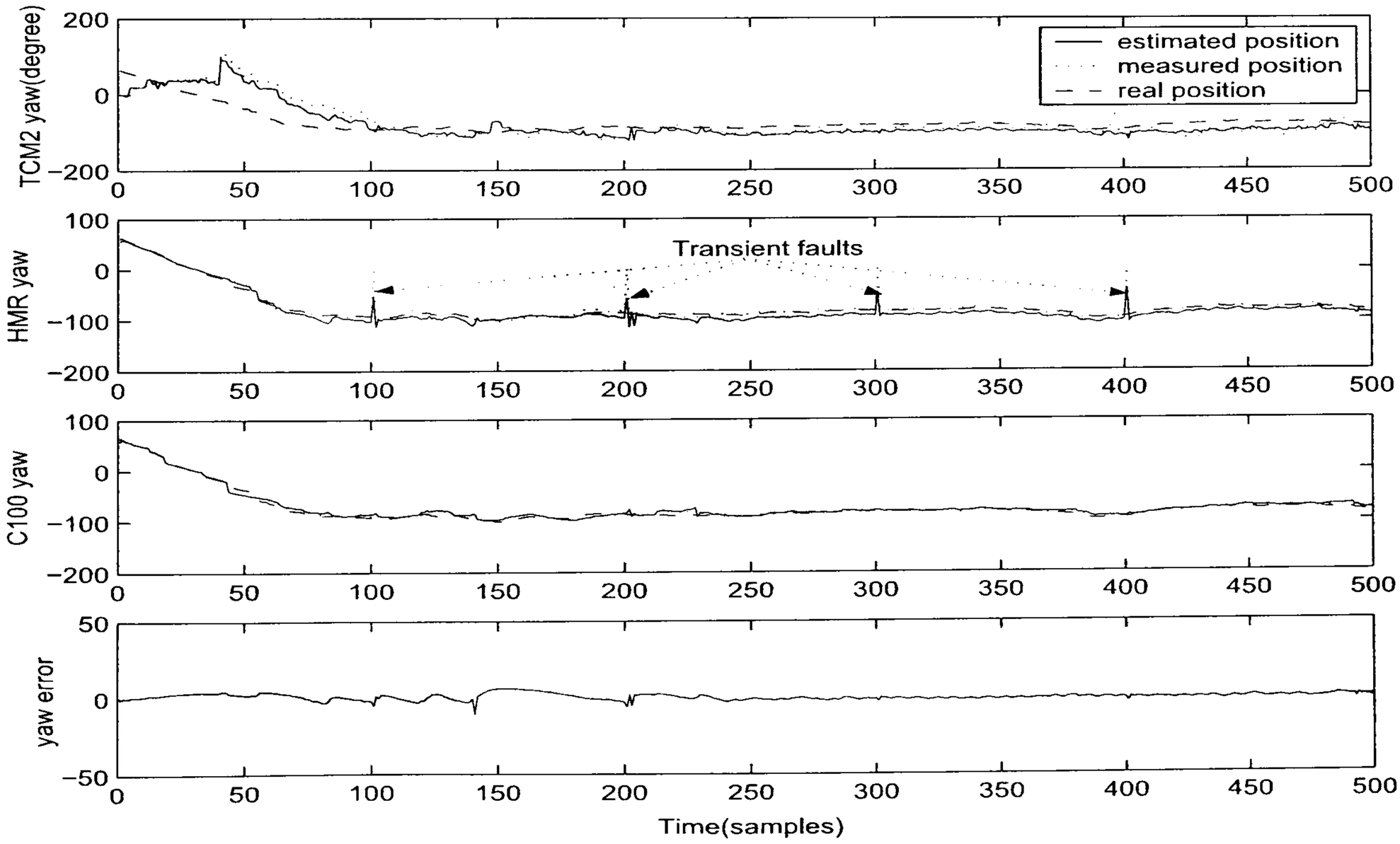

Figure 5.22: FLA-FKF performance with adaptive feedback factors under transient faults on the HMR 3000 compass

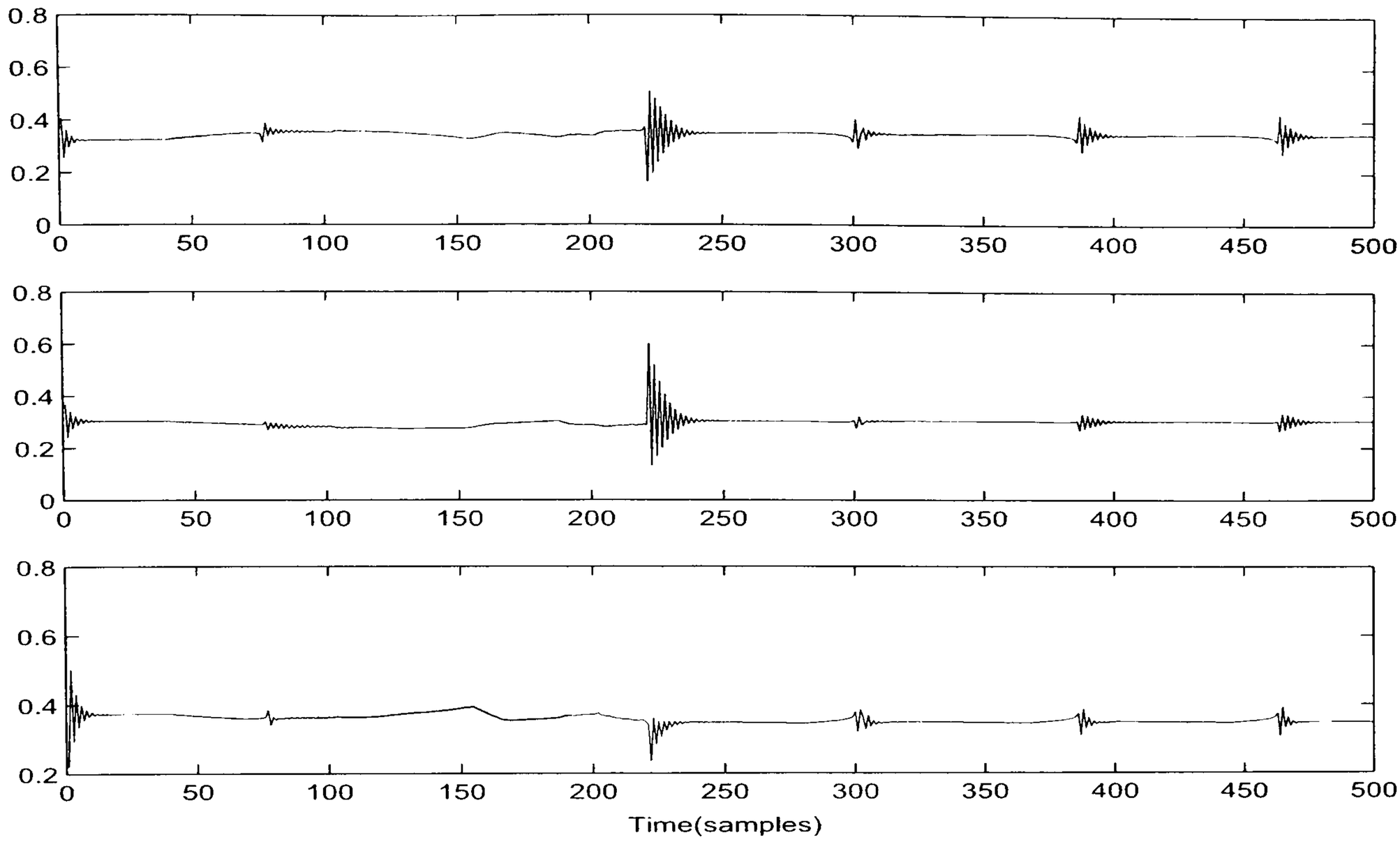

Figure 5.23: Information feedback factors (β_i)under transient faults on the HMR 3000

5.6.5 Fuzzy logic based MSDF algorithms with persistent faults on the HMR 3000 compass

FLA-DKF

The simulation result shown in Figure 5.24 presents the FLA-DKF algorithm performance under persistent faults on the HMR 3000 compass. The persistent faults a re generally reduced by local fuzzy logic KF.

FLA-FKF with fixed feedback factors

Results for the FLA-FKF with fixed feedback factors (same as in Section 5.6.1) running with transient sensor faults on the HMR 3000 compass are shown in Figure 5.25. The fault disturbances are reduced and a better fusion accuracy is achieved than FLA-DKF.

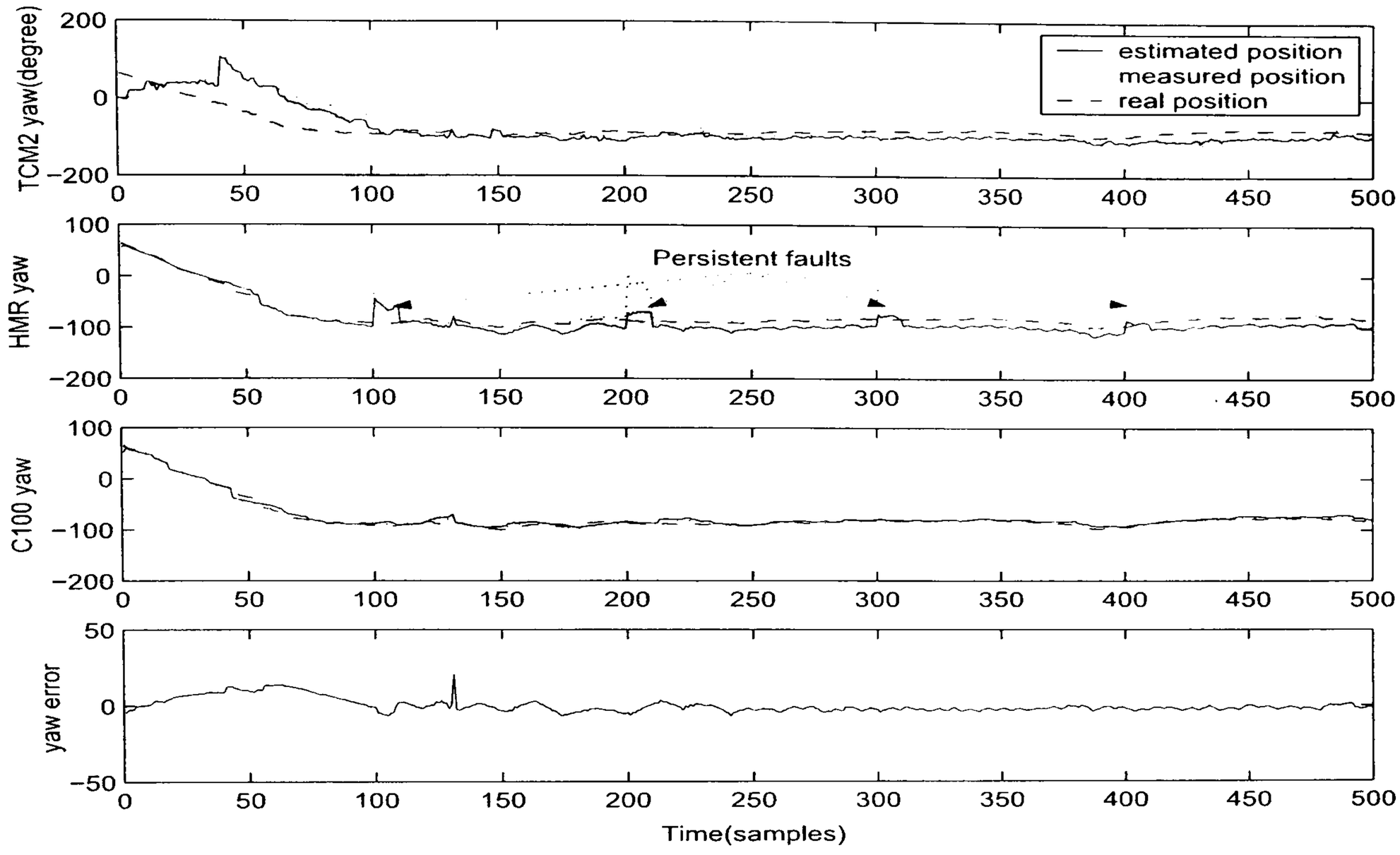

Figure 5.24: FLA-DKF performance under persistent faults on the HMR 3000 compass

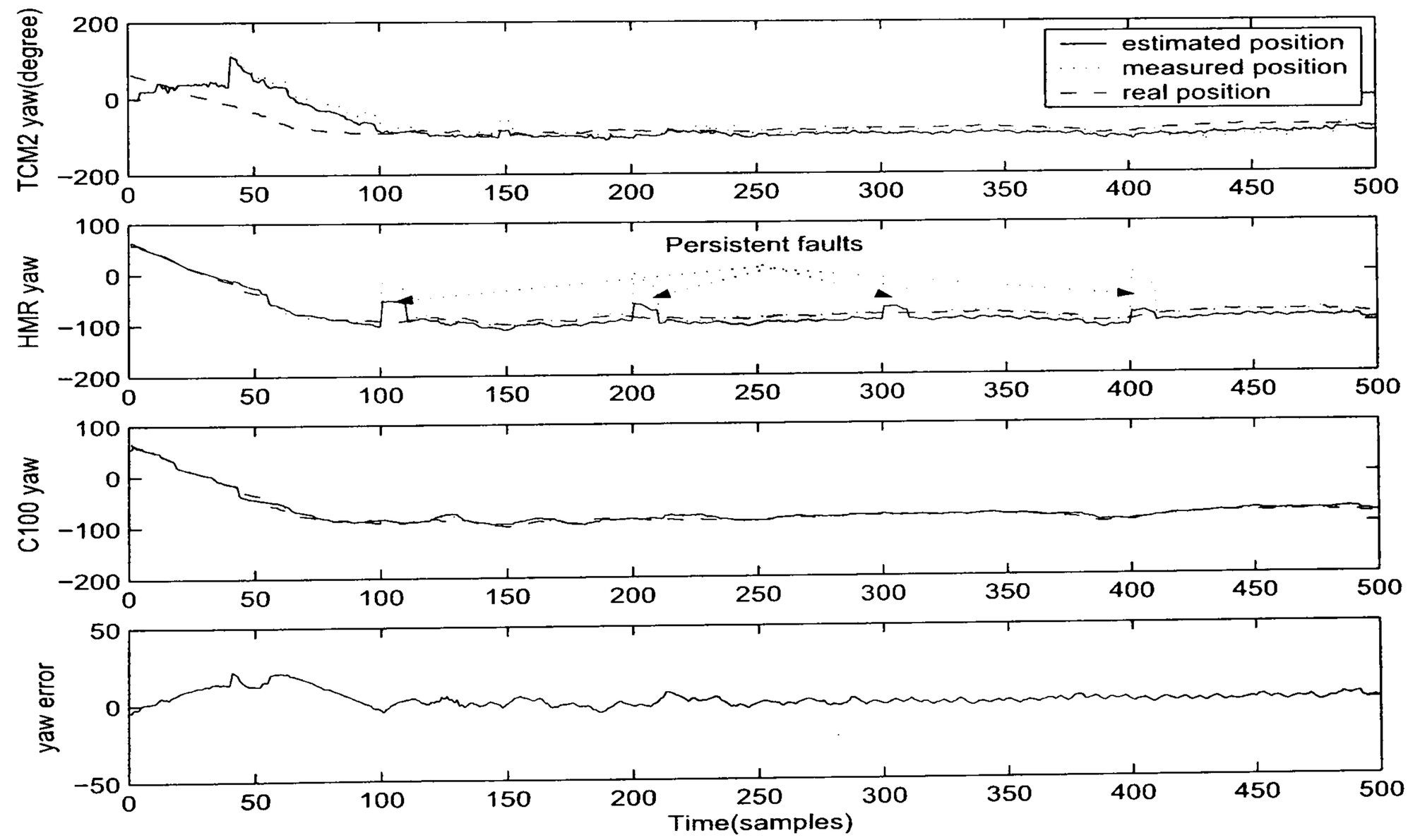

Figure 5.25: FLA-FKF performance with fixed feedback factors under persistent faults on the HMR 3000 compass

FLA-FKF with adaptive feedback factors

In Figure 5.26, FLA-FKF with an adaptive feedback algorithm is implemented, the feedback factors are shown in Figure 5.27. Similar as the simulation above, this approach generate the best fault tolerant and most accurate fusion results.

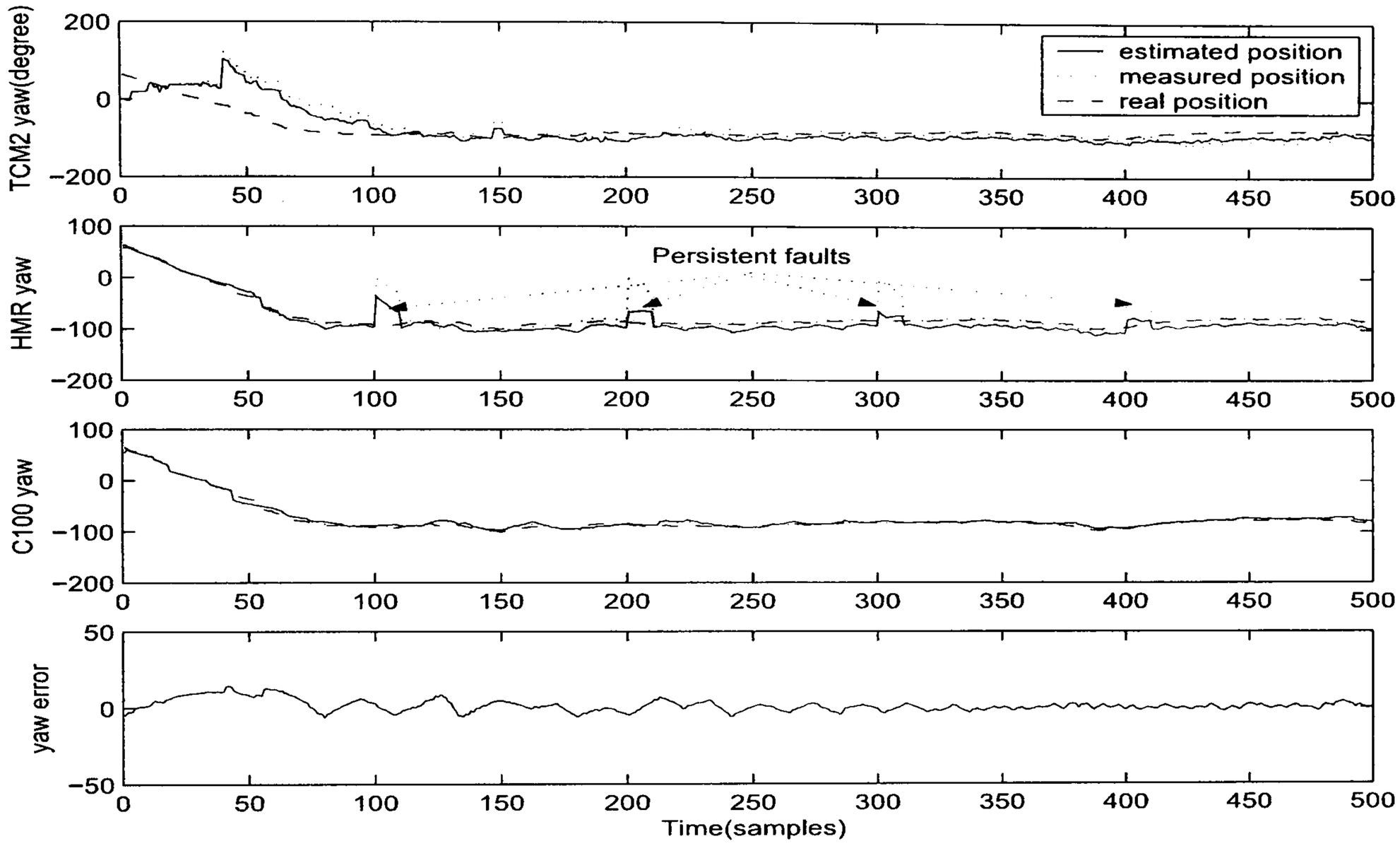

Figure 5.26: FLA-FKF performance with adaptive feedback factors under persistent faults on the HMR 3000 compass

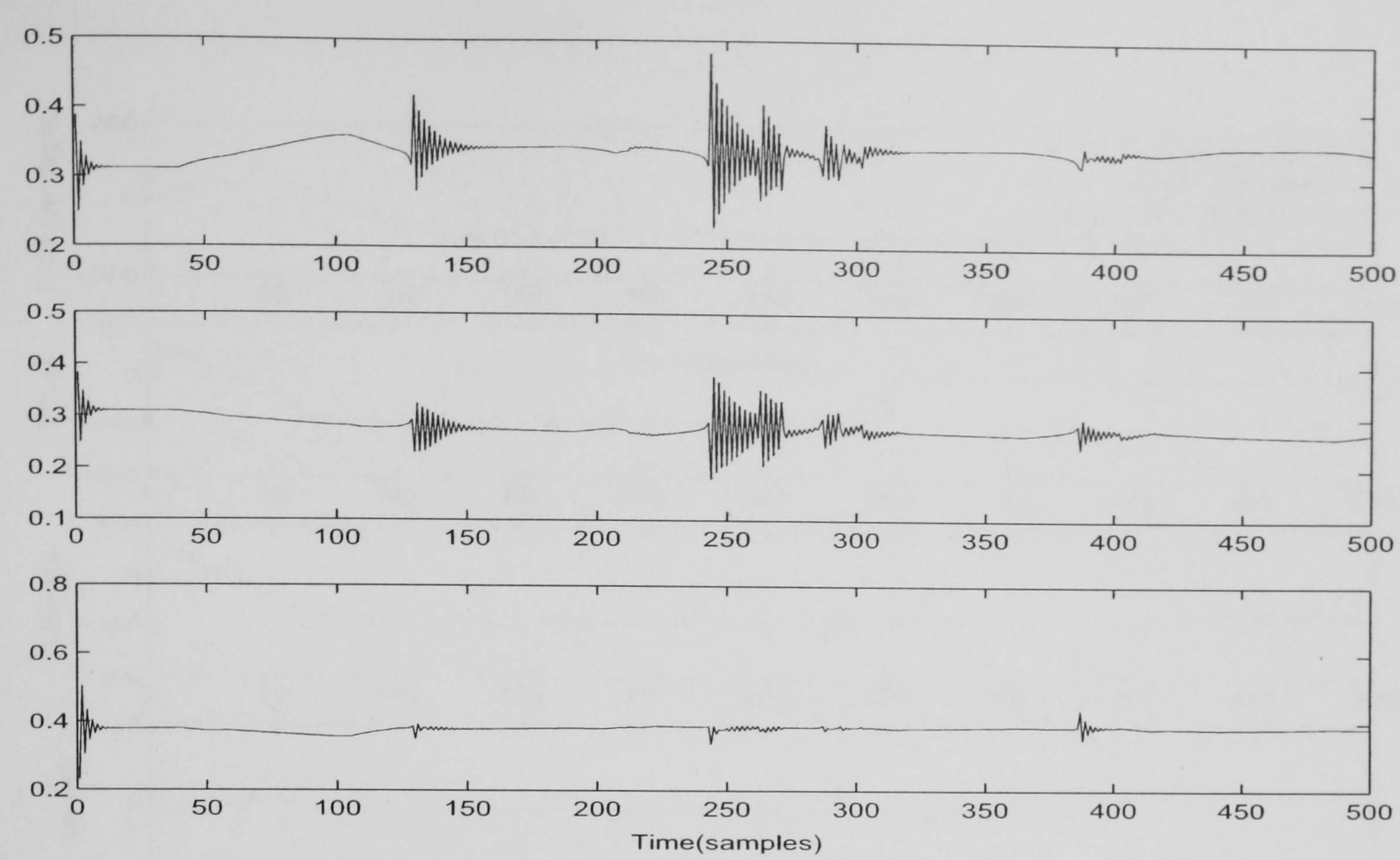

Figure 5.27: Information feedback factors (β_i)under persistent faults on the HMR 3000

5.6.6 Fuzzy logic based MSDF algorithms with a permanent fault on the HMR 3000 compass

FLA-DKF

A permanent fault occurred at the HMR 3000 compass, the FLA-DKF is employed to test the fault tolerant capabilities, the result is shown in Figure 5.28. From the result, apparently, the local filter cannot minimize the permanent fault and the overall fusion accuracy is reduced.

FLA-FKF with fixed feedback factors

Also under the permanent situation, the FLA-FKF with fixed feedback factors (same as in Section 5.6.1) performance is presented in Figure 5.29. The permanent fault disturbance is generally reduced. The overall fusion accuracy is better than FLA-DKF.

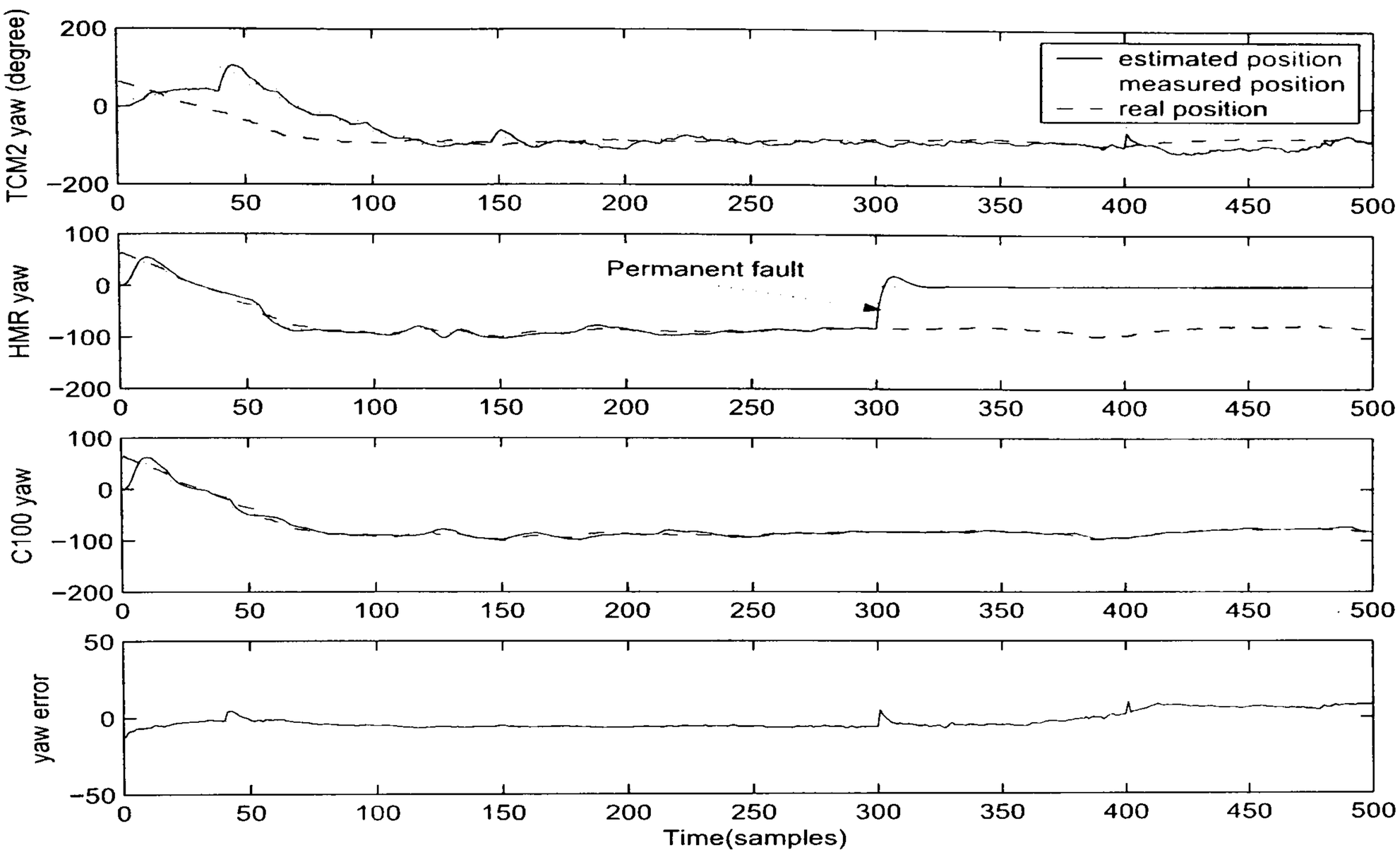

Figure 5.28: FLA-DKF performance with a permanent fault on the HMR 3000 compass

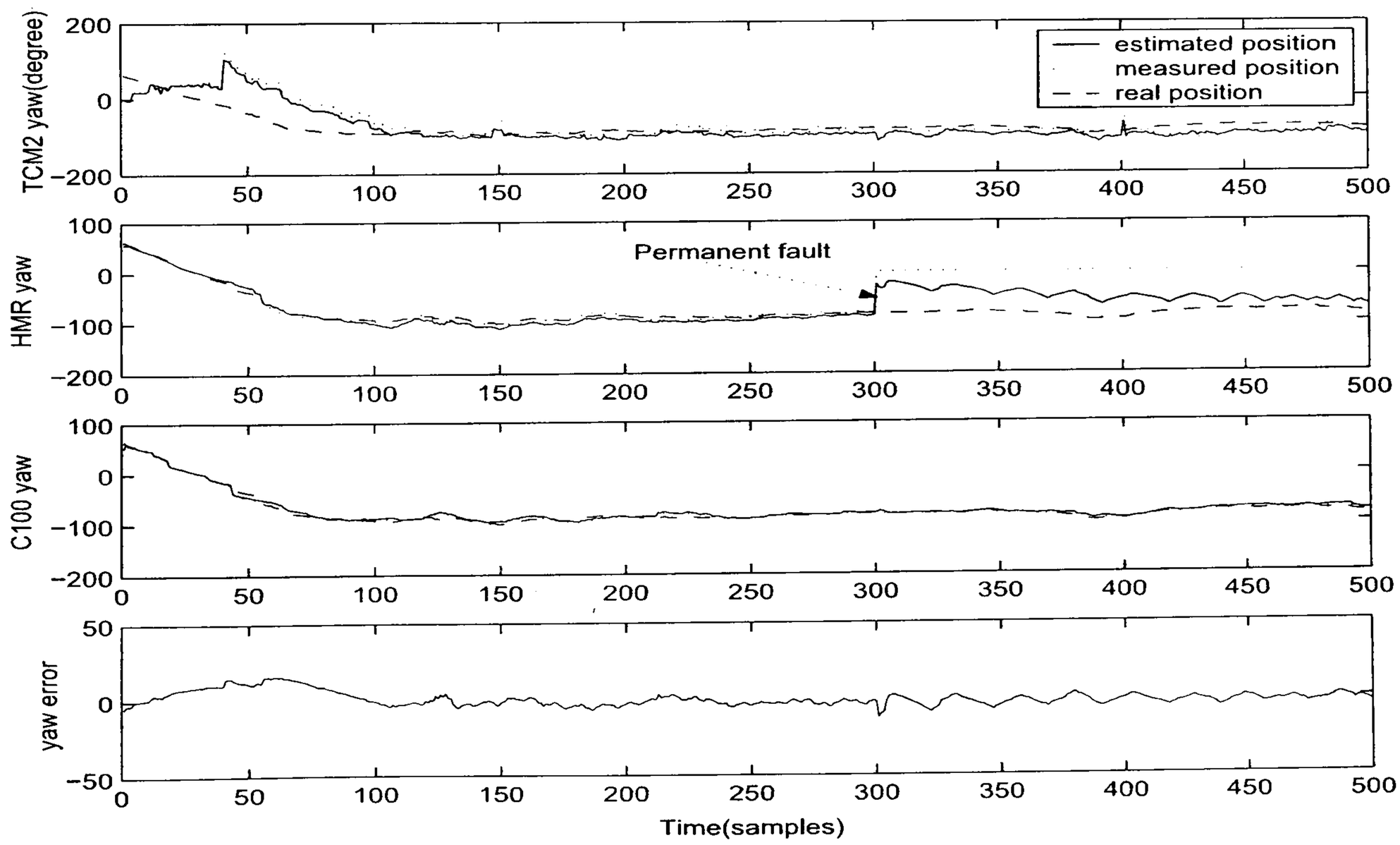

Figure 5.29: FLA-FKF performance with fixed feedback factors under a permanent fault on the HMR 3000 compass

FLA-FKF with adaptive feedback factors

Finally, the FLA-FKF with an adaptive feedback factor performance is shown in Figure 5.30, the adaptive feedback factors are shown in Figure 5.31. Again, this approach output the most accurate fusion result under a permanent fault on the HMR 3000 compass. The adaptive feedback factors play a vital role in improving the fusion accuracy.

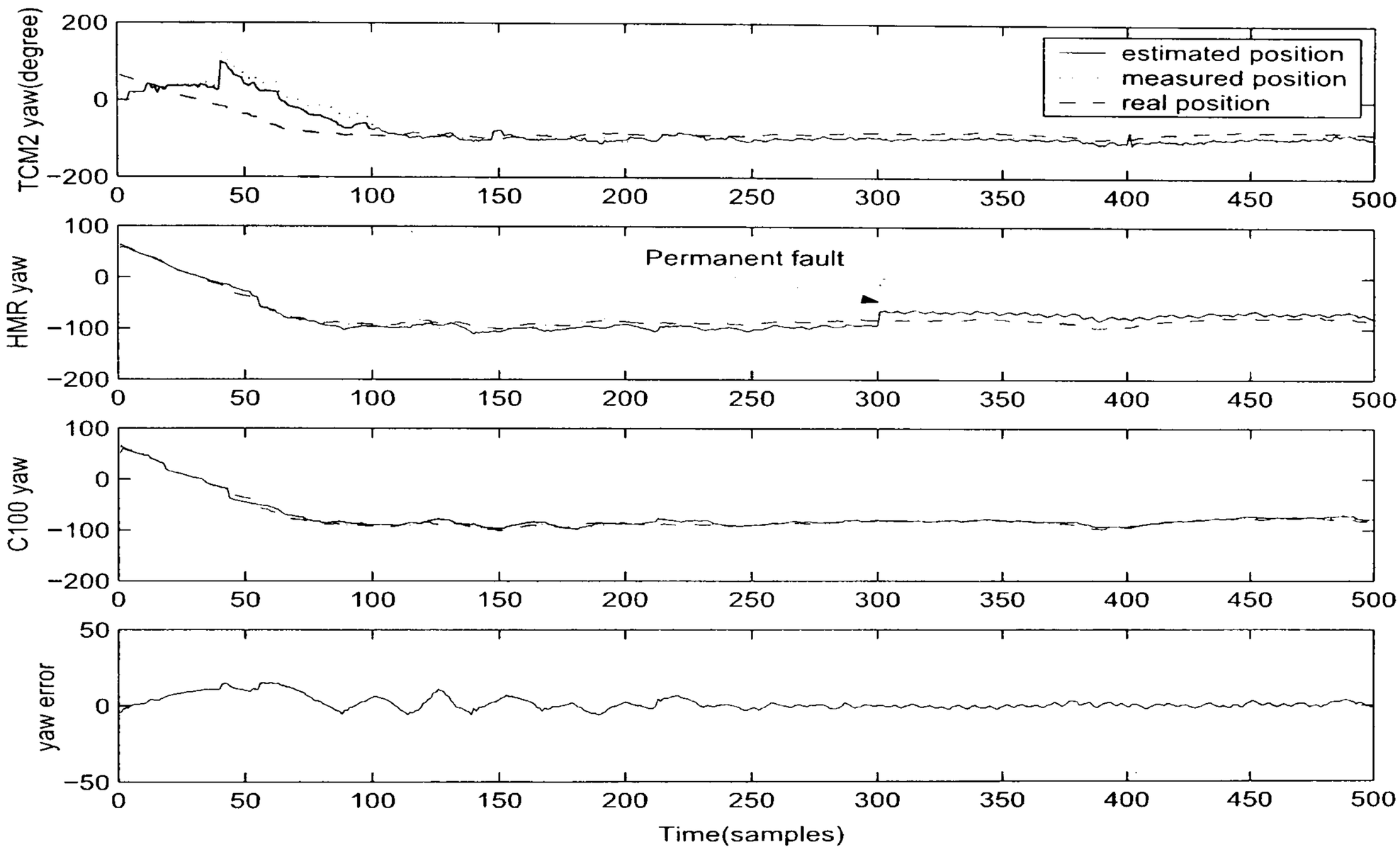

Figure 5.30: FLA-FKF performance with adaptive feedback factors under a permanent fault on the HMR 3000 compass

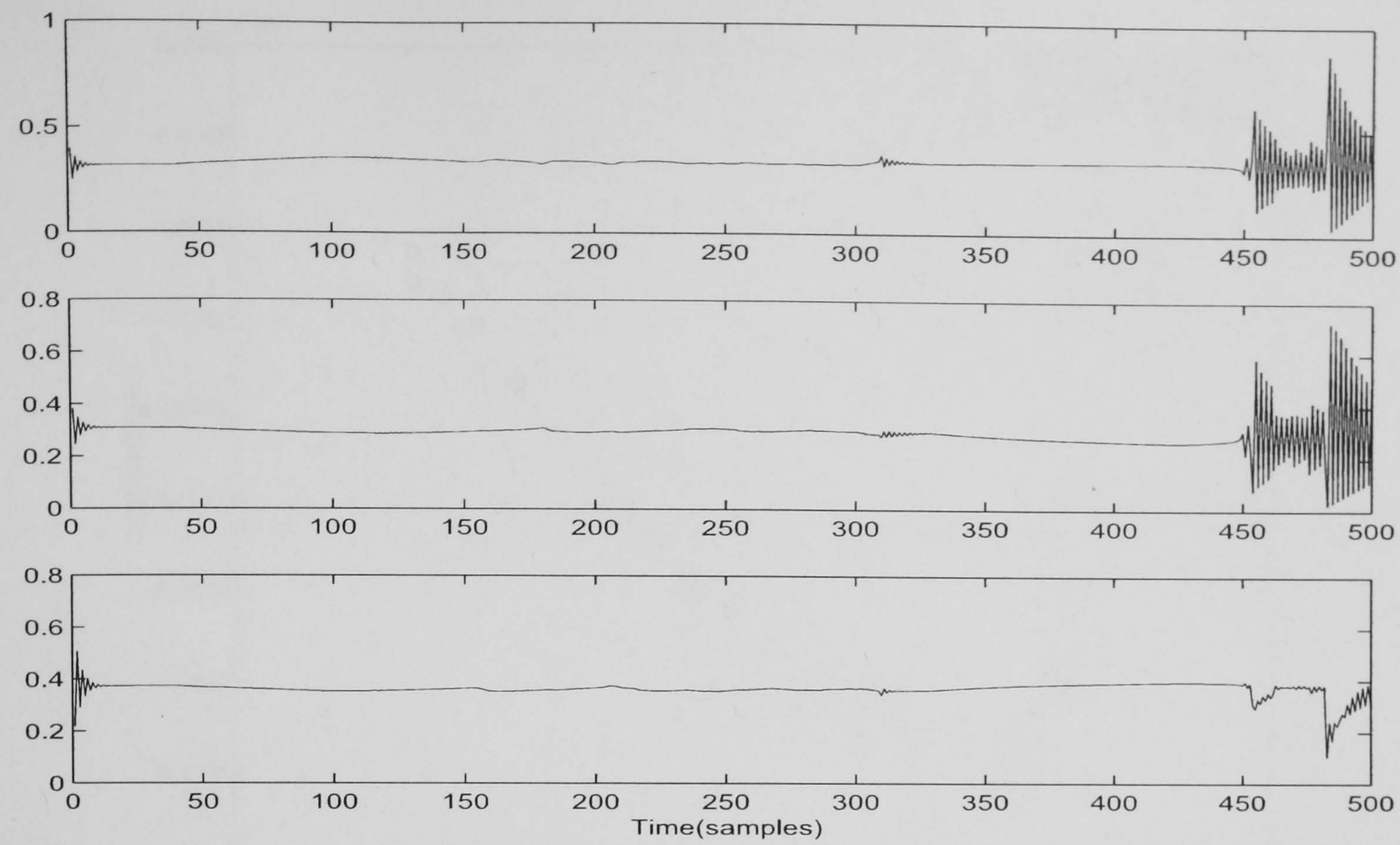

Figure 5.31: Information feedback factors (β_i)under a permanent fault on the HMR 3000

5.7 GPS fusion simulation results

In Figure 5.6, apart of the main FLA-FKF structure, a reference sensor GPS is also included. It is used to provide real time vehicle position including longitude, latitude as well as the vehicle heading and speed. Also it can be used as an individual navigation system if all of the compasses have permanent faults. This can be done by changing the parameters via user interface.

The GPS outputs the vehicle's real time longitude and latitude in degrees, however, when the vehicle undertake surveying tasks, in order to provide the information of the distances from the vehicle to the waypoints, the degree of the Longitude and Latitude components needs to be changed to meters by the following rules(Loebis 2005).

One degree of Latitude= 111 Km and

One minute of Longitude= $1855 \times \cos(Latitude)$ m

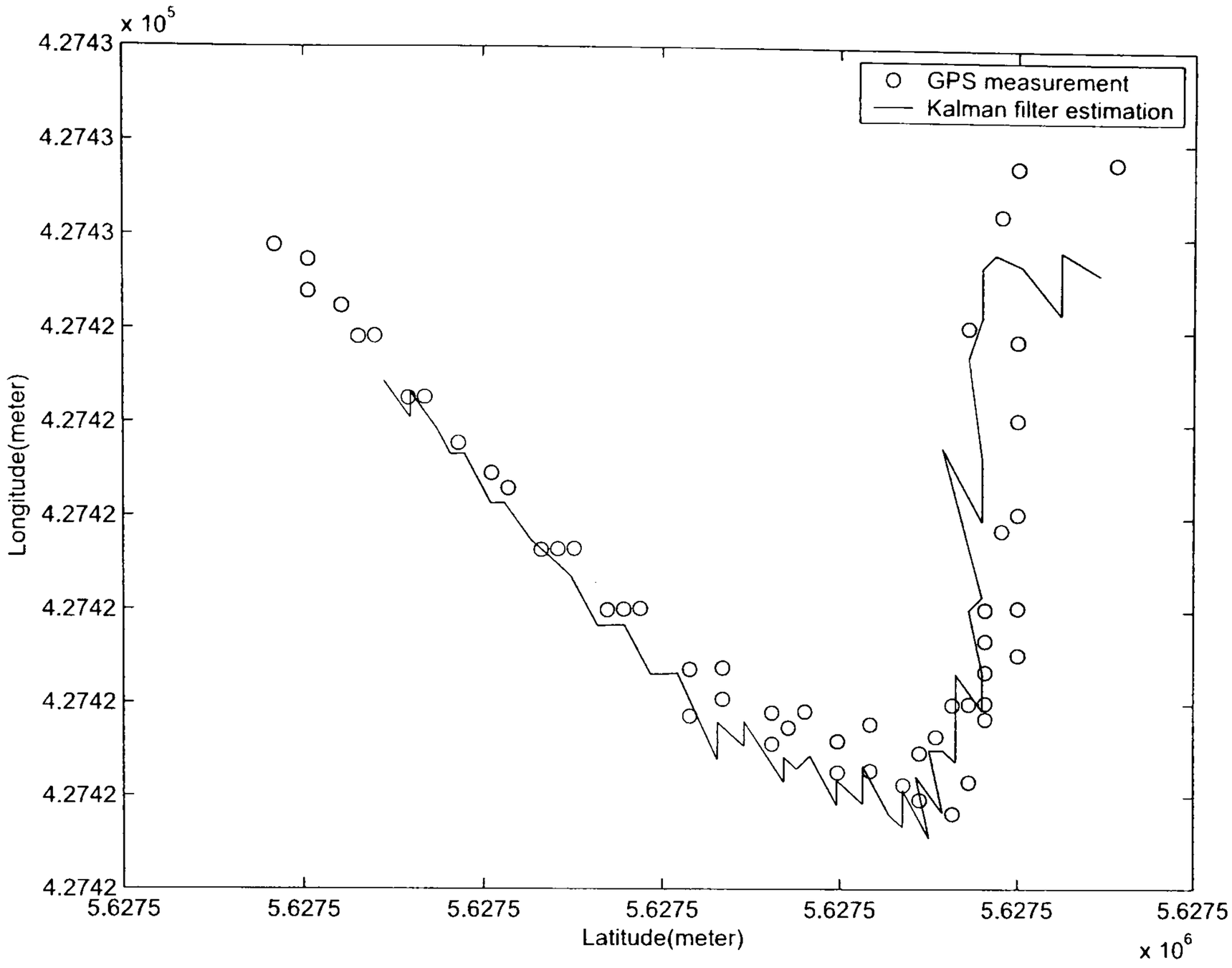

Figure 5.32: GPS fusion result

A GPS model has been derived at Section 4.1, a fuzzy logic based standard Kalman filter is implemented to the onboard GPS, the fusion results are shown in Figure 5.32.

5.8 Concluding remarks

In this chapter, various cascaded Kalman filter strategies integrating fuzzy logic have been presented for use in the *Springer* vehicle.

Various fault situations where is shown in Section 5.6 are simulated, the RMSE values of the MSDF headings are recorded in Table 5.3 and 5.4.

Table 5.3: RMSE (degree) comparison under the TCM2 compass faults

Algorithms	Transient faults on the TCM2 compass		Persistent faults on the TCM2 compass		Permanent fault on the TCM2 compass	
	0-200 samples	201-500 samples	0-200 samples	201-500 samples	0-200 samples	201-500 samples
FLA-CKF	4.1499	1.8280	/		/	
FLA-DKF	4.5582	0.8520	3.9290	0.9230	3.4214	2.5131
FLA-FKF with fixed feedback	4.3143	0.8395	4.1782	0.8500	3.7206	1.7765
FLA-FKF with adaptive feedback	5.3025	0.7930	5.1014	0.8150	5.2004	1.2452

Table 5.4: RMSE (degree) comparison under the HMR 3000 compass faults

Algorithms	Transient faults on the HMR 3000 compass		Persistent faults on the HMR 3000 compass		Permanent fault on the HMR 3000 compass	
	0-200 samples	201-500 samples	0-200 samples	201-500 samples	0-200 samples	201-500 samples
FLA-DKF	3.9032	1.6400	4.1052	1.8770	3.6152	4.6253
FLA-FKF with fixed feedback	6.5207	1.2036	6.5230	1.5396	5.6830	3.5010
FLA-FKF with adaptive feedback	6.0720	0.9870	5.2196	1.1631	5.2274	1.9414

5.8.1 Discussion

In USVs, navigation sensors operate under unpredictable conditions. As a consequence, transient and persistent faults are always a possibility in a multi-sensor navigation system which can lead the system to instability. Thus the system needs a fault tolerant MSDF algorithm to overcome such problems.

In order to achieve an accurate data analysis, the RMSE values were calculated from 1 to 200 samples and 201 to 500 samples separately. Therefore the RMSE value of the first 200 samples can be used to analysis initial parameter tuning speed. Whereas the RMSE value of the last 300 samples can indicate the fault tolerant capabilities. In the various simulations above, the heading and relevant parameters choose 0 as the initial value. The MSDF algorithms need to tune the parameters to the corresponding state, consequently instability results always occurred at the first 200 samples. From the RMSE results shown in Table 5.3 and 5.4, at the first 200 samples, the FLA-DKF gives a more accurate result than both FLA-FKF algorithms, whilst the FLA-FKF with the fixed feedback factor approach outputs better results than the adaptive feedback FLA-FKF approach.

It is worth noting that initially the adaptive feedback factors were very oscillatory at the beginning of the simulation and then settled down in approximately 20 samples. The feedback factors were in a self adaptive process, where they attempt to find suitable values instead of the current values. This self adaptive process took place not only at the beginning of the simulation but also when the local fuzzy logic Kalman filters gave unsatisfactory values to the master filter. Also from the results of the feedback factors, it is found that they did not start to tune the values at 100, 200, 300 and 400 samples. The reason for this is that the self-tuning strategy changed the feedback factor values after the local fuzzy logic Kalman filter process. Thus, the fault disturbances were modified by the fuzzy logic strategy.

5.8.2 Q and R matrices analysis

According to the simulation results and discussion above, owing to an outstanding fault tolerant capabilities, FLA-FKF with adaptive feedback algorithm is selected as the onboard navigation system for *Springer*.

For a MSDF system design, an accurate model and adaptive R and Q matrices are crucial to improve the system fault tolerant capabilities. Consequently, the R and Q matrices of the FLA-FKF are analysised here.

An inappropriate value of the Q matrix can result in the Kalman filter becoming unstable or divergent. An propriate Q matrix enables the Kalman gain (K) to rapidly settle down to steady state values (Grewal and Andrew 2001), therefore the fusion result can be accurate and efficient to reduce the noise/fault measurement.

In the FLA-FKF algorithm, the Q matrix is tuned according to the information feedback factors. From the simulation results and RMSE values from Table 5.3 and 5.4, the overall fusion accuracy is improved by employing adaptive information feedback. The adaptive information feedback allows the Q matrix to find in suitable values by utilising the eigenvalues. The value of the Q matrix under a permeant fault on the TCM2 is presented in Figure 5.33, the adaptive process is similar with the information feedback factors (β_i).

The fuzzy logic adaptive strategy introduced in Section 5.3 allows the R matrix to be adaptive according to the difference of the the value of the theoratical innovation covariance and the practical innovation covariance. For a FLA-FKF under a permanent fault on the TCM2, the adaptive R matrix values are shown in Figure 5.34.

In order to verify that the fuzzy logic strategy has been effectively improve the MSDF fusion accuracy, now, the FKF with adaptive feedback factor strategy (without fuzzy logic)

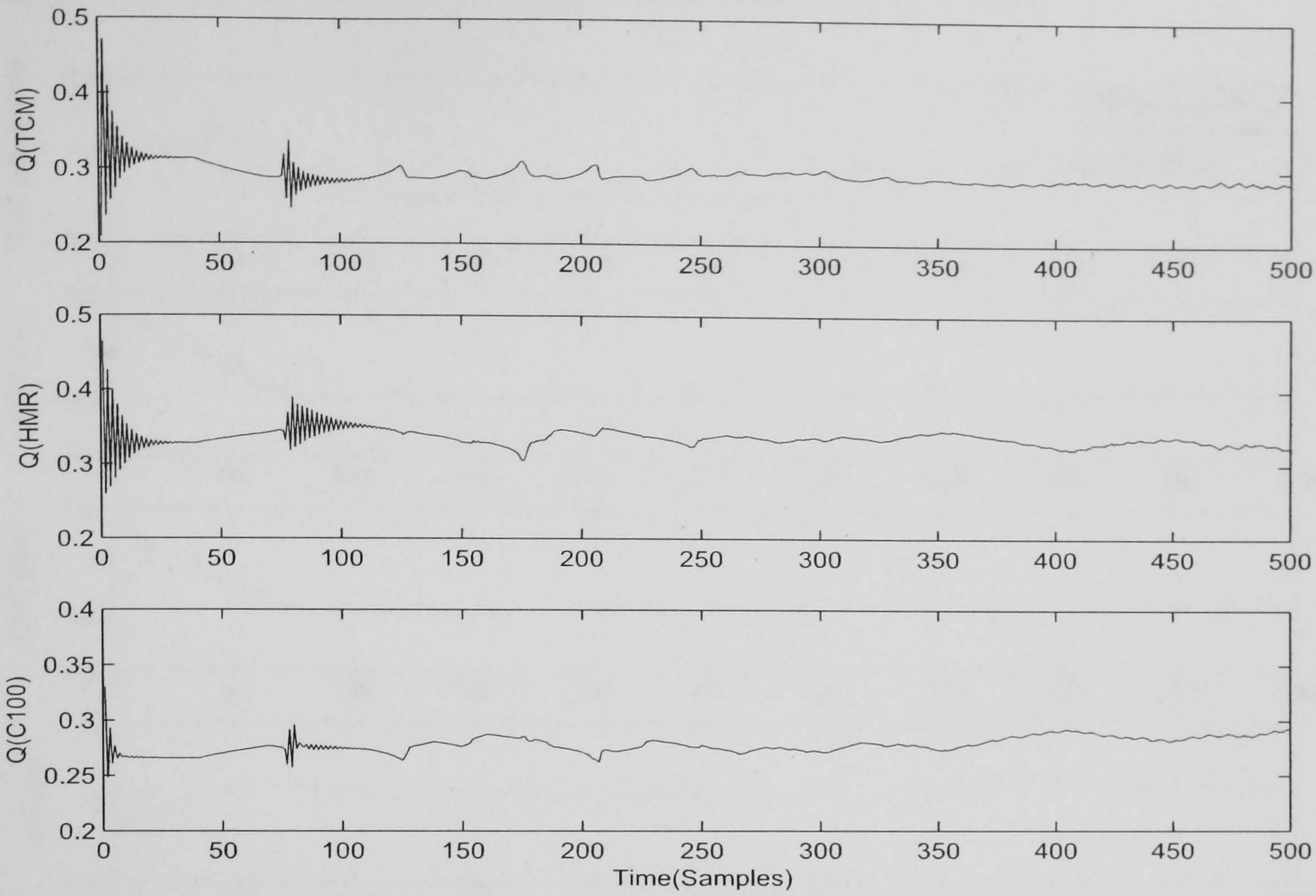

Figure 5.33: Adaptive Q matrix of a FLA-FKF with a permanent fault on the TCM2

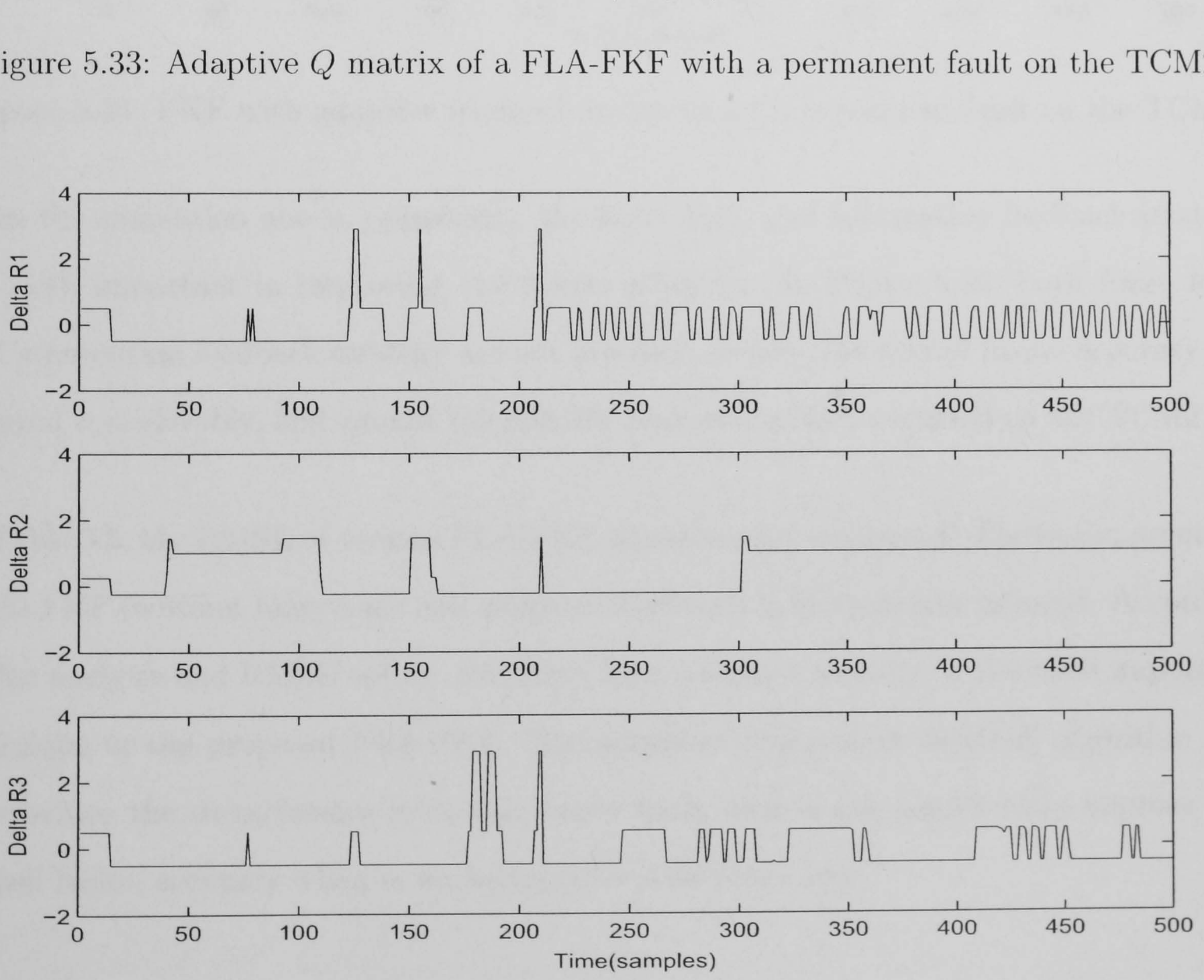

Figure 5.34: ΔR of a FLA-FKF with a permanent fault on the TCM2

is implemented on the sensors with a permanent fault on the TCM2.

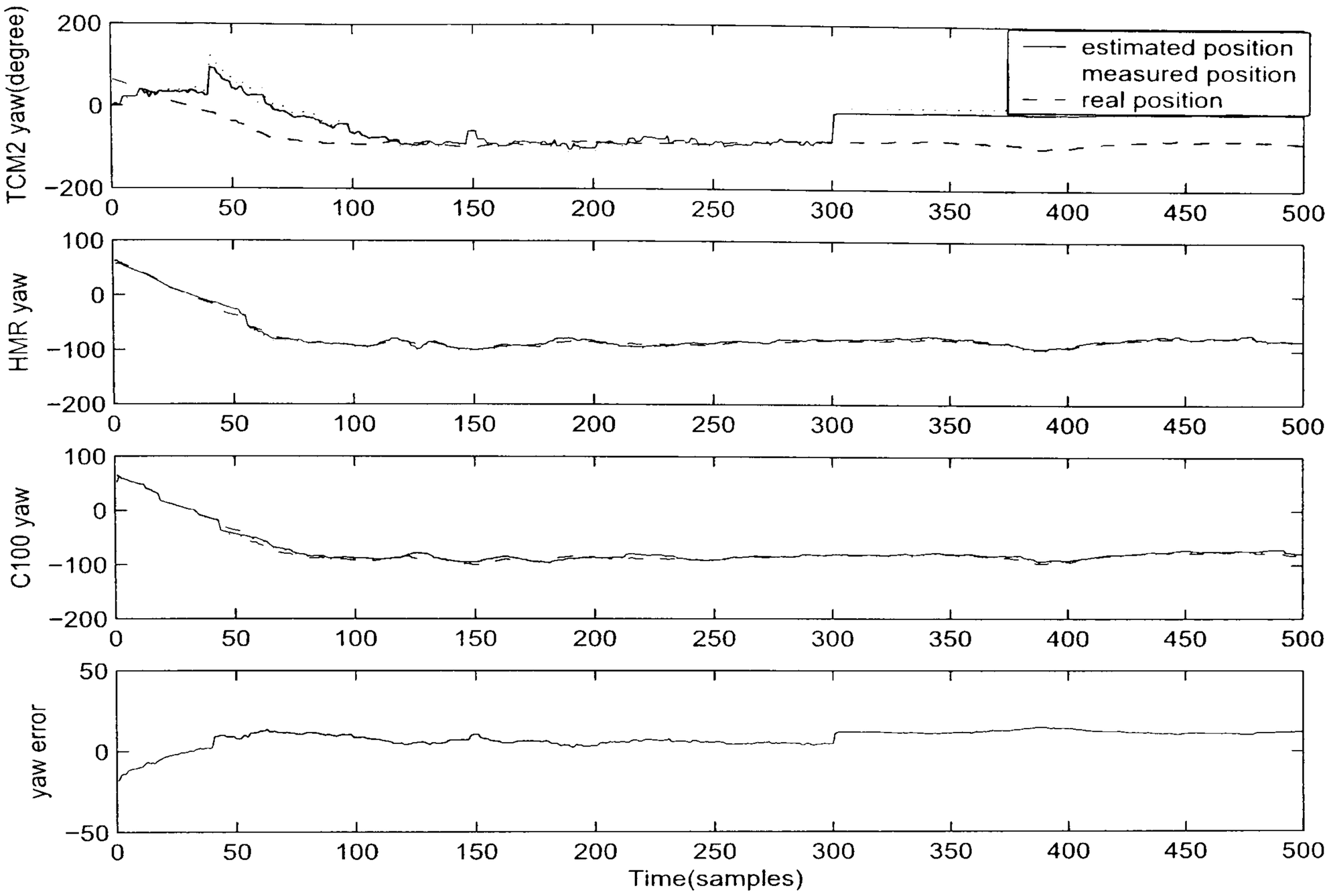

Figure 5.35: FKF with adaptive feedback factor under a permanent fault on the TCM2

From the simulation above, apparently, the fuzzy logic and information feedback strategy are both important in improving the fusion accuracy. In Figure 5.36, both fuzzy logic and information feedback strategy are not involved, clearly, the overall fusion accuracy are reduced considerably, and cannot tolerate the permanent fault occurred on the TCM2.

In Table 5.5, the RMSE of various FLA-FKF situations are compared. The fusion accuracy of the FKF (without fuzzy logic and adaptive feedback) is dramatically reduced. According to the analysis and RMSE values, the fuzzy logic adaptive strategy is the most important technique in the proposed FLA-FKF. The adaptive information feedback algorithm can also reduce the disturbances from the sensor fault, and it can significantly improve the overall fusion accuracy when it works together with fuzzy logic.

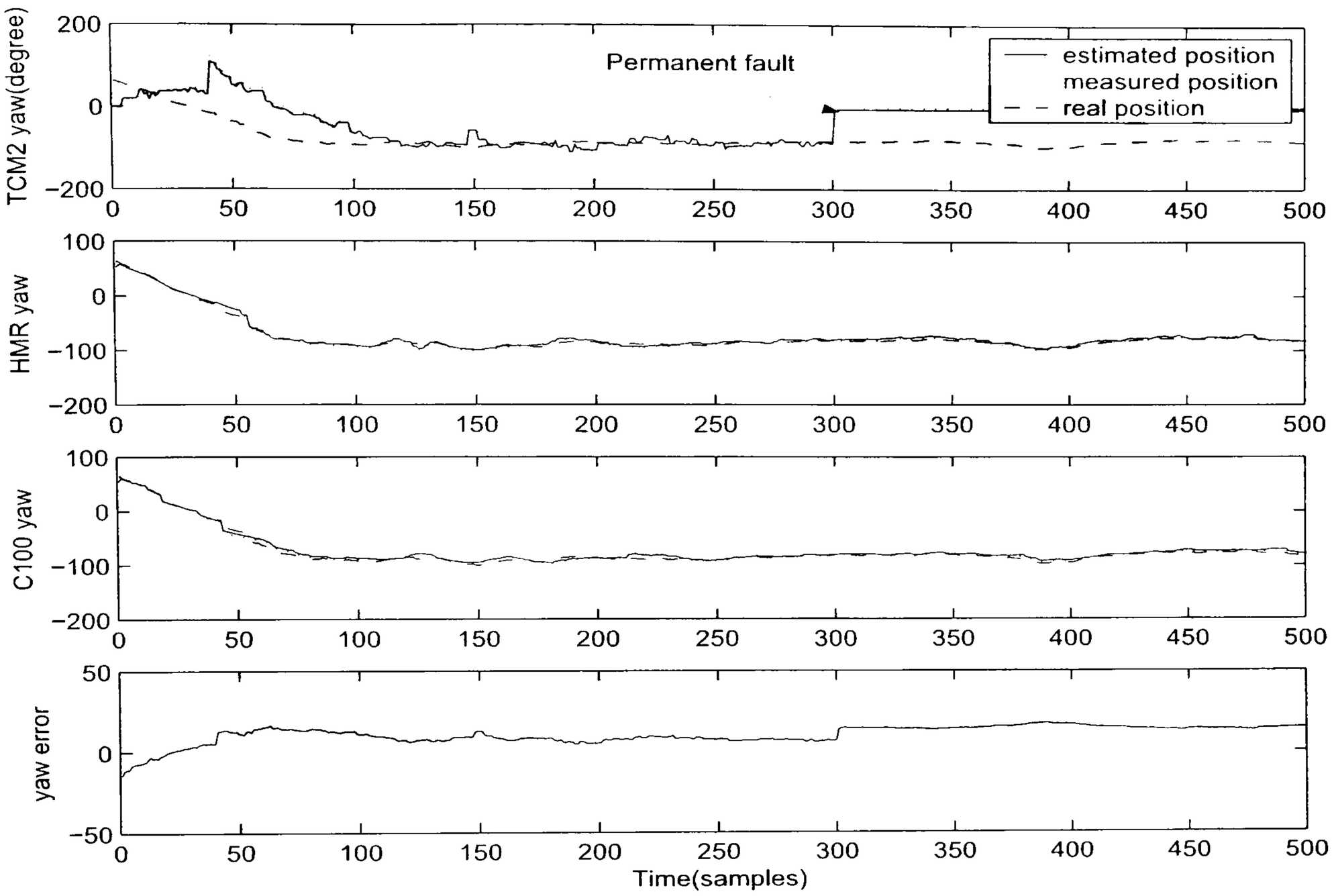

Figure 5.36: FKF without fuzzy logic and adaptive information feedback with a permanent fault on the TCM2

Table 5.5: FLA-FKF RMSE (degree) comparison under a permanent fault on the TCM2 compass

Algorithms	RMSE	
	0-200 samples	201-500 samples
FLA-FKF with adaptive feedback factors adaptive Q and adaptive R	5.2004	1.2452
FLA-FKF with fixed feedback factors fixed Q and adaptive R	3.7206	1.7765
FKF with adaptive feedback factors adaptive Q and fixed R	5.796	9.0460
FKF with fixed feedback factors fixed Q and fixed R	6.774	14.6510

5.8.3 Concluding remarks

In this chapter, three types of cascaded FLA-KF were examined under different sensor fault situations. An adaptive determination method was proposed to improve the fault tolerant capability for the FLA-FKF. In addition a FLO was designed to assess the fuzzy logic performance.

Comparing these FLA-KF algorithms, they are all seem to have their advantages and disadvantages.

The FLA-CKF is a very straightforward method with one level fusion process, however, it does not recover transient faults very well. In addition it has a heavy computation load.

Whereas, the FLA-DKF and FLA-FKF are both two level fusion methods and fuzzy logic has been implemented on both of these levels to adapt the R matrix. From the performances, it appears that the FLA-DKF is more adequate to give an accurate global estimation, nevertheless, its fault tolerance capability is not as good as the FLA-FKF. However, the FLA-DKF has the advantage of a higher computation efficiency.

The FLA-FKF has been featured, and its potential for fault detection and recovery has been demonstrated through simulation. The adaptive information feedback factors improve the robustness of this algorithm. Thus the FLA-FKF is more suitable for the fault detection and recovery purposes.

The FLA-FKF algorithm with adaptive feedback factors will be implemented in the *Springer* vehicle. This algorithm combines in a synergetic way all the advantages that the various applied techniques offer. Fuzzy logic based Kalman filter improves the individual local Kalman filter estimation by tuning the R matrix. Also the FLO provides an interface for the user to monitor the on-line tuning process. The FKF architecture offers enhanced

capability to deal with imprecise sensor measurement. In addition, the adaptive feedback factors can strengthen the estimation accuracy according to the performance of the sensor subsystem.

This chapter concentrates on the design of a fault tolerant MSDF, in the next chapter, a novel fuzzy logic based MMAE is developed for *Springer* navigation system.

Chapter 6

MULTIPLE MODEL ADAPTIVE ESTIMATION

In Kalman filter design, there are usually large uncertainties in some parameters because of inadequate *prior* knowledge about the process. Or some parameters might be expected to vary slowly with time, however, the nature of the change is not predictable. Therefore, Multiple Model Adaptive Estimation (MMAE) technique was proposed by Magill (1965) after Kalman's original paper. In the following years, MMAE has been widely adopted and modified, and it is recognized as a feasible approach in a number of applications, such as, precision geodesy, fault classification, target tracking, ballistic missile interception etc. (Brown and Hwang 1984, Girgis and Brown 1985, Blair and Bar-shalon 1996, Shima *et al.* 2002).

In this Chapter, a modified MMAE algorithm combined with a FLA-CKF is implemented on the multiple sensors to achieve an accurate and adaptive heading for *Springer*. Simulation results are presented to verify the algorithm's robustness by varying the measurement noise covariance (R) and the process noise covariance (Q) respectively.

6.1 Preliminary

In general, a MMAE algorithm can be shown diagrammatically in Figure 6.1. The MMAE algorithm employs a bank of parallel Kalman filters, termed as elementary filters. Each elementary filters is based on a hypothesized parameter vector.$a(1), a(2), \cdots, a(n)$, where $a(i)$ is the constant parameter vector for the i^{th} elemental filters. The elemental filters act upon a measurement vector z to derive a state estimate $\hat{x}_i$, a residual vector r_i which is the difference between the measurements and the filter's prediction of the measurements, and a residual covariance S_i.

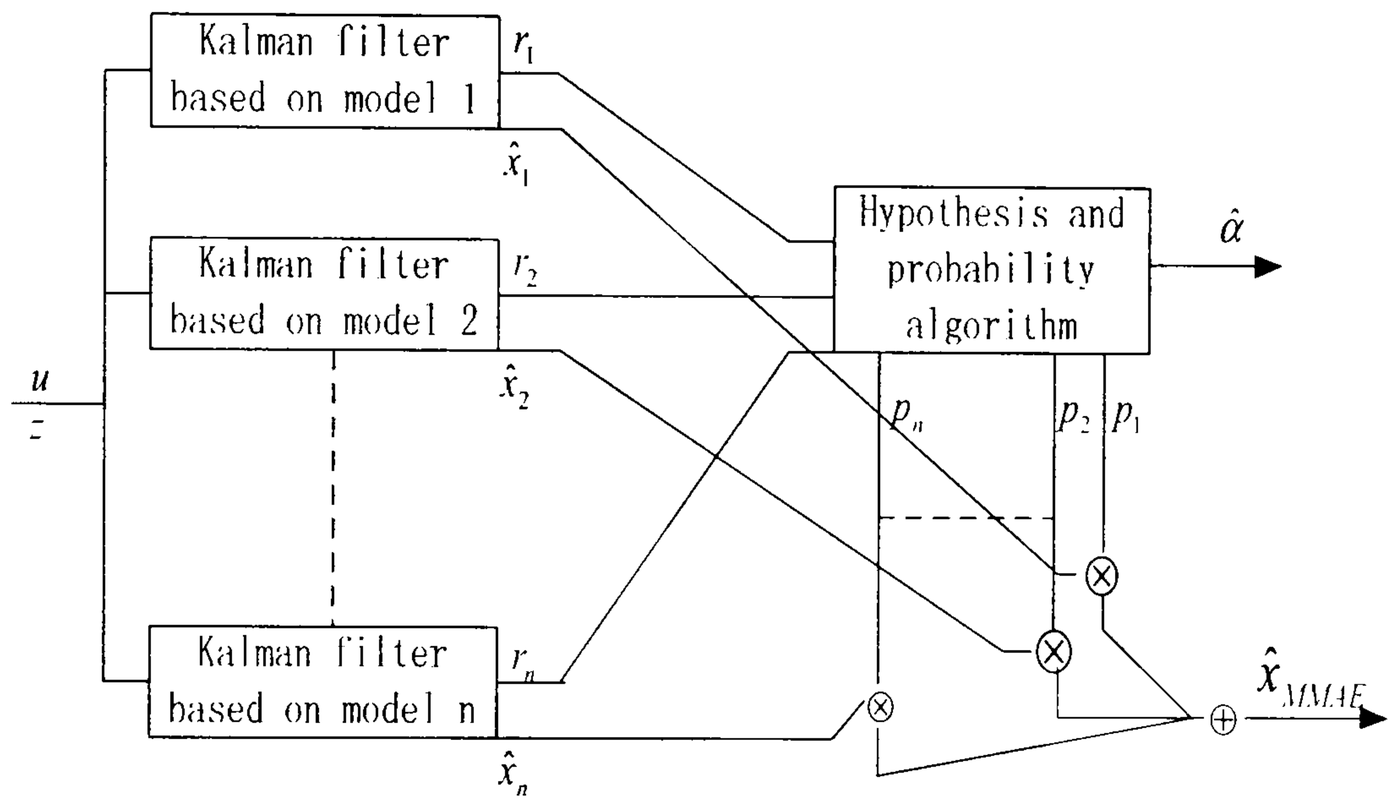

Figure 6.1: MMAE algorithm
(Hanlon and Maybeck 1998)

The residuals are used by the hypothesis algorithm as a relative indication of how close each of the filter's models is to the true model. The smaller the residual the closer the filter model matches the true model.

The hypothesis algorithm computes the conditional probabilities (p_i) for each of the elemental filters. These probabilities are then used to weight the individual elemental Kalman filter state estimates ($\hat{x}_i$) to produce an optimal estimate for the true states ($\hat{x}_{MMAE}$).

When the MMAE algorithm is used for system failure identification, each of the elemental

Kalman filters models a different failure situation. The residuals of each Kalman filter specify how close that filter's model is to the actual failure condition. The hypothesis algorithm is therefore an estimate of the current failure status of the system ($\hat{\alpha}$).

Comparing with the standard Kalman filter, the MMAE is generally able to determine the correct parameter values more accurately. In addition, by running multiple elemental filters in parallel, the residual information at each update is used to identify the system parameters or system failures and offer an adaptive solution while a system failure occurs. On the other hand, the MMAE algorithm produces the state estimates using multiple elemental filters, particularly if a large number of filter states are needed to capture the nature of the system dynamics. The computation, therefore, can be intensive. In order to improve the computation efficiency, several algorithms, such as, 'moving bank', 'filter spawning' have been proposed (Vasquez and Maybeck 2004, Fisher and Maybeck 2002. Li and Bar-shalon 2000). The research carried out here assumes that efficient computational power exists, so methods to increase computational efficiency are not emphasized.

6.2 Theory development

Recalling Equation 5.1 and 5.2, for MMAE, there are n elementary Kalman filters:

$$z_k(n) = H_k(n)x_k(n) + \nu_k(n) \tag{6.1}$$

$$x_{k+1}(n) = \Phi_k(n)x_k(n) + G_k(n)u_k(n) + \omega_k(n) \tag{6.2}$$

The residual of the Kalman filter can be calculated as:

$$r_k(n) = z_k(n) - H_k(n)\hat{x}(n)_k^- \tag{6.3}$$

The residual covariance is defined in Equation 5.36 as:

$$S_k(n) = H_k(n)P_k(n)^- H_k{}^{\mathrm{T}}(n) + R_k(n) \tag{6.4}$$

Herein, Z_k^* is defined as a growing length measurement history vector consisting of all measurement vectors from z_0 to z_{k-1}. Let a represent an uncertain parameter which can affect any model matrices in the system model of Equation 6.2.

A goal of MMAE is to find the joint conditional Probability Density Function (PDF) for the state and a conditioned on the entire measurement history Z_k^*, this process is represented in Equation 6.5:

$$f_{x_k,\alpha|Z_k^*}(\xi,\alpha|Z_k^* = Z_k) = \underbrace{f_{x_k|\alpha,Z_k^*}(\xi|a=\alpha, Z_k^* = Z_k)}_{f1}\underbrace{f_{\alpha|Z_k^*}(\alpha|Z_k^* = Z_k)}_{f2} \tag{6.5}$$

where ξ and Z_k are variables representing the state vector and measurement history.

Consider the first density $f1$ of equation6.5, this density is conditioned on a particular realization of a, and it is analogous to the standard conditional density used in a Kalman filter for state estimation.

The second density $f2$ in Equation 6.5 can be expressed as:

$$f_{\alpha|Z_k^*}(\alpha|Z_k^* = Z_k) = \frac{f_{Z_k^*|a,Z_{k-1}}(\xi|a=\alpha, Z_{k-1}^* = Z_{k-1}) f_{a|Z_{k-1}^*}(\alpha|Z_{k-1}^* = Z_{k-1})}{\int_A f_{Z_k^*|a,Z_{k-1}}(\xi|a=\alpha, Z_{k-1}^* = Z_{k-1}) f_{a|Z_{k-1}^*}(\alpha|Z_{k-1}^* = Z_{k-1}) d\alpha} \tag{6.6}$$

The priori density for a can be defined by Equation 6.7:

$$f_{a_0}(\alpha) = \sum_{n=1}^{N} p_0(n)\delta(\alpha - a(n)) \tag{6.7}$$

The hypothesis conditional probability $p_k(n)$ is expressed in equation6.8.where $a = a(n)$ with a realized measurement history Z_k.

$$p_k(n) \triangleq prob[a = a(n)|Z_k^* = Z_k] \tag{6.8}$$

Substituting Equation 6.7 and Equation6.8 into Equation6.5 yields:

$$p_k(n) = \frac{f_{Z_k^*|a,Z_{k-1}}(z_k|a = a(n), Z_{k-1}^* = Z_{k-1})p_{k-1}(n)}{\sum_{j=1}^{N} f_{Z_k^*|a,Z_{k-1}}(z_k|a = a(j), Z_{k-1}^* = Z_{k-1})f_{a|Z_{k-1}^*}p_{k-1}(j)} \tag{6.9}$$

where the prior conditional probabilities,$p_{k-1}(j)$ is used to weight the conditional densities of the current measurements, assuming each hypothesis, and then normalizes it over the complete set of such numerator terms.

In equation6.9, $f_{Z_k^*|a,Z_{k-1}}(z_k|a = a(n), Z_{k-1}^* = Z_{k-1})$ can be calculate in Equation 6.10(Brown and Hwang 1997):

$$f_{Z_k^*|a,Z_{k-1}}(z_k|a = a(n), Z_{k-1}^* = Z_{k-1}) = \frac{1}{(2\Pi)^{1/2}|S_k^-(n)|^{1/2}} \exp\{-\frac{1}{2}r_k^{-T}(n)S_k^{-1}(n)r_k^-(n)\} \tag{6.10}$$

Therefore the optimal state estimation can be represented as:

$$\begin{aligned}
\hat{x}_k^+ &= E[x_k|Z_k^* = Z_k] \\
&= \int_{-\infty}^{\infty} \xi[\int_A f_{x_k,a|Z_k^*}(\xi,\alpha|Z_k^* = Z_k)d\alpha]d\xi \\
&= \int_{-\infty}^{\infty} \xi[\int_A f_{x_k,a|Z_k^*}(\xi|a=\alpha, Z_k^* = Z_k) f_{a|Z_k^*}(\alpha|Z_k^* = Z_k)d\alpha]d\xi \\
&= \int_{-\infty}^{\infty} \xi[\int_A f_{x_k,a|Z_k^*}(\xi|a=\alpha, Z_k^* = Z_k) \sum_{n=1}^{N} p_k(n)\delta(\alpha - a(n))d\alpha]d\xi \qquad (6.11) \\
&= \int_{-\infty}^{\infty} \xi[\sum_{n=1}^{N} f_{x_k|a,Z_k^*}(\xi|a=a(n), Z_k^* = Z_k)p_k(n)]d\xi \\
&= \sum_{n=1}^{N}[\int_{-\infty}^{\infty} \xi f_{x_k|a,Z_k^*}(\xi|a=a(n), Z_k^* = Z_k)]p_k(n)
\end{aligned}$$

In Equation 6.11, the term inside the square brackets refer to the optimal state estimate conditioned upon a given parameter value $a(n)$ and the realized measurement history Z_k. Therefore, this equation can be rewrite as:

$$\hat{x}_k^+ = \sum_{n=1}^{N} \hat{x}_k(n)p_k(n) \qquad (6.12)$$

Equation6.12 shows that the final state estimate is the weighted sum of the elemental filter state estimates, weighted by the probability that the parameter for that particular elemental filter is the correct parameter.

The covariance update for the MMAE can be derived by Equation 6.13.

$$
\begin{aligned}
P_k^+ &= E\{[x_k - \hat{x}_k^+][x_k - \hat{x}_k^+]^T | Z_k^* = Z_k)\} \\
&= \int_{-\infty}^{\infty} [\xi - \hat{x}_k^+][\xi - \hat{x}_k^+]^T \int_A f_{x_k,a|Z_k^*}(\xi, \alpha | Z_k^* = Z_k) d\alpha d\xi \\
&= \int_{-\infty}^{\infty} [\xi - \hat{x}_k^+][\xi - \hat{x}_k^+]^T \int_A f_{x_k|a,Z_k^*}(\xi | a = \alpha, Z_k^* = Z_k) f_{a|Z_k^*}(\alpha | Z_k^* = Z_k) d\alpha d\xi \\
&= \int_{-\infty}^{\infty} [\xi - \hat{x}_k^+][\xi - \hat{x}_k^+]^T \sum_{n=1}^{N} f_{x_k|a,Z_k^*}(\xi | a = a(n), Z_k^* = Z_k) p_k(n) d\xi \\
&= \sum_{n=1}^{N} p_k(n) \{ \int_{-\infty}^{\infty} [\xi - \hat{x}_k^+][\xi - \hat{x}_k^+]^T f_{x_k|a,Z_k^*}(\xi | a = a(n), Z_k^* = Z_k) d\xi \} \\
&= \sum_{n=1}^{N} p_k(n) \{ \int_{-\infty}^{\infty} \xi\xi^T f_{x_k|a,Z_k^*}(\xi | a = a(n), Z_k^* = Z_k) d\xi \\
&\quad - \int_{-\infty}^{\infty} \hat{x}_k^+ \xi^T f_{x_k|a,Z_k^*}(\xi | a = a(n), Z_k^* = Z_k) d\xi \\
&\quad - \int_{-\infty}^{\infty} \xi \hat{x}_k^+ f_{x_k|a,Z_k^*}(\xi | a = a(n), Z_k^* = Z_k) d\xi \\
&\quad + \int_{-\infty}^{\infty} \hat{x}_k^+ \hat{x}_k^{+T} f_{x_k|a,Z_k^*}(\xi | a = a(n), Z_k^* = Z_k) d\xi \}
\end{aligned}
\tag{6.13}
$$

$$
\begin{aligned}
&= \sum_{n=1}^{N} p_k(n) \{ \int_{-\infty}^{\infty} \xi\xi^T f_{x_k|a,Z_k^*}(\xi | a = a(n), Z_k^* = Z_k) d\xi \\
&\quad - \hat{x}_k^+ \int_{-\infty}^{\infty} \xi^T f_{x_k|a,Z_k^*}(\xi | a = a(n), Z_k^* = Z_k) d\xi \\
&\quad - [\int_{-\infty}^{\infty} \xi^T f_{x_k|a,Z_k^*}(\xi | a = a(n), Z_k^* = Z_k) d\xi] \hat{x}_k^{+T} \\
&\quad + \hat{x}_k^+ \hat{x}_k^{+T} \int_{-\infty}^{\infty} \xi^T f_{x_k|a,Z_k^*}(\xi | a = a(n), Z_k^* = Z_k) d\xi \} \\
&= \sum_{n=1}^{N} p_k(n) \{ \int_{-\infty}^{\infty} \xi\xi^T f_{x_k|a,Z_k^*}(\xi | a = a(n), Z_k^* = Z_k) d\xi \\
&\quad - \hat{x}_k^+ \hat{x}_k^{+T}(n) - \hat{x}_k^+(n) \hat{x}_k^{+T} + \hat{x}_k^+ \hat{x}_k^{+T} \} \\
&= \sum_{n=1}^{N} p_k(n) \{ P_k(n) + [\hat{x}_k^+(n) - \hat{x}_k^+][\hat{x}_k^+(n) - \hat{x}_k^+]^T \}
\end{aligned}
$$

6.3 Modified MMAE design

A modified MMAE algorithm which is combined with a FLA-CKF is designed in this section and shown in Figure 6.2.

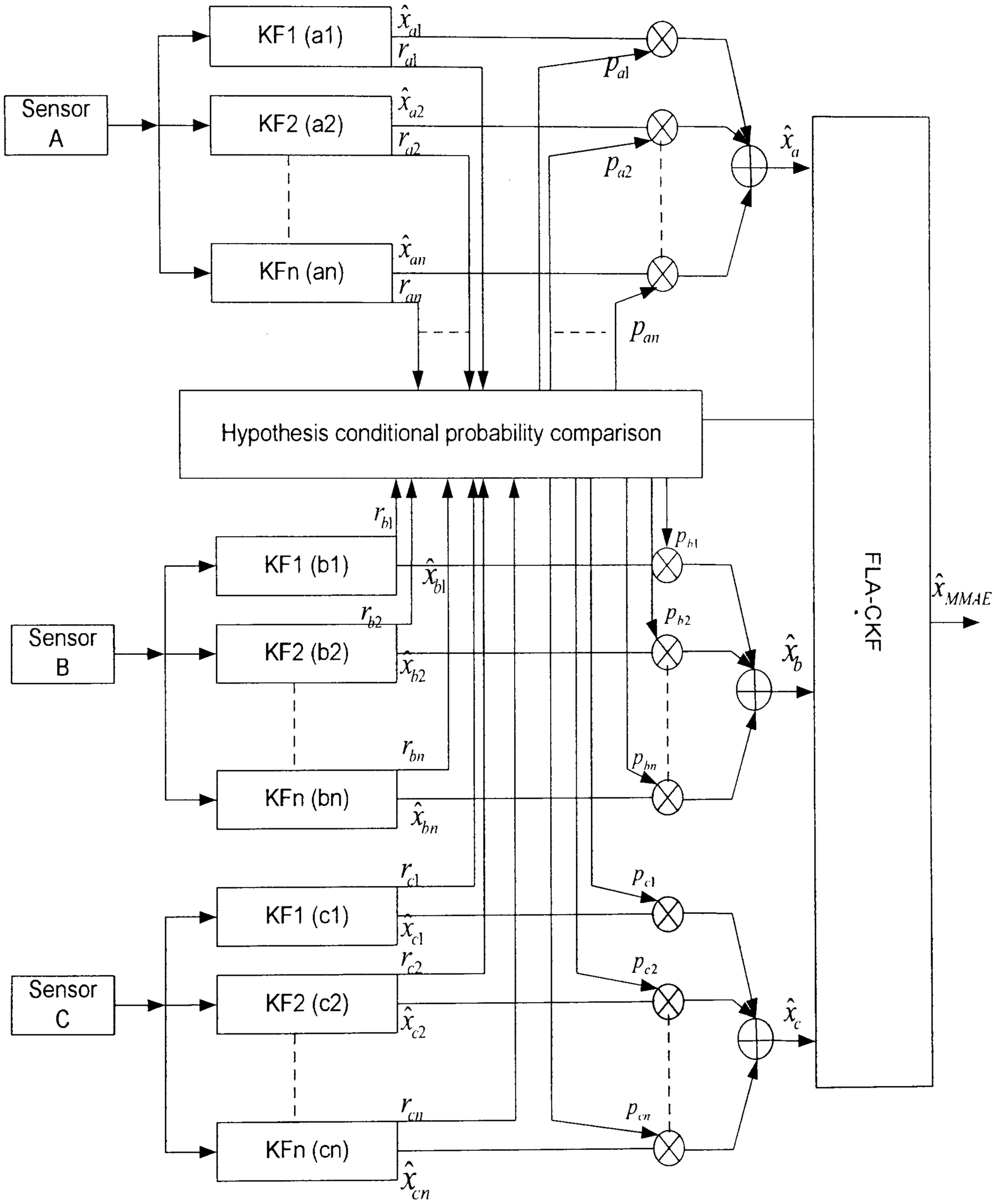

Figure 6.2: MMAE algorithm for *Springer*

For *Springer*, the three onboard compasses are employed to provide the vehicle heading.

In Figure 6.2, sensor A refers to the TCM2 compass, sensor B represents the HMR3000 compass, and sensor C is the KVH C100 compass. The standard MMAE algorithm is employed by each compass to derive its own heading estimate $\hat{r}_a$, $\hat{r}_b$ and $\hat{r}_c$ respectively. The MMAE is a complex system with high computation load, in order to reduce the overall complexity, simple FLA-CKF is selected as the master fusion technique in this proposed technique. The estimated headings are combined and fused by a FLA-CKF to produce an accurate and adaptive heading for *Springer*.

For each MMAE algorithm, the number of elemental filters was set to $n = 3$. The measurement noise covariance, $(R_k(n))$, or process noise covariance, $(Q_k(n))$,are considered to be varied in different elemental filters. In this situation, three measurement noise covariance matrices or process noise covariance are hypothesized in three elemental filters. The MMAE determines which elemental filters contain the more accurate $R_k(n)$ or $Q_k(n)$.

6.4 Simulation results

Simulation studies were performed on the three compasses in order to test the MMAE algorithm. The models produced in Section 4.2 are recalled here.

In order to verify the robustness of the MMAE algorithm, a set of simulated noise shown in Figure 6.3 is added to the sensor measurements. The noise characteristic is generally increased over time, therefore the probabilities of each elemental filter will change over time.

As a result, the simulated measurement outputs and real headings are presented in Figure 6.4

The process of each MMAE is now described step by step:

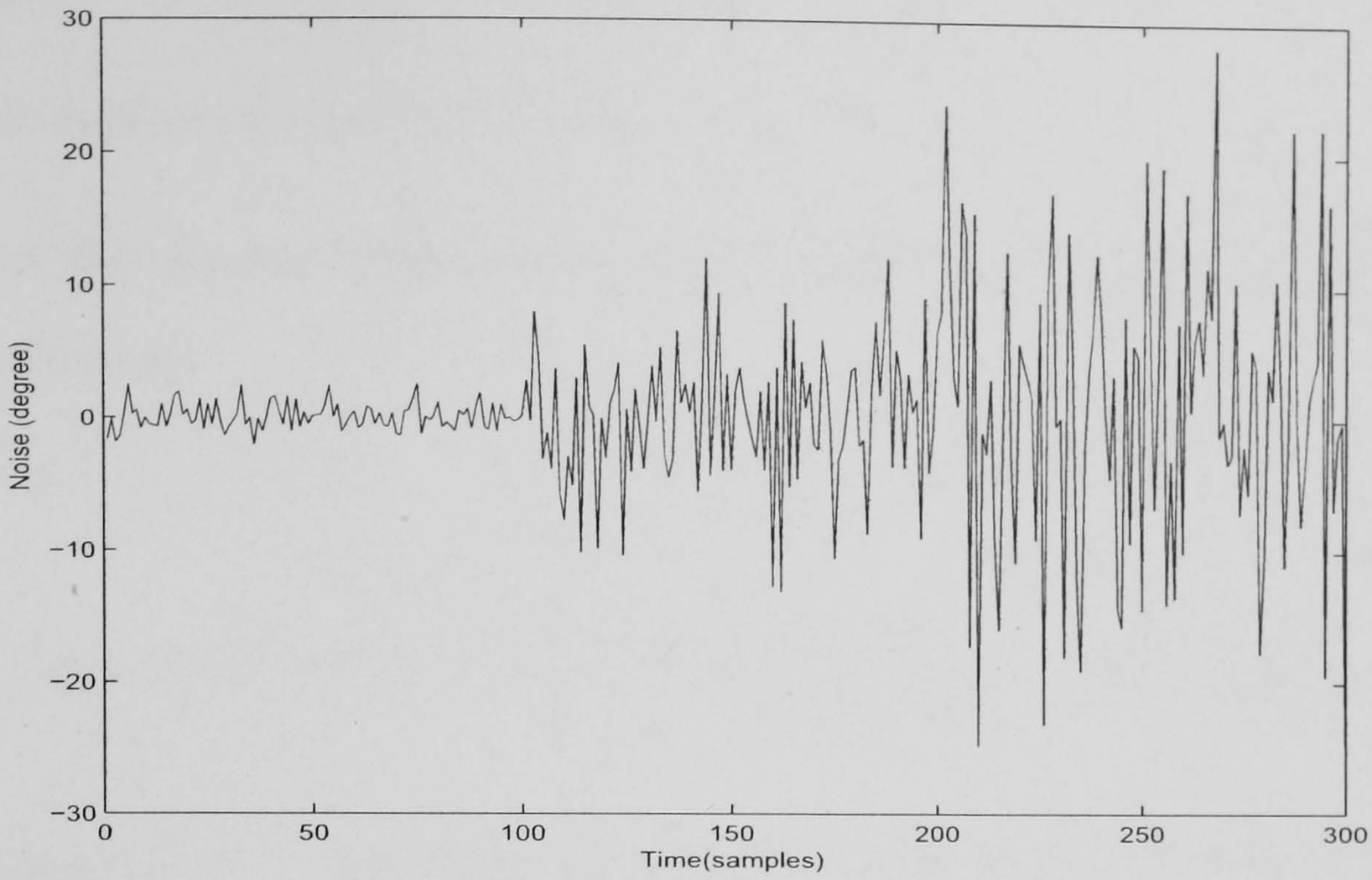

Figure 6.3: Added noise profile to the compasses

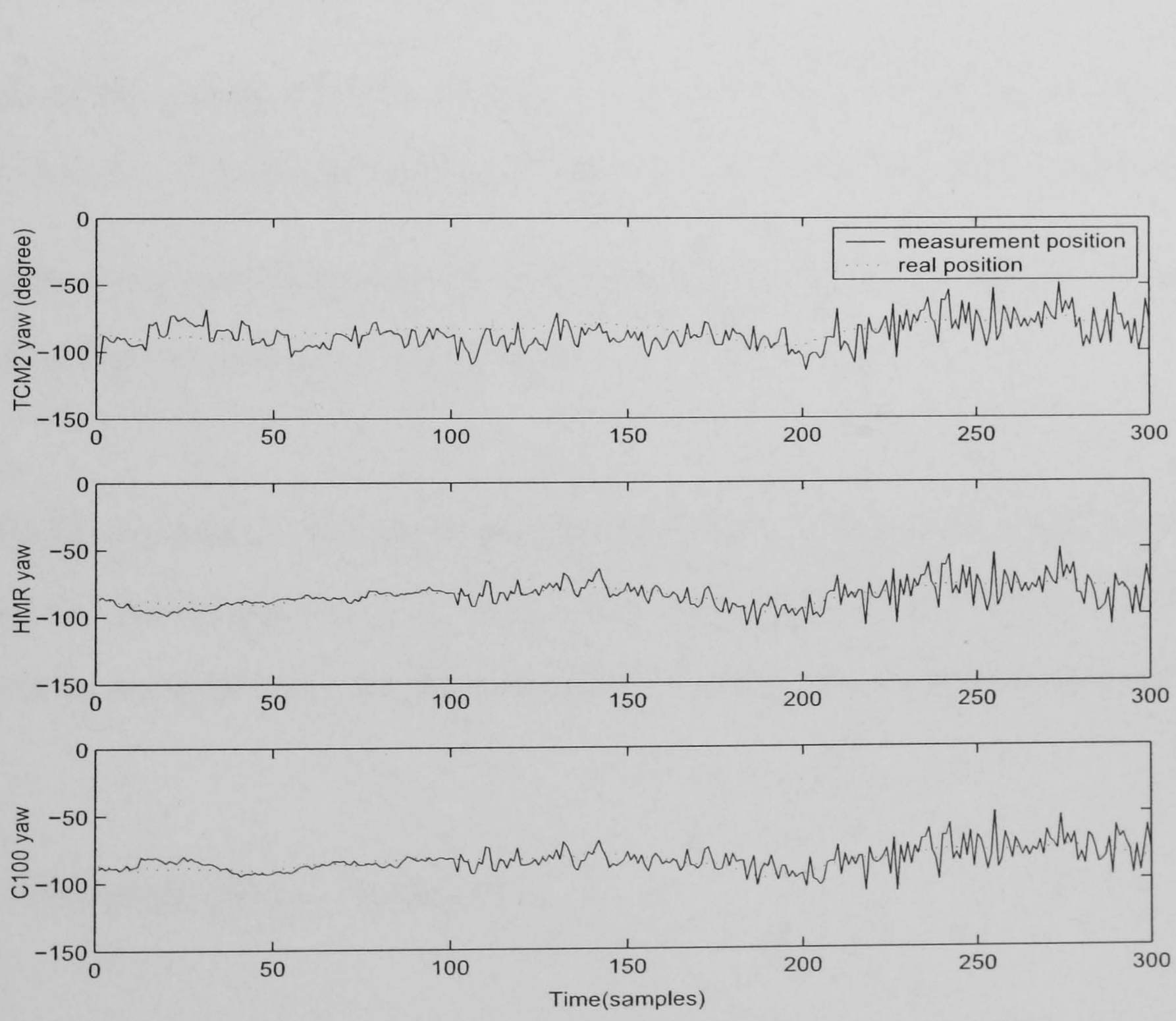

Figure 6.4: The compass outputs with added noise

- Assuming the prior distribution of a is uniform and all the weight factors are equal initially.

- The initial prior state estimate,$\hat{x}_0$, is set equal to 0.

- At $k = 0$ the elemental filters receive the first measurement z_0, so Equation 6.10 can be rewritten as:

$$f_{Z_0^*|a,Z_0}(z_k|a = a(n), Z_0^* = Z_0) = \frac{1}{(2\Pi)^{1/2}|S_0^-(n)|^{1/2}} \exp\{-\frac{1}{2}\frac{z_0^2}{S_0^-(n)}\} \tag{6.14}$$

- Once $f_{Z_0^*|a,Z_0}(z_k|a = a(n), Z_0^* = Z_0)$ has been determined for each elemental filter, Equation 6.9 is employed to calculate the weighting factors. As a result, the updated state estimates $\hat{x}_0^+(n)$ can be derived by each elemental filter.

- Each of the elemental filter estimates and their error covariance is then projected ahead to $k = 1$, and the hypothesis algorithm compute the probability for each a.

- Finally, the weight factors for $k = 1$ can be determined in equation6.9. This recursive process can be performed ad infinitum.

Three MMAE algorithms are run in parallel in order to derive the adaptive heading for each compass. At the same time, a FLA-CKF (see Chapter 5 for details) takes the state estimates from each MMAE algorithm as input to derive the final heading angle.

6.4.1 Varying $R_k(n)$ scenario

Recalling the sensor models produced in Section 4.2, three values for the $R_k(n)$ were arbitrarily chosen based on:

$R_k(1) = R_k$, $R_k(2) = 2.5R_k$ and $R_k(3) = 5R_k$, where $R_k = diag(2^2)$

The simulated sensor measurement errors are increased over time, therefore R_k values are correspondingly increased from R_k to $5R_k$, also the corresponding probabilities will change over time.

The conditional probabilities $p(n)$ of the TCM2 elemental filters are depicted in Figure 6.5.

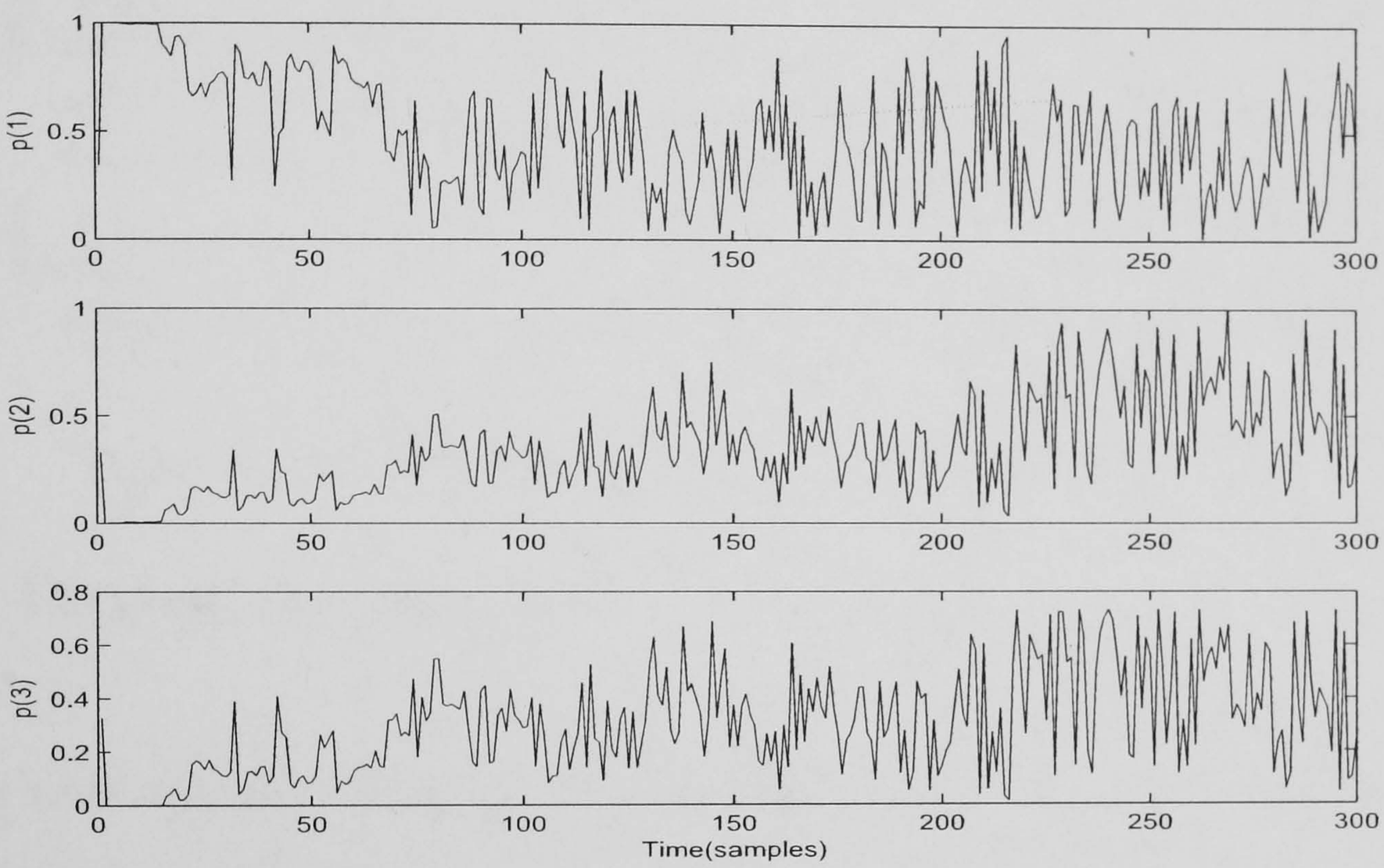

Figure 6.5: The elemental filter probabilities (TCM2 with varying $R_k(n)$ matrices)

Eventually a final heading output is produced, and individual sensor heading estimates and overall vehicle heading residuals are shown in Figure 6.6:

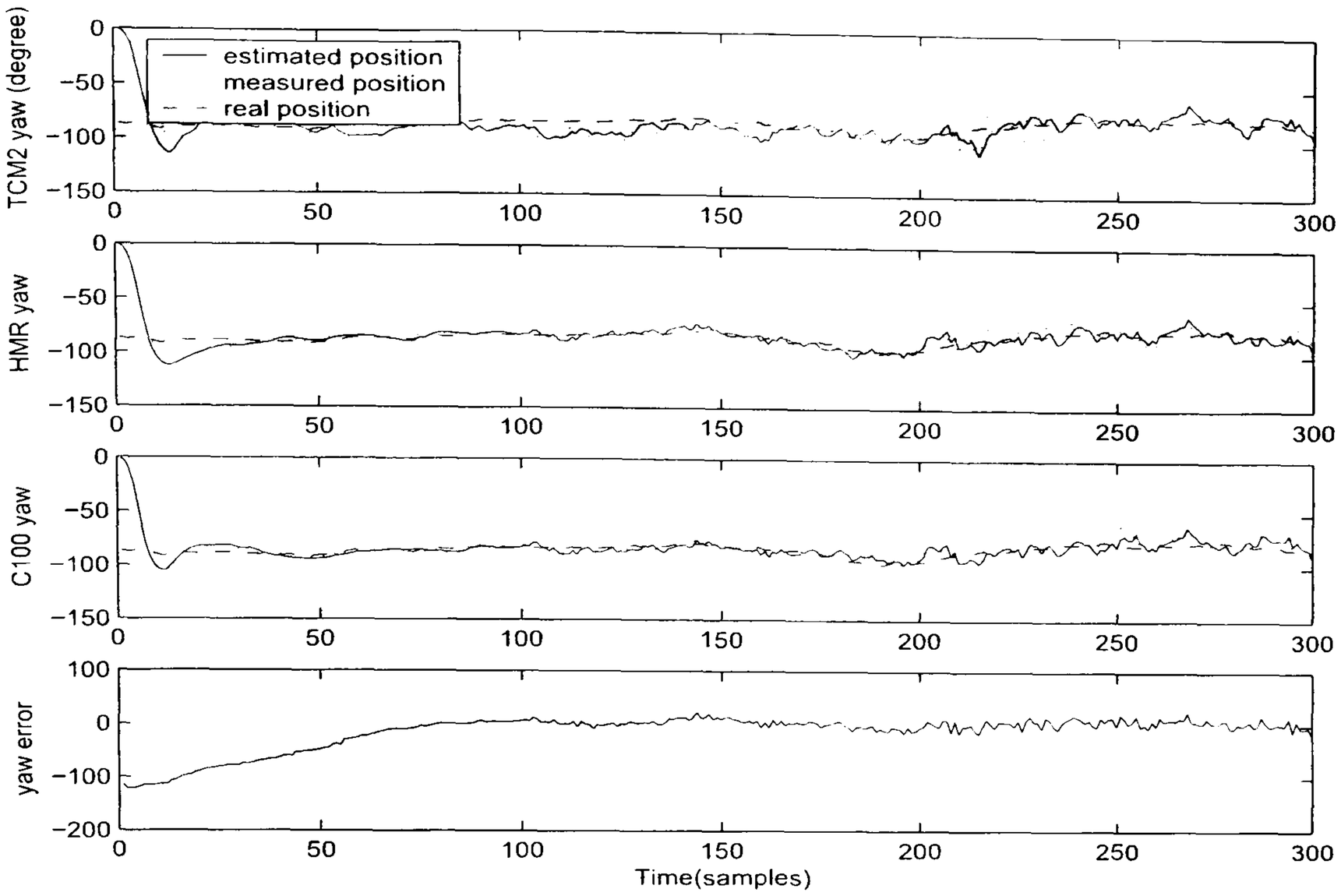

Figure 6.6: MMAE with varying $R_k(n)$ algorithm fusion result

6.4.2 Varying $Q_k(n)$ scenario

Using the same ARMAX model produced in Section 4.2, three values for the $Q_k(n)$ were arbitrarily chosen based on:

$Q_k(1) = Q_k$, $Q_k(2) = 2Q_k$ and $Q_k(3) = 3.5Q_k$, where $Q_k = diag(0.102)$

The simulated sensor measurement errors are increased over time, therefore Q_k values are correspondingly increased from Q_k to $3.5Q_k$, also the corresponding probabilities will change over time.

The elemental filter probabilities are shown in Figure 6.7, Whereas the final fusion heading and three compass MMAE outputs are depicted in Figure 6.8.

In order to compare the fusion accuracy, FLA-FKF with adaptive feedback algorithm which proposed in Chapter 5 is implemented here. The RMSE are compared in Table 6.1, the analysis of the simulation and RMSE results will be presented in the next section.

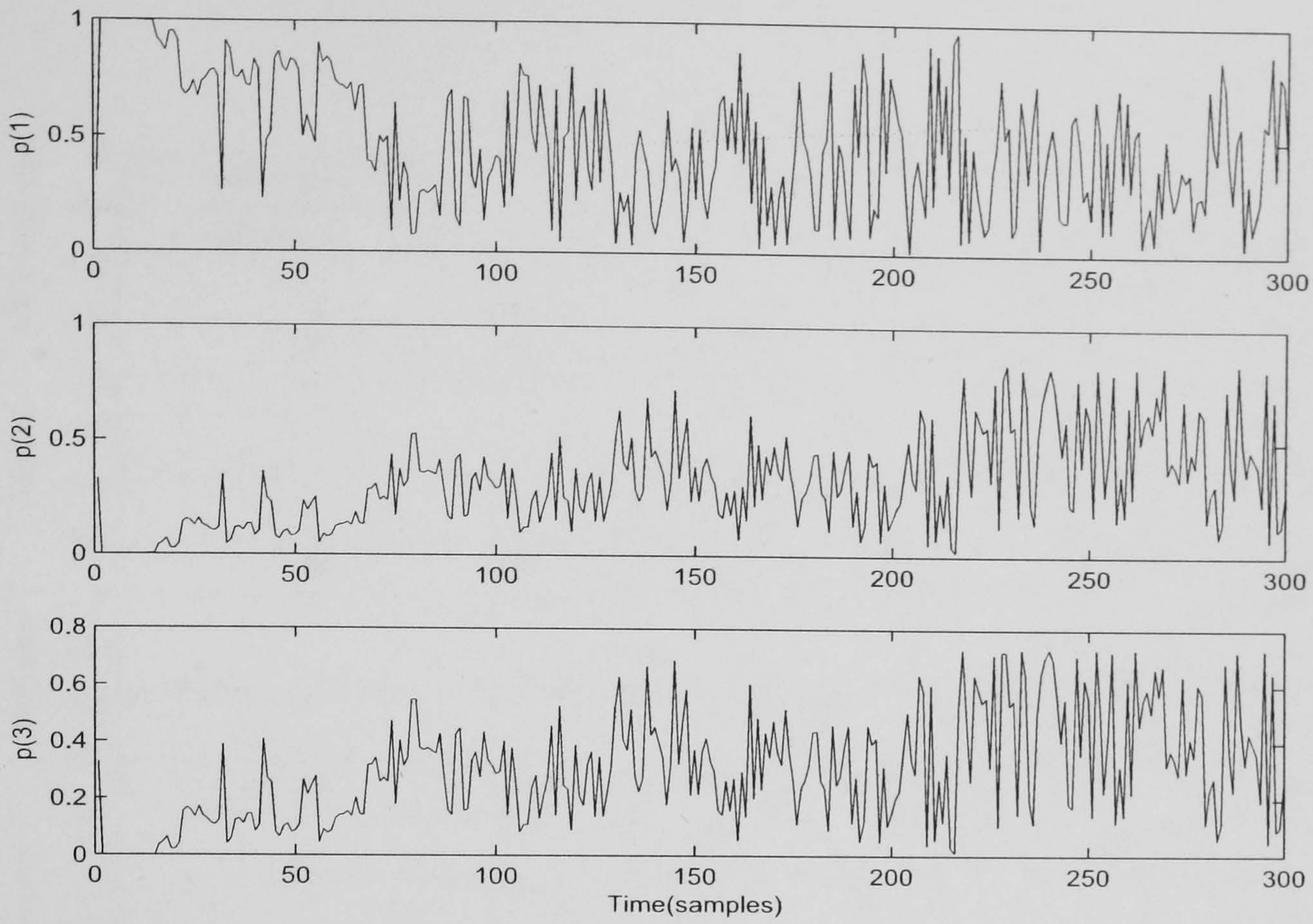

Figure 6.7: The elemental filter probabilities (TCM2 with varying $Q_k(n)$ matrices)

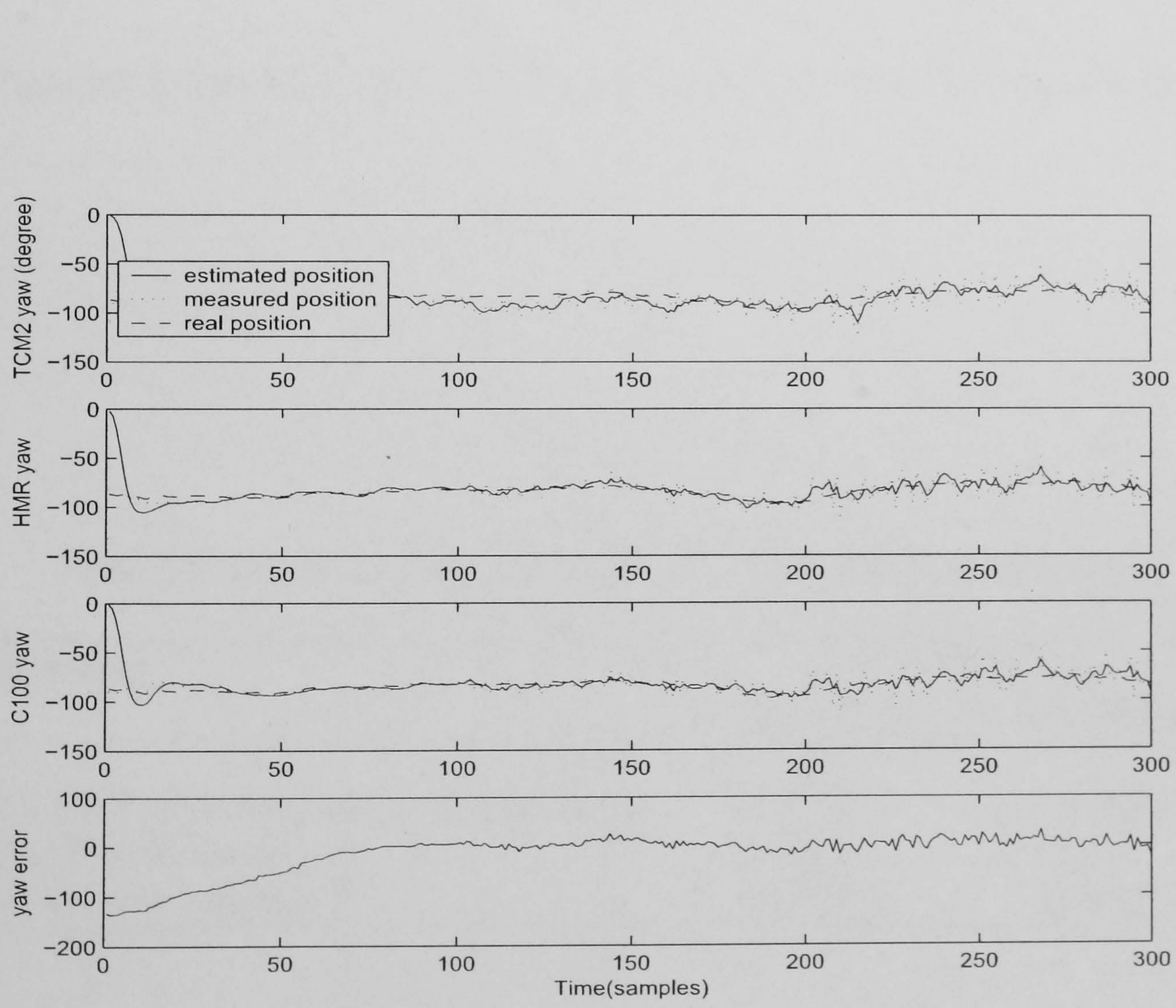

Figure 6.8: MMAE with varying $Q_k(n)$ algorithm fusion result

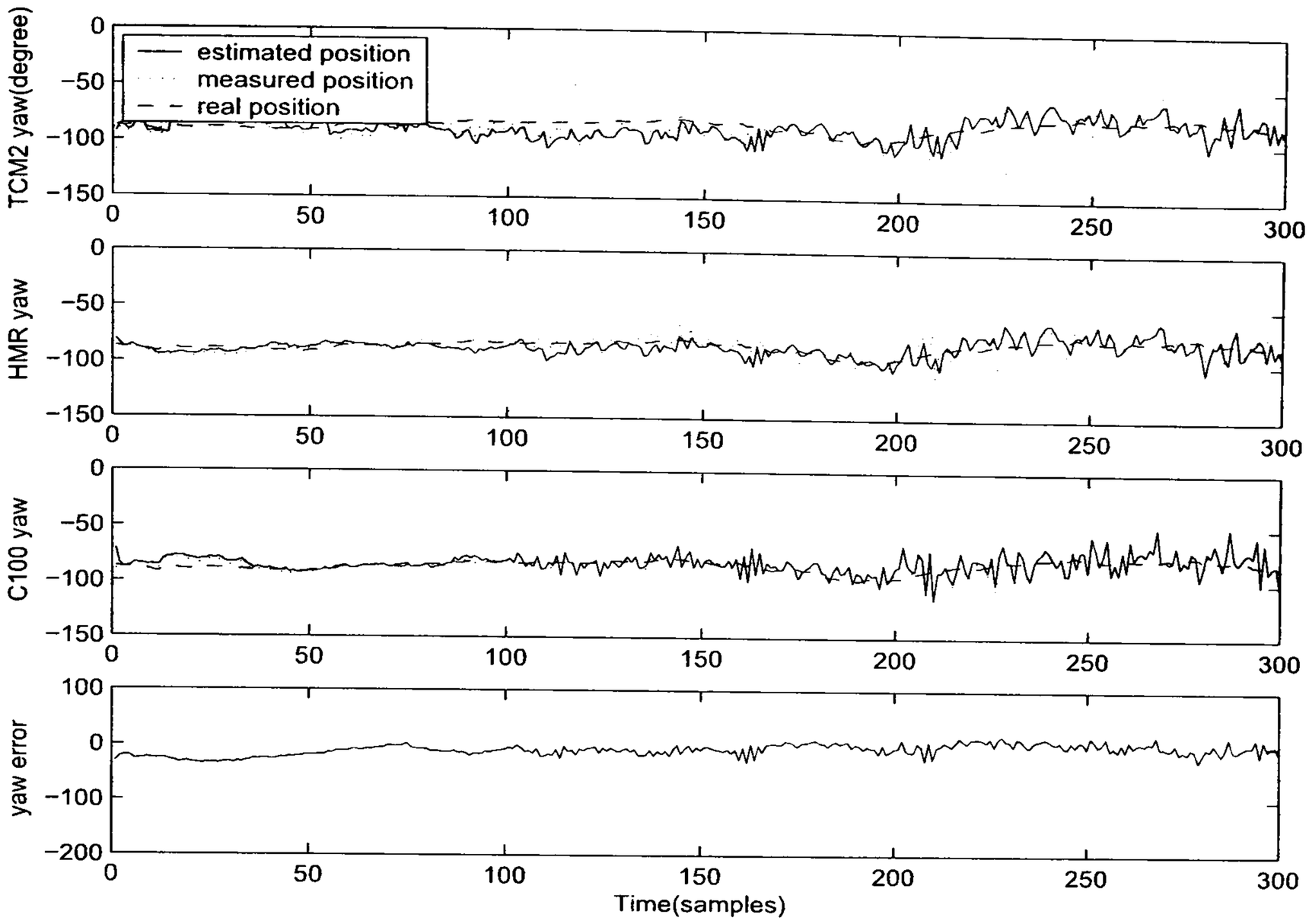

Figure 6.9: The FLA-FKF with adaptive feedback algorithm fusion result

Table 6.1: RMSE comparison of MMAE and FLA-FKF algorithm

Algorithms	RMSE	
	0-100 samples	201-300 samples
FLA-FKF with adaptive feedback factors	9.1795	1.4573
MMAE with varying R	34.6330	4.5320
MMAE with varying Q	38.1396	6.0460

6.4.3 Discussion

The simulation and RMSE results shown above attempt to verify the proposed MMAE algorithm's accuracy and robustness. The $R_k(n)$ and $Q_k(n)$ matrices vary with different elemental filters separately. and very similar results are achieved.

The elemental filters' probabilities results are presented in Figure 6.5 and Figure 6.7 respectively. The measurement noise has smaller values at the beginning, therefore the probability for the first elemental filter ($R_k(1) = R_k$)is approximately equal to 1. When the residual values increase over time, the probability for the second elemental filter ($R_k(1) = 2.5R_k$) becomes larger. For the third elemental filter ($R_k(1) = 5R_k$), the probability is also increased. Similar situation also occurs on the MMAE with varying $Q_k(n)$ matrix. This tuning process of the probabilities for elemental filters assures that the MMAE algorithm output the best state estimates by utilising optimal weighting factors.

The fusion results shown in Figure 6.6 and Figure 6.8 presents the overall heading residuals, as well as the individual MMAE estimates for each compass. The overall fusion result accuracy is compared with the MSDF algorithm presented in Chapter 5, the RMSE results are shown in Table 6.1. However, for MMAE, as the initial state is 0 which has a big difference with the first measurement. Therefore the overall yaw errors is about 4 times of FLA-FKF at the first 100 samples. As a comparison, the FLA-FKF can quickly adapt with the sensor measurement from the initial state (equals 0). Apparently, the FLA-FKF has faster speed in tuning the initial parameters than MMAE.

Comparing the RMSE values from 101 to 300, the RMSE value of FLA-FKF is 1.4573, whilst the RMSE of MMAE with varying R algorithm is reduced to 4.5320 and RMSE of MMAE with varying Q algorithm is 6.0460. Apparently, FLA-FKF produced a more accurate result than MMAE, the MMAE can also reduce the sensor noise but the overall accuracy is not as good as FLA-FKF.

6.5 Concluding remarks

In this chapter, alternative MMAE fusion algorithms are presented. The standard MMAE techniques were introduced and a modified MMAE combined FLA-CKF algorithm is provided. Three elemental filters are implemented for each compass in order to test the algorithm's robustness. Also, an overall heading is provided to compare with the FLA-FKF. The proposed MMAE algorithm has the potential to be utilised as a fault tolerant navigation system by increasing the number of elemental filters. Nevertheless the more elemental filters will increase the computation load. An investigation to determine the optimal number of the elemental filters for the MMAE is recommended for the furture research.

Chapter 7

EXPERIMENTATION WITH THE *SPRINGER* USV

The ultimate step in a navigation system design is to evaluate its performance in a real time environment, as well as its cooperation performance with the onboard guidance and control system. This chapter concentrates on real time experiments onboard the *Springer* USV, and results and analysis of the recorded data.

As the the fuzzy logic based MSDF algorithm which is presented in Chapter 5 presents robust simulation results, it has been selected as the onboard navigation system. Therefore, the MMAE algorithm developed in Chapter 6 has not been tested experimentally. To the author's knowledge this is the first successful application of using a FLA-FKF with an adaptive information feedback algorithm for an onboard navigation system. Therefore this thesis makes an extremely novel and useful contribution to navigation system design in general.

7.1 Experiments introduction

7.1.1 Introduction

The primary aim of this research is to develop an intelligent navigation system which can implemented on the *Springer* in real time. Also the *Springer* is envisaged as a testbed for other research groups to test their NGC system. Hence the navigation system should be flexible enough to accommodate various requirements set by the user, for instance, the user could change navigation parameters via user interface.

It has been observed that most of the on-going USVs can only operate in remote control mode, the operation of the vehicle relies on the sensor/video feedback to the control console, then the command is sent to the vehicle by an operator. Therefore the onboard navigation system does not cooperate with the control system. Currently in the literature, there are only few USVs that can operate in a fully autonomous mode (Pascoal *et al.* 2000, Dynamical Systems and Ocean Robotics (DSOR) Laboratory 2000, Majohr and Buch 2006), however the real time experimentation results are focused on the performance of the control system. Consequently, there is a distinct lack of results and analysis relating to onboard navigation systems.

7.1.2 Experiment setup

In Chapter 3, onboard sensors, user interface, data transmitting/receiving are introduced. Herein more details of the experiment setup are presented.

As mentioned in Section 3.2.3, the DAQ PC collects all the sensor data and transmits the data in a form of a string to the navigation PC. In addition to the sensor data, the string provides the information on the run type, the file name of the recorded data, the

desired heading, navigation parameters, controller parameters, and a counter which allows MATLAB data to be synchronized with the LabView data. The run types, NGC parameters as well as the file name can be altered during a mission.

The run type 'rX' dictates a mission to be executed followed by the string and some other parameters to be used by the controller. Currently, 15 run types have been designed for the NGC program, the details are shown in Table7.1. The user can easily add their own run type by modifying the user interface.

Table 7.1: The details of the run type designed for NGC system

Run type	Operation
r0	Stop the vehicle and wait for a valid command
r1	Change reference heading as the specified value from the user interface
r2	Alter the LQG controller parameters
r3	Alter the MPC controller parameters
r4	Alter the navigation strategy parameters
r5	Change the acceptance range for waypoints
r6-r14	Operate different navigation and control programs as specified

It worth noting that the 'r0' run type is used when the user wants to stop the motors. It is also used when the user needs to change the run type. For example, the vehicle is running in 'r8' which utilizes a fuzzy logic MPC control strategy. When the user would like to change the parameters of the MPC controller, the user has to input 'r0' before 'r3', this strategy enables the NGC system has enough time to alter the programs.

7.2 Experiment results

Now the results of the application of FLA-FKF are presented. All of the experiments were carried out at the Roadford Reservoir in north Devon, UK. A heading reference guidance law is employed in the guidance system, whereas the MPC strategy is used to control the vehicle, more information of the MPC algorithm can be found in Appendix D.

During the experimentation, one of the compass KVH C100 outputs exhibited an unstable performance, therefore, it was isolated as a permanent fault. Consequently, the result shown here is fused by the TCM2 and HMR 3000 compasses only.

Two sets of trial were set up to test the proposed navigation strategy, the sensor models derived in Chapter 4 were applied here. The initial values of the Q and R matrices were chosen as follows:

$$Q_{TCM2} = \begin{bmatrix} 0.1 & 0 \\ 0 & 0.1 \end{bmatrix}$$

$$R_{TCM2} = \begin{bmatrix} 3^2 & 0 \\ 0 & 3^2 \end{bmatrix}$$

$$Q_{HMR} = \begin{bmatrix} 0.1 & 0 \\ 0 & 0.1 \end{bmatrix}$$

$$R_{HMR} = \begin{bmatrix} 1.5^2 & 0 \\ 0 & 1.5^2 \end{bmatrix}$$

7.2.1 FLA-FKF with adaptive feedback factors

The proposed FLA-FKF algorithm with adaptive feedback was applied on *Springer*, the TCM2 and HMR 3000 compass measurements and estimated heading are shown in Figure

7.1, the corresponding information factors are shown in Figure 7.2. The vehicle heading result processed by the MPC controller is shown in Figure 7.3.

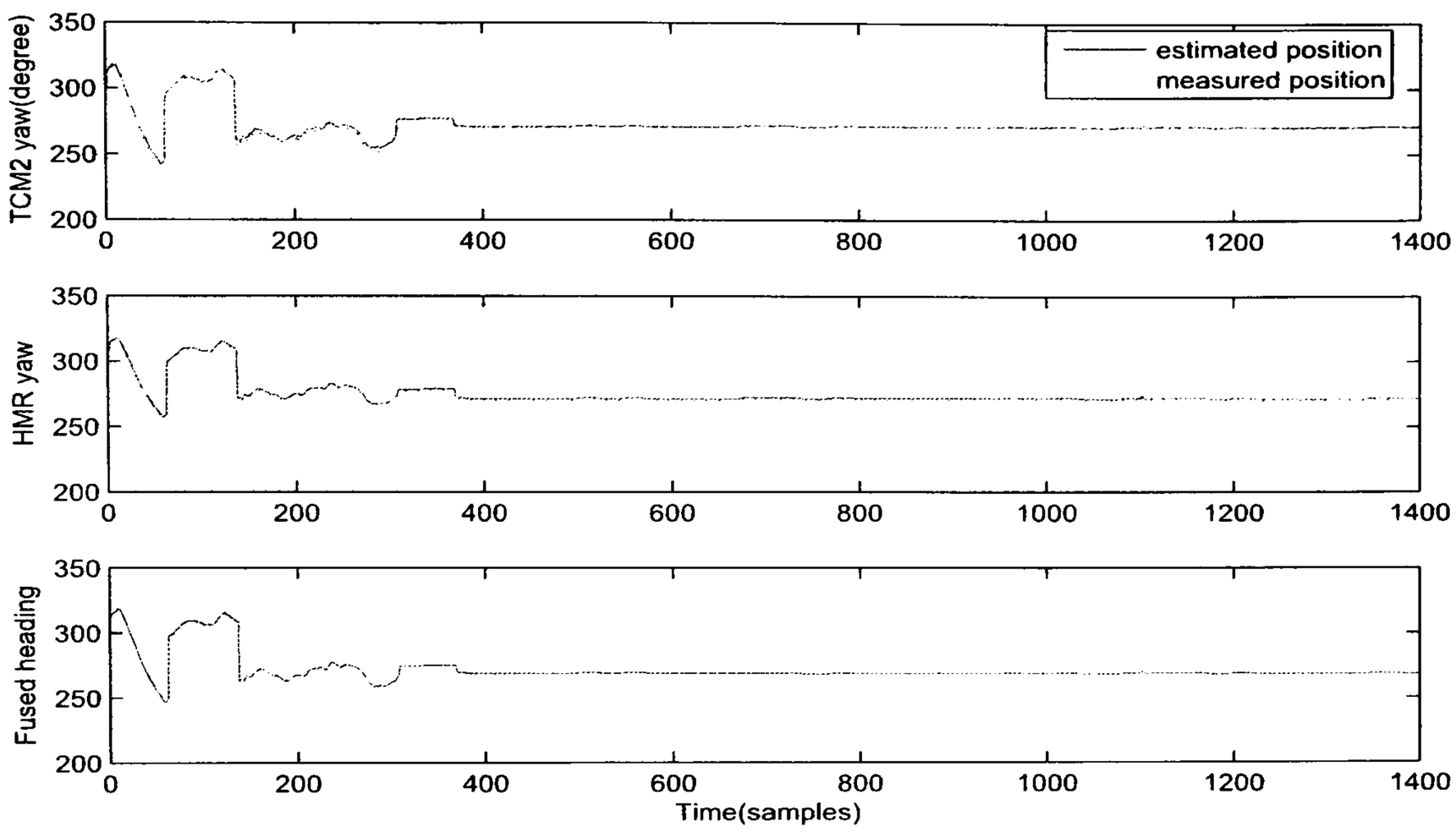

Figure 7.1: Experimental heading output using FLA-FKF with adaptive feedback factors

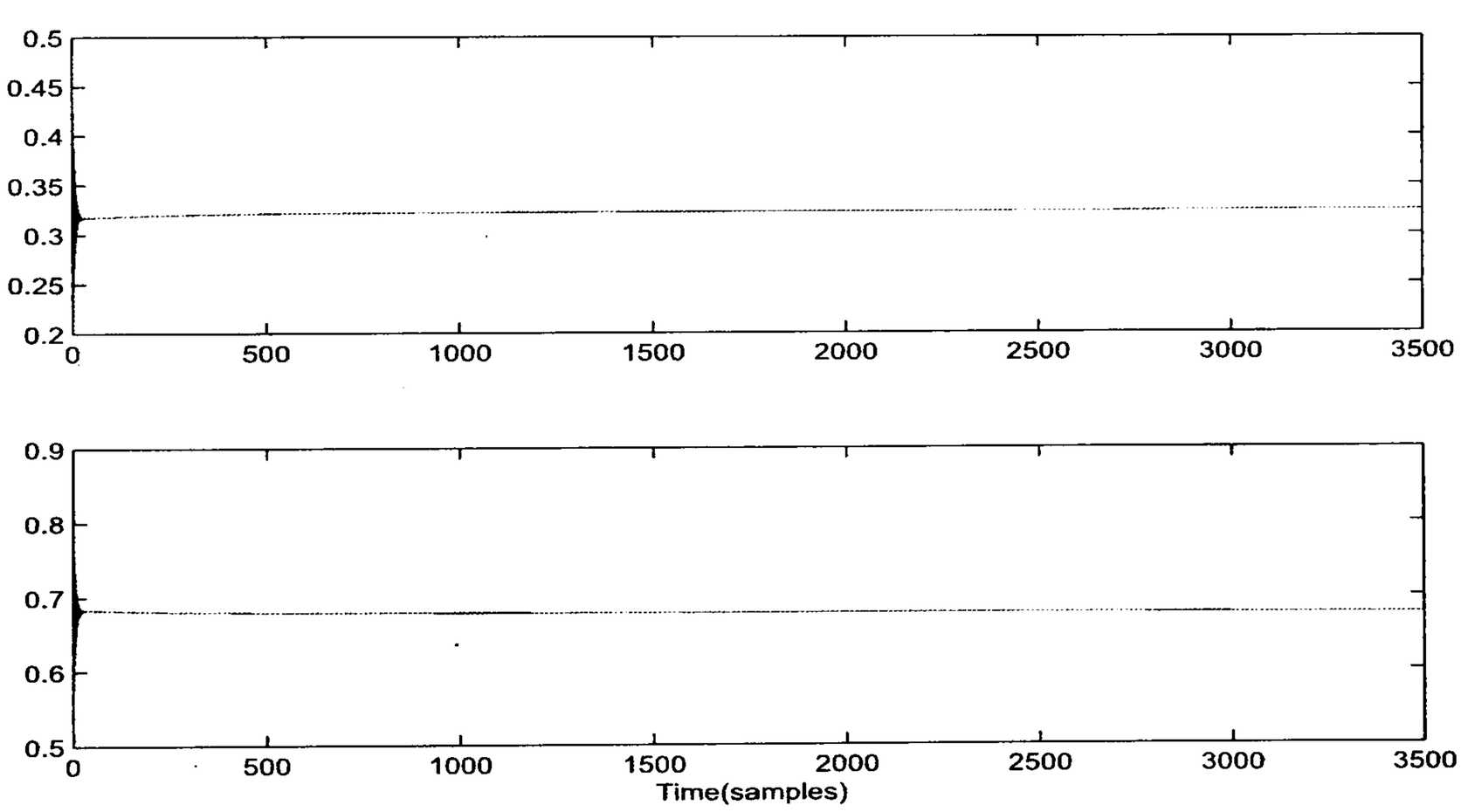

Figure 7.2: Information feedback factors (β_i)

The vehicle reached the desired the course after the 400 samples, the fused heading can effectively reduced the small random noise. Consequently a stable estimation is achieved. The corresponding information factors were initially chosen as 0.5 for each sensor, as the HMR 3000 compass is stable and accurate sensor. The feedback factors for the HMR 3000 finally were chosen as 0.68 according to its performance. Consequently, the HMR

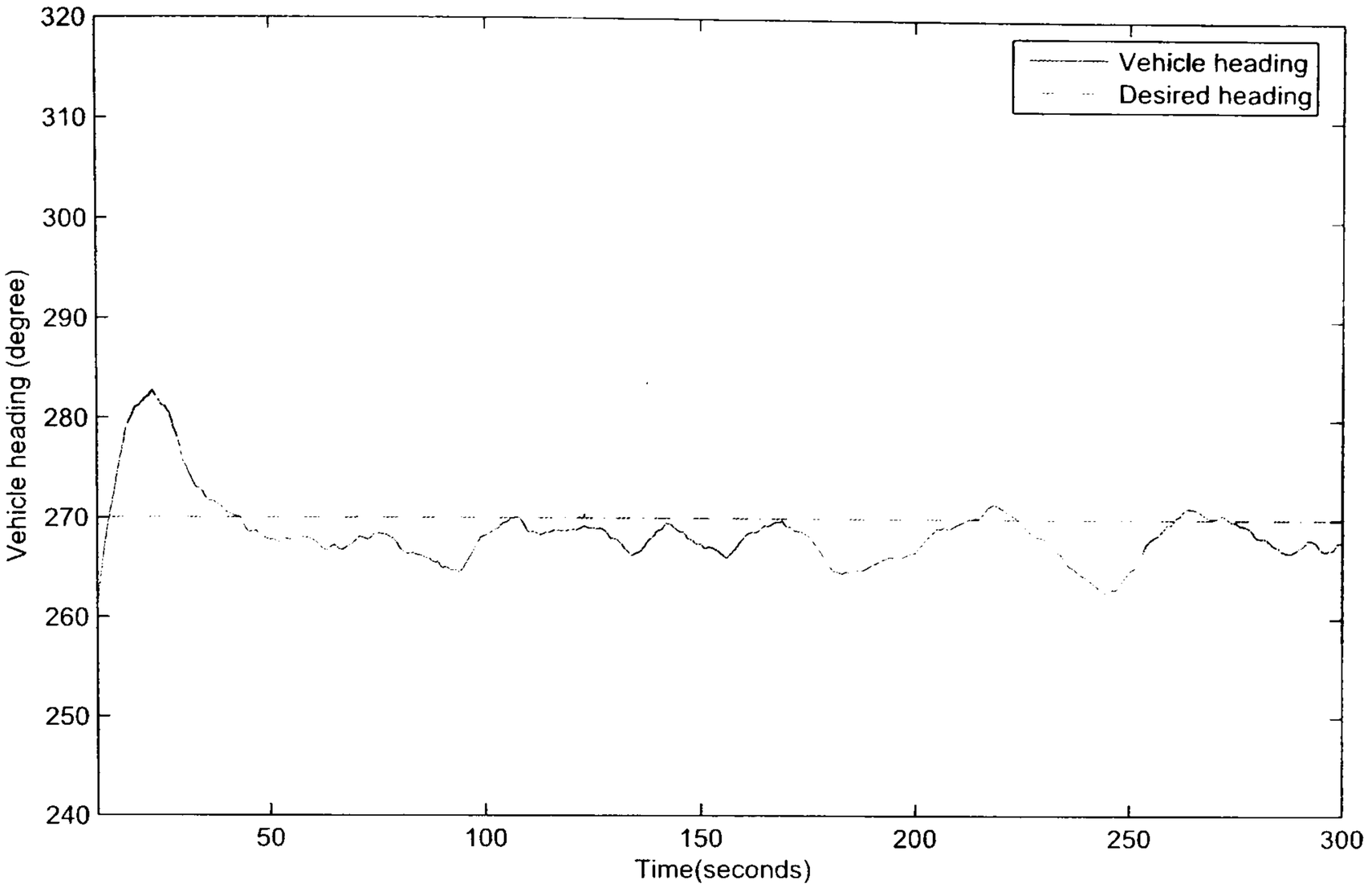

Figure 7.3: The vehicle heading output by utilising MPC controller (Courtesy of Dr. Naeem)

3000 compass performs more contributions to the global estimation. The MPC controller received the fused heading results from the navigation system continuously, therefore the vehicle heading reached the desired heading within 1 minute. The GPS position is presented in Figure 7.4.

Because the unstable performance form the compass KVH C100, the experiments shown above were conducted by utilising two sensors only. The recorded KVH C100 data is employed in the following simulation as a noisy sensor measurement. The simulation result is shown in Figure 7.5 as a comparison with the result shown in Figure 7.1

In Figure 7.5, there was not significant difference between the experimental result shown in Figure 7.1 which use two sensors only. As the KVH C100 is unstable (sometimes outputing a garbage sentence), it is better to ignore this sensor for the following experiments.

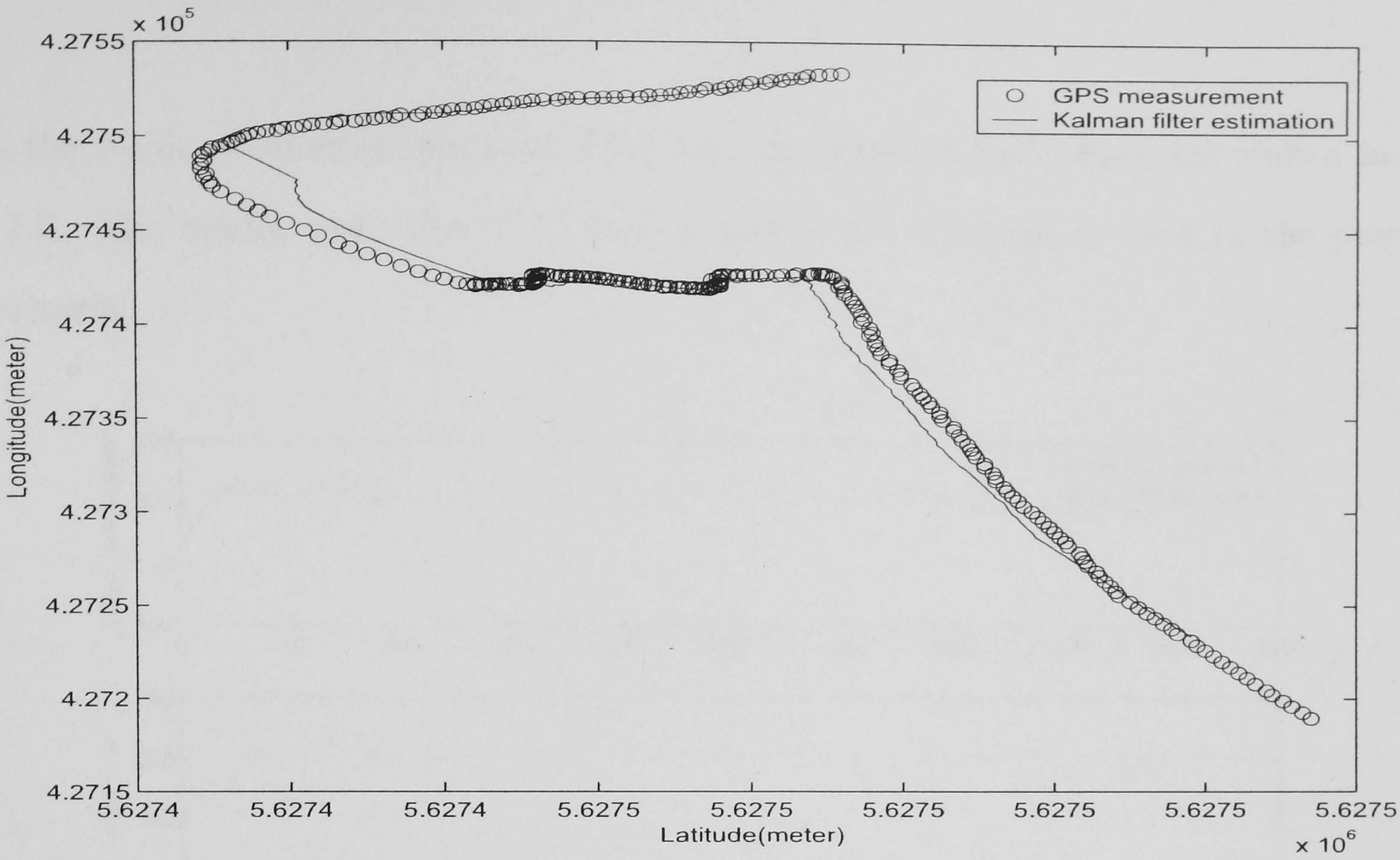

Figure 7.4: The GPS position

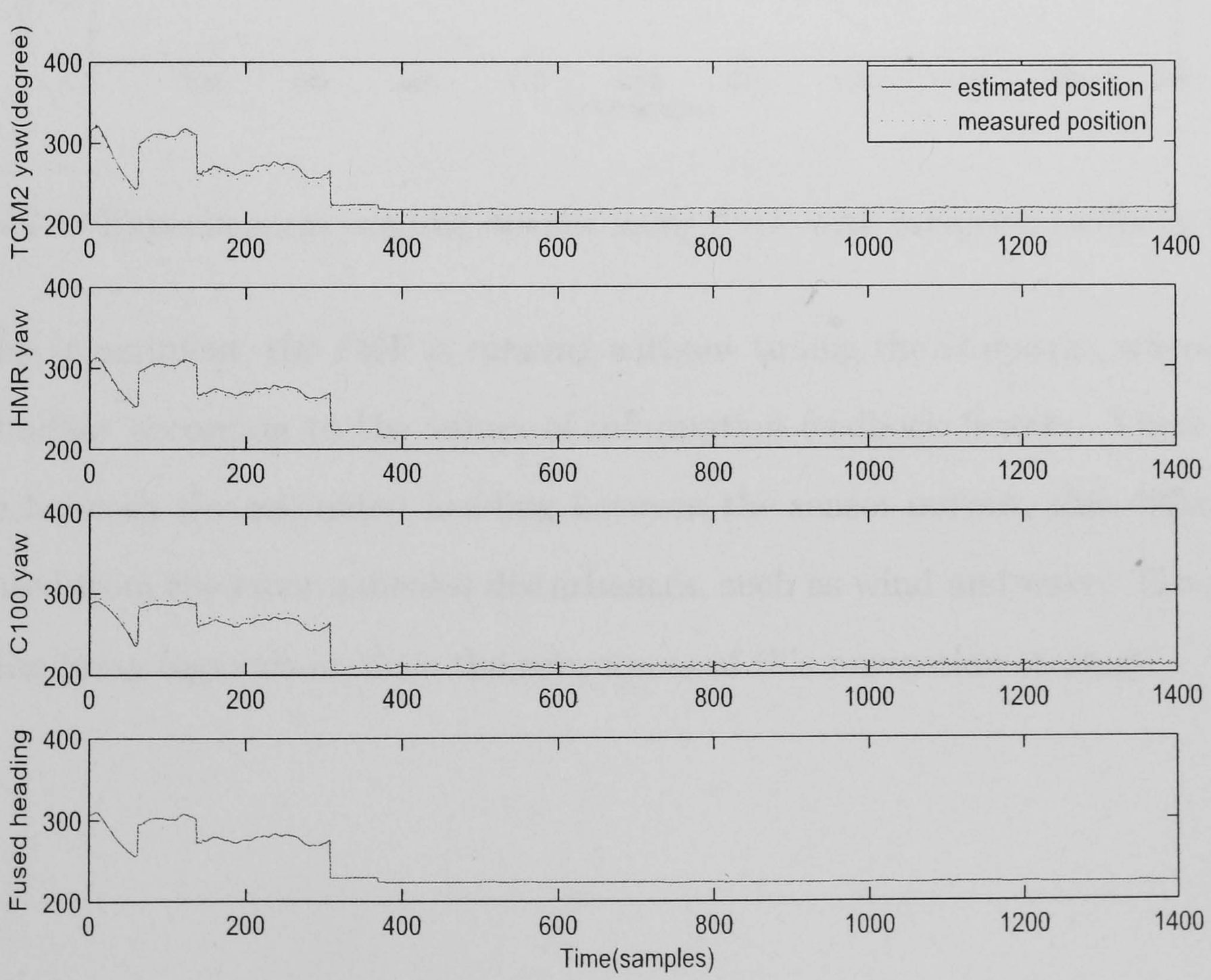

Figure 7.5: Simulation result with noisy measurement from the KVH C100

7.2.2 FKF with adaptive feedback factors

Now the result of adaptive feedback FKF running without fuzzy logic are shown in Figure 7.6. The model and value of Q and R matrix are identical as that in the previous experiment.

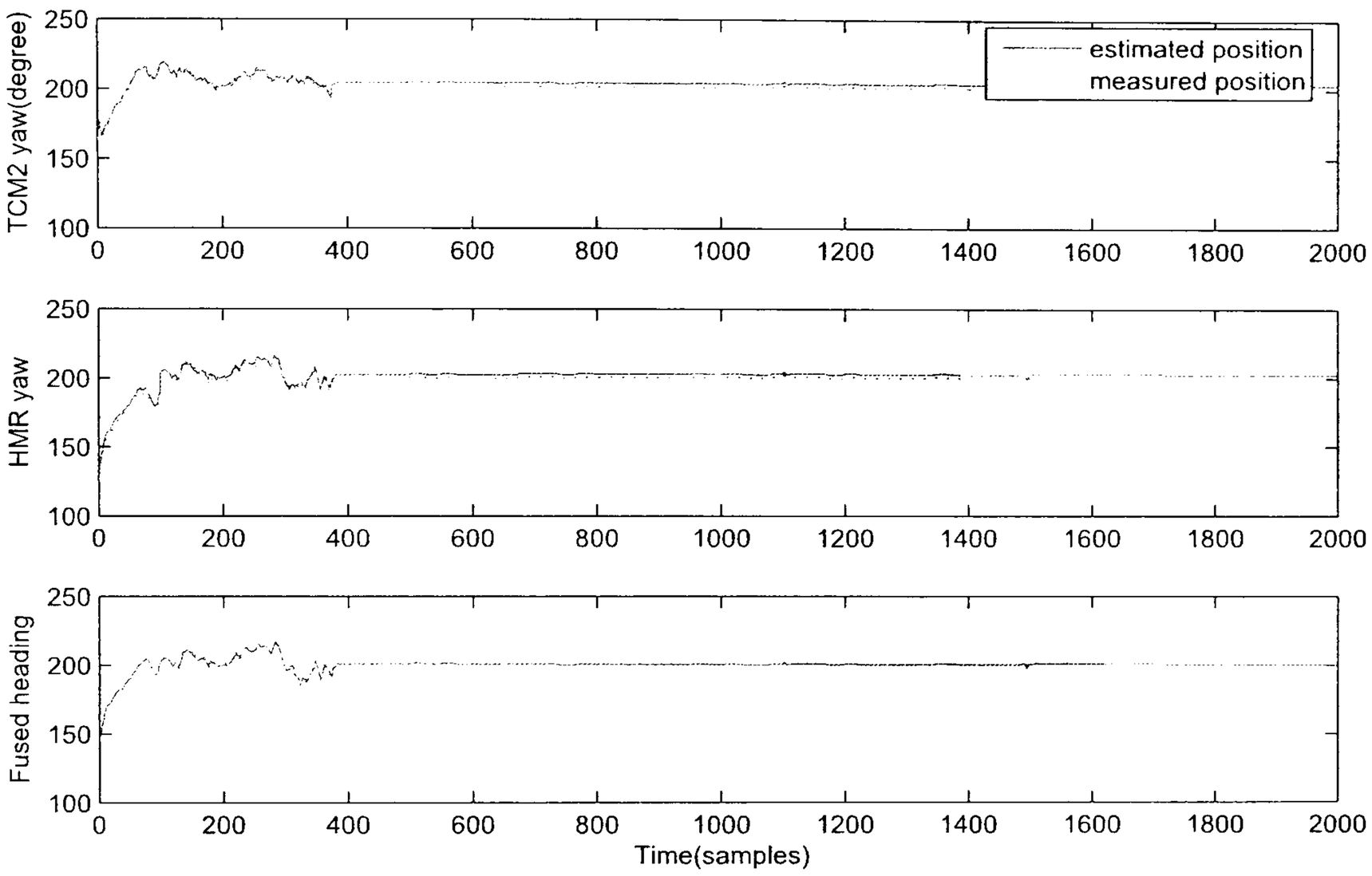

Figure 7.6: Experimental heading output using FKF with adaptive feedback factors

During this experiment, the FKF is running without tuning the R matrix, where as the Q matrix is adapt according to the values of information feedback factors. There are some difference between the estimated heading between the sensor output, this different could be generated from the environmental disturbances, such as wind and wave. The algorithm without the fuzzy logic also reduce the robustness of this navigation strategy.

7.3 Concluding remarks

Simulation results can provide a good insight during the process of the navigation strategy development. however the true potential can only be judged through experimentations. In this chapter, the results of the FLA-FKF strategy have been revealed. It is shown that the proposed algorithm is capable of producing outstanding results under unpredictable environment circumstances. Comparing with FKF without fuzzy logic, the FLA-FKF presents more accurate fusion results. However, real time experiments and simulation presented in Chapter 5 are carried out in different situations, therefore the experiment results cannot compared against simulated results.

The prevailing weather conditions were severe with a force six to force eight wind, and as a result, the overall accuracy of the fused results were found to be reduced but was still of an acceptable level.

After the analysis of the experimental results, summary, conclusions and recommendations for further research will be presented in the next Chapter.

Chapter 8

SUMMARY, CONCLUSIONS AND FUTURE WORK

In this final chapter, the overall research objectives is revisited. A brief summary of each chapters followed by a conclusions drawn with respect to what was anticipated and what has been achieved in terms of the aim and objectives of the research programme. Lastly, recommendations for future research are provided that could stimulate further research projects in this field of study.

8.1 Objectives of the research revisited

The aim and objectives of the overall project, as defined in Chapter 1 are reproduced here for ease of reference.

- Critically review current autonomous navigation techniques.
- Survey current USV projects and analysis the features of different applications.

- Develop a friendly user interface which can allow the user access an onboard NGC system remotely. Also design a practicable communication manner between the NGC system for real time trials.

- Design a novel fault tolerant fuzzy logic based MSDF system for *Springer* as an onboard navigation system.

- Design a multi-model adaptive estimation (MMAE) algorithm as an alternative navigation solution.

- Evaluate the proposed navigation strategy performances in simulations for various scenarios.

- Employ a simulated navigation strategy in the full scale trials, and evaluate the experimental performance results.

8.2 Summary

In Section 8.1, the objectives of this research was revisited. Therefore a summary is given here according to these objectives.

USV research and development is on the verge of reaching maturity yet applications are very few. The cost associated with USV development particularly of the power requirement, onboard sensors and communication system have imposed a significant constraint on their development. The aim of this project as defined in Chapter 1 was to design and develop a low cost USV with an electric propulsion system that would be responsible of undertaking multiple surveys and pollution tracking in shallow waters. To satisfy such requirements, the vehicle needed a robust and effective NGC system onboard which could accommodate different environment condition. In particular, a fault tolerant navigation system plays a vital role in any NGC system.

Chapter 2 provides comprehensive background material on autonomous navigation strategies. Satellite navigation utilizing GPS/DGPS has been widely applied in modern navigation system. Dead reckoning as a traditional navigation strategy has been developed with the advanced technology where electronic, magnetic sensors are involved. INS is a relevant new process, however the cost of an IMU has limited the growth of this technique. Recently, multiple sensor navigation has been widely used with respect to its flexibility along with low cost sensors that can be manipulated together in order to achieve a robust and fault tolerant system. Especially, an enhanced performance can be accomplished when AI techniques are included. Apart of the navigation strategies reviewed, several on-going USVs for military, scientific research and commercial applications are introduced and compared respectively.

The *Springer* has been proposed as the first USV for research purpose in the UK. The *Springer* hardware configuration was detailed in Chapter 3. The Chapter demonstrated the overall physical structure and electrical installation of *Springer*. A low pass filter is implemented on the TCM2 compass in order to reduce the noise of the sensor. The onboard NGC system communication between the Peli cases and user, the onboard navigation sensor suite, as well as the user interface were briefly explicated. The user interface allowed the user to monitor and modify the NGC program in a flexible way over a long distance.

There is no doubt, sensor modelling is a key factor in designing a Kalamn filter. Sensor models are investigated in Chapter 4 by using first principle and SI techniques. Experiments have been carried out to obtain data sets whereby SI techniques were suggested and applied to derive the models for the onboard compasses. Multiple level signals are given to the compasses as the input, SI techniques were used to derive the ARMAX model for each compass. The evaluation results show that the models are suitable to be employed in a Kalman filter.

With the knowledge of the sensor models, two distinct multiple sensor strategies combining

fuzzy logic technique were developed. The first strategy was presented in Chapter 5, it is a fuzzy logic MSDF using a cascaded Kalman filter structure. FLA-CKF, FLA-DKF and FLA-FKF strategies were examined under various sensor fault scenarios. The simulation results show that the FLA-FKF with adaptive information feedback method has the best fault tolerant capabilities among other proposed algorithms.

Another multiple sensor navigation strategy is presented in Chapter 6 by using MMAE and fuzzy logic. MMAE is renowned as an effective way in estimating the state for the system using a bank of elemental Kalman filters. The same fuzzy logic rules and membership functions are implemented in a FLA-CKF. Three elemental Kalman filters are utilised, different values are chosen for Q or R matrices for each elemental filter. The simulated results shown the weight of each elemental filters are changed all over the time according to the result of a hypothesis algorithm. This result indicate how close each of the filter's models is to the true model. The simulated fusion accuracy is comparable with the MSDF strategy, however the drawback of this system is the high computation load generated by each elemental Kalman filters.

Finally in Chapter 7, the MSDF algorithm developed in Chapter 5 was implemented on *Springer*. This is considered one of the principle novelties of this research where a fuzzy logic strategy is employed for optimization purposes in a MSDF system. Also it is the first time a fuzzy logic based MSDF navigation system has been applied on an USV. Moreover, the implementation of a MSDF navigation algorithm in *Springer* USV was imperative to gauge its robustness and cooperating activities with the guidance and control system. The experiments were carried out with the wind and wave disturbances. The experimental results presented show a remarkable performance, and the effective interactive cooperation with the guidance and control system. However the overall accuracy was reduced according to the environment reasons.

8.3 Conclusions

Most of the current military and commercial USVs can only operated in remote control mode exception of a few USVs developed for scientific research purposes. The military USVs feature with high speed and various surveillance capabilities. Whilst for the commercial USVs, a friendly user interface and easy maintenance are the main concern. The *Springer* USV was designed to be a mobile, rapidly sampling, remotely operated sensor platform which can undertake various hydrological surveys. Therefore, the design of a fault tolerant NGC system became a research focus for the *Springer* project.

The thesis focuses on the investigation of the MSDF method utilizing fuzzy logic and CKF techniques to provide enhanced accuracy of navigation information for *Springer*. To the author's knowledge, this hybrid algorithm of its kind to be applied on an USV and is thus considered as the major contribution in relation to autonomous navigation system design and USV techniques. All the contributions of the work presented in this thesis are summarized in Section 1.4.

A FLA-FKF with adaptive information feedback algorithm was selected as an onboard navigation system because of its remarkable robustness and fault tolerant capabilities. In this FLA-FKF approach, the requirement to have complete *a priori* knowledge of the filter statistic, represented by the Q and R matrices, are relaxed.

The fuzzy logic strategy employed adapt the R matrix according to the difference between the value of the theoratical innovation covariance and the practical innovation covariance. A moving window is used to capture the practical innovation. The size of this window is determined empirically in such a way so that it is large enough to capture the dynamic of slowly varying covariance values or small enough to capture the dynamic of fast varying covariance values.

The adaptive information feedback method tune the Q matrix according to the value of the information feedback factors. This adaptive feedback factor method enables the more accurate sensor make more contribution to the global estimation.

The simulation results shown in Chapter 5 was demonstrated that in cases where sensor data is very poor or ambiguous, this FLA-FKF method can effectively combine sensor information and produce a more accurate heading than other proposed methods. It should be noted that this algorithm is highly implementable in real time. This is because it can reduce the sensor fault situations by using simple check process before the FLA-FKF algorithm. This algorithm allows the user to add more sensors or isolate sensors without stoping the program. This algorithm also employs a reference sensor, therefore the program can still output navigation information even when all of the compasses having serious faults.

An alternative navigation strategy was proposed in Chapter 6 by using MMAE. This method is suitable for fault detection and classification. The various elemental models can be used to express the different sensor fault situation. Consequently, the sensor fault can be detected and disturbances can be effectively reduced. At the moment only 3 elemental filters are employed for each compass, therefore the overall heading accuracy is not as good as FLA-FKF. However it does provide another solution for fault tolerant navigation system.

It is important to note that the computation techniques set forth in this study were developed for an USV. However they are not restrictive and can effortlessly be applied to other autonomous vehicles either in the land and aerospace domains. Also the hybrid MSDF technique can also be applied in any system equipped with multiple sensors by modifying the system models.

8.4 Recommendations for future work

A number of achievements have been made throughout the course of this thesis. Nevertheless, scientific research is an ongoing process and clearly there are several topics for future research involving *Springer* USV. A list of the recommended follow ups based on this work are provided below.

8.4.1 Further experiments and research on the MMAE

The most obvious and important work to be conducted is to carry out further experiments involving the MMAE algorithm which have not yet been tested on *Springer*. Furthermore, for the MMAE, more elemental filters are recommended in order to improve the overall fusion accuracy. As a result, a higher computation load will be generated. Therefore to find an optimal number of the elemental filters for the MMAE is recommended.

In the literature, several algorithms were proposed in order to improve the computation efficiency (Li and Bar-shalon 2000, Fisher and Maybeck 2002, Vasquez and Maybeck 2004). For this particular research, a new approach in this field is recompounded.

8.4.2 Consideration of disturbances from pitch and roll

The generic USV is a three Degree Of Freedom (DOF) system , where pitch and roll movement generate disturbances to the yaw output. However, in this thesis, the pitch and roll signals are only used to generate a warning for the user when the limitations are reached ($\pm 45^o$). The cross-coupling effect from pitch and roll signals were ignored in extracting the sensor linear mathematical models. For further research, three DOF data are recommended to estimate a nonlinear model for the sensors using SI. An Extended Kalman Filter (EKF)

can be used to develop a MSDF system.

8.4.3 Collision avoidance system for *Springer*

During the last two decades, CAS has been designed for various vehicles including ROV, AUV, AAV etc. A comprehensive review has been provided by Tan (2004). An intelligent CAS has been designed for an AUV by Tan (2006), and Larson et. al designed a CAS for an USV (2006). As the *Springer* will be operated in open water with little environment knowledge, therefore the risk of collision with other vessels or obstructions could be high and consequence serious. A vision (eg. sonar, onboard camera etc.) based CAS should be designed and implemented for safe operation.

8.4.4 Multi-vehicle navigation system

In Section 2.3, several multi-vehicle coordinate network applications were reviewed in detail. From the literature, a network operation will expand the USV operation form two dimension to multiple dimensions. For instance, an AUV can undertake various tasks underwater, however its positioning signal is very low, therefore an USV can provide the information to the AUV via communication link. Consequently, in order to realize the multiple dimension, synchronize operation, a hierarchical structure navigation system and powerful communication system are required.

REFERENCES

Aeronautics Defense systems Ltd. (2003). Seastar. Available from http://www.aeronautics-sys.com/Index.asp?CategoryID=41&ArticleID=23&Page=1. Data accessed: October 2006.

Amditis, A., A. Polychronopoulos, N. Floudas and L. Andreone (2005). Fusion Of Infrared Vision And Radar For Estimating The Lateral Dynamics Of Obstacles. *Information Fusion* **6**(2), 129–141.

Aris, R. (1995). *Mathematical Modelling Techniques*. Wiley-Interscience.

Autonomous Flight Systems Laboratory, University of Washington (2005). Autonomous Guidance, Control and Communications for Unmanned Surface Vehicles. Available from http://www.aa.washington.edu/research/afsl/research/usv.shtml. Data accessed: October 2006.

BAE Systems, North America (2003). The Protector USV: Delivering Proven Anti-Terror and Force Protection Capabilities. Available from http://www.ws-wr.com/epk/BAE_Protector/. Data accessed: October 2006.

Bells, M. (2000). The Compass and other Magnetic Innovations. Available from http://inventors.about.com/od/cstartinventions/a/Compass.htm. Date Accessed, April 10th 2005.

Blair, W D. and Y. Bar-shalon (1996). Tracking Maneuvering Targets with Multiple Sensors: Does More Data always Mean Better Estimates?. *IEEE Trans. Aerospace Electronic System* **32**(1), 450–456.

Boucher, C., J C. Noyer and M. Benjelloun (2001). 3D structure and motion recovery in a multisensor framework. *Information Fusion* **2**(4), 271–285.

Bowditch, N. (1995). The American Practical Navigator. Available from http://www.irbs.com/bowditch/. Date Accessed, April 10th 2005.

Brooke, C. (2005). Brooke's Sensors page. Available from http://www.pacificsites.com/~brooke/Sensors.shtml. Data accessed: October 2006.

Brooks, R. and S. Iyengar (1998). *Multi-Sensor Fusion: Fundamentals and Applications with Software*. Prentice Hall.

Brown, R G. and P Y C. Hwang (1984). A Kalman Filter Approach to Precision Geodesy. *Journal of the Institute of Navigation* **30**(4), 338–349.

Brown, R G. and P Y C. Hwang (1997). *Introduction to Random Signals and Applied Kalman Filtering with MATLAB Exercises and Solutions*. John Wiley & Sons, Inc.

Butler, B. and V. Hertog (1993). Theseus: A Cable-Laying AUV. *IEEE International Symposium on Unmanned, Untelhered, Submersible Technology* pp. 1–6.

Caccia, M., R. Bono, Ga. Bruzzone, Gi. Bruzzone, E. Spirandelli, G. Veruggio, G. Capodaglio, A M. Stortini and G. Capodaglio (2005). An Autonomous Crafe for the Study of Sea-Air Interactions: Sampling Sea Surfaces with SESAMO. *IEEE Robotics & Automation Magazine* **September**, 95–105.

Chen, Y M. and H C. Huang (2001). Application of Neural Networks in Target Tracking Data Fusion. *Neural. Parallel and Scientific Computations* **9**(3), 267–278.

Corfield, S J. (2002). Unmanned Surface Vehicles and Other Things. *Proceedings of the Unmanned Underwater Vehicle Showcase Conference* pp. 83–91. Southampton, UK.

Corfield, S J. and J. Young (2006). Unmanned Surface Vehicles- Game Changing Technology for Naval Operations. Roberts, G. N. and Sutton, R. (Eds). Advances in Unmanned Marine Vehicles. *IEE Control Series* pp. 311–328.

Doyle, R S. and C J. Harris (1996). Multi-Sensor Data Fusion for Helicopter Guidance using Neuro-Fuzzy Estimation Algorithms. *Aeronautical Journal* pp. 241–251. June–July.

Duwaish, H. and W. Naeem (2001). Nonlinear Model Predictive Control Of Hammerstein and Wiener Models Using Genetic Algorithms. *Proceedings of the 2001 IEEE International Conference on Control Applications (CCA01)* pp. 465–469. Mexico City, Mexico.

Dynamical Systems and Ocean Robotics (DSOR) Laboratory (2000). DSOR laboratory project information web site. Available from http://dsor.isr.ist.utl.pt/Projects. Data accessed: October 2006.

Ebken, J., M. Bruch and J. Lum (2005). Applying UGV Technologies to Unmanned Surface Vessel's. *Unmanned Ground Vehicle Technology VII, Proceedings of the SPIE* pp. 5804–5816. Orlando, USA, March 29-31.

Elbit Systems (2005). Stingray Unmanned Surface Vehicle (USV). Available from http://www.defense-update.com/products/s/stingray.htm. Data accessed: October 2006.

Enderle, B., T. Yanagihara, M. Suemori, H. Imai and A. Sato (2004). Recent Developments in a Total Unmanned Intergrated System. *AUVSI Unmanned System Conference.* Anaheim, USA, 3-5 August.

Escamilla-Ambrosio, P J. and N. Mort (2003). Hybrid Kalman Filter-Fuzzy Logic Adaptive Multisensor Data Fusion Architectures. *Proceedings of The IEEE Conference on Decision and Control* pp. 5215–5220.

Escamilla-Ambrosio, P J. and N. Mort (2004). Comparision of Three Fuzzy Logic-based Adaptive Multisensor Data Fusion Architecture. *Proceedings of the 3rd IFAC on Symposium on Mechatronic Systems* pp. 103–108. September, Sydney,Australia.

Farrell, J A. and M. Barth (1999). *The Global Positioning System and Inertial Navigation.* McGraw-Hill.

Fisher, K A. and P S. Maybeck (2002). Multiple Model Adaptive Estimation with Filter Spawning. *IEEE Trans. Aerospace Electronic System* **38**(3), 755–768.

Gao, Y K. and M A. Abousalem (1993). Comparison and Analysis of Centralized, Decentralized, and Federated Filters. *Journal of the Institute of Navigation* **40**(1), 69–86.

Gershenfeld, N. (1998). *The Nature of Mathematical Modeling.* 2 ed.. Cambridge University Press.

Girgis, A A. and R G. Brown (1985). Adaptive Kalman Filtering in Computer Relaying: Fault Classification Using Voltage Models. *IEEE Trans. Power Apparatus Systems* **104**(5), 1168–1177.

Grewal, M S. and A P. Andrew (2001). *Kalman Filtering, Theory and Practive Using MATLAB.* 2 ed.. John Wiley & Sons, Inc.

Grewal, M S., L R. Weilland and A P. Andrews (2000). *Global Positioning Systems, Inertial Navigation.* Wiley-Interscience.

Griffiths, G., P. Stevenson, A. Webb, N. Milard, S. Pebody and J. Perrett (1999). Open Ocean Operation Experience with the AUTOSUB-1 AUV. *IEEE International Symposium on Unmanned, Untelhered, Submersible Technology* pp. 1–12.

Hanlon, P D. and P S. Maybeck (1998). Interrelationship of Single-Filter and Multiple-Model Adaptive Algorithms. *IEEE Trans. Aerospace Electronic System* **34**(3), 934–946.

Heal, G. and B. Kriström (2002). Uncertainty and Climate Change. Available from http://www2.gsb.columbia.edu/faculty/gheal/General%20Interest%20Papers/climatereview.pdf. Date Accessed, October 18th 2005.

Honeywell International, Inc. (2004). HMR 3000 Compass Manual. Available from http://www.ssec.honeywell.com/magnetic/datasheets/hmr3000_manual.pdf. Data accessed: October 2006.

Hornsby, H. (2005). In-Stride USV Force Multipliers. Available from http://www.dtic.mil/ndia/ewc/Hornsby.pdf. Data accessed: October 2006.

ISE group of companies (2000). Search and Rescue Autonomous Marine Vehicles. Available from http://www.ise.bc.ca/SearchNRescue.html#sarpalpub. Data accessed: October 2006.

Kalman, R E. (1960). A New Approach to Linear Filtering and Prediction Theory. *Journal of Basic Engineering* **82**, 34–45.

Kennedy, M. (2002). *The Global Positioning System and GIS: An Introduction*. 2 ed.. Taylor and Francis Group.

Kim, H J., D H. Shim and S. Sastry (2002). Flying Robots: Modeling, Control and Decision Making. *IEEE International Conference on Robotics and Automation* **1**, 66–71.

Kobayashi, F., F. Arrai and T. Fukuda (1999). Sensor Selected Fusion System. *Proceedings of The IEEE International Conference on Multisensor Fusion and Interation for Intelligent System* pp. 123–128.

KVH Industries, Inc. (2004). KVH C100 Compass User Manual. Available from http://www.kvh.com/pdf/540044H.pdf. Data accessed: October 2006.

Larson, J., M. Bruch and J. Ebken (2006). Autonomous Navigation and Obstacle Avoidance for Unmanned Surface Vehicles. *Unmanned Systems Technology VIII. Proceedings of the SPIE* pp. 6230–6242. Orlando, USA, 17-20 April.

Lawrence, A. (1998). *Modern Inertial Technology Navigation, Guidance and Control*. 2 ed.. Springer-Verlag.

Li. X R. and Y. Bar-shalon (2000). Multiple Model Estimation with Variable Structure. *IEEE Trans. Aerospace Electronic System* **36**(2), 448–466.

Lin, C F. (1992). *Modern Navigation, Guidance. and Control Processing.* Prentice Hall.

Liu, F., R. Tao, Y. Wang and Z Y. Li (2003). Multisensor-Multitarget Location Information Fusion Based on Improved Genetic Algorithm. *Avionics Technology* **1**, 26 41.

Ljung, L. (1999). *System Identification, Theory for the User.* 2 ed.. Prentice Hall.

Loebis, D. (2005). An Intelligent Navigation System for an Autonomous Underwater Vehicles. *Ph.D Thesis.*

Loebis, D., R. Sutton and J. Chudley (2003). A Fuzzy Kalman Filter Optimized Using a Genetic Algorithm for Accurate Navigation of an Autonomous Underwater Vehicle. *Proceedings of the* 6^{th} *IFAC Conference on Manouvring and Control of Marine Crafts (MCMC)* pp. 19–24. September, Girona, Spain.

Loebis, D., R. Sutton, J. Chudley and W. Naeem (2004). Adaptive tuning of a Kalman filter via fuzzy logic for an intelligent AUV navigation system. *Control Engineering Practice* **12**(12), 1531–1539.

Loebis, D., W. Naeem, R. Sutton, J. Chudley and A. Tiano (2006). Navigation, Guidance and Control of the Hammerhead Autonomous Underwater Vehicle, Roberts, G. N. and Sutton, R. (Eds), Advances in Unmanned Marine Vehicles. *IEE Control Series* pp. 127–155.

Luo, R C., C. Yih and K L. Su (2002). Multisensor Fusion and Integration: Approaches, Application and Future Research Direction. *IEEE Journal of Sensors* **2**(2), 107–119.

Magill, D T. (1965). Optimal Adaptive Estimation of Sampled Stochastic Process. *IEEE Trans. Automatic Control* **10**(4), 434–439.

Majohr, J. and T. Buch (2006). Modelling, Simulation and Control of an Autonomous Surface Marine Vehicle for Surveying Applications Measuring Dolphin (MESSIN^{TM}).

Roberts, G. N. and Sutton, R. (Eds), Advances in Unmanned Marine Vehicles. *IEE Control Series* pp. 329–346.

Majohr, J., T. Bush and C. Korte (2000). Navigation and Automatic Control of the Measuring Dolphin (MESSIN^{TM}). *Proceedings of the* 5^{th} *IFAC Conference on Manouvring and Control of Marine Crafts (MCMC)* pp. 405–410. Aalborg, Denmark.

Manlay, J E., A. Marsh, W. Cornforth and C. Wiseman (2000). Evolution of the Autonomous Surface Craft AutoCat. *Proceedings of OCEANS 2000 MTS/IEEE* **1**, 403–408. September, Providence, USA.

McGhee, R B., J R. Clynch, A J. Healey, S H. Kwak, D P. Brutzman, X P. Yun, N A. Norton, R H. Whalen, E R. Bachmann, D L. Gay and W R. Schubert (1995). An Experimental Study of an Intergrated GPS/INS System for Shallow water AUV Navigation. 9^{th} *International Symposium on Unmanned Unthetered Submersible technology* pp. 153–167.

Mebra, R K. (1970). On the Identification of Variances and Adaptive Kalman Filtering. *IEEE Trans. Automatic Control* **AC-15**, 175–184.

MIT AUV Lab (2000). AutoCat Autonomous Surface Craft. Available from http://auvlab, mit,edu/research/mvo.html. Data accessed: October 2006.

Mohamed, A H. and K P. Schwarz (1999). Adaptive Kalman Filtering for INS/GPS. *Journal of Geodesy* **73**, 193–203.

Moiré Inc. (2003). The Growing US Market for Unmanned Surface Vehicles (USVs). Available from http://www.moireinc.com/USVmarketMoire.pdf. Data accessed: October 2006.

Moore, M., C. Rizos and J. Wang (2003). Issues Concerning the Design of a Low-Cost Attitude Determination System for an Unmanned Airborne Vehicle. 11^{th} *International Associate of Institutes of Navigation World Congress, CD-ROM Proceedings, paper 111.*

Morari, M. and J. Lee (1997). Model Predictive Control: Past, Present and Future. Available from citeseer.ist.psu.edu/morari97model.html. Date Accessed, April 10th 2005.

Naeem, W., R. Sutton and S M. Ahmad (2004). A Review of Guidance Laws Applicable to Unmanned Underwater Vehicles. *Journal of the Institute of Navigation* **56**(1). 15–29.

Naeem, W., R. Sutton, J. Chudley, F R. Dalgleish and S. Tetlow (2005). An Online Genetic Algorithm Based Model Predictive Control Autopilot Design with Experimental Verification. *International Journal of Control* **78**(14). 1076–1090.

Naeem, W., T. Xu, J. Chudley and R. Sutton (2006). Design of an Unmanned Surface Vehicle for Environmental Monitoring. *World Maritime Technology Conference.* March, London, UK.

Naeem, W., T. Xu, R. Sutton and A. Tiano (2007). The Design of a Navigation, Guidance and Control System for an Unmanned Surface Vehicle for Environmental Monitoring. *Proceedings of the Institution of Mechanical Engineers, Part M: Journal of Engineering for the Maritime Environment.*

National Research Council,USA (2003). Exploration of the Seas: Voyage into the Unknown. Available from http://www.nap.edu/catalog/10844.html. Date Accessed, October 18th 2005.

Pascoal, A. and P. Oliveira (2003). On the Design of Multirate Complementary Filters for Autonomous Marine Vehicle Navigation. 1^{st} *IFAC Workshop on Guidance and Control of Underwater Vehicles GCUV2003.* Newport, United Kingdom, April 2003.

Pascoal, A., C. Silvestre and P. Oliveira (2006). Vehicle and Mission Control of Single and Multiple Autonomous Marine Robots. Roberts, G. N. and Sutton, R. (Eds), Advances in Unmanned Marine Vehicles . *IEE Control Series* pp. 353–380.

Pascoal, A., P. Oliveira, C. Silvestre, L. Sebastiao, M. Rufino, V. Barroso, J. Gomes, G. Ayela, P. Coince, M. Cardew, A. Ryan, H. Braithwaite, N. Cardew, J. Trepte.

N. Seube, J. Champeau, P. Dhaussy, V. Sauce, R. Moitie, R. Santos, F. Cardigos, M. Brussienx and P. Dando (2000). Robotic Ocean Vehicles for Marine Science Applications: the European ASIMOV Project. *Proceedings of 2000 OCEANS MTS/IEEE* **1**, 409–415. September, Providence, Rhode Island, USA.

PNI, Co. (2004). TCM2 Compass User Manual. Available from https://www.pnicorp.com/downloadResource/c40c/manuals/5/Operation+Manual+TCM2+28MANUAL+1000281+R0329.pdf. Data accessed: October 2006.

Prajitno, P. and N. Mort (2001). A Fuzzy Model-based Multi-Sensor Data Fusion System. *Proceedings of SPIE, Sensor Fusion: Architecture, Algorithms and Applications* **4385**, 301–312.

Qin, S J. (2000). An Overview of Industrial Model Predictive Control Technology. Available from http://www.che.utexas.edu/~qin/cpcv/cpcv14.html. Date Accessed, April 10th 2005.

Raymarine, Ltd. (2001*a*). Raymarine ST40 Depth Sensor User Manual. Available from http://www.raymarine.com/raymarine/SubmittedFiles/Handbooks/Instruments/40depth.pdf. Data accessed: October 2006.

Raymarine, Ltd. (2001*b*). Raymarine ST40 Speed Log User Manual. Available from http://www.raymarine.com/raymarine/SubmittedFiles/Handbooks/Instruments/40speed.pdf. Data accessed: October 2006.

Roberts, G N. and R. Sutton (2006). Editorial: Navigation, Guidance and Control of Unmanned Marine Vehicles Roberts, G. N. and Sutton, R. (Eds), Advances in Unmanned Marine Vehicles. *IEE Control Series* pp. 1–11.

RoboTek Engineering Inc. (2004). Roboski. Available from http://www.thirdhemisphere.com/products/roboski/. Data accessed: October 2006.

Roboteq, Inc. (2005). RoboteQ AX2550/2850 User's Manual. Available from http://www.roboteq.com. Data accessed: October 2006.

Shahbazian, E., L. Gagnon, J. Duquet, M. Macieszczak and P. Valin (1997). Fusion of Imaging and Non-imaging Data for Surveillance Aircraft. *Proceedings of SPIE. Sensor Fusion: Architecture, Algorithms and Applications.* Montreal, Canada, July 1997.

Shahbazian, E., R. Hallsworth and D. Turgeon (2000). Target Tracking and Identification Issues When Using Real Data. *Proceedings of the Third International Conference on Information Fusion.* Montreal, Canada, July 2000.

Shearer, S A., J P. Fulton, S P. Higgins and S G. McNeill (2005). Differential Global Positioning System (DGPS): Application to Precision Agriculture. Available from http://www.bae.uky.edu/precag/PrecisionAg/Pages/gpsext.html. Data accessed: October 2006.

Shima, T., Y. Oshman and J. Shinar (2002). Efficient Multiple Model Adaptive Estimation in Ballistic Missile Interception Scenarios. *Journal of Guidance, Control, and Dynamics* **25**(4), 667–675.

Simone, G., F C. Morabito and A. Farina (2000). Radar Image Fusion by Multiscale Kalman Filtering. *Proceedings of the Third International Conference on Information Fusion* **2**, 10–17.

SPAWAR Systems Center San Diego (2002). SSC-SD Unmanned Surface Vehicle. Available from http://www.nosc.mil/robots/surface/usv/usv.html. Data accessed: October 2006.

Tan, C S. (2006). A Collision Avoidance Systems for Autonomous Underwater Vehicles. *Ph.D Thesis.*

Tan, C S., R. Sutton and J. Chudley (2004). Collision Avoidance Systems for Autonomous Underwater Vehicles, Part B: Obstacle Avoidance. *Journal of Marine Science and Enviroment, IMarEST* **C2**, 51–62.

The University of Azores (2001). Mapping of Marine Habitats of the Azores using Robotic Ocean Vehicles (MAROV) project. Available from http://www.horta.uac.pt/projectos/marov/index1.html. Data accessed: October 2006.

Tiron, R. (2002). High Speed Unmanned Craft Eyed for Surveillance Role. Available from http://www.nationaldefensemagazine.org/issues/2002/May/High-Speed.htm. Data accessed: October 2006.

Vaneck, T. (1997). Fuzzy Guidance Controller for an Autonomous Boat. *IEEE Control Systems* **17**(2), 43–51. April.

Varshney, P K. (1997). Multisensor Data Fusion. *Journal of Electronics and Communciation Engineering* pp. 245–253.

Vasquez, J R. and P S. Maybeck (2004). Enhanced Motion and Sizing of Bank in Moving-Bank MMAE. *IEEE Trans. Aerospace Electronic System* **40**(3), 770–779.

Veers, J. and V. Bertram (2006). Development of the USV Multi-Mission Surface Vehicle III. Available from http://www.tudelft.nl/live/binaries/7d10b02b33c4/doc34620Veers20Development20of20the20USV20MultiMission20Surface20Vehicle20III.pdf. Data accessed: October 2006.

Wall, M. (2000). Introduction to Genetic Algorithms. Available from http://lancet.mit.edu/~mbwall/presentations/IntroToGAs/. Date Accessed, May 14th 2005.

Welch, G. and G. Bishop (2004). An introduction to the Kalman filter. Available from http://www.cs.unc.edu/~welch/media/pdf/kalman_intro.pdf. Date Accessed, October 18th 2005.

Xu, T., J. Chudley and R. Sutton (2006*a*). A Fault Tolerant Multi-Sensor Navigation System for an Unmanned Surface Vehicle. *IFAC Symposium Fault Detection, Supervision and Safety of Technical Processes-SAFEPROCESS*. August, Beijing, China.

Xu, T., J. Chudley and R. Sutton (2006*b*). Soft Computing Design of a Multi-Sensor Data Fusion System for an Unmanned Surface Vehicle Navigation. *Proceedings of the* 7^{th} *IFAC Conference on Manouvring and Control of Marine Crafts (MCMC)*. September. Lisbon, Portugal.

YAMAHA Motor Co., Ltd (2003). First Unmanned Atmospheric Survey Boat. Kan-Chan. Available from http://www.yamaha-motor.co.jp/buzz/marine/boats/ken-chan. Data accessed: April 2006.

Yan, J., M. Ryan and J. Power (1995). *Using Fuzzy Logic: Towards Intelligent Systems*. 1 ed.. Prentice Hall.

Yoerger, D., A M. Bradley, B. Walden and M. Cormier (2000). Fine-Scale Seafloor Survey in Rugged Deep-Ocean Terrain with an Autonomous Robot. *IEEE International Conference on Robotics and Automation* pp. 34–55.

YSI, Inc. (2005). YSI Environmental Operations Manual. Available from http://www.YSI.com. Data accessed: October 2006.

Appendix A

Publications

The work within this thesis has significantly contribute to the USV navigation research literature via the following list of publications. This includes all the papers which have either been published, accepted or under preparation.

Journal Papers

- W. Naeem, T Xu, R Sutton and A. Tiano(2007). *The design of a navigation, guidance and control system for an unmanned surface vehicle for environmental monitoring*, Proceedings of the Institution of Mechanical Engineers, Part M: Journal of Engineering for the Maritime Environment. Accepted.

- T Xu, J Chudley and R Sutton (2007). *A multi-sensor data fusion navigation system for an unmanned surface vehicle*, Proceedings of the Institution of Mechanical Engineers, Part M: Journal of Engineering for the Maritime Environment. Submitted.

Refereed Conference Papers

- T Xu, J Chudley and R Sutton (2006). *A fuzzy logic based mnlti-sensor navigation system for an unmanned surface vehicle*, United Kingdom Automatic Control council (UKACC) International Control Conference, August 2006, Glasgow, Scotland.

- T Xu, J Chudley and R Sutton (2006). *A fault tolerant multi-sensor navigation system for an unmanned surface vehicle*, IFAC Symposium Fault Detection, Supervision and Safety of Technical Processes-SAFEPROCESS. August 2006, Beijing,China.

- W. Naeem, T. Xu, J. Chudley and R. Sutton (2006). *Design of an unmanned surface vehicle for environmental monitoring*, World Maritime Technology Conference, March, London, UK.

- T Xu, J Chudley and R Sutton (2006). *Soft computing design of a multi-sensor data fusion system for an unmanned surface vehicle navigation*, 7th Conference on Manoeuvring and Control of Marine Craft (MCMC'2006), September. 2006. Lisbon, Portugal.

Appendix B

USV feature comparisons

The features of various on-going USVs are compared in Table B.1.

Table B.1. USV feature comparisons

USV name	Navigation Sensor Suite	Operation Mode	Operation Time (max)	Operation Speed (max)	Other Features
Owl MK II	Side scan sonar; Visual sensor; Magnetometer; Bathymetry sensor	Remote manoeuvre.	7.5 h	45 knots	
Spartan	Side scan sonar;	Remote manoeuvre.	8 h	>28 knots	
Protector	GPS; INS, Radar, Video camera	Remote manoeuvre.	N/A	40 knots	Day/night operation
SWIMS	GPS, Compass,	Remote manoeuvre.	N/A	40 knots	NI control equipment and user interface
Seastar	GPS, Sonar, Video camera	Remote manoeuvre.	N/A	40 knots	Day/night operation
SSC San Diego	GPS, gyro-enhanced orientation sensor, Video cameras	Remote manoeuvre; Waypoint pre-programmed manoeuvre; Autonomous operation.	N/A	N/A	PID control Collision avoidance ability
Sea Fox	Radar, Sonar, Video cameras	Remote manoeuvre.	N/A	40 knots	Swimmer detection ability

Roboski	GPS, Video camera	Remote manoeuvre.	N/A	42 knots	Multiple vehicles can be monitored and controlled from a single location
Stingray	N/A	Remote manoeuvre; Waypoint pre-programmed manoeuvre.	N/A	N/A	Day/night operation
Basil	N/A	Remote manoeuvre	7 days	3 knots	
Measuring Dolphin	DGPS, Echo sounder, Speed log, Compass, Impeller-log, Electromagnetic two component log, Magnetic compass, Yaw rate gyroscope, Hydro acoustic depth sensor	Remote manoeuvre; Waypoint pre-programmed manoeuvre; Automatic manoeuvre based on DGPS; Anti-collision manoeuvre.	10 h (for hybrid power supply) 3 h (for battery power supply)	4 knots	Hybrid power supply; Hierarchical steering system including steering equipment for rudder machine and propellers.
Delfim	DGPS, Attitude reference unit, Doppler log	Remote manoeuvre; Waypoint pre-programmed manoeuvre.	NA	5 knots	This vehicle can cooperate with AUV Infante.
Caravela 2000	GPS/DGPS, Doppler log, Gyrocompass, Heave, pitch and roll sensors	Remote manoeuvre; Waypoint pre-programmed manoeuvre; Anti-collision manoeuvre.	3 weeks	5 knots	Development of a inboard computer distributed network unit and a energy generation and distribution system.

Roboski	GPS, Video camera	Remote manoeuvre.	N/A	42 knots	Multiple vehicles can be monitored and controlled from a single location
Stingray	N/A	Remote manoeuvre; Waypoint pre-programmed manoeuvre.	N/A	N/A	Day/night operation
Basil	N/A	Remote manoeuvre	7 days	3 knots	
Measuring Dolphin	DGPS, Echo sounder, Speed log, Compass, Impeller-log, Electromagnetic two component log, Magnetic compass, Yaw rate gyroscope, Hydro acoustic depth sensor	Remote manoeuvre; Waypoint pre-programmed manoeuvre; Automatic manoeuvre based on DGPS; Anti-collision manoeuvre.	10 h (for hybrid power supply) 3 h (for battery power supply)	4 knots	Hybrid power supply; Hierarchical steering system including steering equipment for rudder machine and propellers.
Delfim	DGPS, Attitude reference unit, Doppler log	Remote manoeuvre; Waypoint pre-programmed manoeuvre.	NA	5 knots	This vehicle can cooperate with AUV Infante.
Caravela 2000	GPS/DGPS, Doppler log, Gyrocompass, Heave, pitch and roll sensors	Remote manoeuvre; Waypoint pre-programmed manoeuvre; Anti-collision manoeuvre.	3 weeks	5 knots	Development of a inboard computer distributed network unit and a energy generation and distribution system.

Appendix C

Sensor strings

Each sensor output is in a specified form. The strings normally include the the string head, main body of the string as well as check sum at the end.

GPS

An archetypal GPS sentence is shown below starting with a GPRMC that provides various information including time, position, velocity and magnetic variation etc.

$GPRMC,235959,A,5041.9364,N,00413.9804,W,002.4,021.7,170806,004.0,W*69

$\underline{\$GPRMC}$ is the sentence head,

$\underline{235959}$ is UTC time in hhmmss,

$\underline{A}$ indicates the GPS information is valid,

$\underline{5041.9364}$ refers latitude in ddmm.mmmm, $\underline{N}$ is latitude hemisphere (N or S).

$\underline{00413.9804}$ is longitude in dddmm.mmmm, $\underline{W}$ is longitude hemisphere (E or W).

$\underline{002.4}$ represents speed over ground in knots,

$\underline{021.7}$ gives course over ground in degree,

170806 is UTC date in ddmmyy.

004.0 is magnetic variation, W is magnetic variation direction (E or W)

*69 is the check sum for this string.

TCM2

A typical TCM2 output string is given by

$C63.5P2.1R3.3*29

$ marks the beginning of string,

*C*63.5 represent the heading angle with respect to the magnetic North in degree and it ranges from 0^o to 360^o,

*P*2.1 provides the pitch angle in the limit of $\pm 20^o$,

*R*3.3 is the roll angle in degree and saturates at $\pm 20^o$,

*29 is the check sum for this string.

HMR3000

A standard output of HMR3000 is

$PTNTHPR,85.9,N,-0.9,N,0.8,N*2C

$*PTNTHPR* is the sentence head,

85.9 is the true heading angle ranges from 0^o to 360^o,

-0.9 is the pitch angle in the limit of $\pm 45^o$,

0.8 is the roll angle in the limit of $\pm 45^o$,

N indicates the sensor operate in normal situation.

**2C* is the check sum for the string.

KVH C100

A typical KVH C100 output string is given as

$HCHDT,271.8,T*2C

$\underline{HCHDT}$ is the standard lead in indicating that the message is true heading angle.

$\underline{271.8, T}$ provides the compass true heading to the tenth of a degree.

$\underline{*2E}$ is the check sum for the string.

Depth and speed sensor

Depth and speed sensors output several different strings. In the strings, '$' marks the beginning of strings, II means integrated instrumentation,

For the depth sensor, the information is given by

$IIDBT,8.3,f,2.53,M,1.38,F*14

$\underline{DBT}$ refers depth below transducer,

$\underline{8.3, f}$ is the water depth in feet,

$\underline{2.53, M}$ represents the water depth in meters,

$\underline{1.38, F}$ is the water depth in Fathoms,

$\underline{*14}$ is the check sum for the string.

$IIMTW,16.0,C*14

$\underline{MTW}$ indicates the water temperature,

$\underline{16.0, C}$ is $16C^o$,

$\underline{*14}$ is the check sum for the string.

For the speed sensor, the information is provided by

$IIVHW,005,T,008,M,0.00,N,0.00,K*55

VHW refers vessel speed and heading relative to the water.

005, *T* is the true heading angle in degree,

008, *M* provides magnetic heading angle in degree,

0.00, *N* indicates the speed of vessel relative to the water in knots,

0.00, *K* is the travel distance in kilometers.

Appendix D

Model predictive control

Model predictive control (MPC) is widely adopted in industry as an effective means to deal with large multi-variable constrained control problems (Qin 2000). The main idea of MPC is to choose the control action by repeatedly solving on line an optimal control problem (Morari and Lee 1997). This aims at minimizing a performance criterion over a future horizon, possibly subject to constraints on the manipulated inputs and outputs, where the future behavior is computed according to a model of the plant.

A GA-MPC algorithm was first proposed by Duwaish and Naeem (2001) for chemical processes identified as Hammerstein and Wiener models. This was later modified and implemented in the Hammerhead AUV in real time (Naeem *et al.* 2005) which provided adequate results even in the presence of modelling uncertainty. The GA based controller uses the process model to search for the control moves, which satisfy the process constraints and optimizes a cost function (Wall 2000). The cost function to be minimised here is given by Equation D.1:

$$J = \sum_{i=1}^{H_p} e(k+i)^T T e(k+i) + \sum_{i=1}^{H_c} \Delta u(k+i)^T D \Delta u(k+i) + \sum_{i=1}^{H_p} u(k+i)^T W u(k+i) \quad \text{(D.1)}$$

subject to;

$$u^l \leq u(k+i) \leq u^u$$

$$\Delta u^l \leq \Delta u(k+i) \leq \Delta u^u \quad \text{(D.2)}$$

where the superscripts l and u represents the lower and upper bounds respectively. T is the weight on the prediction error,

$$e(k) = \hat{y}(k) - \omega(k) \quad \text{(D.3)}$$

where $\omega(k)$ is the reference or the desired setpoint. D and W are weights on the change in the input Δu and magnitude of the input u respectively. Adjusting the input weighting matrices could add damping to the closed loop control system. The following steps describe the operation of the GA based MPC algorithm (Naeem *et al.* 2005). At time step k:

- Evaluate process outputs using the process model.
- Use GA search to find the optimal control moves which optimize the cost function and satisfy process constraints. This can be accomplished as follows.
  - generate a set of random possible control moves. The control moves or population consists of real values which is reasonable in a real world environment.
  - find the corresponding process outputs for all possible control moves using the process model.

- evaluate the fitness of each solution using the cost function and the process constraints. The fitness function used here is given by:

$$fitness = \frac{1}{1+J} \tag{D.4}$$

where J is the cost function given by Equation D.1.

- apply the genetic operators (selection, crossover and mutation) to produce new generation of possible solutions. Roulette wheel and single point crossover is used for parents selection and mating respectively.

- repeat until predened number of generations is reached and thus the optimal control moves are determined.

- Apply the optimal control moves to the second step to the process.

- Repeat the first step to the third step for time $k+1$.

D.1 Constraints formulation

Constraints represent limitations on different physical quantities involved in a process. For instance, the input or output of a certain process is restricted beyond a specified value due to economical or environmental reasons or the input cannot be changed abruptly due to the hardware dynamics. One of the most powerful and distinguishing features of MPC is its ability to handle constraints in a natural way during the controller design at every sample time. Generally, two types of constraints are considered in controller design. Soft constraints are employed in the cost function as a penalty factor and can be violated to fulfil some other criteria. On the other hand, hard constraints represent physical limitations on actuators and cannot be violated. Herein, only hard constraints are placed on the input variables in order to determine the suitability of the controller. In this case, since the

population in a GA represents the input variable. therefore, constraints are implemented by generating random initial population in the desired range i.e..

$$u^l \leq u \leq u^u \tag{D.5}$$

GA-MPC has been successfully applied on the *Springer* for real time experiments. More details of the MPC design can be found at Naeem et al. (2006).